AN ABSTRACT OF THE THESIS OF

Grant C. Blake for the degree of Master of Science in Nuclear Engineering presented on September 20, 2016

Title: Scaling Analysis of the Direct Reactor Auxiliary Cooling System for Gas-cooled Fast Reactors during a Depressurized Loss of Forced Convection Event

Abstract approved:

Brian G. Woods

The Direct Reactor Auxiliary Cooling System (DRACS) is a passive safety system capable of removing decay heat directly from the reactor core. Its modularity makes it scalable for use in reactors with various power levels. Work has previously been completed to support inclusion of the DRACS in liquid metal reactors and fluoride-salt cooled reactors. This work supports the inclusion of DRACS in gas-cooled reactors, similarly.

A scaling analysis has been completed for a DRACS module. The target prototype for this scaling analysis is a DRACS for gas-cooled fast reactor (GFR), such as in the Energy Multiplier Module (EM^2). The target model for the scaling analysis is a conceptual design for the inclusion in the High Temperature Test Facility (HTTF) at Oregon State University (OSU). Also included herein is the conceptual design requirements for said scaled-down DRACS module including an instrumentation plan and SolidWorks models. Python was used with Engineering Equation Solver to determine the operating characteristics. These physical dimensions and operating characteristics were used to build models in RELAP5-

3D of the scaled-down and full-scale DRACS with the intent to inform the scaling analysis results.

Results from the RELAP5-3D models support the scaling analysis performed. The error was analyzed between the resulting scaling for each value from RELAP5-3D and the theoretical scaling value as found in the scaling analysis. The errors found for most of the quantities were minimal, and well within reason for simulations in RELAP5-3D. There was a significant error found in the intermediate loop velocity scaling from the RELAP5-3D model results, and this error led to other errors which are dependent on the intermediate loop velocity. The scaling of the heat transfer rates in the intermediate loop also experienced an error from the theoretical results, leading to an error in the intermediate loop DRACS heat exchanger (DHX) and natural draft heat exchanger (NDHX) numbers. The velocity error is thought to be the result of an improperly scaled intermediate loop resistance number, which cannot be investigated directly from RELAP5-3D outputs. The heat transfer error is likely due to different Nusselt number correlations in the intermediate loop from those used in the direct and natural draft loops. These correlations are selected automatically by the code, and measures could be taken in a future design to correct for this.

Scaling Analysis for the Direct Reactor Auxiliary Cooling System for Gas-cooled Fast Reactors during a Depressurized Loss of Forced Convection Event

by
Grant C. Blake

A THESIS

submitted to

Oregon State University

in partial fulfillment of
the requirements for the
degree of

Master of Science

Presented September 20, 2016
Commencement June 2017

Master of Science thesis of Grant C. Blake presented on September 20, 2016.

APPROVED:

Major Professor, representing Nuclear Engineering

Head of the School of Nuclear Science and Engineering

Dean of the Graduate School

I understand that my thesis will become part of the permanent collection of Oregon State University libraries. My signature below authorizes release of my thesis to any reader upon request.

Grant C. Blake, Author

ACKNOWLEDGEMENTS

I would like to thank first and foremost my advisor Dr. Brian Woods, my wife Rachel, and my son Malcolm for being so very patient during the duration of writing this thesis. The counseling provided by Dr. Woods was invaluable. The service provided by Rachel was equally important.

I would also like to thank the following for their various contributions:

Dr. Wu for the knowledge gained during his Scaling and Advanced Thermal Hydraulics classes.

Aaron Weiss for advice on instrumentation.

Matt Hertel for advice on SolidWorks.

Kyle Hoover for exchanging ideas about RELAP5-3D.

Dr. Woods, Dr. Cadell, Rachel, and Ben Blake for proof-reading.

Dr. Woods, Dr. Reese, Dr. Cadell, and Dr. Stetz for serving on my examination committee.

My parents and grandparents for always believing I could do it.

TABLE OF CONTENTS

TABLE OF CONTENTS (Continued)

LIST OF FIGURES

LIST OF TABLES

LIST OF TABLES (Continued)

LIST OF FIGURE SOURCES

Figure 1-1 is used with permission from Nuclear Engineering and Technology [1].

Figure 1-2 is used with permission from personal correspondence with Dr. Schleicher.

Figure 1-3 is used with permission from personal correspondence with Dr. Schleicher.

Figure 1-4 is used with permission from personal correspondence with Dr. Schleicher.

Figure 4-1 is used with permission from originator, Dr. Choi [2].

Figure 4-2 is open domain from Canon Institute for Global Studies [3].

Figure 4-3 is used with permission from Nuclear Technology, Copyright 2013 by the American Nuclear Society, LaGrange Park, Illinois [4].

Figure 4-4 is used with permission from Nuclear Technology, Copyright 2013 by the American Nuclear Society, LaGrange Park, Illinois [4].

Figure 4-5 is open domain from Canon Institute for Global Studies [3].

Figure 4-6 is open domain from Canon Institute for Global Studies [3].

Figure 4-7 is original work.

Figure 5-1 is original work.

Figure 5-2 is original work.

Figure 5-3 is original work.

Figure 5-4 is used with permission from Nuclear Technology, Copyright 2013 by the American Nuclear Society, LaGrange Park, Illinois [4].

Figure 5-5 is original work.

Figure 5-6 is original work.

Figure 5-7 is original work.

Figure 8-1 is original work.

LIST OF ABBREVIATIONS

ABTR	Advanced Burner Test Reactor
AFR-100	100 MWe Advanced sodium-cooled Fast Reactor
AHTR	Advanced High Temperature Reactor
ALMR	Advanced Liquid Metal Reactor
AP600	Advanced Passive PWR, ~600 MWe capacity
AP1000	Advanced Passive PWR, ~1000 MWe capacity
APEX	Advanced Plant Experiment
ASME	American Society of Mechanical Engineers
ATWS	Anticipated Transient without SCRAM
CFD	Computational fluid dynamics
CV	Containment vessel
D-LOFC	Depressurized Loss of Forced Convection
DFBR	Demonstration Fast Breeder Reactor
DHX	DRACS Heat Exchanger
DNBR	Departure from nucleate boiling ratio
DOE	United States Department of Energy
DRACS	Direct Reactor Auxiliary Cooling System
DRHX	Direct Reactor Heat Exchanger
DSS	Dynamical system scaling
EBR-II	Experimental Breeder Reactor-II
ECS	Emergency cooling system
EES	Engineering Equation Solver
EFR	European Fast Reactor
EM^2	Energy Multiplier Module
FCM	Fractional change metric
FFTF	Fast Flux Test Facility
FHR	Fluoride Salt-cooled High Temperature Reactor
FLiNaK	Fluoride salt, molar percentages LiF-NaF-KF 46.5-11.5-42
FOM	Figure of merit
FRC	Fractional rates of change
FSA	Fractional scaling analysis
GA	General Atomics
GFR	Gas-cooled Fast Reactor
H2O	Elemental designation for water
He	Elemental designation for Helium
H2TS	Hierarchal two-tiered scaling
HTDF	High Temperature DRACS Test Facility

LIST OF ABBREVIATIONS (Continued)

HTR-10	10 MW High Temperature Gas-cooled Test Reactor
HTR-PM	High Temperature Gas-cooled Reactor Pebble-bed Modular
HTTF	High Temperature Test Facility
IAEA	International Atomic Energy Agency
IEEE	Institute of Electrical and Electronics Engineers
INL	Idaho National Laboratory
JSFR	Japanese Sodium-cooled Fast Reactor
kW	Kilo Watts (1 000 Watts)
LMFBR	Liquid Metal Fast Breeder Reactor
LMR	Liquid Metal-cooled Reactor
LOCA	Loss of coolant accident
LOFC	Loss of forced convection
LS-VHTR	Liquid Salt-cooled Very High Temperature Reactor
LTDF	Low Temperature DRACS Test Facility
LWR	Light Water Reactor
MASLWR	Multi-application small light water reactor
MHTGR	Modular High Temperature Gas-cooled Reactor
MSR	Molten Salt-cooled Reactor
MWe	Electrical power measured in Mega Watts (1 000 000 Watts)
MWt	Thermal power measured in Mega Watts (1 000 000 Watts)
NaK	Sodium-Potassium eutectic
NDDCT	Natural draft dry cooling tower
NDHX	Natural Draft Heat Exchanger
NEUP	Nuclear Energy University Program
NPP	Nuclear Power Plant
NURETH	Nuclear Reactor Thermal Hydraulics (conference)
OSU	Oregon State University
P-LOFC	Pressurized loss of forced convection
PB-AHTR	Pebble Bed Advanced High Temperature Reactor
PCS	Power conversion system
PCU	Power conversion unit
PFBR	Prototype Fast Breeder Reactor
PFR	Prototype Fast Reactor
PHX	PRACS Heat Exchanger
PIRT	Phenomenon identification and ranking table
PPV	Primary pressure vessel
PRACS	Pool Reactor Auxiliary Cooling System

LIST OF ABBREVIATIONS (Continued)

PWR	Pressurized Water Reactor
RCCS	Reactor Cavity Cooling System
RELAP	RELAP5-3D
RPV	Reactor pressure vessel
RVACS	Reactor Vessel Auxiliary Cooling System
S-CO2	Supercritical Carbon Dioxide
SAFR	Sodium-cooled Advanced Fast Reactor
SASM	Severe Accident Scaling Methodology
SFR	Sodium-cooled Fast Reactor
SSC	Super System Code
TWR	Traveling Wave Reactor
TWR-P	Prototype Traveling Wave Reactor
V&V	Verification and validation
VHTR	Very High Temperature Reactor

Scaling Analysis for the Direct Reactor Auxiliary Cooling System for Gas-cooled Fast Reactors during a Depressurized Loss of Forced Convection Event

1. Introduction

1.1. Background

A major accident was caused at the Fukushima Daiichi nuclear power plant (NPP) in 2011 by a major earthquake off the coast followed by a massive tsunami. These natural disasters led to the total loss of electrical power throughout the power station. This lack of power meant that safety systems in place could not be operated to keep the reactor cores cool over the long term. Through operator intervention the amount of time to plant failure was prolonged, but inevitable. Partial core meltdown was ultimately experienced in units 1, 2, and 3 at Fukushima Daiichi [5].

In 1979, it was demonstrated in unit 2 of the Three Mile Island nuclear power station that operator error can lead to a major accident in a NPP. Operators misinterpreted a signal on the control panel and took action that ultimately turned a system malfunction into a partial core meltdown [6]. Had the NPPs in Fukushima had passive safety systems which can function over a long term without the need for operator action or electrical power, the outcome may have been different. Had the operators at the Three Mile Island NPP understood the signals and taken the proper action, or if the system included a passive system which could function without the operator action, the outcome may have been different. Both of these accidents demonstrate the need for advanced nuclear plant designs with passive safety systems which will safely maintain core

temperature without power and without operator action in the event of abnormal situations.

The DRACS is a passive safety system, conceptualized to increase the safety of advanced nuclear plant designs by removing decay heat directly from the core in the event of an accident. It performs this function without operator action. The Experimental Breeder Reactor-II (EBR-II) featured a passive cooling system which the DRACS was derived from [7] [8]. The DRACS has been included in several different advanced reactor concepts, including sodium-cooled fast reactors (SFR), molten salt-cooled reactors (MSR), and GFRs. Specific concepts include an SFR, TerraPower's Traveling Wave Reactor (TWR) [1], an MSR, the Advanced High Temperature Reactor (AHTR) [9] or Fluoride Salt-cooled High Temperature Reactor (FHR), and a GFR, General Atomics' EM^2 [4]. EM^2 has been chosen as the design to focus on for this work in order to encourage the use of DRACS in more gas-cooled reactor designs in the future.

1.1.1. The Direct Reactor Auxiliary Cooling System

The Direct Reactor Auxiliary Cooling System transports heat directly from the reactor to ambient air by means of buoyancy driven flow through three loops, connected by two heat exchangers. An example schematic of the DRACS is presented in Figure 1-1, from TerraPower's TWR. Although the specific design of this system varies with specific reactor design, the DRACS is typically a passive system, with flow driven by natural circulation. Some designs, such as the TWR and EM^2, include additional features to boost performance when electrical power is available, such as pumps and blowers.

Activation of the DRACS is also performed passively, typically by an air damper or fluidic diode. Air dampers are held closed during reactor operation by an electromagnetic latch which opens after loss of power or at a trip signal [8] [10] [11]. Fluidic diodes are included between the core and DHX, providing high resistance to flow in the direction of flow during normal operations, with low flow resistance in the opposite direction, which is the case after the onset of natural circulation [12].

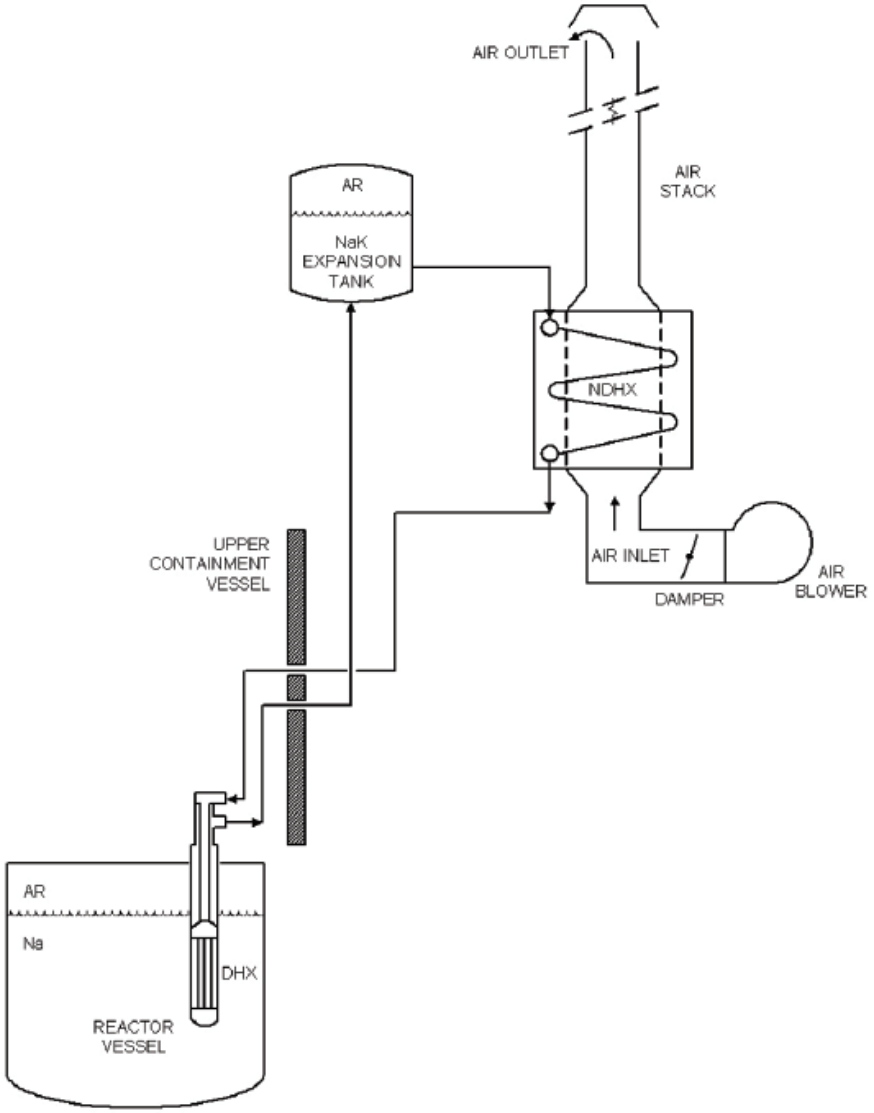

Figure 1-1: DRACS loop schematic from TerraPower's TWR-P

The heat exchanger which absorbs heat from the fluid which flows through the core is called the DHX. The DHX is located within the primary system pressure boundary, and is the link to the rest of the DRACS. In earlier reports on the DRACS, the DHX was instead called the direct reactor heat exchanger (DRHX) [13] [14]. The heat exchanger which rejects heat to ambient air is called the NDHX. It has been suggested that both heat exchangers make use of a shell-and-tube design, due to their low pressure drop and mature design concept compared to other heat exchanger types [12]. Other heat exchanger types have also been suggested, including a finned-tube heat exchanger [10], a twisted tube-and-shell heat exchanger [15], and a multi-tube helical coil heat exchanger [4]. The finned-tube heat exchanger was suggested for the NDHX, with the fins included to enhance heat transfer to the ambient air. The multi-tube helical-coil heat exchanger is included as the DHX for the EM^2 design. Both the helical-coil heat exchanger and twisted tube-and-shell heat exchangers enhance heat transfer by mixing of fluid inside the tubes due to the geometry of those tubes.

Three coupled natural circulation loops transport decay heat to ambient air from the core. Natural circulation depends only on temperature related density differences in the working fluid, with gravity driving the higher density fluid to lower elevations relative to the lower density fluid. Natural circulation as a flow driver is relatively weak compared to forced circulation [16], and is therefore more sensitive to friction and form loss. Limiting these losses in each of these natural circulation loops is essential to maximizing flow rate and therefore heat transport rate. There have been many natural circulation

studies done [17] [18] [19] [20] [21] [22], and although it is weaker at driving fluid flow than forced circulation, it also has benefits. Natural circulation is a physical phenomenon and does not require operator activation or electrical power, as a forced convection system does. The activation of the DRACS is automatic, as discussed at the beginning of this section by air dampers or a fluidic diode. A system that operates by natural circulation can therefore be fully passive, as the DRACS typically is.

The natural circulation loop which includes flow through the core to the DHX is the direct loop. In some designs the direct loop includes piping which leads to the DHX, such as in the EM^2 [4], while others have the DHX submerged in the buffer pool and the direct loop is only natural circulation flow within that pool [23]. In a conceptual design for very high temperature gas-cooled reactors, heat is absorbed directly from core structural material through radiative heat transfer by the DHX [24]. In the FHR, a fluidic diode is included in the direct loop to reduce parasitic flow and heat loss from the primary system during normal operations [12].

Heat absorbed from the core in the direct loop is transferred to the intermediate loop through the DHX. The intermediate loop is a closed loop, again dependent on natural circulation as the flow driver. The working fluid in this loop is also dependent on reactor type, but may be sodium [10], fluoride salt [12], lead [23], or water [4]. In the case of the first three working fluids listed, some attention needs to be given to keeping the intermediate loop unfrozen during normal operations, though heat leakage through the DRACS during normal operation may be enough for this purpose [9] [10] [24]. An

expansion tank is included in the intermediate loop for some designs to account for thermal expansion of the working fluid [1] [10]. Heat which is transferred to the intermediate loop through the DHX is transferred to the natural draft loop through the NDHX.

The natural draft loop is the open flow path of air through a natural draft dry cooling tower (NDDCT). A NDDCT is a cooling tower which does not use blowers to move the air or evaporative cooling. The NDDCT rejects heat to the ambient air by heating from the NDHX. The heated air rises due to natural circulation and cooler air flows past the NDHX in turn. The cooling tower is natural-draft in order to preserve the passive nature of the DRACS. A dry-cooling tower is attractive for many parts in the world where access to water is limited [25] [26] [27]. A dry cooling tower is also attractive for an accident situation where compromised infrastructure makes it difficult to obtain feed water. Air dampers are often included in the cooling tower in order to limit the flow during normal operations, thus limiting the undesired heat loss through the DRACS when it is not needed.

1.1.2. The Energy Multiplier Module

The Energy Multiplier Module is a GFR concept by General Atomics (GA). GFRs take advantage of the inert properties of Helium as a coolant and fast neutron spectrum in order to breed fissile fuel (i.e. Pu-239) from fertile material (i.e. U-238). The EM^2 boasts a thirty-year fuel cycle due to the convert-and-burn fuel concept, similar to TerraPower's TWR [1] [28]. It is proposed that enrichment of fuel won't be necessary

after the first generation of reactors, as fuel pulled out of one reactor will be able to jumpstart subsequent generations as the fissile starter [3]. A fissile starter is needed to initiate the chain reaction, and the neutron inventory, while producing power from fission, will also convert the fertile material included in the core into fissile material, to be burned over the extended fuel cycle. Spent fuel from light water reactors which are now operating in the US and around the world will be able to be used in this convert-and-burn fuel cycle, and the need for radioactive waste storage will be reduced as a result [28].

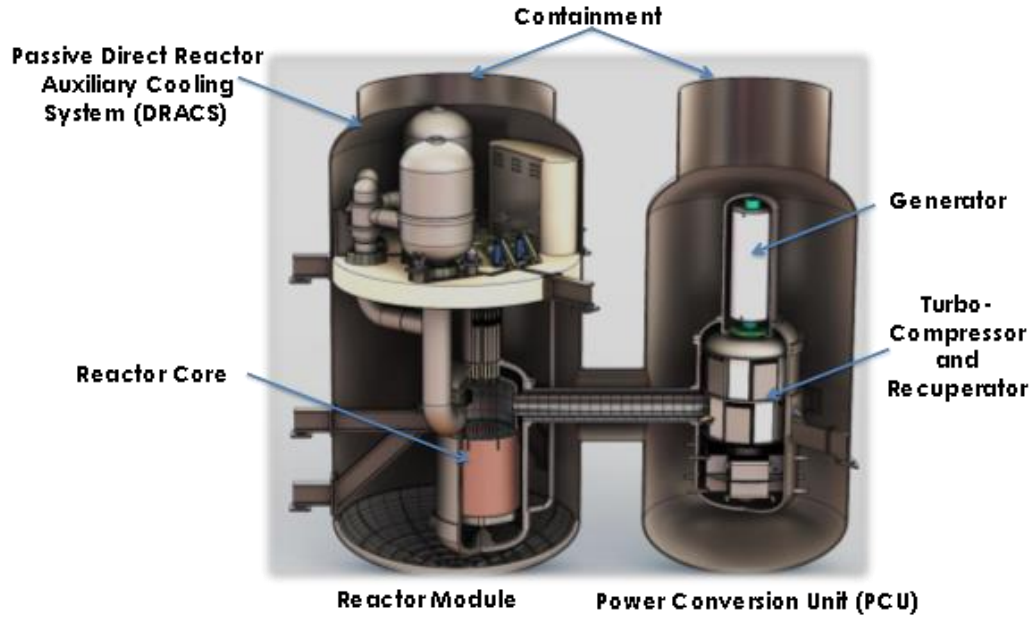

Figure 1-2: The Energy Multiplier Module system cut-away

The power output is 500 MWt with a reactor output temperature of 850 °C [29]. Due to a power conversion design that includes a closed cycle gas turbine and the high peak coolant temperature made possible by Helium, the net efficiency is significantly higher than LWRs [4]. The electrical power output each reactor is expected to achieve is 265

MWe (53% net efficiency) with evaporative cooling, or 240 MWe (48% net efficiency) with dry cooling, compared to 34% net efficiency for the AP1000 [28]. A variable high speed turbine generator set is employed, where the generator output can be rectified and inverted to the grid frequency when necessary [29]. Process heat can also be utilized given the high reactor output temperature. The design life of each plant is 60 years, and reactor modules are small enough to be transported by truck to the site [28]. The modular design is envisioned to be deployed in groups of 4 reactors to rival the power output of the AP1000, and located below grade for extra protection from missiles or planes crashes. The reactor utilizes 6.5% enriched vented porous uranium carbide fuel with silicon carbide clad for high temperature operation. Two independent reactor shutdown systems are included, being control drums and shutdown rods, which absorb neutrons to reduce the number of fission reactions to a safe shutdown state [29].

Two DRACS modules are included in the design of the EM^2, each capable of independently removing decay heat from the core. Each DRACS module is capable of operation in active mode, with the use of a helium circulator in the direct loop and jet pumps in the intermediate loop, or passive mode with neither pump nor circulator running. The direct loop fluid is helium, while intermediate loop fluid is water.

During a pressurized loss of forced convection (P-LOFC) cooldown, one DRACS module is capable of maintaining core temperature at a safe level without the use of the helium circulator or water pumps. A single DRACS module is capable of maintaining safe core temperature during a depressurized loss of forced convection (D-LOFC) cooldown only

while the helium circulator is operational, with either air or helium at atmospheric pressure [4]. With both DRACS modules operating passively during a D-LOFC, a safe shutdown condition will still be reached.

The purpose of the DRACS in the EM^2 design is to remove residual heat in shutdown condition when the power conversion unit system is unavailable for operation [4]. The DRACS was only added to the EM^2 design after a review by the Department of Energy (DOE) raised concerns about the reactor stability during a D-LOFC scenario [29].

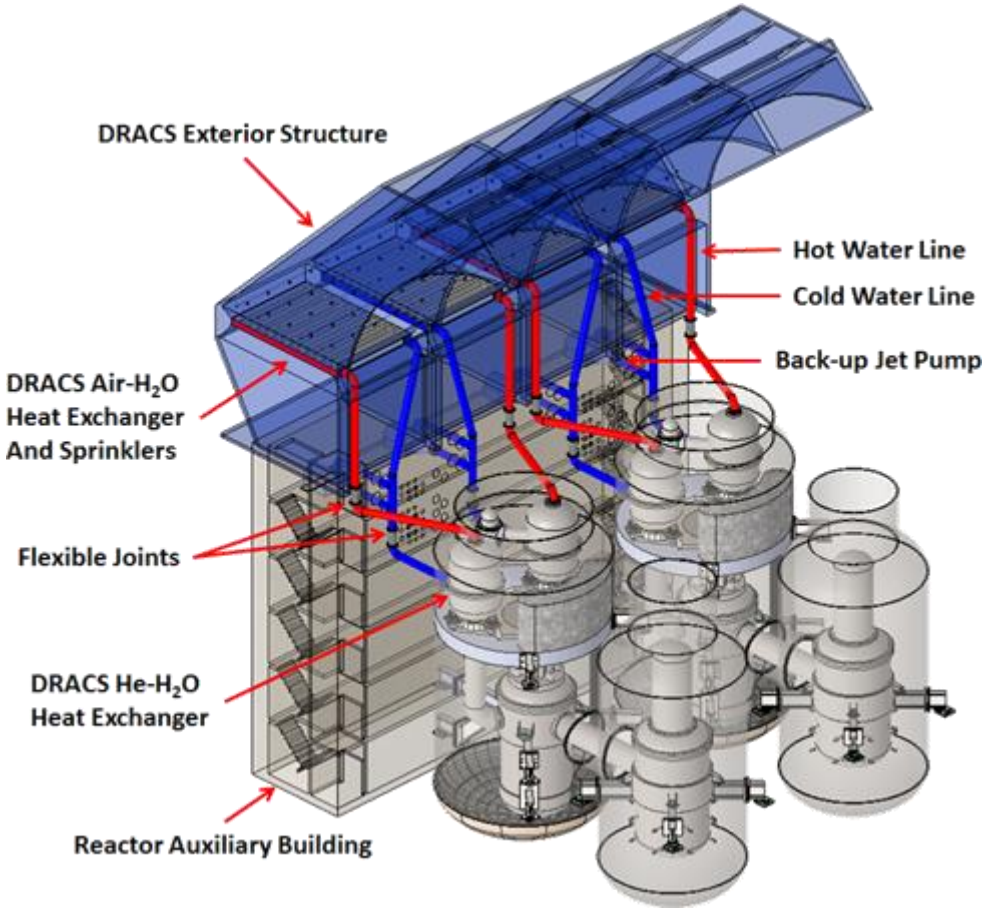

Figure 1-3: Full piping schematic of DRACS in two EM^2 modules

Specific details are not available on the design of the DRACS included in the EM^2 design, but a full list of the information collected is presented in chapter 4. One example is the gas in containment, beyond the fact that it is inert [4], no more specifics are provided. For this work, the containment gas is assumed to be nitrogen. It is clear by reviewing information from over the last five years that there have been design iterations on the EM^2 DRACS.

1.2. Purpose and Goal

The purpose of this work is to perform a scaling analysis and develop the design requirements for a scaled test facility capable of accurately modeling the phenomena of interest for a DRACS design similar to the EM^2. These phenomena of interest are explored in the preliminary phenomenon identification and ranking table (PIRT) in section 3.2. A scaling analysis was performed for the DRACS in GFRs using the Hierarchal Two-Tiered Scaling (H2TS) methodology including the quantification of scaling distortions. Due to limited information available on the EM^2 DRACS, a small-scale DRACS design has been developed to fit the HTTF at OSU, using what information is available. This small-scale design was used to build a computer model in RELAP5-3D, and the model was scaled up to full-scale in a separate RELAP5-3D model. The results of each model built in RELAP5-3D are then used to analyze the validity of the scaling analysis performed.

1.3. Importance

It has been demonstrated by the list of reactor designs in section 2.1 which include DRACS that there is interest in the system and in passive means of cooling the reactor core in both shutdown and accident conditions. Most of the reactor designs listed are sodium cooled, and this is likely because the DRACS was examined first for SFRs by the EBR-II [7]. The RVACS test facility was used to run additional tests on the cooling capability of the DRACS for liquid metal-cooled reactors (LMR) [14]. The construction of the low temperature DRACS test facility (LTDF) [30] [31] [32] and succeeding high temperature DRACS test facility (HTDF) [33] for the AHTR prove that the technology is spreading into the space of FHRs.

Accidents in nuclear reactors have potentially severe consequences, so an emphasis on safety in the nuclear industry is expected. Before designs for new reactors can be licensed to be built, the safety of the design has to be demonstrated. It would be expensive to build a full size prototype of a new reactor design in order to demonstrate its safety, so other less costly methods are employed.

Computer codes are developed to run a reactor through a variety of scenarios and accident conditions to demonstrate how a reactor will respond. These simulations can be run at a lower cost than a physical model, but the computer model must be validated before it can be used for licensing. Test facilities are scaled and constructed to run tests on a physical system to compare data taken to that generated by a computer code in order to validate the code.

A scaled test facility utilizing a DRACS needs to be developed in order to collect validation data for gas-cooled reactors. Licensing of new designs requires that those designs be demonstrated for their safety and effectiveness. This demonstration takes place using computer models of the system in question, but those computer models must undergo verification and validation first. A more complete discussion on the verification and validation process is included in section 2.5, but the collection of validation data in a physical test facility is required for this process. This work includes a scaling analysis and design requirements for the DRACS such that it could be included in a test facility for this purpose. A RELAP5-3D model of DRACS is used to support the scaling analysis. The scaling analysis performed as part of this work does not contribute directly to the verification and validation of a computer model for licensing, but it is necessary for the design of a physical test facility and to relate a scaled-down model to a full-scale model.

1.4. Assumptions

Assumptions were made in order to perform the scaling analysis and supporting work. Flow through each loop is assumed to be one-dimensional along the axial dimension of the loop. The fluid properties are therefore assumed to be uniform at each cross-section such that there is no change in the radial or azimuthal dimensions. All piping is assumed to be well insulated such that heat transfer only occurs between the working fluid and each of the heat exchangers. Heat transport occurs primarily through advection through each loop, such that conduction is negligible by comparison. At steady-state, the

pressure drop due to acceleration through the natural draft loop is assumed negligible, which allows for the steady-state velocity solution. It is assumed that the HTTF can accurately model the accident progression of the D-LOFC, such that the mass fraction of nitrogen in the primary system, and therefore the direct loop, will be the same as in the prototypical EM^2 DRACS.

Due to limited information available on the specifics of the EM^2 DRACS, some assumptions have to be made on the design in order to form the design requirements for the scaled DRACS module. Without physical dimensions of the prototype, a separate model was designed with the intent to be similar to the EM2 DRACS, but differences are inevitable. It is assumed in order to assess the scaling analysis that the flow path of the prototype matches that of the model designed, so there is no comparison to the actual EM^2 DRACS prototype.

The pressure and temperature in the intermediate loop are not referenced for the EM^2 DRACS, so it is assumed that the scaled model will be able to achieve full pressure and temperature, and therefore full fluid property similarity can be assumed. Specific dimensions are not given for the DHX, so it is assumed that the ratio of transverse to stream wise pitch between the tubes will be preserved between the model and prototype, as well as the number of turns of the helical coil. Modeling a helical coil heat exchanger is difficult in RELAP5-3D because there is no built-in capability to deal with this type of geometry. A vertical pipe is used in the RELAP5-3D models and it is assumed

that this geometry most closely matches the flow conditions in a helical coil. A more complete discussion on this model choice is contained in section 8.3.2.7.

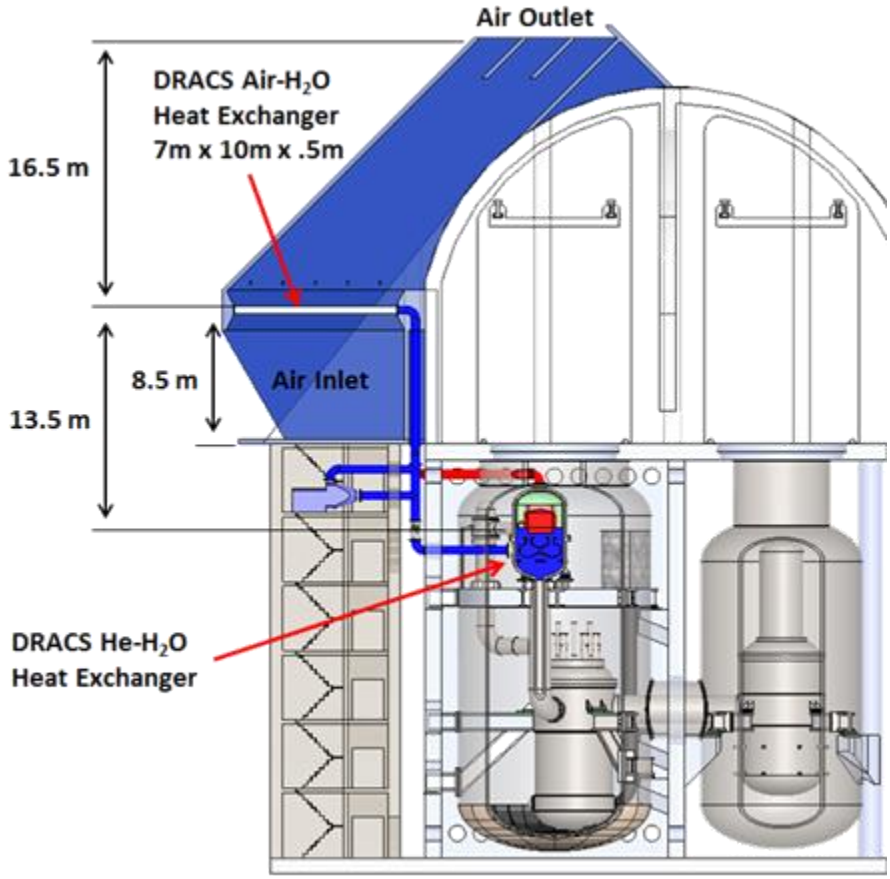

Figure 1-4: EM² full DRACS view with dimensions

Figure 1-4 includes the overall height for the intermediate and natural draft loop, which are used for the prototype dimensions. The intermediate loop height is scaled down and applied to the model according to the length scaling ratio. The remaining elevation between the roof air cooler and the core in the HTTF is then assumed to be the scaled height of the direct loop. This direct loop height is then scaled up from the model for the prototype dimensions. Also, shown in this figure is the NDHX with overall dimensions,

and the fact that it is oriented horizontally. It is assumed that this heat exchanger has finned tubes, the dimensions of which match the dimensions called out in Figure 1-4. The rest of the specific design for the NDHX was completed by engineering judgement.

While the D-LOFC is used as the conditions to model in RELAP5-3D, the model is run with constant boundary conditions to a steady-state condition. The conditions used are at the peak temperature, as shown in Figure 5-4, assumed to be the limiting condition.

1.5. Limitations

A conceptual design is proposed to configure the HTTF with the addition of the DRACS, but not enough specifics are laid out for the full implementation. The conceptual design applied to the HTTF is limited by the current configuration and the current operational abilities cannot be affected by the conceptual DRACS addition. The pressure vessel on the HTTF cannot be modified, so only ports which already exist are available for connections to the conceptual DRACS direct loop. The roof of the bay which houses the HTTF cannot support the weight of an additional cooling tower, so the existing cooling tower will be included in the design. No implementation of the DRACS addition to the HTTF is included as part of this work. No experiments are therefore run, and no test data is collected.

The EM^2 DRACS includes two independent modules as it is a safety rated system. Only one module is included in the initial design requirements presented as part of this work. This difference can be easily accounted for as the DRACS is modular and the two modules function separately. Although the design proposed uses some information

from the EM^2 DRACS and is meant to apply to that design, it is not a match of the EM^2 DRACS and should not be used as a reference for the DRACS included in the EM^2.

The scaling analysis performed is not comprehensive, and does not cover every scenario or accident condition. The scaling analysis performed focuses on a D-LOFC with station blackout. In other words, an event with reduced pressure and no active features. Some scaling ratios are also investigated for normal operations in the direct loop, with the pressure distortion accounting for some differences from the D-LOFC event.

1.6. Document overview

- Chapter 1: Introduction

An introduction to the work presented in this thesis. The background, the purpose of the work, importance, assumptions, and limitations are listed.

- Chapter 2: Literature review

The state of the art is explored and described relating to the DRACS, its inclusion in reactor concepts and designs, general scaling methodologies, previous applications of the H2TS methodology, previous scaling and test facilities related to DRACS, and code models involving the DRACS.

- Chapter 3: Scaling analysis

The H2TS methodology is briefly discussed, followed by a discussion on PIRTs. A preliminary PIRT is presented for the DRACS for gas-cooled reactors. A top-down and bottom-up scaling analysis is performed for the DRACS.

- Chapter 4: Design requirements

Design requirements are laid out and a specific design is suggested for the addition of a scaled DRACS module to the HTTF. An instrumentation plan is presented for the model designed for the HTTF.

- Chapter 5: RELAP5-3D analysis

The model built in RELAP5-3D is presented with nodalization and relevant information for both full-scale prototype and scaled model. Model building is described. A discussion of the results with specific attention to the relation to the scaling analysis is included.

- Chapter 6: Conclusions

Conclusions of the work undertaken, with relevant results, discussion, and summary of work performed. Future work is suggested.

- Chapter 7: References

A list of references used throughout this thesis is presented in the bibliography style maintained by the Institute of Electrical and Electronics Engineers (IEEE).

- Chapter 8: Appendices

Additional work completed which was not included in the thesis body is included in the appendices. Included are a python script, an engineering equation solver script, a detailed description of the RELAP5-3D models, two RELAP5-3D model decks, and SolidWorks drawings of parts which make up the conceptual scaled-down design to work with the HTTF.

2. Literature review

The Direct Reactor Auxiliary Cooling System is a general concept for a passive decay heat removal system, and has been around since 1980 or earlier, with the earliest mention found in a quarterly progress report, discussing seismic event failures [34]. Over the years, the DRACS has been included in a number of articles without any major temporal gaps between 1980 and the present. Although discussion of DRACS has been present in literature for over 35 years and has been included in a number of proposed designs, it has yet to be implemented in commercial applications. This may be due to a lack of construction of new nuclear plants for around 30 years in the United States [35].

2.1. DRACS inclusion in reactor designs

Although there is a wide variety of DRACS designs for varied reactor designs, the base DRACS was included in the EBR-II [12] [23] [36]. This base DRACS consisted of two redundant sodium-potassium (NaK)-to-air coolers which transported heat from the primary pool to outside air as passive back-up to the normal shutdown heat removal path [7]. A heat exchanger submerged in the primary pool absorbed heat generated in the core, and a second heat exchanger connected by piping to the first rejected heat to atmospheric air. Many advanced reactor designs include a DRACS as part of the safety systems to cool the core, and there are some variations from the base DRACS for different reactor designs.

The variations from this base DRACS design discussed above include heat exchanger type and placement, intermediate fluid type, and even the heat rejection system. While

most DRACS designs are entirely passive, some include active features to enhance cooling when available [1] [4]. Different heat exchanger designs have even been proposed, including tube and shell [12], twisted tube and shell [15], and multi-tube helical coil [4]. The specific location of the DHX varies with respect to the reactor core, but always has direct access to the coolant which cools the core. Intermediate fluid varies from sodium, NaK eutectic, lead, fluoride salts, water, and gas. While most designs employ convection to environmental air through the NDHX, some use evaporative cooling [9]. The ultimate similarity in all designs is that there are two heat exchangers connected by piping to transport heat from the core to the outside air.

Many SFRs contain a DRACS in their design for passive decay heat removal. Some examples are the Prototype Fast Reactor (PFR) Dounreay, European Fast Reactor (EFR), KALIMER-600, Prototype Fast Breeder Reactor (PFBR), Advanced Burner Test Reactor(ABTR), Japanese SFR (JSFR) [23], Demonstration Fast Breeder Reactor (DFBR) [37], 100 MWe Advanced SFR (AFR-100) [15], Sodium Advanced Fast Reactor (SAFR) [11], and TerraPower's TWR-Prototype (TWR-P) [1]. Westinghouse also included the DRACS as part of its approach to inherently safe liquid metal reactors [13].

The AHTR is an example of a liquid-salt-cooled very high-temperature reactor (LS-VHTR) which incorporates a DRACS for passive decay heat removal [9]. Different decay heat removal systems were explored for use in the AHTR before settling on the DRACS, including the Reactor Vessel Auxiliary Cooling System (RVACS) and the Pool Reactor Auxiliary Cooling System (PRACS) [8].

The Modular High-Temperature Gas-cooled Reactor (MHTGR) does not have the potential to release large quantities of radionuclides into the environment under any conceivable scenario [9]. This desirable characteristic results from the designed heat removal path, which relies on the conduction from the core through the core structural material to the reactor pressure vessel (RPV), which is in turn cooled by radiative heat transfer to the Reactor Cavity Cooling System (RCCS). The efficiency of radiative heat transfer is increased at a greater rate than other heat transfer mechanisms when the temperature difference between the heat source and sink is increased. The rate of heat transfer is then maximized such that the RPV never reaches its design limit before the rate of decay heat production is met. Although this heat removal path is effective as it is designed, it limits the maximum size of the reactor because the heat removal path effectiveness is related to surface area of the reactor vessel. The reactor cannot be scaled up in power in a cost effective manner, requiring a huge increase in the size of the RPV for an increase in power. It has been proposed that using DRACS for decay heat removal rather than a vessel cooling system could increase the maximum power output of these gas-cooled very high temperature reactors (VHTR) because the DRACS is a volume-based heat removal system rather than a surface area-based heat removal system [24]. The modularity of the DRACS allows removal of more heat by adding more DRACS modules, and the RPV does not have to be increased in size as with the RCCS.

The EM^2 is a GFR which includes DRACS in its design [3] [4] [28]. No other gas-cooled reactors have included a DRACS as part of their designs at this time.

The DRACS has been included in quite a few advanced reactor designs, and sodium-cooled reactors seem to have adopted the system more than any other coolant type. Benefits of using a DRACS in other systems have been pointed out, including the modularity.

2.2.General scaling methodologies

Scaling has been identified as an important part of the Severe Accident Research Program [38], and the United States Nuclear Regulatory Commission implemented the Severe Accident Scaling Methodology (SASM) development program for that reason. Scaling is important to both experimentation and analyses of special models or code calculations so they can be planned and interpreted appropriately [38]. The first general scaling methodology developed as part of the SASM was the H2TS methodology. Three general scaling methodologies are presented here, although this is not a complete list.

The H2TS methodology is published as appendix D of NUREG/CR-5809 [39]. H2TS works well for complex systems with interacting components and subsystems. The general approach is broken into four elements. The first of these four elements is system decomposition, in which the system as a whole is divided into subsystems, which are divided into modules, and so on, all the way down to processes. The second element is called scale identification, in which the scaling level is determined for each subsystem or process. The third element is the top-down scaling analysis, where the system level scaling occurs to determine how all of the processes affect the system. The fourth element is the bottom-up scaling analysis, where a more detailed scaling analysis is

performed for important processes which were not fully covered during the top-down scaling analysis. The H2TS methodology is well established and has been successfully applied, as is discussed in section 2.3. A more detailed discussion on H2TS is contained in section 3.1.

A scaling analysis investigates the effects of scaling a system down to a smaller physical size. When a system is reduced in physical size, the processes which affect the conserved properties, mass, momentum, and energy, are affected. For example, reduction in diameter throughout the system will reduce the heat transfer area for each heat exchanger, reducing the heat transfer rate. The scaling analysis is performed in order to compare the prototype to the scaled model so the differences can be accounted for. This is used so that scaled test facilities can be built to model accident scenarios safely, and the data collected can be used to validate computer models of the system. PIRTs are constructed by a panel of experts in order to rank phenomena by the need for more investigation. Those phenomena which have high importance and low knowledge level can be the focus of the scaling analysis such that they are preserved over those phenomena with low importance or high knowledge level.

The Fractional Scaling Analysis (FSA) was originally presented at the International Topical Meeting on Nuclear Reactor Thermal Hydraulics (NURETH) in 2005 by three companion papers [40] [41] [42]. The idea was discussed in some terms by Zuber in 2001, although not given the name of FSA as presented in that conference [43]. FSA appears as a way to eliminate the need for complex computer codes, it breaks down

complex systems into simpler scaling pieces. Two key parameters are defined as part of the FSA, namely Fractional Rates of Change (FRC) and Fractional Change Metric (FCM). The FRC quantifies the fraction of the total change on a given state variable each transfer process, or agent of change, contributes. This allows ranking of the importance of these agents of change on the state variable. The FCM represents the effect of scaling on the fractional change of the state variable. It is intended that the quantification through the FRC and FCM will eliminate the need for PIRTs, which are seen as subjective [44]. The presentation of the FSA included example applications, and it has since been applied to a pressurizer test facility [45].

The Dynamical System Scaling (DSS) methodology was developed recently and presented in 2015 at NURETH-16 [46]. The DSS quantifies time-dependent distortions of scaled processes through methods of differential geometry. Physical processes are described as geometric objects in a normalized coordinate system, and are scaled using methods from dynamical systems and differential geometry. Process similarity is viewed as an invariance of a process metric under a coordinate transformation. By similar methods, five distinct scaling approaches, including power-to-volume, are yielded through a two-parameter affine transformation of the normalized coordinates. This approach is still new and has not yet been applied, but allows for the assessment of time-dependent scaling effects as opposed to previous methods, which evaluate scaling at a steady-state.

2.3. Previous applications of the H2TS methodology

The scaling of the AP600 was the first comprehensive application of the H2TS methodology. The scaling analysis was performed cooperatively between Westinghouse Electric company and OSU. The scaling analysis was performed in order to ensure that the Advanced Plant Experiment (APEX) at OSU would be capable of obtaining the thermal hydraulic data key to the validation of the AP600 safety analysis codes. The APEX is an integral test facility which ran a series of tests for the collection of necessary data which led to the validation of the codes used for the thermal hydraulic safety analysis of the AP600 design [47], and the AP600 was licensed as a result. That scaling analysis made the application of data from a scaled test facility to the full-scale prototype design license possible.

After the successful scaling and application of the AP600 to the APEX test facility at OSU, further scaling analysis was performed for the AP1000, which is a larger scale reactor with many of the same passive design features of the AP600. This scaling analysis was performed using the H2TS methodology. The APEX facility was able to model the AP1000 after updates to the original facility created for the purpose of licensing the AP600. A series of tests were run successfully from June 2003 to July 2004 which contributed to the licensing of the AP1000 design, detailed in the report by Welter et. al [48].

The multi-application small light water reactor (MASLWR) facility is another reduced-scale test facility at OSU which was built as a result of a scaling analysis performed using

the H2TS methodology [49]. A concept reactor called the MASLWR was developed by OSU in cooperation with INL and NEXANT-Bechtel [50]. After the construction of the scaled MASLWR facility, a design based on the MASLWR concept was developed at a new company, NuScale Power. Currently NuScale is seeking design certification on their design of this small passive LWR.

The MHTGR has also been scaled using the H2TS methodology. The scaling analysis was performed for the design of the HTTF, which is currently the latest scaled-down integral test facility at OSU. The HTTF has not yet collected any test data, but the facility construction is almost complete and tests should begin around late 2016. The data collected will be applicable to the validation of safety analysis codes for the prototype MHTGR, and it has been determined by models built both in system codes (RELAP5-3D) and computational fluid dynamics (CFD) software (STAR-CCM+) that the HTTF experiments will give a reasonable representation of the behavior of the MHTGR [51].

2.4. DRACS scaling and test facilities

Test facilities are constructed in order to collect data to prove a concept before full prototypes are built. In the nuclear industry, experimental data is needed to validate computer codes for licensing by comparing results from the code to experimental data. A computer model can be used in the licensing of the prototypical design by running simulations on design basis accident scenarios only after the verification and validation process has been completed.

Test facilities which incorporate a DRACS have already been designed and built. One such test facility is the RVACS test facility, which in addition to testing an RVACS for advanced liquid metal reactors (ALMR), also ran experiments with a DRACS. Two experiments were run in 1990 in this test facility, which uses electrically heated rods to simulate the core, and liquid sodium as the coolant. The first of these experiments tested the heat removal capability of the DRACS alone, with a constant input power of 100 kW throughout the test. There was significant thermal stratification in the hot pool. The second test used both the DRACS and the RVACS to remove heat generated by the electrically heated core. These tests showed thermal stratification in the hot pool was greatly reduced, while the cold pool began to experience thermal stratification. These experiments were run for the validation of a computer code called COMMIX [14].

Another facility was the EBR-II which, although it was built in order to demonstrate a range of inherent safety features of pool-type sodium-cooled fast breeder reactors, included two modules that became the base DRACS. This base DRACS consisted of NaK to air shutdown coolers designed to be direct, safety related means of removing heat from the primary pool, where the core resides, to outside air [7]. Although not directly referred to as a DRACS in the listed reference, all of the basic elements are present which more recent DRACS designs include.

Two sets of tests were run with the EBR-II which demonstrated the cooling capability of the DRACS for the pool-type SFR. The first set of tests involved a SCRAM at full power with loss of the balance-of-plant, so that the two passive heat removal paths were the

only ones present. The second set of tests involved the passive heat removal paths from a shutdown condition instead of full power. The second set of tests were shown to be less severe, and the first set demonstrated that the passive heat removal systems were sufficient to bring the reactor to a safe condition. It was concluded that natural circulation can provide passive decay heat removal in a reliable, predictable manner, and that it may be used as the primary means of safety related decay heat removal in future LMR plants [7].

The Ohio State University, with Oak Ridge and Idaho National Labs have been working to develop test facilities for the DRACS to support the AHTR over the past several years for the DOE Nuclear Energy University Program (NEUP). First, the prototypical design for a modular DRACS for the AHTR was developed [52]. A scaling analysis was then performed for this prototypical design as the full-scale height and power could not be supported for a test facility in the available lab space [30]. Based on this scaling analysis, a scaled-down test facility in both physical dimension and source power was developed to provide experimental data for model validation. This LTDF uses water as the fluid for both the direct and intermediate loops [33]. The HTDF was also designed, which uses FLiNaK (molar percentages LiF-NaF-KF 46.5-11.5-42) as the coolant for both the direct and intermediate loops [31]. A scaling analysis was also performed for DRACS in FHRs [12].

2.5.Computer modeling of DRACS

Test facilities are generally scaled-down because a scaled facility is cheaper to build than a full-scale prototype, and the facility can be designed to safely put the system through accident scenarios. While scaled-down physical models are cheaper than building a full-scale prototype, computer models of an individual system are even cheaper to build than that. Computer models are also able to safely run the system through any transient, as no physical system has to be run through the transient.

Before a computer model can be used to license a new design, it has to undergo the verification and validation (V&V) process, where the purpose of V&V is to assess the accuracy of a computer model [53]. Validation is defined by the American Society of Mechanical Engineers (ASME) as “the process of determining the degree to which a model is an accurate representation of the real world from the perspective of the intended uses of the model.” Verification is broken into code and solution verification. Code verification deals with ensuring that the code accurately solves the mathematical models which the code is built on. Solution verification assesses the accuracy of a calculation. Typically, the code should undergo verification before the process of validation begins.

The process of using computer models to predict performance was discussed for DRACS for the 1000-MWe liquid metal fast breeder reactor (LMFBR) Development Plant. Two major development needs were listed, being the development of a DRACS flow control device, and the quantification of DRACS natural circulation performance. For this second

development need, a computational tool to predict natural-circulation phenomena should be implemented, and code validation should take place using phenomenological experiments and integral experiments. Computational tools suggested were SASSYS and COBRA. Integral test facilities available for this purpose were the fast flux test facility (FFTF) and the EBR-II. As testing the natural-circulation cooling phenomena of the DRACS was the main goal, a separate effects test facility was suggested for the validation of the computer model predictions [10].

A generic DRACS applied to liquid-metal fast breeder reactors was modeled as part of the Super System Code (SSC), where the momentum and energy conservation equations are coupled thermally and hydraulically. The tests run involved a normal scram with forced circulation, and a loss of electrical power with coast down to natural circulation. Both tests were run with and without the DRACS functional. The conclusion of these tests was that the DRACS lowers the core inlet temperature, increasing core flow rate, ultimately decreasing the peak core temperatures [54].

The experiments for the DRACS and DRACS-RVACS as previously discussed were also modeled in COMMIX. COMMIX is a computer code for general fluid and heat transfer analysis in a multicomponent system, with the ability to model in one, two, or three dimensions. In this case, a porous media formulation was used in order to reduce computation cost. The mass, momentum, and energy equations are solved using a first order finite differencing method, which is not very accurate, so improving the accuracy with a fine grid is important. Three-dimensional transient calculations with a fine grid

leads to excessive computation, however, so a coarse grid was selected. The conclusion of the authors was that after some adjustments to correct pressure drop, the code predictions were in “good agreement” with the experimental results, but they were limited by the computation power of the day to make many simplifying approximations [14].

A RELAP5-3D model was built for the pebble-bed AHTR (PB-AHTR), which includes 8 modular DRACS. A number of non-standard correlations were used in this model, but these deal with the pebble-bed core and fluidic diode, which are not part of the DRACS. Two transients were modeled, the first a loss of forced convection (LOFC), and the second an anticipated transient without scram (ATWS), which consisted of the LOFC without scram. Parametric studies were also performed for the PRACS heat exchanger (PHX), but not for any part of the DRACS. This modeling shows that the emergency core cooling provided by the PRACS/DRACS is effective at keeping coolant temperatures below critical levels, even though the ATWS results in temperatures up to 150°C higher than LOFC alone [55].

A GFR with a passive emergency cooling system (ECS) which resembles the DRACS was modeled in RELAP5-3D. In both this ECS and the DRACS, a heat exchanger absorbs heat from coolant directly from the core, which transfers that heat to a natural circulation loop. A second heat exchanger absorbs heat from the natural circulation loop and rejects it to atmospheric air. Natural circulation cooling presents challenges in gas-cooled reactors because of its relatively low heat transfer rate, being as low as 30% of

forced convection values. The concern is raised for loss of coolant accidents in this paper, as natural circulation was shown to be effective while system pressure is maintained [16]. This concern is relevant for gas-cooled reactors because heat transfer capability is affected more dramatically by changes to pressure in a gas than in a fluid.

In order to show the feasibility of using DRACS in VHTRs, a lumped parameter analysis was used as a first-order estimation for the transient response following a depressurized conduction cooldown event. 2-D steady state CFD calculations were also run to obtain spatial temperature distributions for 3 different placements of DHX in VHTRs [24]. All three placements of the DHX resulted in better cooling than an RVACS, with lower peak fuel temperature reached sooner. The DHX placed in the inner reflector had the best results of all.

3. Scaling analysis

3.1. The Hierarchal Two-Tiered Scaling methodology

The H2TS methodology has been applied to the design of several reduced-scale test facilities. A full outline of this scaling methodology is contained in Appendix D of NUREG/CR-5809 [39]. The basics of the H2TS have been presented in section 2.2. More detail is presented herein on the four basic elements of this scaling methodology, being system decomposition, scale identification, top-down scaling, and bottom-up scaling.

The system decomposition element forms a hierarchy by breaking up the system into interacting subsystems. The subsystems are further decomposed into modules, constituents, phases, geometrical configurations, fields, and finally into processes. Each field is described by a field equation (conservation of mass, momentum, energy). Each of these equations describes the applicable processes which affect the conserved quantity. This system hierarchy is illustrated in Figure D.3.1 of Appendix D of NUREG/CR-5809 [39]. Through the system decomposition, characteristic concentrations, geometries and processes are identified.

The scale identification element identifies the level at which scaling criteria should be developed. The identification of scale occurs by examining the processes which the scaling criteria are being developed for. If the process occurs between two constituents, such as between the coolant and the solid structure of the heat exchanger, then the similarity criteria for that process should be scaled at the constituent level. If, on the

other hand, the process occurs between a liquid and vapor phase within a constituent, then the similarity criteria should be developed at the phase level.

The top-down or system scaling analysis involves using the field equations identified during the system decomposition in order to derive scaling groups and characteristic time ratios. The PIRT helps to identify the important interaction of constituents which will have significant effects on the system. Processes to be addressed in the bottom-up scaling will be identified.

Finally, the bottom-up scaling analysis develops the similarity criteria for processes which the PIRT has identified as important. This addresses the gaps which were left by the top-down scaling analysis, and all scaling ratios should be determined. These scaling ratios dictate the relative scale between the prototype and the scaled model for each transfer process, conserved quantity, and physical dimension.

3.2. Phenomenon Identification and Ranking Tables

Phenomenon Identification and Ranking Tables are generally constructed by a panel of experts relating to the system or area for which the PIRT is being presented. The technical experts identify safety related phenomena and rank them according to importance, and then assess the current knowledge level of each phenomenon [56]. By doing so, it becomes clear that if there are phenomena ranked with high importance and low knowledge level, those phenomena require further study.

As mentioned in section 3.1, a PIRT is important in a scaling analysis. It identifies those processes and phenomena which are important to preserve through the scaling so that they may be appropriately captured by the scaled model. In the top-down portion of the scaling analysis, the PIRT is used to identify the interacting constituents and their effect on the system. In the bottom-up portion of the scaling analysis, the PIRT is used to identify those processes which are important to capture as part of the scaling.

3.2.1. DRACS preliminary PIRT for GFR

For the DRACS in gas-cooled reactors, a preliminary PIRT has been developed. Rather than using a panel of technical experts, Table 3-1 was outlined as part of this work for the purposes of the scaling analysis. A final PIRT would require a panel of technical experts to identify and rank a more complete list of phenomena in terms of importance and knowledge level. For Table 3-1, a review of relevant literature to the phenomena listed was conducted and the availability of information was used to determine the knowledge level. Below are listed the phenomena uncovered and some information on the sources found for each. Following the discussion is the preliminary PIRT captioned as Table 3-1.

The first phenomenon outlined here is heat leakage through the DRACS heat exchanger (DHX) during normal operations. The DHX is designed to absorb heat directly from the core during shutdown, but even under normal operations some percentage of the total heat generated by the core will be transferred through the DHX. Heat losses are inevitable because the fluid in the intermediate loop will be cooler than the coolant in

the primary system, especially near the core where the DHX resides. Designs often include measures to lessen this effect, such as electromagnetic louvers in the cooling tower [8] [10] [11] or a fluidic diode to limit flow during normal operations to the DHX [8] [12] [23] [36] [52]. This phenomenon does not affect the operation of the DRACS as the purpose of the DRACS is not to operate during normal operations, but it does affect the operation of the reactor itself. Any heat removed by the DRACS during normal operations is heat that cannot be used as process heat, and the overall reactor efficiency is decreased. Heat leakage rate estimations were provided for the thermal radiation based DRACS for VHTRs as a result of modeling [24]. Heat leakage and methods to reduce it are discussed in other papers, but these all focus on molten salt or sodium-cooled reactors [1] [10] [33].

The second phenomenon is natural circulation. This is essential to the operation of the DRACS as its purpose is to operate inherently under shutdown conditions, including total station blackouts. The EM^2 design involves forced circulation if power is available, but it also functions under natural circulation. Most designs for the DRACS run entirely on natural circulation. Therefore, the density difference in the fluids due to variation in temperature leading to gravity driven circulation is an essential component of the DRACS. This effect will be greatest in an accident scenario when the core temperature rises. There have been many studies on natural circulation over the years. Experiments and analytical analysis were completed for both sodium and water with the conclusion that natural circulation is sufficient for decay heat removal [17]. In another experiment,

the heat transfer coefficient was measured from a tube bundle under natural circulation conditions [19]. A simple natural circulation loop was constructed and the data was compared to a one-dimensional analytical model with less than 7% deviation at steady state [20]. More recent analysis has determined that natural circulation has a reduced heat transfer rate as low as 30% of forced convection values and discussed that data and correlations have potentially large uncertainties [16].

The third phenomenon is heat exchanger effectiveness, which is a measure of how much heat is transferred through a heat exchanger vs. the theoretical maximum value. It is a method for classifying heat exchangers and will be important for both heat exchangers present in the DRACS, the DHX and the NDHX. The rate at which the DRACS can transfer heat from the reactor core to the ambient air is what is important, and based on the heat exchanger effectiveness, one or both of these heat exchangers may be the limiting factor. Heat exchanger effectiveness is a well-known concept, and there are a few different measures [57].

The fourth phenomenon is heat transport rate. As mentioned above, this is the measure of how well the DRACS is fulfilling its intended purpose. It is the rate at which the decay heat is removed from the core and rejected to the ambient air. The specific rate will change depending on transient conditions, and will be limited by the component or constituent which most slowly transports the heat. For the AFR-100, 3 DRACS modules have been proposed, each capable of removing 0.25% of total operating power, and only two modules are required to remove decay heat [15]. A modular DRACS capable of

removing 200 kW has been proposed [36]. For the thermal radiation based DRACS for VHTRs, a heat removal rate equation is provided and charts based on the computer modelling show heat removal matches the decay heat production between 11 and 45 hours depending on the accident scenario with a value of about 0.4-0.5% of total operating power [24].

The fifth phenomenon is dry heat rejection through the NDDCT. There are two classifications to break down cooling towers in general: natural vs. forced draft and dry vs. wet or evaporative cooling. Evaporative cooling is common for many NPPs, but dry cooling towers are attractive for parts of the world without large amounts of water readily accessible which allows for more siting flexibility. Dry cooling towers will have reduced efficiency compared to wet cooling towers, and natural draft will also have reduced efficiency compared to forced draft. The result is a cooling tower which is much less affected by a variety of scenarios because there's no worry of loss of power or dry out. A small scale experiment was conducted and CFD modeling results were compared to scaled data from a full-scale prototype in order to investigate scaling effects on dry heat rejection [27].

The sixth phenomenon addressed is wind effects on cooling tower performance. Wind effects have been demonstrated to have a significant effect on dry cooling tower performance, especially in small NDDCTs. Many experiments using wind tunnels and CFD models have been made to test this effect. Wind tunnel experiments showed that crosswind of velocities greater than 4 meters per second significantly affect cooling

tower performance [25]. A CFD study on windbreak walls shows thermal effectiveness reduced by more than 30% for crosswind velocities greater than 10 meters per second, and concluded that the effect is great enough that designs should consider proper crosswind velocity profiles over no crosswind conditions [58]. Experimental and numerical results show windbreak walls can recover up to 50% of losses due to crosswind in a large NDDCT [26]. CFD studies show that windbreak walls significantly improve thermal performance of NDDCTs during crosswind, that porous windbreak walls are as effective as solid walls. The CFD study also found that for high wind speeds, interior windbreak walls are most effective and exterior walls are most effective for low wind speeds [59]. CFD modeling of vertically oriented heat exchangers shows that the efficiency of NDDCTs is heavily influenced by wind speed and direction [60]. CFD modeling of a 15-meter tall NDDCT showed a 37% reduction in heat rejection rate with a crosswind of 5 meters per second [61]. Another CFD study showed that three specifically placed interior windbreak walls could improve the thermal efficiency with crosswind over no crosswind at all [62].

The seventh phenomenon outlined is an intermediate fluid ingress, in the case there is a rupture in the DHX. The outcome of this phenomenon is very dependent on the specific reactor design and intermediate fluid. For molten salt reactors, the intermediate fluid often matches the primary coolant. Fluoride salts and lead are both suggested for VHTRs in the thermal radiation based DRACS [24]. The specific outcome of an intermediate fluid ingress is again dependent on the intermediate fluid, so for gas-cooled reactors,

this phenomenon would have to be evaluated on a case-by-case basis. Intermediate fluid ingress can be mitigated by ensuring that the primary system pressure is higher than the intermediate loop pressure.

The intermediate fluid in the EM^2 DRACS is water, so a steam-water ingress event is the concern. There is a helium purification system included in the EM^2 to keep primary-coolant helium free of oxidants and radioactivity [4], which will likely be effective for small breaks. Steam-water ingress is concerning for gas reactors which use graphite as a moderator and core structural material, as graphite will readily oxidize in the presence of oxygen and heat. Steam can be broken down into the components of hydrogen and oxygen gas through the process of thermal decomposition. Steam-water ingress is a beyond design basis accident for another helium-cooled reactor, the HTR-PM, and some study has been done on the event for that reason [63]. The probability of a water-ingress event is reduced in the HTR-10 by the arrangement of the steam generator vessel in a side by side arrangement such that there is not a large elevation difference to drive water to the core [64]. The scaling for steam-water ingress is already in progress at OSU, and is not included as part of this work.

The final phenomenon is the interaction of two decay heat removal systems when a RCCS is present. This is a phenomenon which could be easily investigated with a DRACS module added to the HTTF because the RCCS is already present. No reactor designs have been found which include both systems to remove heat, however, so this study would be of little importance. Many gas reactor designs include an RCCS, but do not include a

DRACS. The AHTR design includes both a DRACS and a RVACS, but the RVACS differs from the RCCS [65].

Table 3-1: Preliminary PIRT for the DRACS in gas-cooled reactors

System or Component	Phenomenon	Importance	Knowledge Level and References	Rationale
DHX	Heat Leakage (Normal Operations) {Some portion of the heat generated in the reactor core is diverted through DRACS}	H	L [1] [10] [24] [33]	• FOM: $\dot{q}_{loss}$ Any percentage of heat leaked through DRACS during normal operations is heat that can't be used to generate electricity or be used as process heat, reducing reactor efficiency
Each loop in DRACS	Natural Circulation (LOFC) {The DRACS is an inherent system dependent on natural circulation}	H	H [16] [17] [19] [20]	• FOM: $\dot{m}_{loop}$ As an inherent safety system, there is no other driving force for circulation in the DRACS besides density gradients due to Temperature variation leading to gravity driven circulation
DHX and NDHX	Heat Exchanger Effectiveness (LOFC) {Under conditions of natural circulation}	H	H [57]	• FOM: $\varepsilon_{DHX}, \varepsilon_{NDHX}$ There are two heat exchangers between the core and the dry heat rejection, DHX and NDHX, which may be the limiting factor for heat rejection

Table 3-1: Preliminary PIRT for the DRACS in gas-cooled reactors (continued)

System or Component	Phenomenon	Importance	Knowledge Level and References	Rationale
DRACS	Heat Transport Rate (LOFC) {How much decay power can a single DRACS module transport away from the core}	H	M [15] [24] [36]	• FOM: $\dot{q}_{DRACS}$ The reason for inclusion of DRACS is decay heat rejection during accidents, so the rate at which the DRACS can reject decay heat is central to its importance
Cooling Tower	Dry Heat Rejection (LOFC) {Heat is rejected through the DRACS ultimately to atmosphere using air}	H	M [27]	• FOM: $\dot{q}_{tower}, \varepsilon_{tower}$ For a DRACS system, using a NDDCT to reject heat is less efficient than an evaporative cooling tower, but yields siting flexibility due to no need for water supply to reject heat to atmosphere
Cooling Tower	Wind Effects (LOFC) {Cooling tower performance related to weather conditions – what is the contribution}	M	H [25] [26] [58] [59] [60] [61] [62]	• FOM: ε_{wind} Wind effects have been demonstrated to have a significant effect on dry cooling tower performance, which is what is used in the prototypical DRACS
DHX	Intermediate Fluid Ingress (DHX break) {A break in the DHX could lead to intermediate fluid in the core}	M	M [63] [64]	• FOM: $\dot{m}_{ingress}$ Core structural material made of graphite will oxidize if there is sufficient thermal decomposition of intermediate water leaked into the primary system
DRACS	Interaction with RCCS (LOFC) {Percent of heat rejected by each}	L	N/A	• FOM: $\dot{q}_{DRACS}, \dot{q}_{RCCS}$ May not be applicable (EM^2 doesn't have an RCCS, most gas reactors don't include DRACS)

3.3.Top-down scaling analysis of the DRACS

3.3.1. General governing equations

This section outlines the general equations which govern the processes in every loop. The equations are applied to each loop in the subsequent sections by eliminating terms which are not applicable to the processes in the given loop. The following loop-integrated momentum equation is found in reference [66, p. 465] as a modified form of the Bernoulli equation.

$$\sum_{i=1}^{N}\left(\frac{l_i}{A_i}\right)\frac{d\dot{m}}{dt} + P_{out} - P_{in} + (\rho_{out} - \rho_{in})gL_{loop} + \tag{3.1}$$

$$+\frac{\dot{m}^2}{2}\left(\frac{1}{\rho_{out}A_{out}^2} - \frac{1}{\rho_{in}A_{in}^2}\right) + \Delta \mathrm{P}_{\mathrm{loss}} = 0$$

Where $l, A, \dot{m}, t, P, \rho, g, L_{loop}$ represent length, cross-sectional area, mass flow rate, time, pressure, density, acceleration due to gravity, and the total axial length of the given loop respectively. The subscript i represents a given section of the loop, and N is the total number of sections. The pressure loss term can be expressed in terms of the friction and form losses, combined here shown as equation (3.2).

$$\Delta P_{loss} = \frac{\dot{m}^2}{2}\sum_{i=1}^{N}\left[\left(K_i + \frac{f_i l_i}{D_{e,i}}\right)\left(\frac{1}{\rho_i A_i^2}\right)\right] \tag{3.2}$$

Where K, f, D_e are the form loss coefficient, the Darcy friction factor, and equivalent or hydraulic diameter respectively. The change rate of energy stored in the coolant is

balanced with energy added to the coolant as it flows, expressed in the conservation of energy equation.

$$\rho c_p \frac{\partial T}{\partial t} + \rho c_p w \frac{\partial T}{\partial z} = k \frac{\partial^2 T}{\partial z^2} + q''' \tag{3.3}$$

Where c_p, T, w, z, k, q''' are the constant pressure specific heat, temperature, velocity in the axial direction, axial dimension, conduction heat transfer coefficient, and heat source rate per unit volume respectively. It is assumed that no significant energy transfer occurs in the loop through conduction, and only heat transferred through heat exchangers will have a significant effect on this energy balance. Local temperatures are not the primary concern, so a one-dimensional loop integral is performed across the axial dimension.

$$A \oint \rho c_p \frac{\partial T}{\partial t} dz + A \oint \rho c_p w \frac{\partial T}{\partial z} dz = A \oint q''' dz \tag{3.4}$$

The result of this loop integral is the loop integrated energy equation shown in equation (3.5).

$$\rho c_p A L_{loop} \frac{\partial T}{\partial t} + \dot{m}\left(c_{p,out} T_{out} - c_{p,in} T_{in}\right) = \sum_{j=1}^{J} \dot{q}_j \tag{3.5}$$

Where $\dot{q}$ is the heat sink/source rate. The subscript j represents each heat source/sink, and J represents the total number of heat sources/sinks in each loop. By the assumption of well-insulated pipes, the only heat sources and sinks are heat exchangers, the DHX

and NDHX. The differentiation between sources and sinks is taken care of in the energy equation by means of a positive defining a source and a negative defining a sink.

3.3.2. Direct loop scaling

3.3.2.1. Direct loop momentum equation

Throughout this section, the subscript D will be used to specify that the given property is for the fluid in the direct loop. As an example of this, L_D is the elevation difference between the heat source and sink in the system, being the core and DHX respectively.

The direct loop is a closed loop, made up by the natural circulation flow path between the core and the DHX. Thus the pressure difference term and pressure drop due to acceleration in equation (3.1) will cancel out. After substituting equation (3.2) into (3.1) and removing that term, equation (3.6) is the direct loop momentum equation.

$$\sum_{i=1}^{N}\left(\frac{l_i}{A_i}\right)_D \frac{d\dot{m}_D}{dt} + (\rho_{D,h} - \rho_{D,c})gL_D + \frac{\dot{m}_D^2}{2}\sum_{i=1}^{N}\left[\left(K_i + \frac{f_i L_i}{D_{e,i}}\right)\left(\frac{1}{\rho_i A_i^2}\right)\right]_D = 0 \qquad (3.6)$$

These equations can be made non-dimensional by normalizing each term as shown in equations (3.7)-(3.10) using direct loop inlet conditions at steady-state.

$$\dot{m}^+ = \frac{\dot{m}}{\dot{m}_{D,0}} = \frac{\dot{m}}{\rho_{D,h,0} A_{D,1} w_{D,1,0}} \qquad (3.7)$$

$$(\rho_h - \rho_c)^+ = \frac{\rho_h - \rho_c}{(\rho_{D,c,0} - \rho_{D,h,0})} \qquad (3.8)$$

$$\rho^+ = \frac{\rho}{\rho_{D,h,0}} \qquad (3.9)$$

$$\sum_{i=1}^{N}\left[\left(K_i+\frac{f_iL_i}{D_{e,i}}\right)\left(\frac{1}{\rho_iA_i^2}\right)\right]^+=\frac{\sum_{i=1}^{N}\left[\left(K_i+\frac{f_iL_i}{D_{e,i}}\right)\left(\frac{1}{\rho_iA_i^2}\right)\right]}{\sum_{i=1}^{N}\left[\left(K_i+\frac{f_iL_i}{D_{e,i}}\right)\left(\frac{1}{\rho_iA_i^2}\right)\right]_{D,0}} \tag{3.10}$$

A common time scale is used for all of these equations, which is established by the direct loop residence time, τ, which is related to the following.

$$t^+=\frac{t}{\tau}=t\frac{w_{D,1,0}}{L_D} \tag{3.11}$$

Substituting equations (3.7)-(3.11) into equation (3.6) yields equation (3.12) after some algebra.

$$\frac{A_{D,1}}{L_D}\sum_{i=1}^{N}\left(\frac{l_i}{A_i}\right)_D\frac{d\dot{m}_D^+}{dt^+}+\frac{\left(\rho_{D,c,0}-\rho_{D,h,0}\right)gL_D}{\rho_{D,h,0}w_{D,1,0}^2}\left(\rho_{D,h}-\rho_{D,c}\right)^+ + \tag{3.12}$$

$$+\sum_{i=1}^{N}\left[\left(K_i+\frac{f_iL_i}{D_{e,i}}\right)\left(\frac{\rho_{D,h,0}A_{D,1}^2}{\rho_iA_i^2}\right)\right]_{D,0}\frac{(\dot{m_D^+})^2}{2}\sum_{i=1}^{N}\left[\left(K_i+\frac{f_iL_i}{D_{e,i}}\right)\left(\frac{1}{\rho_iA_i^2}\right)\right]_D^+=0$$

The non-dimensional primary loop integrated momentum equation is shown in equation (3.13).

$$\Pi_{G,D}\frac{d\dot{m}_D^+}{dt^+}+\Pi_{Ri,D}\left(\rho_{D,h}-\rho_{D,c}\right)^+ + \tag{3.13}$$

$$+\Pi_{F,D}\frac{(\dot{m_D^+})^2}{2}\sum_{i}^{N}\left[\left(K_i+\frac{f_iL_i}{D_{e,i}}\right)\left(\frac{1}{\rho_iA_i^2}\right)\right]_D^+=0$$

The characteristic ratios are then established for the direct loop non-dimensional momentum equation, shown in equations (3.14)-(3.16).

Direct loop reference geometry number:

$$\Pi_{G,D} = \frac{A_{D,in}}{L_D} \sum_{i}^{N} \left(\frac{l_i}{A_i}\right)_D \tag{3.14}$$

Direct loop Richardson number:

$$\Pi_{Ri,D} = \frac{(\rho_{D,c,0} - \rho_{D,h,0}) g L_D}{\rho_{D,h,0} w_{D,1,0}^2} \tag{3.15}$$

Direct loop resistance number:

$$\Pi_{F,D} = \sum_{i}^{N} \left[\left(K_i + \frac{f_i L_i}{D_{e,i}} \right) \left(\frac{\rho_{D,h,0} A_{D,1}^2}{\rho_i A_i^2} \right) \right]_{D,0} \tag{3.16}$$

3.3.2.2. Direct loop energy equation

With the characteristic ratios identified for the direct loop momentum equation, the energy equation becomes the next focus. The direct loop is a closed loop, where heat is absorbed from the core and deposited in the DRACS Heat Exchanger (DHX). This is described by the loop integrated energy equation for the direct loop presented as equation (3.17).

$$\rho_{D,h} c_{p,D,h} A_{D,1} L_D \frac{\partial T_{D,h}}{\partial t} = \dot{q}_{D,core} - \dot{q}_{D,DHX} \tag{3.17}$$

The energy equation requires additional dimensionless quantities, shown below.

$$c_p^+ = \frac{c_p}{c_{p,D,h,0}} \tag{3.18}$$

$$T^+ = \frac{T}{\left(T_{D,h,0} - T_{D,c,0}\right)} \tag{3.19}$$

$$\dot{q}^+_{DHX} = \frac{\dot{q}_{DHX}}{\dot{q}_{D,DHX,0}} \tag{3.20}$$

$$\dot{q}^+_{core} = \frac{\dot{q}_{core}}{\dot{q}_{D,core,0}} \tag{3.21}$$

The direct loop integrated energy equation becomes dimensionless by inserting equations (3.7), (3.9), (3.11), and (3.18)-(3.21) into equation (3.17). Dividing through by a common term yields equation (3.22), the non-dimensional direct loop integrated energy equation.

$$\rho^+_{D,h} c^+_{p,D,h} \frac{\partial T^+_{D,h}}{\partial t^+} = \Pi_{core,D} q^+_{D,core} - \Pi_{DHX,D} q^+_{D,DHX} \tag{3.22}$$

Two characteristic ratios are established in equation (3.22), defined below.

Direct loop core heat transfer number:

$$\Pi_{core,D} = \frac{\dot{q}_{D,core,0}}{\rho_{D,h,0} A_{D,1} w_{D,1,0} c_{p,D,h,0} \left(T_{D,h,0} - T_{D,c,0}\right)} \tag{3.23}$$

Direct loop DHX number:

$$\Pi_{DHX,D} = \frac{\dot{q}_{D,DHX,0}}{\rho_{D,h,0} A_{D,1} w_{D,1,0} c_{p,D,h,0} \left(T_{D,h,0} - T_{D,c,0}\right)} \tag{3.24}$$

3.3.3. Intermediate loop scaling

3.3.3.1. Intermediate loop momentum equation

For the intermediate loop, the pressure and area will be the same at the first and last sections because it is a closed loop. The terms associated with the differences in pressure and area will cancel out leaving the intermediate loop momentum equation.

$$\sum_{i=1}^{N}\left(\frac{l_i}{A_i}\right)_I \frac{d\dot{m}_I}{dt} + (\rho_{I,c} - \rho_{I,h})gL_I + \frac{\dot{m}_I^2}{2}\sum_{i=1}^{N}\left[\left(K_i + \frac{f_i L_i}{D_{e,i}}\right)\left(\frac{1}{\rho_i A_i^2}\right)\right]_I = 0 \tag{3.25}$$

The normalized quantities used to make equation (3.25) non-dimensional are shown below as equations (3.26)-(3.29).

$$\dot{m}^+ = \frac{\dot{m}}{\dot{m}_{I,0}} = \frac{\dot{m}}{\rho_{I,h,0} A_{I,1} w_{I,1,0}} \tag{3.26}$$

$$(\rho_c - \rho_h)^+ = \frac{\rho_c - \rho_h}{(\rho_{I,c,0} - \rho_{I,h,0})} \tag{3.27}$$

$$\rho^+ = \frac{\rho}{\rho_{I,h,0}} \tag{3.28}$$

$$\sum_{i=1}^{N}\left[\left(K_i + \frac{f_i L_i}{D_{e,i}}\right)\left(\frac{1}{\rho_i A_i^2}\right)\right]^+ = \frac{\sum_{i=1}^{N}\left[\left(K_i + \frac{f_i L_i}{D_{e,i}}\right)\left(\frac{1}{\rho_i A_i^2}\right)\right]}{\sum_{i=1}^{N}\left[\left(K_i + \frac{f_i L_i}{D_{e,i}}\right)\left(\frac{1}{\rho_i A_i^2}\right)\right]_{I,0}} \tag{3.29}$$

Equations (3.11), (3.26)-(3.29) are substituted into equation (3.25) where appropriate. The equation is subsequently divided through by a common term to yield equation (3.30), the non-dimensional intermediate loop momentum equation.

$$\frac{A_{I,1}}{L_D}\sum_{i=1}^{N}\left(\frac{l_i}{A_i}\right)_I\frac{d\dot{m}_I^+}{dt^+}+\frac{(\rho_{I,c,0}-\rho_{I,h,0})gL_I}{\rho_{I,h,0}w_{I,1,0}w_{D,in,0}}(\rho_{I,c}-\rho_{I,h})^+ + \tag{3.30}$$

$$+\left(\frac{w_{I,1,0}}{w_{D,in,0}}\right)\sum_{i=1}^{N}\left[\left(K_i+\frac{f_iL_i}{D_{e,i}}\right)\left(\frac{\rho_{I,h,0}A_{I,1}^2}{\rho_iA_i^2}\right)\right]_{I,0}\frac{(\dot{m}_I^+)^2}{2}\sum_{i=1}^{N}\left[\left(K_i+\frac{f_iL_i}{D_{e,i}}\right)\left(\frac{1}{\rho_iA_i^2}\right)\right]_I^+=0$$

Characteristic ratios are identified and replaced by their designators in equation (3.31).

The definitions of these characteristic ratios are shown in equations (3.32)-(3.35).

$$\Pi_{G,I}\frac{d\dot{m}_I^+}{dt^+}+\Pi_{Ri,I}(\rho_{I,c}-\rho_{I,h})^+ + \tag{3.31}$$

$$+\Pi_{w,I}\Pi_{F,I}\frac{(\dot{m}_I^+)^2}{2}\sum_{i=1}^{N}\left[\left(K_i+\frac{f_iL_i}{D_{e,i}}\right)\left(\frac{1}{\rho_iA_i^2}\right)\right]_I^+=0$$

Intermediate loop reference geometry number:

$$\Pi_{G,I}=\frac{A_{I,1}}{L_D}\sum_{i=1}^{N}\left(\frac{l_i}{A_i}\right)_I \tag{3.32}$$

Intermediate loop Richardson number:

$$\Pi_{Ri,I}=\frac{(\rho_{I,c,0}-\rho_{I,h,0})gL_I}{\rho_{I,h,0}w_{I,1,0}w_{D,in,0}} \tag{3.33}$$

Intermediate loop velocity ratio:

$$\Pi_{w,I}=\frac{w_{I,1,0}}{w_{D,in,0}} \tag{3.34}$$

Intermediate loop resistance number:

$$\Pi_{F,I} = \sum_{i=1}^{N} \left[\left(K_i + \frac{f_i L_i}{D_{e,i}} \right) \left(\frac{\rho_{I,h,0} A_{I,1}^2}{\rho_i A_i^2} \right) \right]_{I,0} \tag{3.35}$$

3.3.3.2. Intermediate loop energy equation

The intermediate loop is closed and heat is absorbed in the DHX and rejected through the NDHX. The intermediate loop integrated energy equation, with the appropriate assumptions applied is shown in equation (3.36).

$$\rho_{I,h} c_{p,I,h} A_{I,1} L_I \frac{\partial T_{I,h}}{\partial t} = \dot{q}_{I,DHX} - \dot{q}_{I,NDHX} \tag{3.36}$$

Equations (3.37)-(3.40) establish the additional non-dimensional quantities required for the intermediate loop energy equation to be made dimensionless.

$$c_p^+ = \frac{c_p}{c_{p,I,h,0}} \tag{3.37}$$

$$T^+ = \frac{T}{\left(T_{I,h,0} - T_{I,c,0}\right)} \tag{3.38}$$

$$\dot{q}_{DHX}^+ = \frac{\dot{q}_{DHX}}{\dot{q}_{I,DHX,0}} \tag{3.39}$$

$$\dot{q}_{NDHX}^+ = \frac{\dot{q}_{NDHX}}{\dot{q}_{I,NDHX,0}} \tag{3.40}$$

Equations (3.11), (3.37)-(3.40) are used with equation (3.36), and after some rearrangement, the result is equation (3.41), the non-dimensional intermediate loop integrated energy equation.

$$\frac{L_I}{L_D}\rho_{I,h}^{+}c_{p,I,h}^{+}\frac{\partial T_{I,h}^{+}}{\partial t^{+}} = \frac{\dot{q}_{I,DHX,0}}{\rho_{I,h,0}c_{p,I,h,0}\left(T_{I,h,0}-T_{I,c,0}\right)w_{D,in,0}A_{I,1}}\dot{q}_{I,DHX}^{+} - \\ -\frac{\dot{q}_{I,NDHX,0}}{\rho_{I,h,0}c_{p,I,h,0}\left(T_{I,h,0}-T_{I,c,0}\right)w_{D,in,0}A_{I,1}}\dot{q}_{I,NDHX}^{+} \tag{3.41}$$

Three characteristic ratios are identified from equation (3.41) and replaced by their designators to yield equation (3.42). These three characteristic ratios are defined in equations (3.43)-(3.45).

$$\Pi_{L,I}m^{+}c_p^{+}\frac{\partial T^{+}}{\partial t^{+}} = \Pi_{DHX,I}q_{I,DHX}^{+} - \Pi_{NDHX,I}q_{I,NDHX}^{+} \tag{3.42}$$

Intermediate loop length geometry number:

$$\Pi_{L,I} = \frac{L_I}{L_D} \tag{3.43}$$

Intermediate loop DHX number:

$$\Pi_{DHX,I} = \frac{\dot{q}_{I,DHX,0}}{\rho_{I,h,0}c_{p,I,h,0}\left(T_{I,h,0}-T_{I,c,0}\right)w_{D,in,0}A_{I,1}} \tag{3.44}$$

Intermediate loop NDHX number:

$$\Pi_{NDHX,I} = \frac{\dot{q}_{I,NDHX,0}}{\rho_{I,h,0}c_{p,I,h,0}\left(T_{I,h,0}-T_{I,c,0}\right)w_{D,in,0}A_{I,1}} \tag{3.45}$$

3.3.4. Natural draft loop scaling

3.3.4.1. Natural draft loop momentum equation

The natural draft loop is open, so the term which describes pressure loss due to acceleration remains in the momentum equation. Because a common time scale is shared between all of the loops, additional characteristic ratios appear like in the intermediate loop, being the length and velocity ratios. The subscripts Nd throughout this section specify the natural draft loop.

$$\sum_{i=1}^{N}\left(\frac{l_i}{A_i}\right)_{Nd}\frac{d\dot{m}_{Nd}}{dt}+\left(\rho_{Nd,out}-\rho_{Nd,in}\right)gL_{Nd}+ \tag{3.46}$$

$$+\frac{\dot{m}_{Nd}^2}{2}\left(\frac{1}{\rho_{Nd,out}A_{Nd,out}^2}-\frac{1}{\rho_{Nd,in}A_{Nd,in}^2}\right)+\frac{\dot{m}_{Nd}^2}{2}\sum_{i=1}^{N}\left[\left(K_i+\frac{f_iL_i}{D_{e,i}}\right)\left(\frac{1}{\rho_iA_i^2}\right)\right]_{Nd}=0$$

The normalized quantities used to make equation (3.44) non-dimensional are shown below as equations (3.47)-(3.50).

$$\dot{m}^+=\frac{\dot{m}}{\dot{m}_{Nd,0}}=\frac{\dot{m}}{\rho_{Nd,out,0}A_{Nd,out}w_{Nd,out,0}} \tag{3.47}$$

$$\left(\rho_{out}-\rho_{in}\right)^+=\frac{\rho_{out}-\rho_{in}}{\left(\rho_{Nd,in,0}-\rho_{Nd,out,0}\right)} \tag{3.48}$$

$$\rho^+=\frac{\rho}{\rho_{Nd,out,0}} \tag{3.49}$$

$$\sum_{i=1}^{N}\left[\left(K_i+\frac{f_iL_i}{D_{e,i}}\right)\left(\frac{1}{\rho_iA_i^2}\right)\right]^+=\frac{\sum_{i=1}^{N}\left[\left(K_i+\frac{f_iL_i}{D_{e,i}}\right)\left(\frac{1}{\rho_iA_i^2}\right)\right]}{\sum_{i=1}^{N}\left[\left(K_i+\frac{f_iL_i}{D_{e,i}}\right)\left(\frac{1}{\rho_iA_i^2}\right)\right]_{Nd,0}} \tag{3.50}$$

Equations (3.11), (3.47)-(3.50) are substituted into equation (3.46) where appropriate. The equation is subsequently divided through by a common term to yield equation (3.51), the non-dimensional intermediate loop momentum equation.

$$\frac{A_{Nd,out}}{L_D}\sum_{i}^{N}\left(\frac{l_i}{A_i}\right)_{Nd}\frac{d\dot{m}^{+}_{Nd}}{dt^{+}}+\frac{\left(\rho_{Nd,in,0}-\rho_{Nd,out,0}\right)gL_{Nd}}{\rho_{Nd,out,0}w_{Nd,out,0}w_{D,in,0}}\left(\rho_{Nd,out}-\rho_{Nd,in}\right)^{+}+ \quad (3.51)$$

$$+\left(\frac{A^2_{Nd,in}}{\rho^{+}_{Nd,out}A^2_{Nd,out}}-\frac{1}{\rho^{+}_{Nd,in}}\right)\frac{(\dot{m}^{+}_{Nd})^2}{2}$$

$$+\frac{w_{Nd,out,0}}{w_{D,in,0}}\sum_{i=1}^{N}\left[\left(K_i+\frac{f_iL_i}{D_{e,i}}\right)\left(\frac{\rho_{Nd,out,0}A^2_{Nd,out}}{\rho_iA_i^2}\right)\right]_{Nd,0}$$

$$\times\frac{(\dot{m}^{+}_{Nd})^2}{2}\sum_{i}^{N}\left[\left(K_i+\frac{f_iL_i}{D_{e,i}}\right)\left(\frac{1}{\rho_iA_i^2}\right)\right]^{+}_{Nd}=0$$

Characteristic ratios are identified and replaced by their designators in equation (3.52). The definitions of these characteristic ratios are shown in equations (3.53)-(3.57).

$$\Pi_{G,Nd}\frac{d\dot{m}^{+}_{Nd}}{dt^{+}}+\Pi_{Ri,Nd}\left(\rho_{Nd,out}-\rho_{Nd,in}\right)^{+}+\left(\frac{\Pi_{A,Nd}}{\rho^{+}_{Nd,out}}-\frac{1}{\rho^{+}_{Nd,in}}\right)\frac{(\dot{m}^{+}_{Nd})^2}{2}+ \quad (3.52)$$

$$+\Pi_{w,Nd}\Pi_{F,Nd}\frac{(\dot{m}^{+}_{Nd})^2}{2}\sum_{i}^{N}\left[\left(K_i+\frac{f_iL_i}{D_{e,i}}\right)\left(\frac{1}{\rho_iA_i^2}\right)\right]^{+}_{Nd}=0$$

Natural draft loop reference geometry number:

$$\Pi_{G,Nd}=\frac{A_{Nd,out}}{L_D}\sum_{i}^{N}\left(\frac{l_i}{A_i}\right)_{Nd} \quad (3.53)$$

Natural draft loop Richardson number:

$$\Pi_{Ri,Nd} = \frac{\left(\rho_{Nd,in,0} - \rho_{Nd,out,0}\right) g L_{Nd}}{\rho_{Nd,out,0} w_{Nd,out,0} w_{D,in,0}} \tag{3.54}$$

Natural draft loop area ratio:

$$\Pi_{A,Nd} = \frac{A_{Nd,in}^2}{A_{Nd,out}^2} \tag{3.55}$$

Natural draft loop velocity ratio:

$$\Pi_{w,Nd} = \frac{w_{Nd,out,0}}{w_{D,in,0}} \tag{3.56}$$

Natural draft loop resistance number:

$$\Pi_{F,Nd} = \sum_{i=1}^{N} \left[\left(K_i + \frac{f_i L_i}{D_{e,i}} \right) \left(\frac{\rho_{Nd,out,0} A_{Nd,out}^2}{\rho_i A_i^2} \right) \right]_{Nd,0} \tag{3.57}$$

3.3.4.2. Natural draft loop energy equation

The natural draft loop is open and heat is absorbed in the NDHX. The loop integrated energy equation, with the appropriate assumptions applied is shown in equation (3.58).

$$\rho_{Nd,out} c_{p,Nd,out} A_{Nd,out} L_{Nd} \frac{\partial T_{Nd,out}}{\partial t} + \tag{3.58}$$

$$+ \dot{m}_{Nd} \left(c_{p,Nd,out} T_{Nd,out} - c_{p,Nd,in} T_{Nd,in} \right) = \dot{q}_{Nd,NDHX}$$

Equations (3.59)-(3.61) establish the additional non-dimensional quantities required for the natural draft loop energy equation to be made dimensionless.

$$c_p^+ = \frac{c_p}{c_{p,Nd,out,0}} \tag{3.59}$$

$$T^+ = \frac{T}{\left(T_{Nd,out,0} - T_{Nd,in,0}\right)} \tag{3.60}$$

$$\dot{q}_{NDHX}^+ = \frac{\dot{q}_{NDHX}}{\dot{q}_{Nd,NDHX,0}} \tag{3.61}$$

Equations (3.11), (3.47), (3.49), (3.59)-(3.61) are used with equation (3.58), and after some rearrangement, the result is equation (3.62), the non-dimensional natural draft loop integrated energy equation.

$$\Pi_{L,Nd}\rho_{Nd,out}^+ c_{p,Nd,out}^+ \frac{\partial T_{Nd,out}^+}{\partial t^+} + \tag{3.62}$$

$$+\dot{m}_{Nd}^+\left(c_{p,Nd,out}^+ T_{Nd,out}^+ - c_{p,Nd,in}^+ T_{Nd,in}^+\right) = \Pi_{NDHX,Nd} q_{Nd,NDHX}^+$$

Two characteristic ratios are identified from equation (3.62). These characteristic ratios are defined in equations (3.63) and (3.64).

Intermediate loop length geometry number:

$$\Pi_{L,Nd} = \frac{L_{Nd}}{L_D} \tag{3.63}$$

Intermediate loop NDHX number:

$$\Pi_{NDHX,Nd} = \frac{\dot{q}_{Nd,NDHX,0}}{\rho_{Nd,out,0} A_{Nd,out} w_{D,in,0} c_{p,Nd,out,0}\left(T_{Nd,out,0} - T_{Nd,in,0}\right)} \tag{3.64}$$

A list of the characteristic ratios discovered for the direct loop is presented below in Table 3-2. Likewise, the intermediate loop and natural draft loop characteristic ratios are presented in Table 3-3 and Table 3-4 respectively.

Table 3-2: List of direct loop characteristic ratios

Name	Symbol	Formula
Direct loop reference geometry number	$\Pi_{G,D}$	$\frac{A_{D,1}}{L_D}\sum_i^N \left(\frac{l_i}{A_i}\right)_D$
Direct loop Richardson number	$\Pi_{Ri,D}$	$\frac{(\rho_{D,c,0}-\rho_{D,h,0})gL_D}{\rho_{D,h,0}w_{D,1,0}^2}$
Direct loop resistance number	$\Pi_{F,D}$	$\sum_i^N \left[\left(K_i+\frac{f_i L_i}{D_{e,i}}\right)\left(\frac{\rho_{D,h,0}A_{D,1}^2}{\rho_i A_i^2}\right)\right]_{D,0}$
Direct loop core heat transfer number	$\Pi_{core,D}$	$\frac{\dot{q}_{D,core,0}}{\rho_{D,h,0}A_{D,1}w_{D,1,0}c_{p,D,h,0}(T_{D,h,0}-T_{D,c,0})}$
Direct loop DHX number	$\Pi_{DHX,D}$	$\frac{\dot{q}_{D,DHX,0}}{\rho_{D,h,0}A_{D,1}w_{D,1,0}c_{p,D,h,0}(T_{D,h,0}-T_{D,c,0})}$

Table 3-3: List of intermediate loop characteristic ratios

Name	Symbol	Formula
Intermediate loop reference geometry number	$\Pi_{G,I}$	$\frac{A_{I,1}}{L_D}\sum_{i=1}^{N}\left(\frac{l_i}{A_i}\right)_I$
Intermediate loop Richardson number	$\Pi_{Ri,I}$	$\frac{(\rho_{I,c,0}-\rho_{I,h,0})gL_I}{\rho_{I,h,0}w_{I,1,0}w_{D,in,0}}$
Intermediate loop velocity ratio	$\Pi_{w,I}$	$\frac{w_{I,1,0}}{w_{D,in,0}}$
Intermediate loop resistance number	$\Pi_{F,I}$	$\sum_{i=1}^{N}\left[\left(K_i+\frac{f_iL_i}{D_{e,i}}\right)\left(\frac{\rho_{I,h,0}A_{I,1}^2}{\rho_iA_i^2}\right)\right]_{I,0}$
Intermediate loop length ratio	$\Pi_{L,I}$	$\frac{L_I}{L_D}$
Intermediate loop DHX number	$\Pi_{DHX,I}$	$\frac{\dot{q}_{I,DHX,0}}{\rho_{I,h,0}c_{p,I,h,0}(T_{I,h,0}-T_{I,c,0})w_{D,in,0}A_{I,1}}$
Intermediate loop NDHX number	$\Pi_{NDHX,I}$	$\frac{\dot{q}_{I,NDHX,0}}{\rho_{I,h,0}c_{p,I,h,0}(T_{I,h,0}-T_{I,c,0})w_{D,in,0}A_{I,1}}$

Table 3-4: List of natural draft loop characteristic ratios

Name	Symbol	Formula
Natural draft loop reference geometry #	$\Pi_{G,\boldsymbol{Nd}}$	$\frac{A_{Nd,out}}{L_D}\sum_{i}^{N}\left(\frac{l_i}{A_i}\right)_{Nd}$
Natural draft loop Richardson number	$\Pi_{Ri,Nd}$	$\frac{(\rho_{Nd,in,0}-\rho_{Nd,out,0})gL_{Nd}}{\rho_{Nd,out,0}w_{Nd,out,0}w_{D,in,0}}$
Natural draft loop area ratio	$\Pi_{A,Nd}$	$\frac{A_{Nd,in}^2}{A_{Nd,out}^2}$
Natural draft loop velocity ratio	$\Pi_{w,Nd}$	$\frac{w_{Nd,out,0}}{w_{D,in,0}}$
Natural draft loop resistance number	$\Pi_{F,Nd}$	$\sum_{i=1}^{N}\left[\left(K_i+\frac{f_iL_i}{D_{e,i}}\right)\left(\frac{\rho_{Nd,out,0}A_{Nd,out}^2}{\rho_iA_i^2}\right)\right]_{Nd,0}$
Natural draft loop length ratio	$\Pi_{L,Nd}$	$\frac{L_{Nd}}{L_D}$
Natural draft loop NDHX number	$\Pi_{NDHX,Nd}$	$\frac{\dot{q}_{Nd,NDHX,0}}{\rho_{Nd,out,0}A_{Nd,out}w_{D,in,0}c_{p,Nd,out,0}(T_{Nd,out,0}-T_{Nd,in,0})}$

3.3.5. Scaling choices

Scaling ratios must be decided as part of a scaling analysis. The non-dimensional governing equations for each loop have revealed the characteristic ratios which are important in the scaling of these loops. The scaling ratio choices determine the scaling distortions which arise through these characteristic ratios and the characteristic time scale. If one can be clever about these choices, the scaling distortions can be minimized for the parameters which affect the most important processes. Distortions are a natural effect of scaling and are therefore unavoidable.

Importance of processes can be determined by the relative size of the characteristic ratios within a given equation. Ratios which are much less than one will not contribute significantly to the transport of the given quantity (mass, momentum, energy).

Two requirements will be imposed on this analysis; that of kinematic similarity and friction and form loss similarity. In order to preserve kinematic similarity between the model and the prototype, area ratios will be preserved in each loop.

$$\left(\frac{A_i}{A_{ref}}\right)_R = 1{:}1 \tag{3.65}$$

In order to preserve friction and form loss similarity, the following must be true:

$$\left(\Pi_{F,D}\right)_R = \left(\Pi_{F,I}\right)_R = \left(\Pi_{F,Nd}\right)_R = 1{:}1 \tag{3.66}$$

This friction and form loss similarity can be ensured by adding form loss to the model if the friction is smaller than in the prototype. This is a common practice and is often accomplished using baffle plates.

The following scaling ratios have been selected additionally. The diameter scaling has been chosen to be the same as the scaling for the HTTF for compatibility. The length scaling is based on the estimated elevation difference between core center and NDHX for both the prototype and model. The elevations of prototype are based on Figure 1-4. Elevations of the model are based on drawings for the HTTF and the air cooler on the roof.

$$(D)_R = 1:4 \tag{3.67}$$

$$(L)_R = 1:4 \tag{3.68}$$

The cross sectional area, surface area, and volume scales can be derived from the two scaling choices shown in equations (3.67) and (3.68).

$$(A)_R = (D^2)_R = 1:16 \tag{3.69}$$

$$(A_S)_R = (DL)_R = 1:16 \tag{3.70}$$

$$(V)_R = (AL)_R = 1:64 \tag{3.71}$$

Furthermore, it is intended that tests involving the scaled DRACS module will be able to run at full temperature, as the HTTF is capable of modeling full temperature accident scenarios.

$$(T)_R = 1{:}\,1 \tag{3.72}$$

The same working fluid will be included in the model as in the prototype for the direct, intermediate, and natural draft loops respectively. This will lead to fluid property similarity in each of these loops as long as there is pressure and temperature similarity. Given the scaling choice in equation (3.72), the temperature will be similar. Direct loop pressure similarity can be achieved for a D-LOFC event after the initial depressurization phase, shown in equation (3.73). The HTTF is a scaled pressure facility, however, and cannot achieve the operating pressure of the EM^2 primary system. Based on the operating limits of the HTTF, the pressure scaling is given during normal operation in equation (3.74). As the focus of this work is on the D-LOFC event, pressure similarity, and therefore fluid property similarity, is achieved.

$$\left(P_{D,d}\right)_R = 1{:}\,1 \tag{3.73}$$

$$\left(P_{D,n}\right)_R = \frac{8\ bar}{131\ bar} = 1{:}\,16.375 \tag{3.74}$$

The intermediate loop pressure is unknown in the prototypical EM^2 DRACS. It is assumed that the intermediate loop will be able to have prototypic pressure, so the intermediate loop can be assumed to have fluid property similarity. The operating pressure of the intermediate loop is chosen based on the pipe size in use for the model and prototype. It is also assumed that fluid property similarity will be achieved in the natural draft loop, as both model and prototype use air at atmospheric conditions as the working fluid.

The reference geometry number ratio for both the direct and intermediate loops will equal unity due to the requirements imposed for kinematic similarity and the same scaling for length and diameter ratio.

$$\left(\Pi_{G,D}\right)_R = \left(\frac{A_{D,1}}{L_D}\sum_i^N \left(\frac{l_i}{A_i}\right)_D\right)_R = 1{:}1 \tag{3.75}$$

$$\left(\Pi_{G,I}\right)_R = \left(\frac{A_{I,1}}{L_D}\sum_{i=1}^N \left(\frac{l_i}{A_i}\right)_I\right)_R = 1{:}1 \tag{3.76}$$

$$\left(\Pi_{G,Nd}\right)_R = \left(\frac{A_{Nd,out}}{L_D}\sum_i^N \left(\frac{l_i}{A_i}\right)_{Nd}\right)_R = 1{:}1 \tag{3.77}$$

The natural draft loop area ratio is defined in equation (3.55). Because of the scaling requirement laid out in equation (3.65), the direct loop area ratio will be unity.

$$\left(\Pi_{A,Nd}\right)_R = \left(\frac{A_{Nd,in}^2}{A_{Nd,out}^2}\right)_R = 1{:}1 \tag{3.78}$$

The intermediate loop length ratio, defined in equation (3.43), has its scaling defined by the scaling choice shown in equation (3.68). All lengths are scaled the same to the given scaling factor, so the ratio of intermediate loop length to direct loop length will be the same in the model as in the prototype. The same follows for the natural draft loop length ratio, defined in equation (3.63).

$$\left(\Pi_{L,I}\right)_R = \left(\frac{L_I}{L_D}\right)_R = 1{:}1 \tag{3.79}$$

$$\left(\Pi_{L,Nd}\right)_R = \left(\frac{L_{Nd}}{L_D}\right)_R = 1{:}1 \tag{3.80}$$

This concludes the characteristic ratios scaled during the top-down scaling analysis. The remaining characteristic ratios describe processes which must be investigated by the bottom-up scaling analysis.

3.4. Bottom-up scaling analysis of the DRACS

Some of the distortions in characteristic ratios could not be determined through the top-down scaling analysis, and a bottom-up scaling analysis for these specific processes is necessary to determine the distortions that will arise in those characteristic ratios. There are many variables that can be set to a specific value in order to limit distortion, and this is included in the top-down scaling analysis. For those parameters which cannot simply be set, the bottom-up scaling analysis is necessary.

The first characteristic ratio to be dealt with is the intermediate loop velocity ratio, which is defined in equation (3.34). The natural draft loop velocity ratio scaling is developed simultaneously, which is defined in equation (3.56). The velocities for each loop have not been defined at this point in the analysis.

The steady-state velocity can be found for the direct loop by finding a steady-state solution to the transient formulation shown in equation (3.13). The time dependent term will be set to zero and all of the terms superscripted with “+” will be set to unity at steady state. The simple result of this steady-state formulation is shown in equation (3.81).

$$\Pi_{F,D} = \Pi_{Ri,D} \tag{3.81}$$

This steady-state natural circulation velocity at the first section of the direct loop can be found with some algebraic manipulation of equation (3.81). The result is shown in equation (3.82).

$$w_{D,1,0} = \left(\frac{\left(\rho_{D,c,0} - \rho_{D,h,0}\right) g L_D}{\rho_{D,h,0} \Pi_{F,D}}\right)^{\frac{1}{2}} \tag{3.82}$$

The steady-state velocity can be found for the intermediate loop in a similar way. The transient formulation for the intermediate loop is shown in equation (3.31). The steady state condition has the same effects as listed for the direct loop. The result is shown in equation (3.83).

$$\Pi_{Ri,I} = \Pi_{w,I} \Pi_{F,I} \tag{3.83}$$

The first examination of this equation is that it is more complicated than the result for the direct loop, but when the terms are expanded, the result is shown to be similar.

$$\frac{\left(\rho_{I,c,0} - \rho_{I,h,0}\right) g L_I}{\rho_{I,h,0} w_{I,1,0} w_{D,in,0}} = \frac{w_{I,1,0}}{w_{D,in,0}} \Pi_{F,I} \tag{3.84}$$

The steady state velocity for the intermediate loop is shown in equation (3.85) after algebraic manipulation of equation (3.84).

$$w_{I,1,0} = \left(\frac{\left(\rho_{I,c,0} - \rho_{I,h,0}\right) g L_I}{\rho_{I,h,0} \Pi_{F,I}}\right)^{\frac{1}{2}} \tag{3.85}$$

The natural draft loop velocity at steady state is found similarly to those in the direct and intermediate loop. Because the natural draft loop is an open loop, there is an additional term which describes the pressure drop due to acceleration. If the natural draft loop area ratio is one, this term drops out at steady-state. It is assumed that the natural draft loop area ratio is close to one, such that this term is negligible at steady-state. The non-dimensional natural draft loop integrated momentum equation is shown in equation (3.52), which at steady-state is shown in equation (3.86).

$$\Pi_{Ri,Nd} = \Pi_{w,Nd}\Pi_{F,Nd} \tag{3.86}$$

The natural draft loop outlet velocity at steady-state is shown in equation (3.87) by manipulation of equation (3.86) similar to the intermediate loop.

$$w_{Nd,out,0} = \left(\frac{\left(\rho_{Nd,in,0} - \rho_{Nd,out,0}\right) g L_{Nd}}{\rho_{Nd,out,0}\Pi_{F,Nd}}\right)^{\frac{1}{2}} \tag{3.87}$$

Now that an expression has been found for the steady-state velocity in each loop, the velocity scaling between model and prototype can be evaluated for each. As stated in section 3.3.5, fluid property similarity is achieved for each loop during a D-LOFC. As shown in equation (3.66), the loop resistance numbers are preserved between model and prototype for each loop. The acceleration due to gravity does not change between model and prototype (assuming that the location is a similar elevation relative to sea level). The scaling of the velocities is then dependent on the length scaling, shown in equation (3.68). The length scaling is consistent for each loop, so the velocity scaling is

therefore consistent for each loop, shown in equation (3.88). Again, this is based on the condition of fluid property similarity, which is achieved during a D-LOFC.

$$\left(w_{D,1,0}\right)_R = \left(w_{I,1,0}\right)_R = \left(w_{Nd,out,0}\right)_R = (L_R)^{\frac{1}{2}} = 1:2 \tag{3.88}$$

The intermediate and natural draft loop velocity ratios are then investigated using the above results. As the velocity scaling ratio is the same for each loop, the result is a scaling of unity for each of these characteristic ratios.

$$\Pi_{w,I} = \frac{\left(w_{I,1,0}\right)_R}{\left(w_{D,1,0}\right)_R} = 1:1 \tag{3.89}$$

$$\Pi_{w,Nd} = \frac{\left(w_{Nd,out,0}\right)_R}{\left(w_{D,1,0}\right)_R} = 1:1 \tag{3.90}$$

The next characteristic ratios that need to be addressed in the bottom-up scaling are the Richardson numbers for the direct, intermediate, and natural draft loops. These are defined in equations (3.15), (3.33), and (3.54) respectively. The parameters included in the Richardson numbers which did not have their scaling defined during the top-down analysis were the velocities. The scaling for velocity was defined in equation (3.88).

The Richardson numbers for each loop depend on densities, acceleration due to gravity, loop height, and loop velocities. The densities are fluid properties, which are similar in all loops during a D-LOFC. The loop height and velocities are scaled according to equations (3.68) and (3.88) respectively. The relationship between the scaling of length

and velocity mean that the Richardson number for all loops is preserved between the model and prototype.

$$\left(\Pi_{Ri,D}\right)_R = \left(\Pi_{Ri,I}\right)_R = \left(\Pi_{Ri,Nd}\right)_R = 1{:}\,1 \tag{3.91}$$

Although the focus of this scaling analysis is on the D-LOFC event, it is interesting to note that even when fluid property similarity is not achieved in the direct loop due to a pressure scaling other than unity, the direct loop Richardson number is preserved. The densities included in the Richardson number will result in a ratio of unity between prototype and model due to the relationship between the densities. The density in the direct loop can be computed using the ideal gas law modified for two gas species. The mass fraction of each species is used along with the molecular weight to determine the composite gas constant. If the mass fractions are preserved between model and prototype, and temperature is still matched, the density ratio will be the same as the pressure ratio between model and prototype, illustrated in equation (3.92).

$$\rho_D = \frac{P_D}{RT_D}\left(X_N M_N + (1 - X_N) M_{He}\right) \tag{3.92}$$

The hot and cold densities differ only due to temperature, using the same loop pressure for both points within the loop. The arrangement of densities which are included in the Richardson number can each be expressed in terms of equation (3.92), and all three densities include the common pressure term. Because this same pressure is included in the numerator and denominator, it cancels out, so the pressure difference between

model and prototype have no effect on the Richardson number. Again, this scaling analysis is not focused on events other than the D-LOFC, but it is interesting to note that the Richardson numbers would be preserved in any case.

The last characteristic ratios necessary to be included in the bottom-up scaling analysis are the direct loop core heat transfer number, direct loop DHX number, intermediate loop DHX number, intermediate loop NDHX number, and natural draft loop NDHX number. These characteristic ratios are defined in equations (3.23), (3.24), (3.44), (3.45), and (3.64) respectively. The scaling ratios for cross-sectional area, temperature, and velocity are defined in equations (3.69), (3.72), and (3.88) respectively. Density and constant pressure specific heat capacity are both fluid properties, and are therefore similar as stated in section 3.3.5.

The only parameter left in all three of these characteristic ratios is the heat source/sink rates, being that of the heat transferred from the core and through the DHX and NDHX. A closure relation ties this heat source/sink rate to the rate of heat transfer from the core and to/from each heat exchanger.

$$\dot{q} = hA_s\Delta T \tag{3.93}$$

Where $h, A_s, \Delta T$ are the heat transfer coefficient, total heat transfer surface area, and difference between bulk fluid temperature and heat exchanger surface temperature. The scaling ratio for surface area or heat transfer area is defined in equation (3.70), and the temperature is full-scale in both loops according to the requirement imposed by

equation (3.72). At steady-state, the heat transfer rates throughout the system should be balanced, such that there is no change in temperature over time in a component or loop. An equation to describe the advection heat transfer rate is used as a reference for scaling in agreement with this requirement, shown in equation (3.94).

$$\dot{q} = \dot{m} c_p \Delta T \tag{3.94}$$

The difference in temperature in equation (3.94) is given by the difference between the bulk fluid temperature hot and cold points. According to the requirement imposed by equation (3.72), this temperature difference will be preserved between model and prototype. The scaling of the heat transfer rate is then dependent only on the mass flow rate scaling.

The mass flow rate is the product of density, velocity, and cross-sectional or flow area. Under the conditions of fluid property similarity as described above, the density is preserved between the model and prototype. The area scaling is given by equation (3.69), and the velocity scaling is given by equation (3.88). The resulting scaling factor for mass flow rate under the conditions of fluid property similarity is given by equation (3.95). The resulting scaling of the advection heat transfer rate, as shown in equation (3.94), is given by equation (3.96). This scaling will be the same as the scaling for the heat transfer rate, as shown in equation (3.93), for steady-state.

$$(\dot{m})_R = (\rho)_R (A)_R (w)_R = 1{:}\,32 \tag{3.95}$$

$$(\dot{q})_R = (\dot{m})_R \left(c_p\right)_R (T)_R = 1{:}\,32 \tag{3.96}$$

Equation (3.96) gives the scaling for heat transfer rates throughout the system imposed by a steady-state condition with fluid property similarity. By combining equations (3.93) and (3.96), the appropriate scaling for the heat transfer coefficient is defined for proper heat transfer scaling.

$$(h)_R = \frac{(\dot{q})_R}{(A_s)_R(\Delta T)_R} = 1{:}\,2 \tag{3.97}$$

The heat transfer coefficient needs to be broken down further in order to determine how it is related between the model and prototype. The Nusselt number is often used in order to determine the heat transfer coefficient. The definition of the Nusselt number is shown in equation (3.98), which can be rearranged to find the overall heat transfer coefficient.

$$Nu = \frac{hL_c}{k_f} \tag{3.98}$$

Where Nu, L_c, k_f are the Nusselt number, characteristic length, and thermal conductivity of the fluid, respectively. The characteristic length depends on the flow conditions, and the heated hydraulic diameter is used for both heat exchangers here. Nusselt number correlations are often used to find the heat transfer coefficient. Nusselt number correlations use non-dimensional numbers which describe the flow conditions in order to characterize heat transfer. Reynolds number, Prandtl number, and Rayleigh number are commonly used for these correlations.

Reynolds number is the ratio of inertial to viscous forces. This number is used to characterize fluid flow regimes, namely laminar and turbulent flow. Reynolds number is important to determine dynamic similitude between two different fluid flows, such as the fluid flows in scaling a model from a prototype. Reynolds number is defined in equation (3.99), and the scaling ratio is defined under conditions of fluid property similarity in equation (3.100). One new term shows up in this equation, μ is the dynamic viscosity.

$$Re = \frac{\rho w L_c}{\mu} \tag{3.99}$$

$$(Re)_R = (w)_R (D)_R = 1{:}8 \tag{3.100}$$

Prandtl number is the ratio of viscous diffusion rate to thermal diffusion rate. The relative thickness of momentum and thermal boundary layers are described by the Prandtl number. All of the quantities which make up the Prandtl number are fluid properties, so it can be tabulated alongside thermal conductivity, density, and viscosity of fluids. Under the condition of fluid property similarity, the scaling ratio is unity between the model and prototype. Equation (3.101) defines Prandtl number while equation (3.102) shows the scaling under the conditions of fluid property similarity.

$$Pr = \frac{\mu c_p}{k_f} \tag{3.101}$$

$$(Pr)_R = 1{:}1 \tag{3.102}$$

Rayleigh number is the product of the Grashof and Prandtl numbers. The Prandtl number has already been discussed, and the Grashof number is the ratio of buoyancy and viscosity of the fluid. The Rayleigh number is used to define the dominant heat transfer mechanism between conduction and convection. The Rayleigh number is often used in natural convection Nusselt number correlations. The Rayleigh number is defined in equation (3.103) and the scaling ratio is defined in equation (3.104) under the conditions of fluid property similarity. $\beta, T_s, T_\infty, \nu, \alpha$ are the volumetric coefficient of thermal expansion, surface temperature, bulk fluid temperature, kinematic viscosity, and thermal diffusivity.

$$Ra = \frac{g\beta(T_s - T_\infty)L_c^3}{\nu\alpha} \tag{3.103}$$

$$(Ra)_R = (L_c^3)_R = 1{:}64 \tag{3.104}$$

The type of Nusselt number correlation used is determined by the specific flow conditions. There are often limits on Reynolds number, Rayleigh number, Prandtl number, length to diameter ratio, depending on the type of correlation. Without knowing the specific flow conditions, Nusselt number correlations cannot be used for scaling. Often these correlations are made up of a coefficient and a combination of the three above numbers raised to some power. Let the appropriate scaling of the Nusselt number between model and prototype suffice for this scaling analysis, developed by equations (3.67), (3.97), and (3.98).

$$(Nu)_R = (h)_R(D)_R = 1{:}8 \tag{3.105}$$

The heat exchanger characteristic ratios can now be evaluated as the scaling ratios have been developed for all of the relevant parameters. First, the direct loop core heat transfer number is given by equation (3.106) under the condition of fluid property similarity.

$$\left(\Pi_{core,D}\right)_R = \frac{(\dot{q})_R}{(A)_R(w)_R} = 1{:}1 \tag{3.106}$$

As the scaling for each of these parameters are consistent between all of the loops, the other heat exchanger characteristic ratios will follow the same scaling, as shown in equations (3.107), (3.108), (3.109), and (3.110).

$$\left(\Pi_{DHX,D}\right)_R = \frac{(\dot{q})_R}{(A)_R(w)_R} = 1{:}1 \tag{3.107}$$

$$\left(\Pi_{DHX,I}\right)_R = \frac{(\dot{q})_R}{(A)_R(w)_R} = 1{:}1 \tag{3.108}$$

$$\left(\Pi_{NDHX,I}\right)_R = \frac{(\dot{q})_R}{(A)_R(w)_R} = 1{:}1 \tag{3.109}$$

$$\left(\Pi_{NDHX,Nd}\right)_R = \frac{(\dot{q})_R}{(A)_R(w)_R} = 1{:}1 \tag{3.110}$$

The only remaining quantity of importance left to evaluate the scaling of between model and prototype is the time scale, defined by the direct loop residence time, shown in equation (3.11). The scaling of this time scale pulls from the length scaling in equation (3.68) and velocity scaling in equation (3.88). The result is shown in equation (3.111),

and the implication is that everything happens twice as fast in the model as in the prototype.

$$(\tau)_R = \frac{(L_D)_R}{(w_D)_R} = 1:2 \tag{3.111}$$

The primary focus of this scaling analysis is to evaluate the scaling ratios between model and prototype for the D-LOFC event after depressurization. This event affects the temperatures which are seen throughout the DRACS, and the pressure in the primary system and direct loop. All the values which are dependent on these quantities are also affected by the event. All geometry scaling in all three loops will remain consistent regardless of the event. The scaling of the intermediate and natural draft loops will remain consistent regardless of the event. The scaling results are summarized for operating characteristic and characteristic ratio during the D-LOFC event after depressurization, when fluid property similarity can be assumed for all three loops. The quantities which will vary from the listed scaling value during other events are the direct loop pressure, density, velocity, heat transfer rate, other fluid properties, and all characteristic ratios which depend on these operating characteristics, with the exception of the direct loop Richardson number. As the scaling for other events is not the main focus of this scaling analysis, the alternate values are not presented in Table 3-5 and Table 3-6.

Table 3-5: Scaling values following depressurization of operating characteristics

Ratio	Scale	Ratio	Scale	Ratio	Scale
$\left(\frac{A_i}{A_{ref}}\right)_R$	1:1	$(D)_R$	1:4	$(L)_R$	1:4
$(A)_R$	1:16	$(A_S)_R$	1:16	$(V)_R$	1:64
$(P)_R$	1:1	$(T)_R$	1:1	$(\rho)_R$	1:1
$(\mu)_R$	1:1	$(w)_R$	1:2	$(\dot{m})_R$	1:32
$(k_f)_R$	1:1	$(\dot{q})_R$	1:32	$(c_p)_R$	1:1
$(Re)_R$	1:8	$(Pr)_R$	1:1	$(Ra)_R$	1:64
$(Nu)_R$	1:8	$(\tau)_R$	1:2		

Table 3-6: Scaling distortions following depressurization of characteristic ratios

Ratio	Scale	Distortion Factor	Ratio	Scale	Distortion Factor
$\Pi_{G,D}$	1:1	0	$\Pi_{F,D}$	1:1	0
$\Pi_{G,I}$	1:1	0	$\Pi_{F,I}$	1:1	0
$\Pi_{G,Nd}$	1:1	0	$\Pi_{F,Nd}$	1:1	0
$\Pi_{Ri,D}$	1:1	0	$\Pi_{L,I}$	1:1	0
$\Pi_{Ri,I}$	1:1	0	$\Pi_{L,Nd}$	1:1	0
$\Pi_{Ri,Nd}$	1:1	0	$\Pi_{DHX,D}$	1:1	0
$\Pi_{A,D}$	1:1	0	$\Pi_{DHX,I}$	1:1	0
$\Pi_{A,Nd}$	1:1	0	$\Pi_{NDHX,I}$	1:1	0
$\Pi_{w,I}$	1:1	0	$\Pi_{NDHX,Nd}$	1:1	0
$\Pi_{w,Nd}$	1:1	0			

4. Design requirements

A scaled-down DRACS which will accurately model the performance of the full-scale prototype for gas-cooled reactors can be designed using the scaling analysis performed in chapter 3 as a guide. Some design requirements must be laid out in order to ensure that the scaled-down test facility will fulfill its purpose. The EM^2 is a GFR which employs the DRACS as its emergency decay heat removal system. Information collected and deduced about the DRACS included in the EM^2 will be discussed first, followed by what the addition of the DRACS might look like at the HTTF at OSU. While it is intended that the scaling analysis will be applicable to the DRACS in the EM^2, the design requirements do not specifically meet this purpose as official information on this design is not available.

4.1. DRACS in the EM^2

There is limited information available on the DRACS in the EM^2, partially because the design is still conceptual. Other parts of the design specifics may be proprietary, or just too much detail to include in scientific articles. Information gathered from text and figures in papers and presentations given on the EM^2 is presented here.

First, DRACS was not always a part of the EM^2 design. The DRACS was added in order to address concerns raised by a DOE review in 2010 related to the D-LOFC event [29]. At the addition of the DRACS to EM^2, it was a fully passive system, much like many examples of DRACS seen in other reactor types. Figure 4-1 was used with permission from a report by the International Atomic Energy Agency (IAEA) on small and medium

reactor designs, and it shows an early concept without the helium circulator attached to each DRACS module [2]. It is likely that the helium circulator and back-up jet pumps were added in order to provide further protection for D-LOFC events.

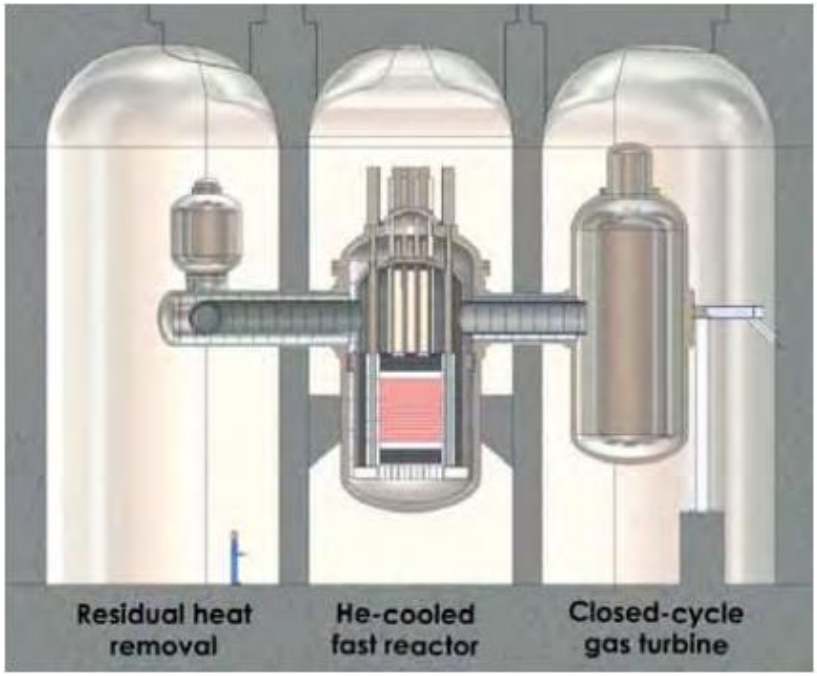

Figure 4-1: Early concept of the EM^2 fully passive DRACS

Figure 4-1 shows the early concept of the EM^2 DRACS when it was fully passive, but more recent reports discuss a helium circulator and a jet pump for each DRACS module. Each DRACS module is capable of functioning in active mode or fully passive mode in the case of total loss of electrical power [4]. It can be seen in the Figure 4-2 that the jet pumps reside in the reactor auxiliary building.

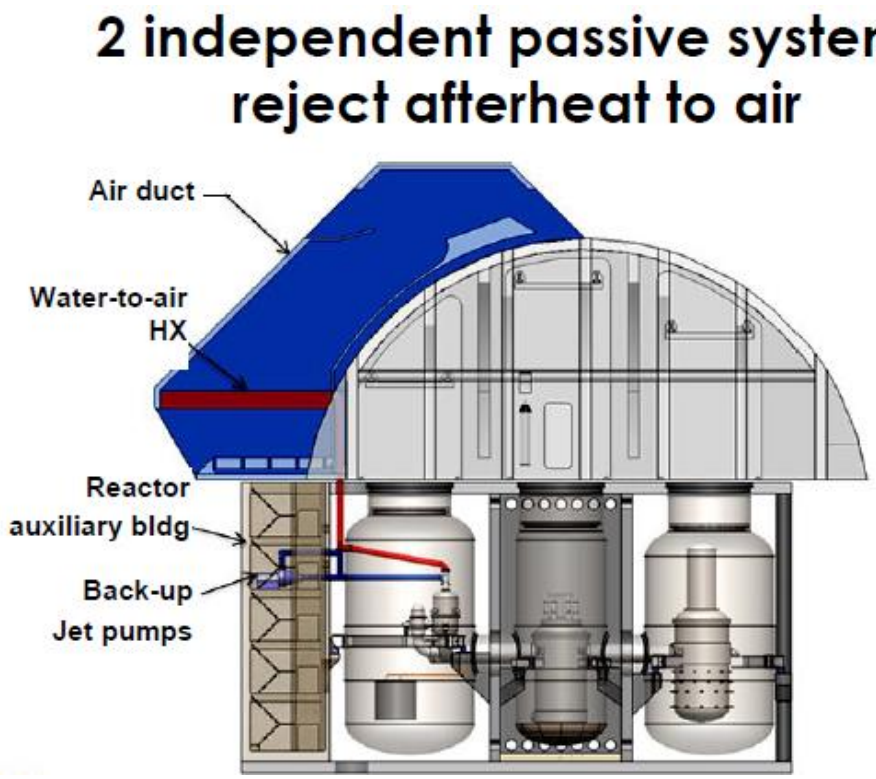

Figure 4-2: The EM^2 DRACS with active cooling, second concept

Figure 4-2 also yields information about the cooling tower and the NDHX. The NDDCT sits above grade to one side of the maintenance hall, and the water-to-air heat exchangers are arranged horizontally near the base of the tower, just above the air intake [28]. The air inlet and outlet of the cooling tower are defined in Figure 1-4. The DRACS heat exchanger (DHX) is a multi-tube helical-coil helium to water heat exchanger [4], and can be seen more closely in the following cut-away of a DRACS module. In Figure 4-3, it can be seen that the intermediate water loop enters the DHX through four pipes and leaves through one larger riser pipe.

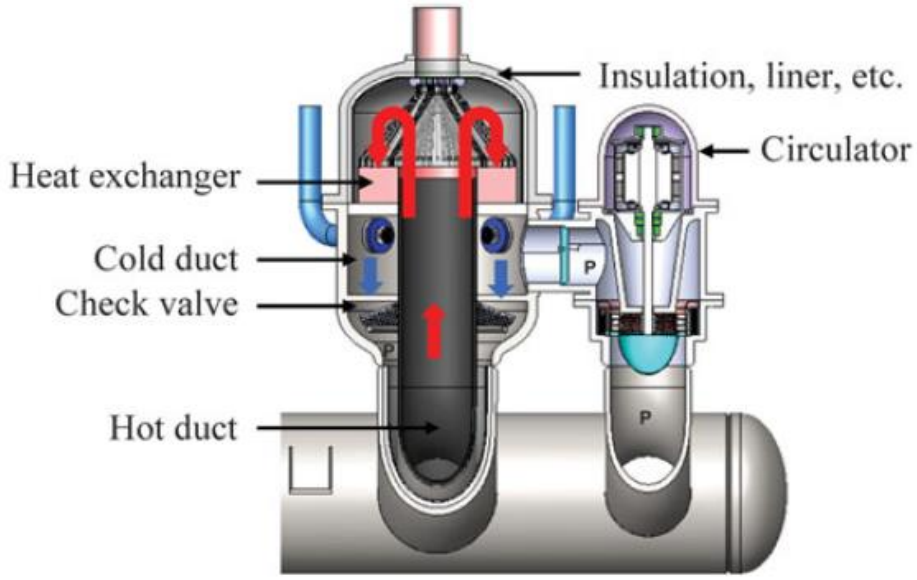

Figure 4-3: The EM^2 DRACS module cutaway, second concept

The flow path of the direct loop is also shown in some detail in Figure 4-3. Hot helium flows through an integrated duct up into a plenum where it turns around as it flows over the multi-tube helical-coil DHX and is cooled. The cool helium then either passively drops down the cold duct or is accelerated by means of the helium circulator back to the reactor vessel. It can be seen in Figure 4-2 and Figure 4-3 that a concentric duct which leads directly to the reactor vessel connects the DRACS to the core. In Figure 4-4, it appears that the concentric duct which leads to the DRACS is the same diameter as the concentric duct that leads to the power conversion unit. There are two DRACS modules for each EM^2 reactor, so the flow area of that concentric duct is shared by both modules. These modules are referred to as redundant because each module is capable of removing enough decay heat to maintain the core temperature at safe levels under the following conditions: during a D-LOFC, a single DRACS module with use of the

helium circulator, and during a P-LOFC, a single DRACS module is capable while running in passive mode [4]. During a D-LOFC without electrical power to run the helium circulator and jet pumps, the EM^2 core is still maintained at or below the tentative design limit of the fuel cladding if both DRACS modules are operating in passive mode [4].

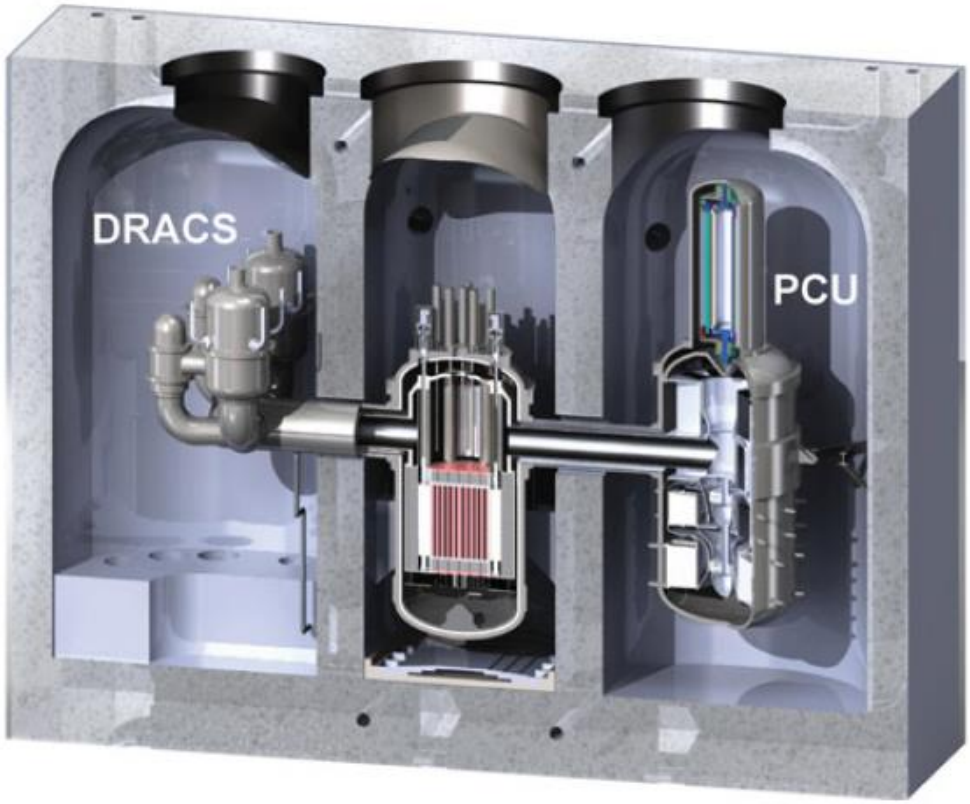

Figure 4-4: The Energy Multiplier Module Containment Cutaway

While all of the early renderings of the reactor show three containment vessels (CV), later renderings show only two CVs. In the first and second DRACS concepts with three CVs, the two DRACS modules are located in one CV at an elevation just above the concentric duct which is at an elevation just above that of the core, the middle CV holds

the RPV, and the third CV holds the power conversion unit (PCU). In the third DRACS concept with only two CVs, the DRACS modules are located in a single CV above the RPV, and the PCU is located its own CV as in the previous concept.

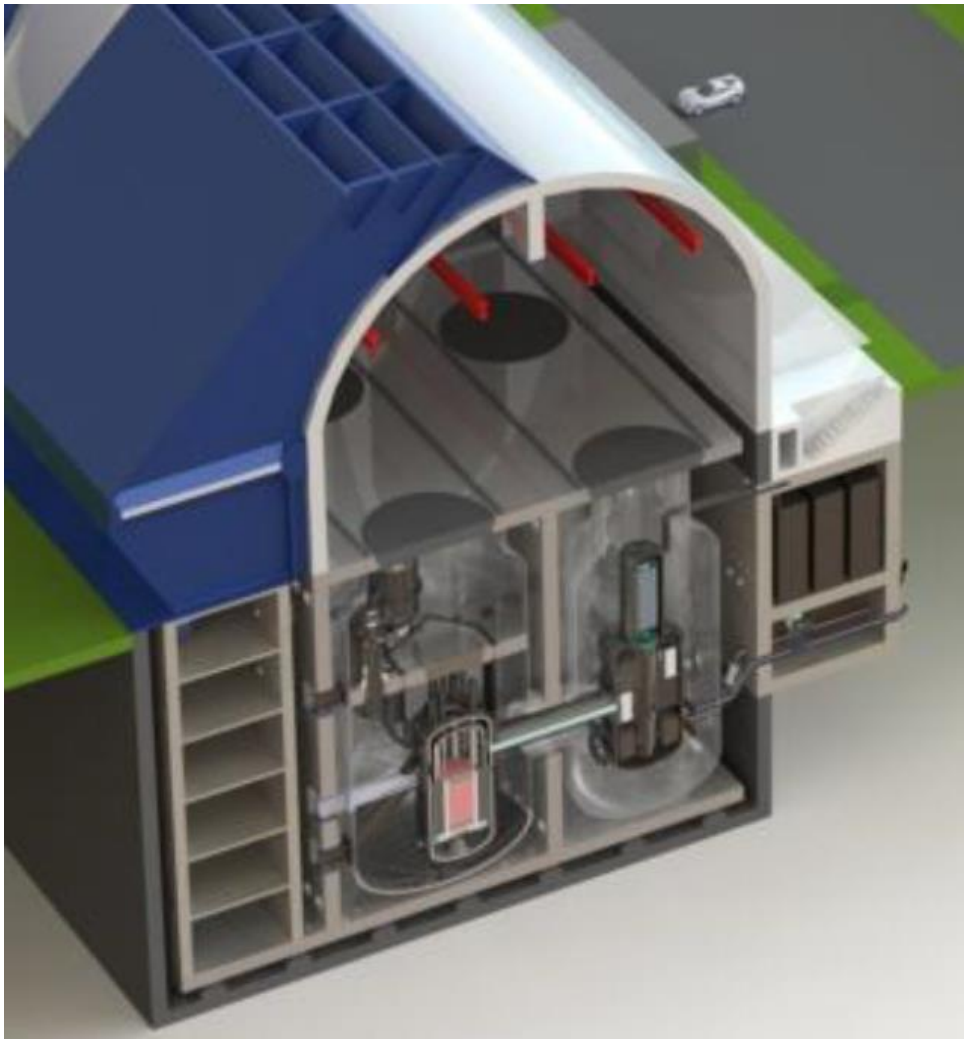

Figure 4-5: Two CV design for the EM^2 DRACS, third concept

The difference between these two design concepts is not directly discussed in currently available literature, so the reason for the change is not clear. Two possibilities are either the elimination of the third CV saves materials and space and therefore capital cost, or

that a greater elevation difference between the core and the DHX were desired for natural circulation flow formation. Figure 4-5 is included to show this two CV design. Figure 1-2, Figure 1-3, and Figure 1-4 were received via email from the author of the presentation which contained Figure 4-5, and they also show this recent two containment vessel design. Figure 1-3 and Figure 1-4 show that the piping for the intermediate loop has also changed so there is only one cold pipe leading to the DHX opposed to the four pipes that were shown in Figure 4-3. These images also give no indication that the hot pipe and cold pipe in the intermediate loop are different diameters.

4.2. DRACS in the HTTF

While limited information is available on the prototypic DRACS design for EM^2, modeling the DRACS in the HTTF will differ than those figures shown above. The first constraint is that the flow path through the HTTF core, which is modeled after the MHTGR, is opposite of the flow path through the EM^2 core. In the HTTF, like the MHTGR, cool helium is directed up to the upper plenum, then down through the core and out through the lower plenum to the concentric hot duct. The flow path for the EM^2 is illustrated in Figure 4-6, and it can be seen that it is opposite that of the MHTGR and HTTF. Cool helium is directed to the bottom of the RPV, up through the lower plenum, up through the core, and out from the upper plenum through the concentric hot duct in the EM^2.

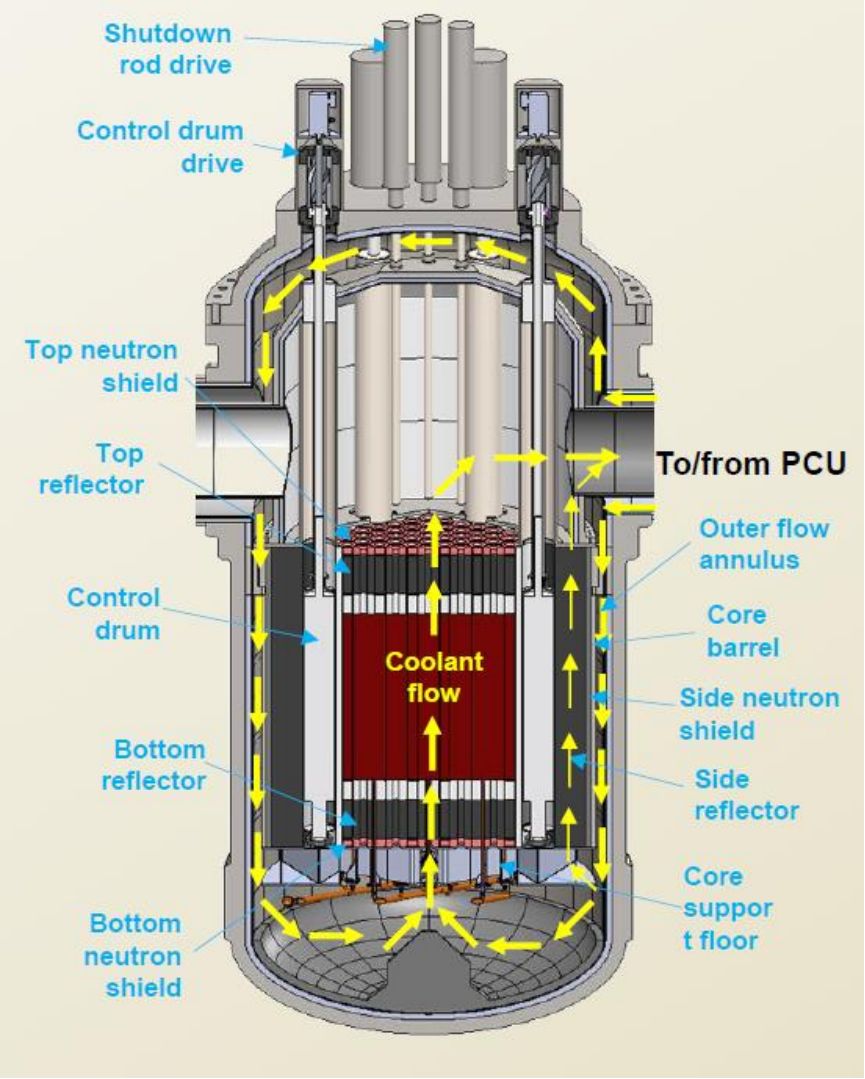

Figure 4-6: Coolant flow path through the EM^2 RPV

The concentric duct in each reactor design is located at the elevation of the outlet plenum. For the MHTGR and HTTF, the outlet plenum is the lower plenum, whereas the outlet plenum of the EM^2 is the upper plenum. This discontinuity demonstrates why piping to the DRACS in the HTTF cannot consist of a concentric duct located opposite of the one for the PCU, as it was originally in the EM^2. In order to avoid the need for a re-certified pressure vessel for the HTTF, existing ports in the upper head have been

selected to serve as the inlet and outlet for the direct loop in the stead of a concentric duct. The location of piping in the upper head allows for natural circulation flow to occur between the core and the DRACS. During normal operations in the HTTF helium flows down through the core, but a loss of forced convection scenario leads to flow reversal to support this natural circulation. The piping from the upper head will lead to the DHX elevated above the HTTF primary pressure vessel (PPV), which will better match the newest concept of the EM^2 as shown in Figure 1-2, Figure 1-3, Figure 1-4, and Figure 4-5.

The dimensions of the piping which lead to the DHX are unknown for the EM^2. In the most recent concept, separate piping leads to each DRACS module from the RPV above the core as illustrated in Figure 1-3. In the second concept, a single concentric duct leads to both DRACS modules, and it appears to be the same size as the concentric duct leading to the PCU. As a reference, there is a concentric duct which leads to the steam generator in the HTTF, which is scaled down in diameter 1:4 from the MHTGR. The same diameter scaling is desired to be matched for the EM^2 DRACS, so the flow area of the concentric duct in the HTTF can be a reference for the flow area of the concentric ducts in the EM^2. The power rating of the EM^2 is 500 MWth and the power rating of the MHTGR used for scaling the HTTF is 350 MWth. It is therefore likely that the concentric duct for the EM^2 will be at least as large as the concentric duct for the MHTGR. If it is assumed that the concentric ducts on these two reactor designs are the same, and that the newest concept of the EM^2 DRACS piping has a flow area of about half of the concentric duct, then the desired flow area can be determined for the model.

The ports available on the upper head limit the ability to match the direct loop piping exactly. The port which has been selected as the direct loop outlet for the model has a flow area approximately half that of both the hot and cold side of the concentric duct in the HTTF. Using the assumptions discussed in the previous paragraph, the flow area of this pipe is appropriate for the direct loop in the model DRACS module. Unfortunately, the port selected for the inlet to the direct loop piping on the HTTF has a flow area just over a third that of the outlet port. A reducer will therefore be necessary to attach the proper size pipe to the inlet port. A concentric duct is used to lead up to and away from the DHX from the point where the inlet and outlet pipes reach the same physical location. These ideas are demonstrated in the model constructed in SolidWorks, for which the part drawings are contained in Appendix F, and images which show the assembled parts are Figure 5-1, Figure 5-2, and Figure 5-3.

As formerly discussed in section 1.5, the model DRACS is envisioned to only model the passive mode, and will therefore not include the helium circulator or jet pump as in the prototype. The performance in passive mode is the limiting case, and forced convection performance is more predictable than natural circulation [16].

The EM^2 DHX is a multi-tube helical-coil heat exchanger, which is located around the outside of the inner pipe, just below a plenum. A helical-coil heat exchanger may have been selected for a few reasons for the DRACS design in EM^2. Helical-coils force the fluid within the tubes to mix more because of the constant acceleration toward the center which leads to mixing and potentially better heat transfer. A helical coil may have also

fit well with the geometry. Dimensions on the DHX are unknown, so engineering judgement is used to size the DHX for the model, and the prototype will be assumed to be scaled up from that according to the scaling analysis.

Information is scarce on the specific design of the NDHX in the prototype. The NDHX sits horizontally near the base of the cooling tower in the prototype, as discussed in section 4.1. Overall dimensions for the NDHX are given in Figure 1-4, which can be used to scale down the design of the model. The cooling of the intermediate loop for the model must be done by the existing equipment on the roof of the bay where the HTTF is housed. This limitation is what drives the length scaling factor, as there is already a defined elevation for the core and what will simulate the NDHX, and those points are fixed.

As mentioned in section 3.3.4, the natural draft loop exists only as a boundary condition for heat to be rejected from the intermediate loop. The existing system is an air fluid cooler, manufactured by General Air Products, used to cool water which cools the primary system helium circulator. It is intended that cooling will be provided to either the DRACS intermediate loop or the circulator, as the DRACS is intended for use during shutdown conditions, especially during a LOFC. The NDHX in the model is cooled with forced draft as opposed to natural draft as it is in the prototype.

With all of these changes listed, it's important to also note what will remain the same between model and prototype. The fluids which flow through each of the loops in the DRACS will remain the same; Helium in the direct loop, water in the intermediate loop,

and air in the natural draft loop. Heat will be transferred ultimately from the core and rejected to outside air.

Temperatures produced for each mode of operation are capable of being matched in the HTTF. Pressure similarity in the direct loop can be achieved during a D-LOFC event, but pressure limitations in the HTTF mean that there will be a pressure distortion during normal operation. Pressure similarity can be achieved in the intermediate and natural draft loops. It is desired that the friction and form loss will be matched, and this can be achieved through the addition of baffle plates if necessary. All of the scaling distortions are listed in Table 3-5, and those operating conditions and characteristic ratios which do not experience distortion can also be seen there.

4.2.1. Instrumentation for DRACS in the HTTF

The Direct Reactor Auxiliary Cooling System is a fairly simple system, especially when compared to the existing HTTF. The instrumentation required will therefore also be less complex than the existing HTTF. Necessary data to collect for the DRACS addition to the HTTF includes temperatures, pressures, and flow rates. The list of instruments planned for the DRACS model for the HTTF is shown in Table 4-1.

Temperatures at specific points throughout the loop will not be necessary as the loop integrated energy equation was employed. Rather, temperatures will be taken before and after each heat source/sink in order to calculate the heat transferred through each heat exchanger. A pressure for each loop will also be read at a single point where it is expected to be the highest, knowing that the system will not have concerns of over-

pressure as long as the pressure read in each loop remain below the design limit. Using the temperatures and pressure in each loop, densities will be available through calculation, which will inform how effective natural circulation is at generating flow. Finally, flow meters will read the flow rate in each loop at the inlet of a heat sink. A simplified schematic of the instrumentation is shown in Figure 4-7.

Table 4-1: Instrumentation list for the DRACS addition to the HTTF

Instrument type	Facility Tag	Loop	Location
Thermocouple	TK-7311	Direct	Loop inlet
Thermocouple	TK-7312	Direct	DHX shell side inlet
Thermocouple	TK-7313	Direct	DHX shell side outlet
Thermocouple	TK-7314	Direct	Loop outlet
Thermocouple	TK-7321	Intermediate	DHX tube side outlet
Thermocouple	TK-7322	Intermediate	NDHX tube side inlet
Thermocouple	TK-7323	Intermediate	NDHX tube side outlet
Thermocouple	TK-7324	Intermediate	DHX tube side inlet
Pressure Tap	PT-7312	Direct	DHX shell side inlet
Pressure Tap	PT-7321	Intermediate	DHX Outlet
Flow Transmitter	FT-7313	Direct	DHX Outlet
Flow Transmitter	FT-7324	Intermediate	DHX Inlet

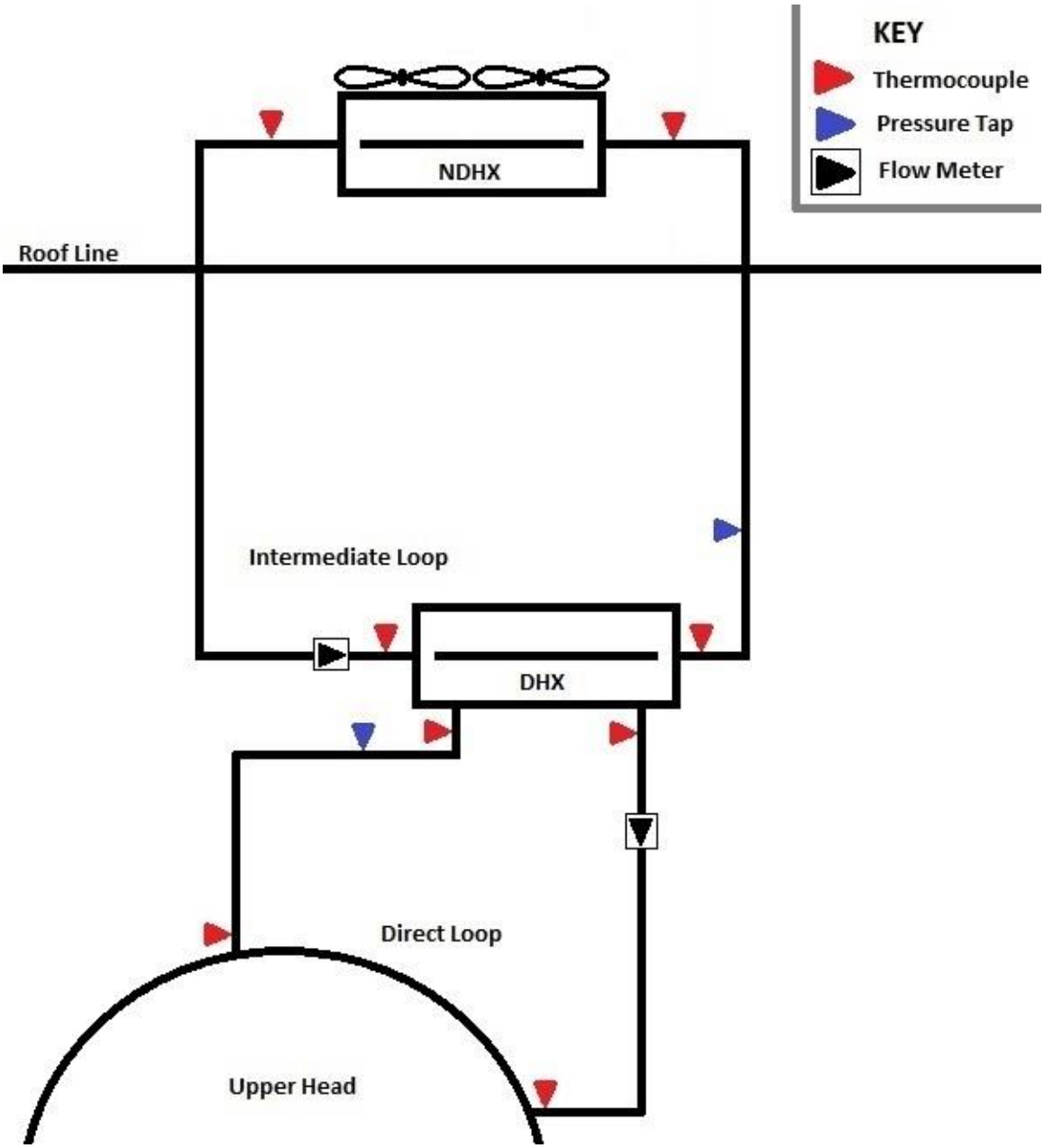

Figure 4-7: DRACS model instrumentation schematic

5. RELAP5-3D analysis

In order to inform the accuracy of the scaling analysis performed for the DRACS for gas-cooled reactors, a computer model has been built of the scaled-down and full-scale prototype. The computer software selected to build these models in is called RELAP5-3D. A discussion on some of the basics of this code are included in section 5.1. Some dimensions and operating parameters were obtained from sources on the EM^2 [3] [4] [28]. Many others could not be located for the EM^2 and were therefore made to fit the scaled-down model, and scaled up to the full-scale prototype according to the scaling analysis.

5.1. RELAP5-3D introduction

RELAP5-3D is the latest version in a code series developed at the Idaho National Laboratory (INL), being the RELAP5 series. While primarily for the use of analyzing transients and accidents in water-cooled NPPs, there is also the capability to model advanced nuclear reactor designs as well. Helium has been included as an option for working fluid in order to support advanced reactor designs. RELAP5-3D is distinguished most from its predecessors in the RELAP5 code series by its capability for multi-dimensional thermal-hydraulic modeling capability.

The RELAP series of codes, along with codes such as RETRAN and TRAC, are known as system codes. System codes are part of the group of codes which are used to analyze the safety of a NPP in a specific configuration. System codes can be used to model entire

NPP systems and simulate accident scenarios. Information from these transient analyses is used as inputs for other codes to solve more specific problems.

Local fluid conditions in the core can be used to inform a sub-channel analysis tool such as COBRA or VIPRE. Neutronics codes are used for core design, which core design is used to inform a power shape, which is compared to a reference shape. The reference shape is also used in the sub-channel analysis code. These sub-channel codes are used to calculate the departure from nucleate boiling ratio (DNBR). This information is used to ensure against cladding failure by including a safety margin which will not be breached by the accidents modeled.

System codes are used to find information on system pressure and temperature, to ensure the pressure boundary will not be breached. System codes can also be used to find information on release into containment. This information is then used in a containment analysis tool such as GOTHIC to analyze whether any release into containment will translate into a containment breach. All of these analyses must be performed for each fuel reload cycle of each NPP before the plant is licensed for operation by the Nuclear Regulatory Commission.

RELAP5 has been in development since the early 1980's, sponsored by the DOE. RELAP5 was chosen as the tool to evaluate the thermal-hydraulic safety of NPPs in the US after the accident at Chernobyl. It was during this evaluation that the need was discovered for more complex analysis tools, especially at the Savannah River NPPs, leading to the

advance to three-dimensional capability [67]. The three main components which were added to RELAP5-3D from RELAP5 are the multi-dimensional hydrodynamic model, multi-dimensional kinetics model, and the new matrix solver for 3D problems. The three-dimensional hydrodynamic model was added in order to deal with multi-dimensional flow exhibited in certain components or regions of a LWR. Primarily the applications were inside the RPV, but this tool is not limited to those regions only. The multi-dimensional neutron kinetics model is based on the NESTLE code developed at North Carolina State University. The new matrix solver is the border profiled lower upper solver, which has been shown to significantly speed up multi-dimensional matrix solves. No significant speed up was shown for 1D problems using the new solver, however.

RELAP5-3D was made for LWR applications, where two-phase flow is of significant interest to be analyzed. For two-phase flow calculations, the balance equations can be solved for each phase, or using mixture models with various assumptions to form the group of equations. A common simplification used for two-phase flow calculations is the homogeneous equilibrium model, which results in four equations to solve. RELAP5-3D uses a six equation model for solving the two-phase flow conservation equations.

The capabilities of RELAP5-3D are vast, and only a small portion has been presented here. The model built of the DRACS uses a small portion of this vast set of capabilities in order to model the necessary processes. Only the DRACS is modeled in RELAP5-3D, with boundary conditions from the primary system to the direct loop, and boundary

conditions for the natural draft loop. The fluids used are helium, water, and air, but none of these fluids should experience two-phase flow. The whole system is modeled in one dimension, so the multi-dimensional capabilities are not being utilized. While only a small portion of the capabilities of RELAP5-3D are in use, it is a tool capable of modeling what complexities are associated with the DRACS.

5.2.Model building in RELAP5-3D

RELAP5-3D models are built with a structure based on the early days of computing, when commands were given to a computer by means of cards which were punched in a way that would deliver specific commands. A stack of cards was called a deck. Similarly, each line in a RELAP5-3D model is called a card, and each card is limited to 80 characters. The full model, stored in a single input file, is called a deck. Each card has an identifier, which is an eight-digit number. The cards need not appear in numerical order, although it is recommended that the title card is followed by the data cards in numerical order, and the terminator card must appear last. If more than one card exists with the same identifier, the card which appears last in the deck will over write any previously appearing. Comment cards can also be added and are helpful for organizing and identifying the information present. It is also recommended that heat structures use the same component number as the hydrodynamic component with which they interact.

The models are described and laid out for both the scaled-down and full-scale as built in RELAP5-3D in the following subsections, followed by a section describing the challenges faced during the model building process.

5.2.1. RELAP5-3D model information collection

Prior to building a model in RELAP5-3D, all of the information needed to be determined for the inputs necessary. Much of the geometrical data necessary was obtained during the design of the scaled-down model in SOLIDWORKS, while operating conditions were determined using a python script to iterate on necessary equations. Necessary information was then compiled in a spreadsheet for both scaled-down model and full-scale prototype versions of each loop and heat exchanger. SOLIDWORKS parts drawings are shown in Appendix F, while the python script is shown in Appendix A.

Overall loop height for the intermediate and natural draft loops was obtained from Figure 1-4. The direct loop height is not identified in that figure. The scaled-down model was used to determine the direct loop height. The NDHX in the scaled-down model is planned to sit just above the elevation of the roof of the Advanced Nuclear Science Engineering Laboratory (ANSEL). The DHX elevation will then be lower than the NDHX by the intermediate loop scaled-down height. The direct loop height is then the remaining elevation difference between the center of the DHX and the core in the HTTF.

The flow area for the direct loop in the scaled-down model is discussed in section 4.2. The pipe size chosen has a flow area of approximately half that of the concentric duct in the HTTF. It is assumed that the concentric duct in the MHTGR is approximately the size of that in the EM^2, and the HTTF was scaled by the same diameter scaling from the MHTGR as the DRACS is from the EM^2. In the second design of the DRACS for EM^2, a single concentric duct leads from the core to both DRACS modules, and has ostensibly

the same flow area as the concentric duct that leads to the PCU. For a single DRACS module, the flow area should therefore be approximately half that of the concentric duct that leads to the PCU. The port which was selected as the outlet for the direct loop in the model is then the appropriate size to use for the piping in the direct loop, and was matched for the piping from the inlet. These attachments can be seen in Figure 5-1.

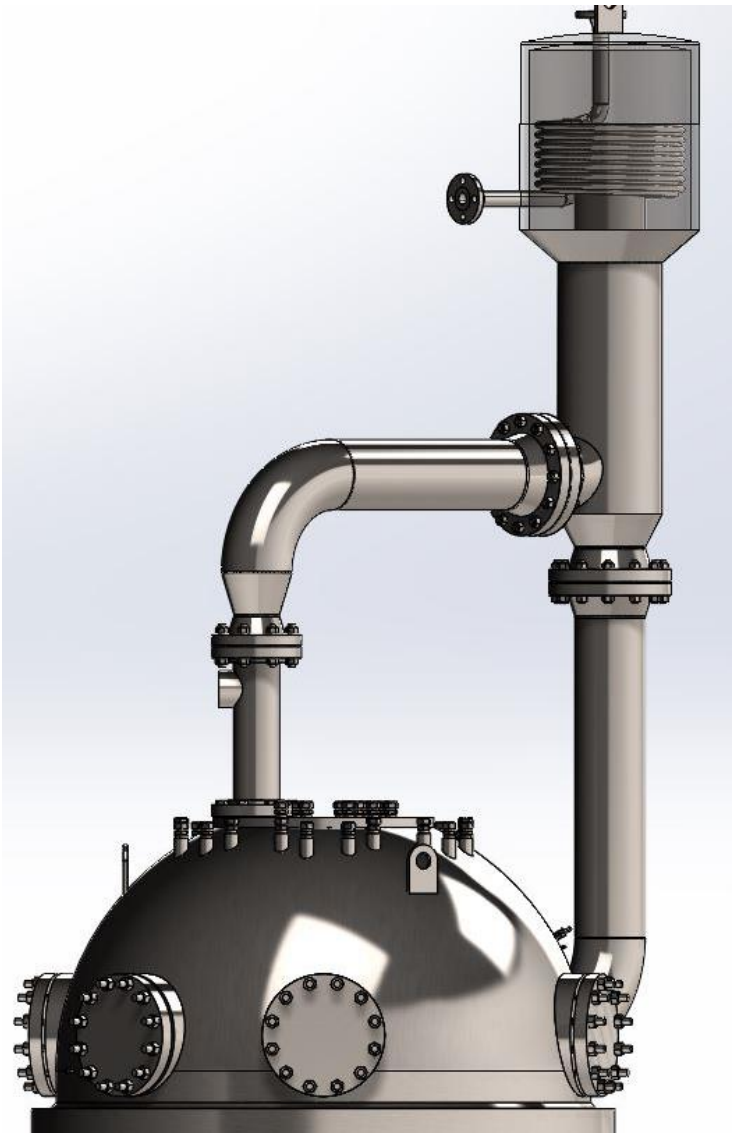

Figure 5-1: Direct loop model attached to upper head

The module which houses the DHX in the EM^2 uses concentric pipes, with a plenum to turn around the hot gas before it flows over the DHX tubes, as seen in Figure 4-3. This module was copied as the detail available allowed for the scaled-down direct loop. Although the pipes for the inlet and outlet connect to separate ports on the HTTF pressure vessel, and are therefore not concentric as shown in the EM^2 DRACS, the inlet pipe meets up with the outlet pipe and is joined such that it flows up through the center in order to preserve the flow characteristics in the module. The inner diameter of the concentric outlet pipe was selected to provide a similar flow area as the inlet pipe. The diameter is expanded for a section in order to accommodate the DHX tubes, which the hot gas flows over. The DHX tubes have a transverse pitch of two and a half times that of the stream-wise pitch, and the stream-wise pitch was selected such that the tubes would lay close with no interference. The major radius of the outermost helical coil tube determined the minimum inner diameter that could be used for that section. Heights were estimated on the various components in the module to resemble the cutaway of the EM^2 DHX module, Figure 4-3. The resulting module is shown in Figure 5-2 including the junction of the inlet and outlet pipes to form the concentric duct. The overall height of the module looks to be larger in the model, but the most recent EM^2 DRACS design includes a long vertical concentric duct leading to it.

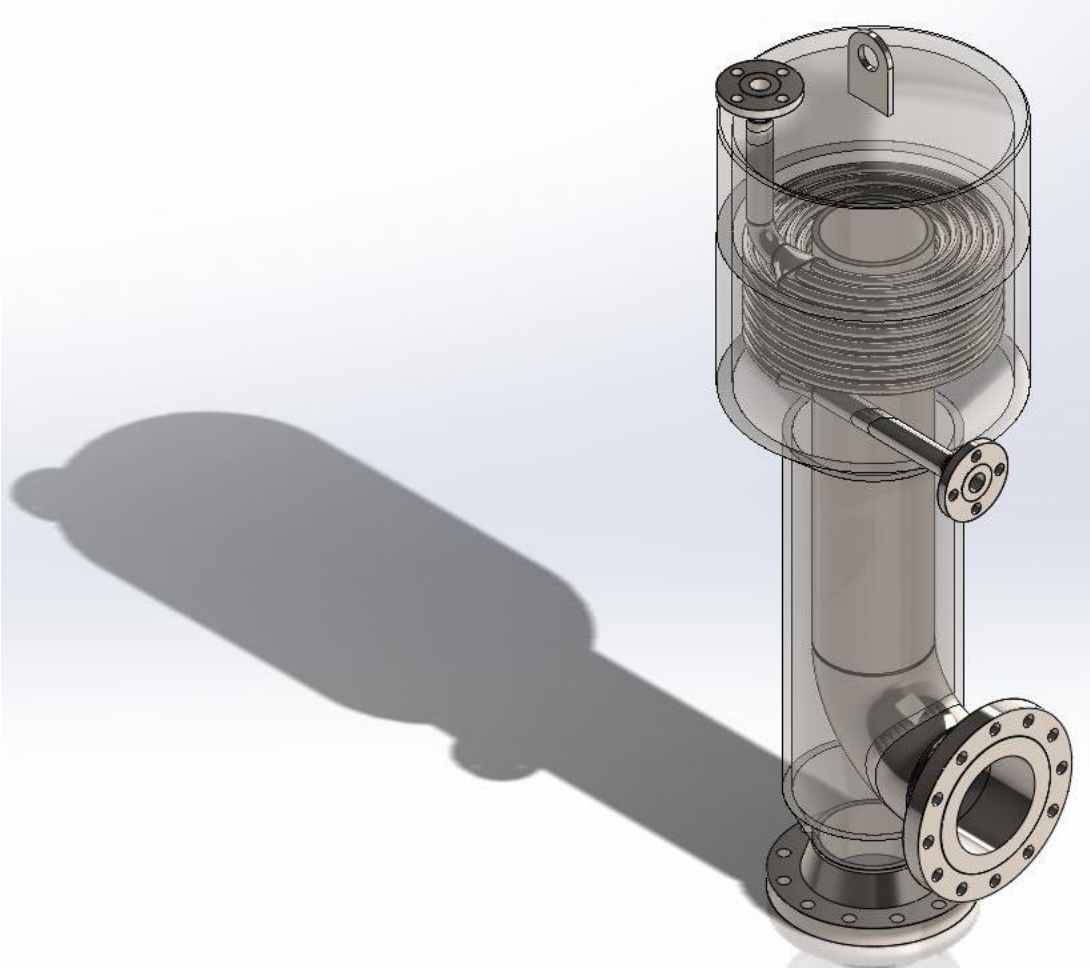

Figure 5-2: Scaled-down model DHX module

Piping for the intermediate loop was chosen to be compatible with the air cooler which was chosen to model the NDHX in the scaled-down model. The diameter and number of DHX tubes was chosen such that the flow area through the DHX would be slightly larger than that of the rest of the intermediate loop piping, resulting in six tubes for the multi-tube helical coil DHX. These design decisions led to the physical dimensions which informed the scaled-down RELAP5-3D model. The intermediate loop can be seen in Figure 5-3.

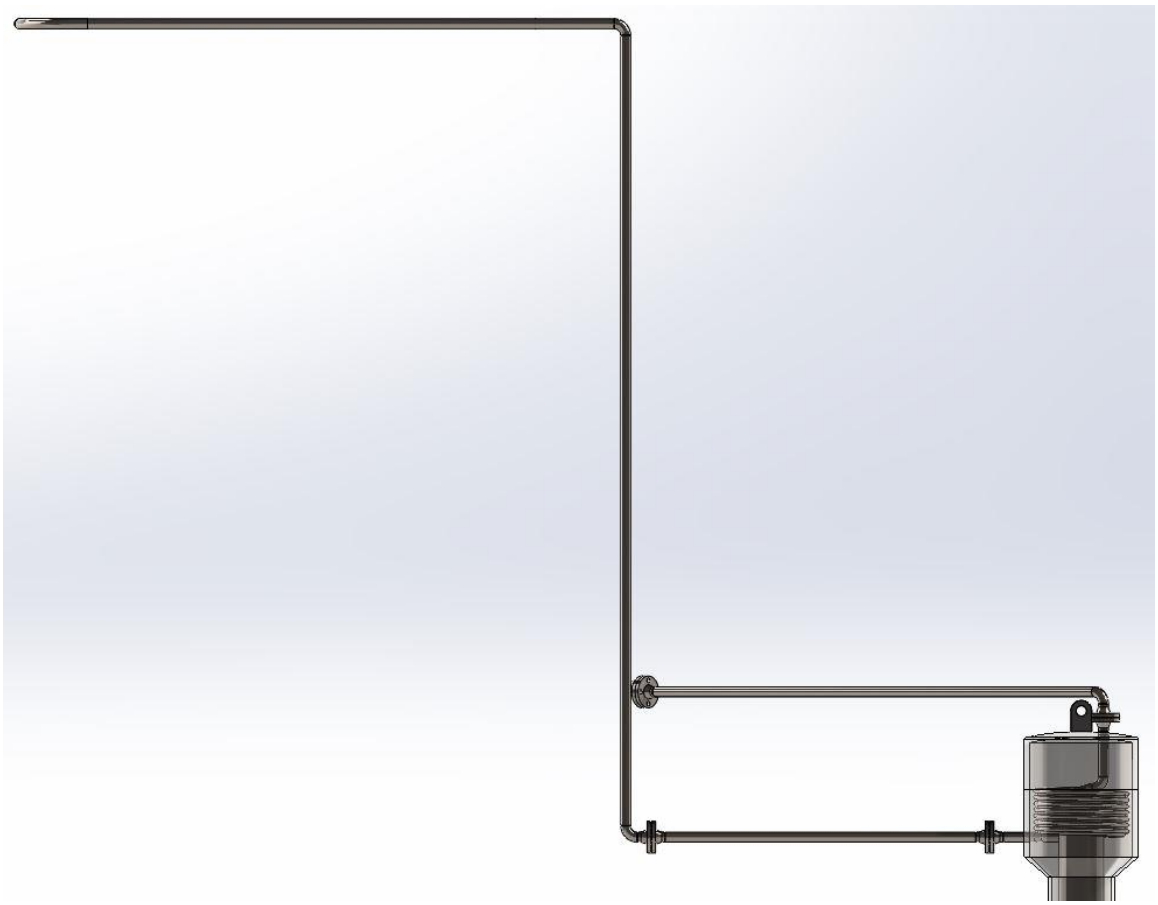

Figure 5-3: Intermediate loop piping in the scaled-down model

Operating characteristics were found using a python script which was written to more easily iterate necessary equations. The heat transfer rates across the DRACS need to be matched at steady state so no energy buildup occurs in any of the components. With the assumption that everything is well insulated such that the only heat transfer that occurs is across each heat exchanger, there are six heat transfer rates through the DRACS: heat transfer into the DHX from the direct loop, through the DHX, from the DHX to the intermediate loop, from the intermediate loop to the NDHX, through the NDHX, and finally from the NDHX to the natural draft loop. The bottom-up scaling analysis revealed that the scaling of the heat transfer rate into the DHX is different than the

scaling of the heat transfer rate from the DHX or to the NDHX. This means that if the full-scale model needs to be at steady-state, the scaled-down model will not be with the same conditions. The python script was therefore built to evaluate the full-scale model.

The geometry of the full-scale model was determined by scaling up the completed scaled-down model design. Heat transfer rates are dependent on the heat transfer coefficient which is determined through a Nusselt number correlation with Reynolds and Prandtl numbers. The Reynolds number is dependent on the flow conditions, whereas the Prandtl number is only dependent on pressure and temperature. The velocity at each point within each loop is found using a mass balance, with the inlet velocity, or mass flow rate, as a reference point. The inlet velocity is determined using equations (3.60) and (3.63) for the direct loop and intermediate loop respectively. These velocities are dependent on the loop resistance numbers, which are dependent on velocity through the friction factor.

This recursive relationship between friction factor and velocity required iteration, which was completed by using a while loop in python to check for convergence. After the proper velocity and Reynolds number was calculated for each loop, the heat transfer coefficient could be determined using the proper Nusselt number correlation. The heat transfer rate could then also be calculated. The Reynolds number range for the direct loop allowed for a straightforward calculation of the friction factor using Reynolds number, shown in equation (5.1). The intermediate loop Reynolds numbers were high

enough that another correlation for the friction factor was necessary, which requires iteration, shown in equation (5.2).

$$f_D = \frac{64}{Re_D} \tag{5.1}$$

$$\frac{1}{\sqrt{f_i}} = -2\log\left(\frac{\varepsilon}{3.7D_h} + \frac{2.51}{Re\sqrt{f_i}}\right) \tag{5.2}$$

Temperatures were known at two places before starting this exercise – at the core outlet, which is assumed to be the same as the direct loop and DHX inlet, and an approximate ambient air temperature. The temperatures in between these two points had to be determined based on the target heat transfer rate through the DRACS. The target heat transfer rate will be the decay heat generation rate. The time selected to analyze is at the peak core outlet temperature for a D-LOFC. The transient is depicted in Figure 5-4. The decay power at the time of this peak core outlet temperature is approximately 2%. This 2% decay power is the point at which two DRACS modules are able to reject enough heat to turn the transient around, so a single DRACS module is capable of removing 1% of decay power. The operating power of the EM^2 is 500 MWt, leading to a target heat removal rate of 5 MW for a single DRACS module in the full-scale prototype.

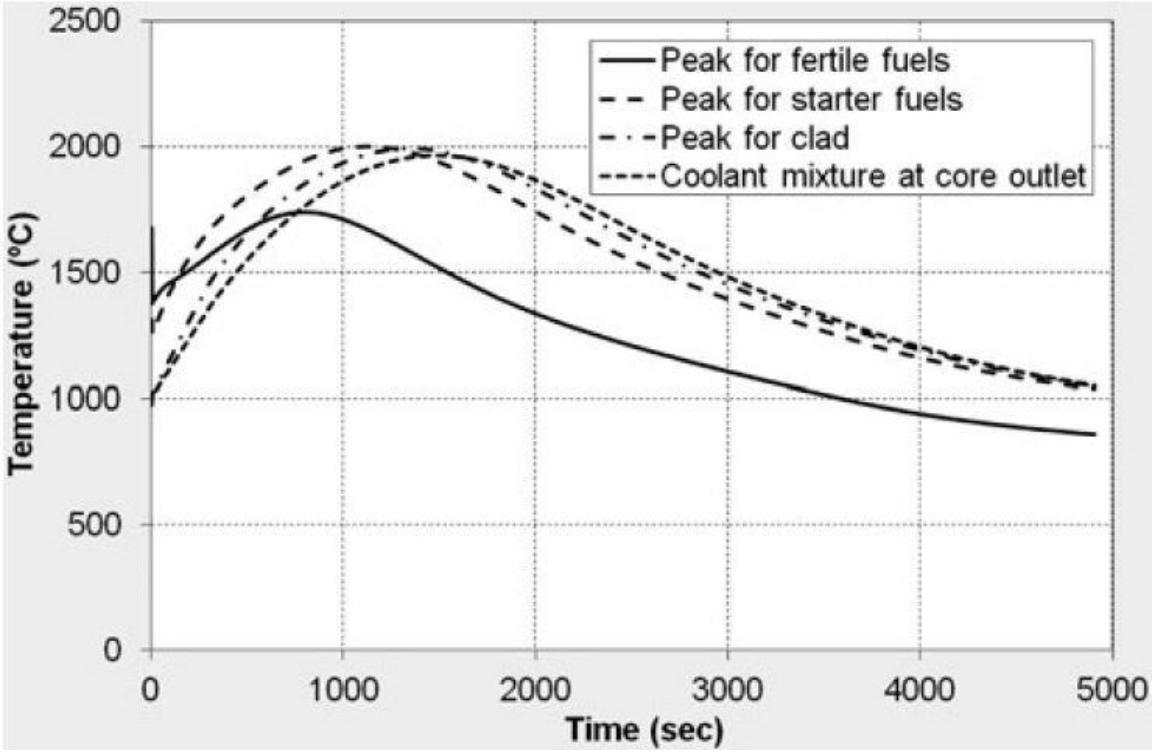

Figure 5-4: EM² depressurization accident with two DRACS modules operating in passive mode

In order to find what the temperature drop needs to be within each loop across a heat exchanger, equation (3.73) is used. The specific heat capacity is the measure of the amount of energy required to raise a mass of fluid by a certain temperature, and this concept is the basis of equation (3.73). The direct loop outlet temperature, natural draft loop outlet temperature, and the difference between hot and cold temperature in the intermediate loop were found using this equation.

The desired average bulk fluid temperature in the intermediate loop was then found by balancing the heat transfer rate from the direct loop to the intermediate loop and from the intermediate loop to the natural draft loop. The heat transfer rate from the direct loop to the intermediate loop is found by the difference between average bulk fluid

temperature in the direct loop and the intermediate loop multiplied by the inverse of the sum of the heat transfer resistances, shown in equation (5.3). Similarly, the heat transfer from the intermediate loop to the natural draft loop is shown in equation (5.4).

$$\dot{q}_{D,I} = \left(\frac{1}{h_{D,DHX}A_{s,D,DHX}} + \frac{t_{DHX}}{k_{DHX}A_{s,DHX}} + \frac{1}{h_{I,DHX}A_{s,I,DHX}}\right)^{-1}\left(T_{D,a} - T_{I,a}\right) \tag{5.3}$$

$$\dot{q}_{I,ND} = \frac{\left(T_{I,a} - T_{ND,a}\right)}{\left(\frac{1}{h_{I,NDHX}A_{s,I,NDHX}} + \frac{t_{NDHX}}{k_{NDHX}A_{s,NDHX}} + \frac{1}{h_{ND,NDHX}A_{s,ND,NDHX}}\right)} \tag{5.4}$$

The heat transfer rates for each of these should be equal for a steady-state formulation, so the two equations are set equal to one another. The average bulk fluid temperature in the intermediate loop is then isolated to find the target value. Equations (5.5) and (5.6) define the overall heat transfer coefficients for the DHX and NDHX respectively. These are then used to shorten the result of the isolation described above, where the target intermediate fluid average bulk temperature is shown in equation (5.7).

$$UA_{DHX} = \left(\frac{1}{h_{D,DHX}A_{s,D,DHX}} + \frac{t_{DHX}}{k_{DHX}A_{s,DHX}} + \frac{1}{h_{I,DHX}A_{s,I,DHX}}\right)^{-1} \tag{5.5}$$

$$UA_{NDHX} = \left(\frac{1}{h_{I,NDHX}A_{s,I,NDHX}} + \frac{t_{NDHX}}{k_{NDHX}A_{s,NDHX}} + \frac{1}{h_{ND,NDHX}A_{s,ND,NDHX}}\right)^{-1} \tag{5.6}$$

$$T_{I,a} = \frac{T_{D,a} + T_{ND,a}\left(\frac{UA_{NDHX}}{UA_{DHX}}\right)}{1 + \left(\frac{UA_{NDHX}}{UA_{DHX}}\right)} \tag{5.7}$$

The intermediate loop bulk fluid hot and cold temperatures are then found using equations (3.73) and (5.7) for the target heat transfer rate. The difference in bulk fluid temperature found in equation (3.73) is centered around the average temperature found in equation (5.7). All of the target temperatures must of course be iterated on as the mass flow rate, heat transfer coefficients, thermal conductivities, and specific heat capacities are dependent on temperature. This iteration was also completed using the python script mentioned previously, which can be found in Appendix A.

At each input temperature, thermo-physical properties needed to be entered in order for the script to be able to produce new target temperatures. These thermo-physical properties were found for the fluids in each loop using Engineering Equation Solver (EES), a program generally used for thermodynamic calculations. The script used to look up thermo-physical properties in EES is included in Appendix B.

All relevant information for the full-scale RELAP5-3D model was compiled in a spreadsheet. The compiled information was then easily entered in a RELAP5-3D model. The direct loop is modeled according to the flow path developed in the scaled-down model in SolidWorks, starting at the first elbow in the inlet flow path above the tee and reducer, and ending with the flange which connects to the outlet port. Boundary conditions are created and attached to these two points using a time-dependent volume and time-dependent junction. The boundary volume specifies pressure and temperature of the incoming/outgoing flow, and the boundary junction specifies the mass flow rate. Non-condensable gas species are used for the direct and natural draft

loops in order to select the proper fluids; an 80:20 helium-nitrogen mixture is present in the direct loop as a D-LOFC after depressurization is being modeled, and air is the non-condensable gas in the natural draft loop. The flow rate and pressure remain constant throughout each loop in the input deck, whereas the temperature varies due to changes through the heat exchangers.

5.2.2. Model nodalization

RELAP5-3D models are made up of volumes and junctions which connect volume. A physical system is modeled in RELAP5-3D by dividing the system into cells or nodes. Each node should have similar properties and physical dimensions. Obvious places to break up a system are therefore at area changes or orientation breaks, or where there is a large pressure or temperature gradient. Nodalization in general can be quite a complex process, and there exist codes for the purpose of creating meshes to be fed into a code which will solve it.

Section 2.2.2.2 of the RELAP5-3D user's manual volume 5 contains nodalization guidelines. Nodalization should take into account 3 factors: the applicability of the constitutive models, run time, and spatial convergence. The constitutive models used for drag, heat and mass transfer were developed in terms of macroscale parameters. To help with this, it is recommended that the node length-to-diameter ratio be greater than or equal to unity [68]. It is also recommended that nodes of interest have a length of 1-3 m, with larger less important nodes. Nodalization diagrams for the direct, intermediate, and natural draft loops follow as Figure 5-5, Figure 5-6, and Figure 5-7.

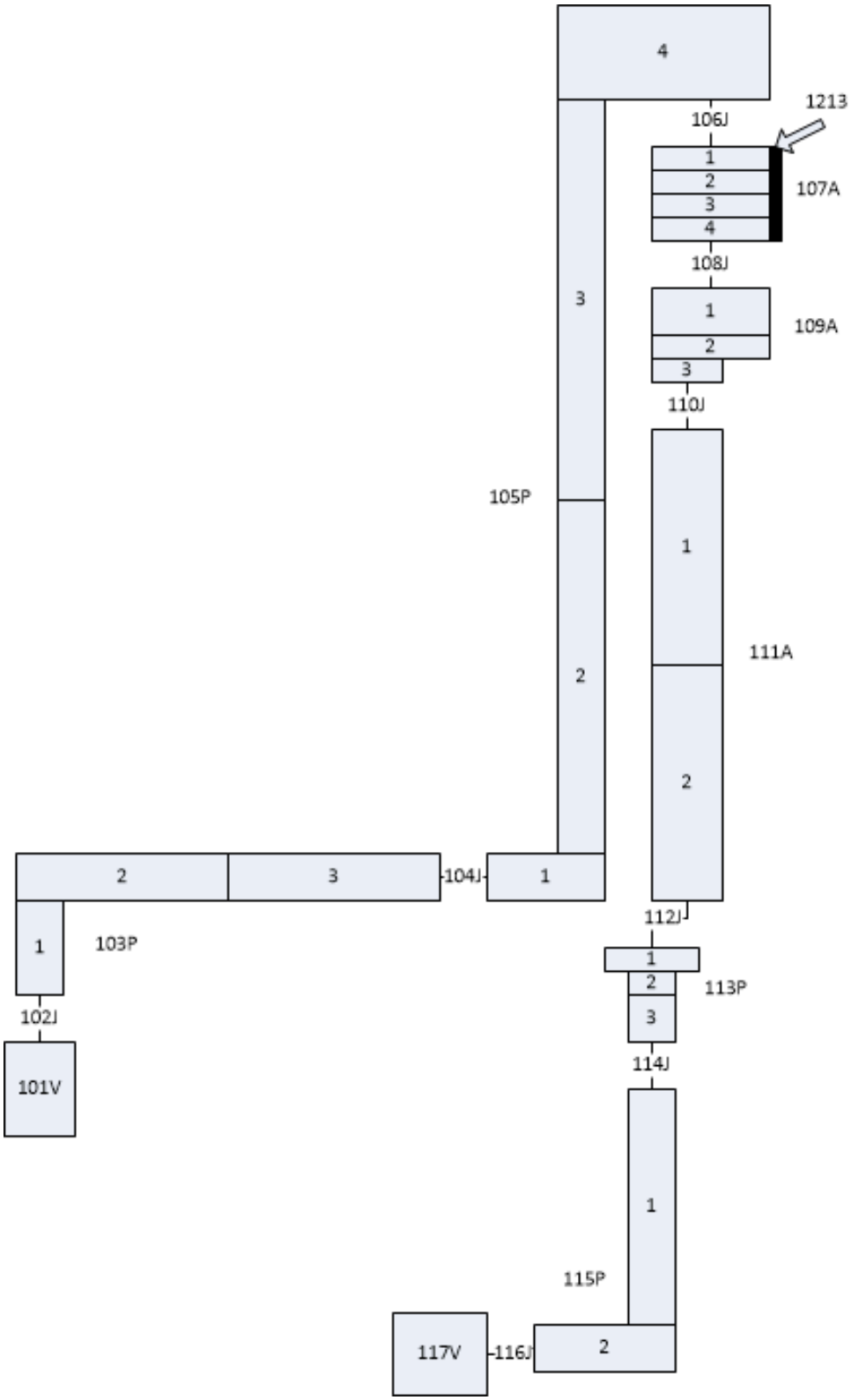

Figure 5-5: Direct loop nodalization diagram

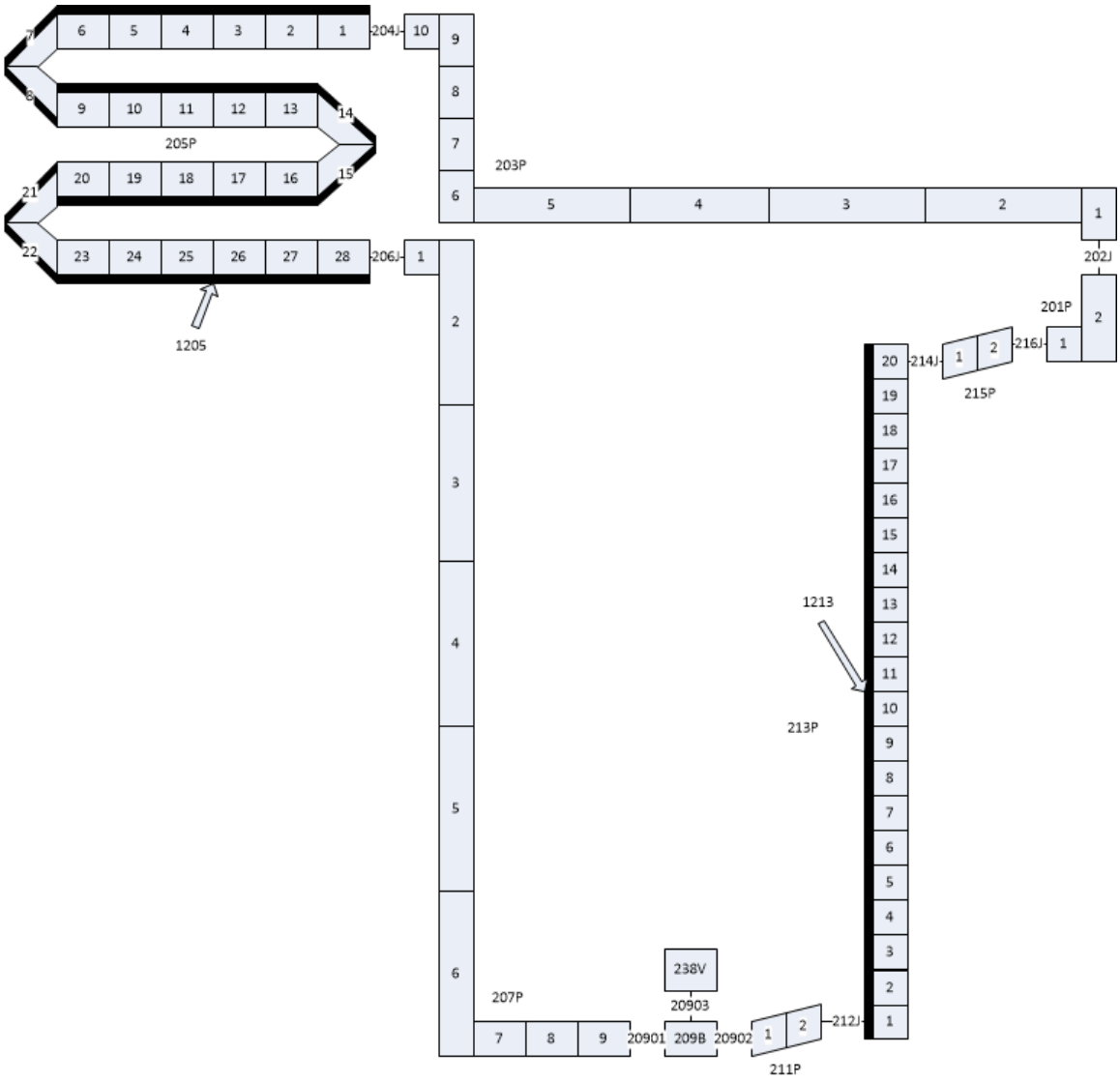

Figure 5-6: Intermediate loop nodalization diagram

The nodalization of these three loops was kept consistent between full-scale prototype and scaled-down model. This choice is appropriate as the length and diameter scaling are the same, and therefore the length-to-diameter ratio of each node is preserved between model and prototype. Preserving the nodalization also simplified deck building for the two models as corresponding components shared volume numbers between scaled-down and full-scale.

Certain components have unique nodalization imposed on them for specific reasons. The reducers in the direct loop are one example, where the length of each volume is smaller than the diameter. The main issue is that the overall length of these reducers is smaller than the diameter already, but this is compounded by the fact that the diameter is changing. In order to inform RELAP5-3D of the smooth area change across these reducers, they were each broken into two volumes, one with the largest area, the other with the smallest area.

The heat exchangers also provide interesting nodalization problems. In each case, the flow length through the inside of the tubes is greater than the flow length over the outside of the tubes. In order to get volume lengths within the desired range of one to three meters for the inside flow, the DHX was divided into 20 volumes while the NDHX was divided into 28 volumes, both in the intermediate loop. Section 8.3.2.7 describes the modeling of the helical coil heat exchanger, which is not supported in RELAP5-3D.

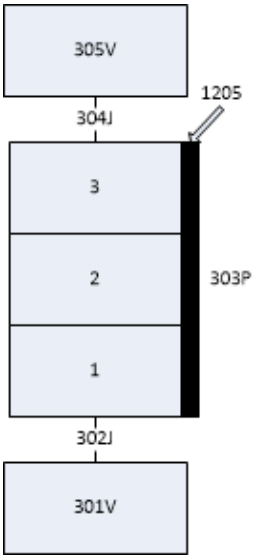

Figure 5-7: Natural draft loop nodalization diagram

Meanwhile, the direct side of the DHX is divided into four volumes, which each have a fairly short flow length, rather than leave it as a single hydrodynamic volume to be connected to all 20 axial heat structures. Likewise, the NDHX was divided into only 3 volumes, and in the end only the middle volume is connected to the 28 axial heat structures associated with the NDHX.

The natural draft loop is to be modeled with a forced draft heat exchanger in the scaled-down model, and the natural draft loop model in RELAP5-3D was kept very simple in order to only model those parts of the system which remain similar. The NDHX is a finned-tube heat exchanger which sits horizontally near the base of the cooling tower in the prototype. The three volumes correspond with just fins, tubes with fins, and again only fins. The scaled-down model is also a horizontally-oriented air-cooled heat exchanger. Where the two differ is mainly outside of the heat exchanger, so only boundary volumes and junctions are connected to the single pipe component.

Detailed discussion on each component within the RELAP5-3D models is contained in Appendix C. The description is only given once as everything remains consistent between the two models except for the scaled values. Tables are also presented which compare the values entered for the scaled-down and full-scale models.

5.3.Results

Models have been constructed in RELAP5-3D as discussed above for both the scaled-down and full-scale DRACS for a GFR. These models have been built based on a design of the scaled-down DRACS to be compatible with the HTTF. Information which was

available and compatible with the HTTF was used in order to inform that model. For example, it is known that the prototypical DRACS uses a concentric duct for the direct loop piping between the RPV and the DHX, but this was not possible in the scaled-down model for the entire flow path as the pressure vessel of the HTTF did not have the proper connection point available for such a duct. The duct was made concentric from the point that the inlet and outlet pipes met, and through the DHX module, where it is most important to preserve the flow path because the heat transfer through the DHX is of a primary concern. Other information was utilized fully, such as water as the fluid for the intermediate loop, and the intermediate and natural draft loop heights.

Both RELAP models use the same flow paths, and all dimensions are scaled according to the scaling analysis performed in chapter 3. Initial conditions were found by calculations previous to building the models using a python script, contained in appendix A, and an EES script, contained in appendix B. The RELAP5-3D input deck for the full-scale model is contained in appendix D, while the RELAP5-3D input deck for the scaled-down model is contained in appendix E. The results of these RELAP5-3D models are used to inform the scaling analysis by comparing the results of the full-scale to scaled-down for those characteristic ratios and operating characteristics.

The following tables contain the results at the final time step of the input decks as shown in appendices D and E. Each model is run as a transient with constant boundary conditions in order to find a steady-state solution. The total transient time for these simulations was 8,000 seconds in the scaled-down and 16,000 seconds in the full-scale

model, according to the scaling of the time scale as shown in equation (3.111). The simulations were run in ATHENA-3D version 2.4.1. The capabilities of ATHENA have been wrapped into RELAP5-3D since version 2.3. These capabilities include the use of new working fluids and the capability to mix non-condensable gas species with water in the vapor/gas phase [69]. Outputs of the RELAP5-3D models are presented, followed by a comparison of these results to the theoretical scaling.

Table 5-1: RELAP5-3D model results for characteristic ratios of both models

Characteristic ratio	Full-scale	Scaled-down
Direct loop Richardson number	0.0164	0.0165
Intermediate loop Richardson number	0.164	0.220
Natural draft loop Richardson number	0.00936	0.00936
Direct loop DHX number	0.999	1.000
Intermediate loop DHX number	0.0120	0.0113
Intermediate loop NDHX number	0.0120	0.0113
Natural draft loop NDHX number	0.199	0.197
Intermediate loop velocity ratio	0.0147	0.0125
Natural draft loop velocity ratio	0.274	0.274

Table 5-2: RELAP5-3D model results for dimensionless numbers of both models

Derived dimensionless number	Full-scale	Scaled-down
Direct DHX Reynolds number	2,111.644	263.950
Intermediate DHX Reynolds number	30,569.737	3,260.307
Intermediate NDHX Reynolds number	70,545.546	7,523.785
Natural draft NDHX Reynolds number	52,136.176	6,515.300
Direct loop Prandtl number	0.514	0.514
Intermediate loop Prandtl number	3.377	3.377
Natural draft loop Prandtl number	0.724	0.724

Table 5-3: RELAP5-3D model results for operating characteristics of both models

Operating characteristic	Full-scale	Scaled-down
Direct loop pressure [Pa]	450,012	450,007
Intermediate loop pressure [Pa]	13,990,900	13,997,600
Natural draft loop pressure [Pa]	95,998	95,999
Direct loop temperature hot [K]	2273.2	2273.2
Direct loop temperature cold [K]	2220.9	2220.9
Intermediate loop temperature hot [K]	325.72	325.72
Intermediate loop temperature cold [K]	314.45	312.42
Natural draft loop temperature hot [K]	300.52	300.53
Natural draft loop temperature cold [K]	299.72	299.72
Direct loop density hot [kg/m^3]	0.11502	0.11502
Direct loop density cold [kg/m^3]	0.11772	0.11773
Intermediate loop density hot [kg/m^3]	992.82	992.87
Intermediate loop density cold [kg/m^3]	997.78	998.56
Natural draft loop density hot [kg/m^3]	1.1128	1.1128
Natural draft loop density cold [kg/m^3]	1.116	1.116
Direct loop dynamic viscosity [µPa s]	68.8787	68.8785
Intermediate loop dynamic viscosity [µPa s]	522.751	522.744
Natural draft loop dynamic viscosity [µPa s]	18.7126	18.7126
Direct loop inlet velocity [m/s]	16.595	8.2973
Intermediate loop section 1 velocity [m/s]	0.24373	0.10397
Natural draft loop inlet velocity [m/s]	4.5416	2.2702
Direct loop thermal conductivity [W/(m K)]	0.59195	0.59195
Intermediate loop therm. cond. [W/(m K)]	0.64257	0.64257
Natural draft loop therm. cond. [W/(m K)]	0.026027	0.0260271
Direct heat transfer rate to DHX [W]	207,546	6,492.6
Intermediate HT rate from DHX [W]	169,195	5,846.2
Intermediate HT rate to NDHX [W]	169,190	5,846.2
Natural draft HT rate from NDHX [W]	207,541	6,492.6

The characteristic ratios shown in Table 5-1 are those which can be constructed through the information contained in Table 5-3, which are the operating characteristics which are available through minor edit requests in RELAP. Information necessary to calculate resistance number is not available as outputs in RELAP5-3D. All characteristic ratios which deal only with geometry are correctly scaled. The resulting distortion factors of each of the applicable characteristic ratios are compared to the target in Table 5-4.

Table 5-4: Distortion factors of characteristic ratios

Characteristic ratio	Target distortion	Distortion	Error
Direct loop Richardson number	0	-0.0038	0.38%
Intermediate loop Richardson number	0	-0.3446	34.46%
Natural draft loop Richardson number	0	-0.0003	0.03%
Direct loop DHX number	0	-0.0011	0.11%
Intermediate loop DHX number	0	0.0630	6.30%
Intermediate loop NDHX number	0	0.0630	6.30%
Natural draft loop NDHX number	0	0.0113	1.13%
Intermediate loop velocity ratio	0	0.1468	14.68%
Natural draft loop velocity ratio	0	0.0002	0.02%

Table 5-5: Distortion factors of relevant non-dimensional numbers

Derived dimensionless number	Target distortion	Distortion	Error
Direct DHX Reynolds number	0.875	0.8750	0.00%
Intermediate DHX Reynolds number	0.875	0.8933	1.83%
Intermediate NDHX Reynolds number	0.875	0.8933	1.83%
Natural draft NDHX Reynolds number	0.875	0.8750	0.00%
Direct loop Prandtl number	0	0.0000	0.00%
Intermediate loop Prandtl number	0	0.0001	0.01%
Natural draft loop Prandtl number	0	0.0000	0.00%

Table 5-6: scaled-down to full-scale model ratio of operating characteristics

Operating characteristic	Target ratio	Ratio	Relative Error
Direct loop pressure	1:1	1:1.0000	0.00%
Intermediate loop pressure	1:1	1:0.9995	0.05%
Natural draft loop pressure	1:1	1:1.0000	0.00%
Direct loop temperature hot	1:1	1:1	0.00%
Direct loop temperature cold	1:1	1:1	0.00%
Intermediate loop temperature hot	1:1	1:1	0.00%
Intermediate loop temperature cold	1:1	1:1.0065	0.65%
Natural draft loop temperature hot	1:1	1:1.0000	0.00%
Natural draft loop temperature cold	1:1	1:1	0.00%
Direct loop density hot	1:1	1:1	0.00%
Direct loop density cold	1:1	1:0.9999	0.01%
Intermediate loop density hot	1:1	1:0.9999	0.01%
Intermediate loop density cold	1:1	1:0.9992	0.08%
Natural draft loop density hot	1:1	1:1	0.00%
Natural draft loop density cold	1:1	1:1	0.00%
Direct loop dynamic viscosity	1:1	1:1.0000	0.00%
Intermediate loop dynamic viscosity	1:1	1:1.0000	0.00%
Natural draft loop dynamic viscosity	1:1	1:1	0.00%
Direct loop inlet velocity	1:2	1:2.0000	0.00%
Intermediate loop section 1 velocity	1:2	1:2.3442	17.21%
Natural draft loop inlet velocity	1:2	1:2.0005	0.03%
Direct loop thermal conductivity	1:1	1:1	0.00%
Intermediate loop thermal cond.	1:1	1:1	0.00%
Natural draft loop thermal cond.	1:1	1:1.0000	0.00%
Direct heat transfer rate to DHX	1:32	1:31.9665	0.10%
Intermediate HT rate from DHX	1:32	1:28.9410	9.56%
Intermediate HT rate to NDHX	1:32	1:28.9401	9.56%
Natural draft HT rate from NDHX	1:32	1:31.9658	0.11%

Distortion factors are used in scaling to evaluate the fractional amount of conserved property transferred by specific processes in the prototype and model during the respective residence times. The distortion factor is defined in equation (5.8). A distortion factor of zero indicates that the process is ideally simulated in the model. Positive distortion factors indicate that the prototype transfers more of the conserved property by the specific process than the model, while a negative distortion factor indicates that the model transfers more of the conserved property by the specific process than the prototype.

$$DF = \frac{[\Pi_i]_P - [\Pi_i]_M}{[\Pi_i]_P} \tag{5.8}$$

Distortion factors are used to describe the characteristic ratios found in Table 5-4 as well as the non-dimensional numbers found in Table 5-5. The errors listed therein are the difference between the theoretical distortion factor and the distortion factor which resulted from RELAP5-3D output, as shown in equation (5.9). Distortion factors are not intended to compare single quantities which have units, but rather characteristic ratios which describe different processes. Distortion factors were therefore not used to evaluate the operating characteristics in the two models, but rather the scale ratios. These scale factors, along with relative error computed according to equation (5.10) are contained in Table 5-6.

$$Error = abs\left(DF_{theory} - DF_{RELAP}\right) \tag{5.9}$$

$$Rel.Error = \frac{abs(scale_{theory} - scale_{RELAP})}{scale_{theory}} \quad (5.10)$$

5.4. Discussion

The results of the characteristic ratio scaling are the most important, as it is the characteristic ratios that define how a system acts. A characteristic ratio value of much less than unity means that the process described by that characteristic ratio has little influence on the system. A characteristic ratio value of much greater than unity means that the process described by that characteristic ratio dominates the system. A value on the order of unity means that the process contributes to the system and can remain in balance with other processes.

The first three characteristic ratios listed in Table 5-4 are the Richardson numbers for the direct, intermediate, and natural draft loops. These characteristic ratios are given by equations (3.15), (3.33), and (3.54) respectively. The Richardson number is the ratio of buoyant term to flow gradient term, and it describes how buoyancy-driven the flow is. This number depends on density differences across a loop, the loop height, acceleration due to gravity, density at the reference point, and velocity at the reference point. Of these values, the densities and velocities are outputs available in RELAP5-3D, and are therefore the only values capable of contributing to the error from theoretical distortion.

The direct loop Richardson number has an error from the theoretical distortion factor of less than a half of a percent. This error is minimal for a quantity which is a composite of

three separate values which could potentially contain improper distortion between the two models. The intermediate loop Richardson number had considerably less desirable results, with an error of just under thirty-four and a half percent. While the theoretical distortion factor was zero, the results from RELAP5-3D showed that the scaled-down intermediate loop transfers momentum more than a third faster than the full-scale by means of buoyancy. The main contributor to this error was the intermediate velocity ratio, while the intermediate loop cold density played a minimal role and intermediate loop hot density played no role. Discussion on the intermediate loop velocity error follows. The natural draft loop Richardson number matches the theoretical value best of all, likely due to the simplicity of the model for that loop.

The following four characteristic ratios in Table 5-4 are the heat exchanger numbers, being the direct loop DHX number, intermediate loop DHX number, intermediate loop NDHX number, and natural draft loop NDHX number. These characteristic ratios are given by equations (3.24), (3.44), (3.45), and (3.64) respectively. The direct loop core heat transfer number is not available for comparison because the full direct loop was not modeled in RELAP5-3D. The distortion in the direct loop DHX number is close to the theoretical value found in Table 3-6. The distortion in the intermediate loop DHX and NDHX numbers are much farther from the theoretical value, with an error in each of just under six and a half percent. These numbers depend on the heat transfer rates to/from the respective heat exchangers, intermediate loop hot density and specific heat capacity, direct loop inlet velocity, intermediate loop section one flow area, and the

difference in temperature of the intermediate fluid from hot to cold. The relative error contributions for each of these dependencies can be seen in Table 5-6. The two quantities which contribute most to the error are the heat transfer rates and the temperature difference between intermediate loop hot and cold fluid. The natural draft loop NDHX number has a relatively small error, and the largest contributor is the heat transfer rate.

The final characteristic ratios which can be evaluated from the RELAP5-3D output are the intermediate and natural draft loop velocity ratios, which are the ratio of the respective loop velocity to direct loop velocity. These characteristic ratios arise from the common time scale between all three loops. The error in the intermediate loop velocity ratio is fairly large, and is the direct result of the error in the intermediate loop velocity scale, which can be seen in Table 5-6. The natural draft loop velocity ratio matches the theoretical scaling very well.

Table 5-5 contains the resulting distortion factors in some additional non-dimensional numbers which are important in the characterization of fluid flow and heat transfer, being Reynolds number and Prandtl number. Reynolds number is evaluated at the heat exchangers in each loop, using the diameter of the heat exchanger tubes as the characteristic length. Prandtl number does not include a characteristic length, so it is evaluated only once for each loop.

The distortion factor matches the theoretical value very well for both the Reynolds and Prandtl number in the direct and natural draft loops. The intermediate loop numbers had more error, though overall within reason for a RELAP5-3D model. The intermediate loop Reynolds numbers in both the DHX and NDHX experienced the same error of just under two percent, which was the result of the intermediate loop velocity error. The Prandtl number for each of the loops matched the theoretical distortion factor well.

Although the error was low for the Reynolds numbers, especially in the direct and natural draft loops, a different issue was revealed. The direct loop and intermediate loop Reynolds number scaling resulted in different flow regimes between the model and prototype. Table 5-2 shows the results from the RELAP5-3D models for these Reynolds numbers. The direct loop DHX Reynolds number shows that the flow past the DHX tubes in the full-scale model is in the transition region, while the scaled-down model is laminar flow. The intermediate loop DHX Reynolds number shows that the flow through the DHX tubes in the full-scale model is fully turbulent, while the scaled-down model is in the transition region from laminar to turbulent. A scaled facility will model the full-scale prototype well as long as the flow conditions are similar. When the flow regime changes between the two models, it becomes harder to predict the behavior in the prototype based on results from the scaled model.

Most of the operating characteristics matched the theoretical scaling very well. There are a few, however, which should be highlighted and discussed. The first, by order of appearance in Table 5-6, is the intermediate loop cold fluid temperature. The

intermediate loop hot temperature between the model and prototype was matched well, and the cold temperature was off ultimately due to the intermediate loop velocity scale results not matching the theoretical scaling. The difference in hot and cold fluid temperature is governed by equation (3.94). The intermediate loop velocity in the full-scale model was about seventeen percent higher than it should have theoretically been according to the scaling analysis. The temperature difference in the intermediate loop must therefore be lower than the theoretical scaling in order for equation (3.94) to be satisfied. The result is that the intermediate loop temperature difference is higher in the scaled-down model compared to the full-scale. The magnitude of the temperature difference scaling is not apparent from Table 5-6, but when the temperature differences are compared between full-scale and scaled-down models, the difference is about five percent from the theoretical scaling of 1:1.

The second operating characteristic with a significant scaling error is the intermediate loop cold density. The error shown in Table 5-6 appears insignificant as a result of being relative error with a large value for density. The significance of this error is best seen in the difference between the hot and cold density, which appears in the Richardson number. The scale of density difference in the intermediate loop between full-scale and scaled-down is about thirteen percent less than the theoretical scaling. This is the direct result of the temperature difference error as described above.

The third operating characteristic with a significant error is the intermediate loop velocity. This is the most significant error present as just about every other error

discussed hitherto can be traced back to it. The reason for the error is not entirely clear, though there are several possibilities that could have led to or contributed to the error. Each RELAP5-3D model deck was checked side-by-side for consistency between the scaled inputs without discrepancies. If the intermediate loop resistance number scaling between the two models does result in unity, this would change the velocity. The modeling of the DHX with a vertical pipe may not have matched the helical coil flow characteristics as well as desired, which could have changed both the velocity and the heat transfer rate. RELAP5-3D also has some modeling limitations which may have led to the error. One such limitation which was not discovered until after the completion of the modeling in RELAP5-3D is that for a closed loop with buoyancy driven flow, the elevation of node breaks need to match between the two sides of the loop. Finer nodes are allowed to break in between, but the breaks in the larger nodes should match up with a node break on the other side. If the nodes do not match up as described, it can lead to a false buoyancy term, which could have had a greater effect in one model compared to the other, leading to the discrepancy. This level nodalization restraint is not discussed in any sort of detail in the manuals, but it is demonstrated in the example nodalization of a PWR RPV in figure 2.2-3 of volume 5 of the code user's manual [68].

The last operating characteristics with significant error are the heat transfer rate from the DHX to intermediate fluid and from intermediate fluid to the NDHX. The error for each of these heat transfer rates is approximately the same, as the heat transfer rate values themselves were approximately the same in each model. One possible reason

that an error is present for the intermediate loop values and not the direct or natural draft loop values is that the Nusselt number correlations which RELAP5-3D used to find the heat transfer coefficient were different between the two sides of each heat exchanger. The default convection boundary condition was used for both sides of each heat exchanger, but the resulting code-selected correlations were different for the intermediate loop than the other loops.

In the output deck of each RELAP5-3D model, the heat transfer mode is shown for both sides of each heat structure. This heat transfer mode is given as a numerical code, and volume 4 of the user's manual presents models and correlations used in RELAP5-3D [70]. Section 4.2.1 lists correlations which are applied to heat transfer modes 1-12. ATHENA provides additional heat transfer modes for working fluids other than light water.

The heat transfer mode used for the intermediate loop in both heat exchangers was mode 2, which is single-phase liquid convection at subcritical pressure, for subcooled wall and low void fraction. The correlation used in this heat transfer mode is the maximum of the Nusselt number correlation results for forced turbulent, forced laminar, or free convection flow. The forced turbulent flow uses the Dittus-Boelter correlation with the McAdams coefficient, and the exponent on the Prandtl number is coded for heating fluid always. This equation is shown as equation (5.11). The forced laminar correlation assumes a constant wall heat flux, shown in equation (5.12). The free convection correlation uses the Churchill-Chu correlation, shown in equation (5.13).

$$Nu = 0.023Re^{0.8}Pr^{0.4} \tag{5.11}$$

$$Nu = 4.36 \tag{5.12}$$

$$Nu = \left\{ 0.825 + \frac{0.387(Ra)^{\frac{1}{6}}}{\left[1 + \left(\frac{0.492}{Pr}\right)^{\frac{9}{16}}\right]^{\frac{8}{27}}} \right\}^2 \tag{5.13}$$

While information is available in volume 4 of the RELAP5-3D code manual on the correlations used in the intermediate loop, information is not given for the ATHENA heat transfer modes, including 20 and 21, which appear in the output deck as the heat transfer modes for the direct loop and natural draft loop respectively. The difference in heat transfer modes, and therefore correlations, is likely why the direct and natural draft loops were much closer to the theoretical scaling values for heat transfer rate than the intermediate loop.

6. Conclusions

The DRACS is a passive safety system, capable of removing decay heat from the reactor core in a manner that is direct and does not depend on other systems or components. The DRACS has been researched liquid metal and fluoride salt-cooled reactors, and the work presented in this thesis aims to advance the knowledge level of the DRACS for gas-cooled reactors. A scaling analysis has been performed for the DRACS in the EM^2 and applied to a basic design for the inclusion in the HTTF at OSU. RELAP5-3D models have been built based on the full-scale and scaled-down designs in order to inform the scaling analysis.

The state-of-the-art has been established related to the work being performed by a review of recent and previous literature on the topics of reactor designs which include the DRACS, general scaling methodologies, successful applications of the H2TS methodology, previous scaling analyses and test facilities for and related to the DRACS, and computer modeling of the DRACS.

A preliminary PIRT was developed for the DRACS in gas-cooled reactors in order to inform the scaling analysis.

The scaling analysis results are summed up by the list of characteristic ratios and the scaling values between model and prototype for operating characteristics and the characteristic ratios. The characteristic ratios govern the function of the system through the processes they describe, and the relative size of each for a given system show which processes are most important. The list of characteristic ratios revealed during the

scaling analysis are presented with their names and formulae in Table 3-2. The scaling ratio results during a D-LOFC after depressurization are presented in Table 3-5

The prototypical DRACS in the EM^2 was investigated in some detail in chapter 4, and inferences were made based on what information is available in public literature. This information was applied to a scaled-down conceptual design to be compatible with the HTTF at OSU. The differences between the prototype and scaled-down conceptual model were investigated as there are some things about the HTTF which cannot be altered for the addition of a DRACS module. An instrumentation plan was presented for the conceptual scaled-down DRACS model, with a summary in Table 4-1. SolidWorks models were completed to support this scaled-down facility addition, and the parts drawings are included in appendix E. This SolidWorks modeling, along with a script written in python, established the dimensions and operating characteristics of the DRACS models to be investigated as part of this work.

The outputs from the design requirements section, including the SolidWorks and python results were used to build models in RELAP5-3D of the full-scale and scaled-down model. These models are described in some detail, and the nodalization of each loop is shown in section 5.2.2. The outputs from these RELAP5-3D models were used to inform the scaling analysis. These results are presented in Table 5-1, Table 5-2, and Table 5-3. The scaling between the two models for each value are presented and compared to the theoretical value in Table 5-4, Table 5-5, and Table 5-6.

The results from the RELAP5-3D models showed good agreement with the theoretical scaling for the most part. There were some values which had significant error when compared to the theoretical scaling/distortion factor. In terms of operating characteristics, these included the intermediate loop velocity, intermediate loop cold fluid temperature and density, and the heat transfer rates from the DHX to the intermediate fluid and from the intermediate fluid to the NDHX. These operating characteristics also led to significant errors in the intermediate loop Reynolds numbers, Richardson number, DHX number, NDHX number, and intermediate loop velocity ratio. The improperly scaled velocity between the two RELAP5-3D models is cited as the root of most of the other issues, with the heat transfer rates being the main cause of the error in the intermediate loop DHX and NDHX numbers.

The reason for the velocity error in the intermediate loop is unknown, but there are a few possibilities. The intermediate loop resistance number may not be properly scaled between the two models, which cannot be checked from the outputs. The way that the DHX was modeled in RELAP5-3D as a vertical pipe may have also led to issues due to the flow characteristics not matching the helical coil as well as desired. RELAP5-3D also experiences numerical instabilities if the elevation of node breaks do not match on the upward and downward sides, leading to a false buoyancy term. RELAP5-3D does have limits to its modeling capability, and this specific model does not account for them all.

The target heat transfer rate scaling throughout the DRACS has a target Nusselt number in order to meet the requirements, shown in equation (3.105). The heat transfer

correlations selected by the code for the intermediate loop were different than those selected for the direct and natural draft loops. It is assumed that this leads to the inconsistent scaling in heat transfer rates between the intermediate loop and the two gas-filled loops. The intermediate loop velocity error likely also plays into the discrepancy, as it is included in Reynolds number, which is used in the Dittus-Boelter Nusselt number correlation.

All of the geometrically based characteristic ratios were preserved, as these were locked in by the design and did not change during the RELAP5-3D transient runs. The characteristic ratios which were based on RELAP5-3D outputs had generally poor results when compared to the scaling analysis results, with the exceptions of the direct loop Richardson number and the direct loop DHX number. The reason why the characteristic ratios saw larger errors than the individual operating characteristics is that they are composites of several values each, and the errors compound. The largest contribution to error was the intermediate loop velocity scale.

Overall the RELAP5-3D results support the scaling analysis performed. In the design of the final scaled-down facility, particular care should be given to preserving the direct and intermediate loop resistance numbers in order to ensure the velocity scaling is properly modeled. The target heat transfer rate scaling ratios may be difficult to match in the scaled-down facility as different Nusselt number correlations are valid for different fluid flow conditions. Scaling of each side of each heat exchanger may need to be adjusted from the default length and diameter scaling in order to achieve the proper

heat transfer rate scaling. Just as fins were added to the outside of the NDHX tubes to increase surface area such that the target heat transfer rate could be matched, geometry may be necessary to adjust in order to compensate for improper scaling of the Nusselt number according to local flow conditions.

The importance of collecting low distortion data in integral effects test has been expressed [29]. The HTTF is an integral test facility, and with the inclusion of a scaled DRACS, would be capable of performing integral effects tests to produce data for the DRACS module inclusion in the EM^2 design, and potentially other advanced gas reactors. This data could contribute to the licensing of the EM^2 design. Future work includes improvement and implementation of a scaled-down DRACS module design to be included in the HTTF so validation data can be collected for DRACS in gas-cooled reactors. Future work should also include a full scaling analysis for this scaled design under scenarios other than the D-LOFC, such as normal operations heat leakage and P-LOFC.

7. References

[1] P. Hejzlar, R. Petroski, J. Cheatham, N. Touran, M. Cohen, B. Truong, R. Latta, M. Werner, T. Burke, J. Tandy, M. Garrett, B. Johnson, T. Ellis, J. McWhirter, A. Odedra, P. Schweiger, D. Adkisson and J. Gilleland, "TerraPower, LLC Traveling Wave Reactor Development Program Overview," *Nuclear Engineering and Technology,* pp. 731-744, 2013.

[2] International Atomic Energy Agency, "Status of Small and Medium Sized Reactor Designs," 2012.

[3] R. W. Schleicher, "Climate Change and the Role of Nuclear Energy," in *Canon Institute for Global Studies Climate Change Symposium*, 2015.

[4] R. W. Schleicher, H. Choi and J. Rawls, "The Energy Multiplier Module: Advancing the Nuclear Fuel Cycle Through Technology Innovations," *Nuclear Technology,* vol. 184, no. 2, pp. 169-180, 2013.

[5] J. M. Acton and M. Hibbs, "Why Fukushima was Preventable," The Carnegie Papers, Washington DC, 2012.

[6] United States Nuclear Regulatory Commission, "Backgrounder on the Three Mile Island Accident," Washington DC, 2013.

[7] H. Planchon, R. Singer, D. Mohr, E. Feldman, L. Chang and P. Betten, "The Experimental Breeder Reactor II Inherent Shutdown and Heat Removal Tests - Results and Analysis," in *Proceedings of the International Topical Meeting on Fast Reactor Safety*, Knoxville, Tennesee, 1985.

[8] C. W. Forsberg, "Alternative Passive Decay-Heat Systems for the Advanced High-Temperature Reactor," in *Proceedings of ICAPP '06*, Reno, NV, 2006.

[9] C. Forsberg, P. Peterson and R. Kochendarfer, "Design Options for the Advanced High-Temperature Reactor," in *Proceedings of ICAPP '08*, Anaheim, CA, 2008.

[10] J. Brunings, J. Hartung, J. Mills and E. Moody, "Direct Reactor Auxiliary Cooling System for the 1000-MWe LMFBR Development Plant," in *Joint ASME/IEEE Power Generation Conference*, St. Louis, Missouri, 1981.

[11] R. Lancet and J. Marchaterre, "Inherent Safety of the SAFR Plant," in *Proceedings of the Internation Topical Meeting on Fast Reactor Safety*, Knoxville, Tennessee, 1985.

[12] Q. Lv, X. Wang, I. Kim, X. Sun, R. Christensen, T. Blue, G. Yoder, D. Wilson and P. Sabharwall, "Scaling Analysis for the Direct Reactor Auxiliary Cooling System for FHRs," *Nuclear Engineering and Design,* pp. 197-206, 2015b.

[13] R. Doncals, J. Schmidt, R. Markley, J. Kalinowski, R. Coffield, J. Lake and R. Sievers, "The Westinghouse Approach to an Inherently Safe Liquid Metal Reactor Design," in *Proceedings of the International Topical Meeting on Fast Reactor Safety*, Knoxville, Tennessee, 1985.

[14] C. P. Tzanos and D. R. Pedersen, "Analysis of DRACS and DRACS-RVACS Decay Heat Removal Experiments," *Nuclear Technology,* pp. 253-265, 1991.

[15] C. Grandy, T. K. Kim, E. Jin, M. Farmer, H. Belch, J. Grudzinski, T. Sumner, Y. Momozaki, L. Krajtl, C. Gerardi, Y. Tang, T. Moran, A. Moisseytsev, R. Vilim, T. Wei, R. Seidensticker and C. Youngdahl, "A 100 MWe Advanced Sodium-cooled Fast Reactor (AFR-100)," Paris, 2013.

[16] M. Pope, J. Lee, P. Hejzlar and M. Driscoll, "Thermal Hydraulic Challenges of Gas Cooled Fast Reactors with Passive Safety Features," *Nuclear Engineering and Design,* pp. 840-854, 2009.

[17] F. Namekawa, K. Ogura and K. Mawatari, "Thermal Hydraulic Phenomena During Decay Heat Removal with Natural Circulation in an LMFBR," in *Proceedings of the International Topical Meeting on Fast Reactor Safety*, Knoxville, Tennessee, 1985.

[18] A. Levin, J. Carbajo, D. Lloyd, B. Montgomery, S. Rose and J. Wantland, "Results of Natural Circulation Tests in Simulated LMFBR Fuel Assemblies and Their Relation to Decay Heat Removal System Design," in *Proceedings of the International Topical Meeting on Fast Reactor Safety*, Knoxville, Tennessee, 1985.

[19] K. Hallinan and R. Viskanta, "Heat transfer from a vertical tube bundle under natural circulation conditions," *International Journal of Heat and Fluid Flow,* pp. 256-264, 1985.

[20] K. Hallinan and R. Viskanta, "Dynamics of a Natural Circulation Loop: Analysis and Experiments," *Heat Transfer Engineering,* pp. 43-52, 1986.

[21] T. Murakami, Y. Eguchi, K. Oyama and O. Watanabe, "Reduced-scale Water Test of Natural Circulation for Decay Heat Removal in Loop-type Sodium-cooled Fast Reactor," *Nuclear Engineering and Design,* pp. 220-231, 2015.

[22] A. Ono, H. Kamide, J. Kobayashi, N. Doda and O. Watanabe, "An Experimental Study on Natural Circulation Decay Heat Removal System for a Loop Type Fast Reactor," *Journal of Nuclear Science and Technology,* pp. 1-12, 2016.

[23] H. Zhang, H. Zhao, V. Mousseau and R. Szilard, "Design Considerations for Economically Competitive Sodium Cooled Fast Reactors," in *Proceedings of ICAPP '09*, Tokyo, 2009.

[24] H. Zhao, H. Zhang, L. Zou and X. Sun, "Enhancing VHTR Passive Safety and Economy with Thermal Radiation Based Direct Reactor Auxiliary Cooling System," in *Proceedings of ICAPP '12*, Chicago, IL, 2012.

[25] Z. Zhai, K. Zhu and S. Fu, "Experimental Study of Effects of Cross Wind on Flow in Natural-draft Dry-cooling Towers," *Tsinghua Science and Technology,* pp. 955-958, 1998.

[26] Z. Zhai and S. Fu, "Improving cooling efficiency of dry-cooling towers under cross-wind conditions by using wind-break methods," *Applied Thermal Engineering,* pp. 1008-1017, 2006.

[27] K. Tanimizu and K. Hooman, "Natural draft dry cooling tower modelling," *Heat Mass Transfer,* pp. 155-161, 2013.

[28] J. Rawls, Z. Johal and J. Parmentola, "Improving the Economics and Long-Term Sustainability of Nuclear Power," *Energy Development Frontier,* pp. 20-29, 2014.

[29] A. R. C. T. R. Panel, "Evaluation and Identification of future R&D on eight Advanced Reactor Concepts," 2012.

[30] X. Wang, Q. Lv, X. Sun, R. Christensen, T. Blue, G. Yoder, D. Wilson and P. Sabharwall, "Scaling Analysis for the Direct Reactor Auxiliary Cooling System for AHTRs," in *Transactions of the American Nuclear Society*, Washington, D.C., 2011b.

[31] X. Wang, Q. Lv, X. Sun, R. Christensen, T. Blue, G. Yoder, D. Wilson and P. Sabharwall, "Design of a Scaled-down DRACS Test Facility for an AHTR," in *Transactions of the American Nuclear Society*, Washington, D.C., 2011c.

[32] Q. Lv, X. Wang, I. Adams, X. Sun, R. N. Christensen, T. E. Blue, G. Yoder, D. Wilson and P. Sabharwall, "Design of a Scaled-down Low-temperature DRACS Test Facility for an AHTR," *Transactions of the American Nuclear Society,* vol. 106, pp. 1071-1074, 2012.

[33] Q. Lv, X. Sun, R. Christensen, T. Blue, G. Yoder and D. Wilson, "Final Report: Design, Testing, and Modeling of the Direct Reactor Auxiliary Cooling System for AHTRs," 2015c.

[34] T. Sandke, "Quarterly Technical Progress Report, January-March, 1980," General Electric, 1980.

[35] A. Rascoe, "U.S. Approves First New Nuclear Plant in a Generation," *Reuters Technology,* 9 February 2012.

[36] Q. Lv, H. Lin, I. Kim, X. Sun, R. Christensen, T. Blue, G. Yoder, D. Wilson and P. Sabharwall, "DRACS Thermal Performance Evaluation for FHR," *Annals of Nuclear Energy,* pp. 115-128, 2015a.

[37] B. Farrar, J. Lefevre, S. Kubo, C. Mitchell, Y. Yoshinari and S. Itooka, "Fast Reactor Decay Heat Removal: Approach to the Safety System Design in Japan and Europe," *Nuclear Engineering and Design 193,* pp. 45-54, 1999.

[38] N. Zuber, G. E. Wilson, M. Ishii, W. Wulff, B. E. Boyack, A. E. Dukler, P. Griffith, J. M. Healzer, R. E. Henry, J. R. Lehner, S. Levy, M. F. J, M. Pilch, B. R. Sehgal, B. W. Spencer, T. G. Theofanous and J. Valente, "An Integrated Structure and Scaling Methodology for Severe Accident Technical Issue Resolution: Development of Methodology," *Nuclear Engineering and Design,* no. 186, pp. 1-21, 1998.

[39] N. Zuber, "Appendix D: A Hierarchal, Two-Tiered Scaling," in *An Integrated Structure and Scaling Methodology for Severe Accident Technical Issue Resolution (NUREG/CR-5809)*, 1991.

[40] N. Zuber, W. Wulff, U. S. Rohatgi and L. Catton, "Application of Fractional Scaling Analysis (FSA) to Loss of Coolant Accidents (LOCA), Part 1: Methodology

Development," in *Proceedings of the International Topical Meeting on Nuclear Reactor Thermal Hydraulics (NURETH-11)*, Avignon, France, 2005.

[41] W. Wulff, N. Zuber, U. S. Rohatgi and L. Catton, "Application of Fractional Scaling Analysis (FSA) to Loss of Coolant Accidents (LOCA) - Part 2: System Level Scaling for System Depressurization," in *Proceedings of the International Topical Meeting on Nuclear Reactor Thermal Hydraulics (NURETH-11)*, Avignon, France, 2005.

[42] L. Catton, W. Wulff, N. Zuber and U. S. Rohatgi, "Application of Fractional Scaling Analysis (FSA) to Loss of Coolant Accidents (LOCA), Part 3: Component Level Scaling for Peak Clad Temperature," in *Proceedings of the International Topical Meeting on Nuclear Reactor Thermal Hydraulics (NURETH-11)*, Avignon, France, 2005.

[43] N. Zuber, "The Effects of Complexity, of Simplicity and of Scaling in Thermal-Hydraulics," *Nuclear Engineering and Design,* vol. 204, pp. 1-27, 2001.

[44] F. D'Auria and G. M. Galassi, "Scaling in Nuclear Reactor System Thermal-Hydraulics," *Nuclear Engineering and Design,* vol. 240, pp. 3267-3293, 2010.

[45] D. A. Botelho, P. A. B. De Sampaio, M. d. L. Moreira and A. C. O. Barroso, "Fractional Scaling Analysis Applied to Scale a Pressurizer Test Facility," in *Proceedings of the 2007 International Nuclear Atlantic Conference (INAC 2007)*, Santos, SP, Brazil, 2007.

[46] J. N. Reyes Jr., "The Dynamical System Scaling Methodology," in *Proceedings of the International Topical Meeting on Nuclear Reactor Thermal Hydraulics (NURETH-16)*, Chicago, IL, USA, 2015.

[47] J. N. Reyes Jr. and L. Hochreiter, "Scaling Analysis for the OSU AP600 Test Facility (APEX)," *Nuclear Engineering and Design,* vol. 186, pp. 53-109, 1998.

[48] K. B. Welter, S. M. Bajorek, J. N. Reyes Jr., B. G. Woods, J. Groome, J. Hopson, E. Young, J. DeNoma and K. Abel, "APEX-AP1000 Confirmatory Testing to Support AP1000 Design Certification (Non-Proprietary), NUREG-1826," United States Nuclear Regulatory Commission, Washington D.C., 2005.

[49] J. N. Reyes Jr., "Integral System Experiment Scaling Methodology," in *IAEA Course on Natural Circulation in Water Cooled Nuclear Power Plants*, Trieste, Italy, 2004.

[50] S. M. Modro, J. E. Fisher, K. D. Weaver, J. N. Reyes Jr., J. T. Groome, P. Babka and T. M. Carlson, "Multi-Application Small Light Water Reactor Final Report," Idaho National Engineering and Environmental Laboratory, Idaho Falls, 2003.

[51] R. R. Schultz, P. D. Bayless, B. D. Hawkes, R. W. Johnson, J. R. Wolf and B. Woods, "Scaling Studies for High Temperature Test Facility and Modular High Temperature Gas-cooled Reactor," Idaho National Laboratory, Idaho Falls, 2012.

[52] X. Wang, Q. Lv, X. Sun, R. Christensen, T. Blue, G. Yoder, D. Wilson and P. Sabharwall, "A Modular Design of a Direct Reactor Auxiliary Cooling System for AHTRs," in *Transaction of the American Nuclear Society*, Hollywood, FL, 2011a.

[53] ASME Performance Test Codes Committee, Standard for Verification and Validation in Computational Fluid Dynamics and Heat Transfer, The American Society of Mechanical Engineers, 2009.

[54] B. Chan, J. Guppy and R. Kennett, "Direct Reactor Auxiliary Cooling System Modeling in SSC," in *Transactions of the American Nuclear Society, Winter Meeting*, 1981.

[55] A. Griveau, F. Fardin, H. Zhao and P. Peterson, "Transient Thermal Response of the PB-AHTR to Loss of Forced Cooling," in *Global 2007*, Boise, ID, 2007.

[56] S. J. Ball and S. E. Fisher, "Next Generation Nuclear Plant Phenomena Identification and Ranking Tables (PIRTs)," United States Nuclear Regulatory Commission, 2008.

[57] F. P. Incropera and D. P. DeWitt, Fundamentals of Heat and Mass Transfer, Wiley, 1990.

[58] R. Al-Waked and M. Behnia, "The performance of natural draft dry cooling towers under crosswind: CFD study," *International Journal of Energy Research,* pp. 147-161, 2004.

[59] R. Al-Waked and M. Behnia, "The Effect of Windbreak Walls on the Thermal Performance of Natural Draft Dry Cooling Towers," *Heat Transfer Engineering,* pp. 50-62, 2005.

[60] X. Du and M. Beyers, "Numerical Studies on Wind Effects on the Cooling Efficiency of Dry Cooling Towers," in *The Fifth International Symposium on Computation Wind Engineering (CWE2010)*, Chapel Hill, 2010.

[61] Y. Lu, Z. Guan and H. Gurgenci, "CFD simulations on small natural draft dry cooling towers," in *18th Australian Fluid Mechanics Conference*, Launceston, 2012.

[62] Y. Lu, Z. Guan, H. Gurgenci and Z. Zou, "Windbreak walls reverse the negative effect of crosswind in short natural draft dry cooling towers into a performace enhancement," *International Journal of Heat and Mass Transfer,* pp. 162-170, 2013.

[63] R. Zhang, X. Sun and Y. Dong, "The CFD Analysis of Hydrogen Behavior in HTR-PM During the Water-Ingress Accident Caused by Double-Ended Guillotine Break of Two Steam Generator Heating Tubes," in *Proceedings of the International Conference on Nuclear Engineering (ICONE-22)*, Prague, Czech Republic, 2014.

[64] Z. Wu, D. Lin and D. Zhong, "The Design Features of the HTR-10," *Nuclear Engineering and Design,* vol. 218, pp. 25-32, 2002.

[65] P. F. Peterson and H. Zhao, "Passive Decay Heat Removal for the Advanced High Temperature Reactor," U.C. Berkeley, Berkeley, 2004.

[66] N. E. Todreas and M. S. Kazimi, Nuclear Systems Volume 1: Thermal Hydraulic Fundamentals, Boca Raton, FL: Taylor & Francis Group, LLC, 2012.

[67] Idaho National Laboratory, "About RELAP5-3D," [Online]. Available: http://www4vip.inl.gov/relap5/relap5-3.htm. [Accessed 14 August 2016].

[68] R. R. Schultz, "Volume V: User's Guidelines," in *RELAP5-3D Code Manual*, Idaho Falls, ID, Idaho National Laboratory, 2005, pp. 1-616.

[69] R. A. Riemke, C. B. Davis and R. R. Schultz, "RELAP5-3D Code Includes Athena Features and Models," in *Proceedings of the International Conference on Nuclear Engineering - (ICONE 14)*, Miami, FL, 2006.

[70] The RELAP5-3D Code Development Team, "Volume IV: Models and Correlations," in *RELAP5-3D Code Manual*, Idaho Falls, ID, Idaho National Laboratory, 2005, pp. 1-590.

[71] "Ventilation Ducts - Roughness & Surface Coefficients," The Engineering ToolBox, [Online]. Available: http://www.engineeringtoolbox.com/surface-roughness-ventilation-ducts-d_209.html. [Accessed 15 August 2016].

[72] N. V. Hoffer, P. Sabharwall and N. A. Anderson, "Modeling a Helical-coil Steam Generator in RELAP5-3D for the Next Generation Nuclear Plant," Idaho National Laboratory, Idaho Falls, ID, 2011.

[73] The RELAP5-3D Code Development Team, "Volume II Appendix A: RELAP5-3D Input Data Requirements," in *RELAP5-3D Code Manual*, Idaho Falls, ID, Idaho National Laboratory, 2005, pp. 1-352.

[74] Q. Lv, I. Adams, X. Wang, X. Sun, R. Christensen, T. Blue, G. Yoder, D. Wilson and P. Sabharwall, "A MATLAB Code for the Thermal Performance Evaluation of a Low-Temperature DRACS Test Facility," *Transactions of the American Nuclear Society,* vol. 107, p. 1374, 2012.

[75] Nuclear Regulatory Commission, "Design Certification Application Review - AP1000 Amendment," United States Nuclear Regulatory Commission, 13 April 2016. [Online]. Available: http://www.nrc.gov/reactors/new-reactors/design-cert/amended-ap1000.html. [Accessed 21 July 2016].

8. Appendices

8.1. Appendix A: Python script

```
import math

# Constants needed for calculations
g = 9.81 # acceleration due to gravity, m/s^2
R_D = 0.8 * 2077 + 0.2 * 297 # Direct loop gas constant after
depressurization, 80% Helium, 20% Nitrogen, J/(kg K)
rough = 1.5e-5 # Surface roughness for SS-316, m
bolt = 1.380658e-23 # Boltzmann's constant, J/K

# Heat exchanger thermal conductivity
kDHX = 0.53606 # from 316_316l_data_sheet for 500 C
kNDHX = 32.44646 # from 316_316l_data_sheet for 100 C

intom = 0.0254 # conversion for inches to meters
ntube = 6 # number of tubes in DHX

# Heat exchanger geometry
tDHX = 0.2 * intom # DHX tube wall thickness, m
tNDHX = 0.8 * intom # NDHX tube wall thickness, m
ODDHX = 3 * intom # DHX tube outer diameter, m
IDDHX = ODDHX - 2 * tDHX # DHX tube inner diameter, m
IDNDHX = 6 * intom # NDHX tube inner diameter, m
ODNDHX = IDNDHX + 2 * tNDHX # NDHX tube outer diamter, m
LDHX = math.pi * 7 * (40.5 + 46.5 + 52.5 + 58.5 + 64.5 + 70.5) /
ntube * intom # average flow length through DHX tubes,
intermediate side, m
LNDHX = (2 * 347.766 + 2 * 293.832 + 3 * math.pi * 91.868 / 2) *
intom # total flow length through NDHX tubes, intermediate side,
m
As_DDHX = LDHX * math.pi * ODDHX * ntube # Heat transfer area
from the direct loop to the DHX
As_IDHX = LDHX * math.pi * IDDHX * ntube # Heat transfer area
from the DHX to the intermediate loop
As_DHX = (As_DDHX + As_IDHX) / 2 # Average heat transfer area
through DHX tube walls
As_INDHX = LNDHX * math.pi * IDNDHX # Heat transfer area from the
intermediate loop to the NDHX
As_NdNDHX = 10155.63626 # Heat transfer area from the NDHX to the
natural draft loop
As_NDHX = math.pi * (IDNDHX + ODNDHX) / 2 * LNDHX # Average heat
transfer area through NDHX tube walls

# Loop heights, elevation difference between heat source and sink
L_D = 19.643 # Direct loop height, m
L_I = 13.5 # Intermediate loop height, m
L_ND = 25 # Natural draft loop height, m
```

```
A_Din = math.pi * (30.5 / 2 * intom)**2 # Direct loop inlet area,
m^2
A_I1 = math.pi * (IDNDHX / 2)**2 # Intermediate loop reference
area, m^2
A_DHX = math.pi * (IDDHX / 2)**2 * 6 # Flow area through DHX
tubes

# Loop pressures
P_D = 4.5e5 # Direct loop pressure, Pa
P_I = 140e5 # Intermediate loop pressure, Pa
P_ND = 1e5 # Natural draft loop pressure, Pa

# Known temperatures
T_Dh = 2273.15 # Direct loop hot temperature, K
T_NDc = 303.15 # Natural draft loop cold temperature, K

# Temperature guesses
T_Dc = 1080.38 # Direct loop cold temperature, K
T_Ic = 407.09 # Direct loop cold temperature, K
T_Ih = 488.38 # Intermediate loop hot temperature, K
T_NDh = 322.77 # Direct loop cold temperature, K
T_Da = (T_Dc + T_Dh) / 2 # Direct loop average temperature for
calculations, K
T_Ia = (T_Ih + T_Ic) / 2 # Intermediate loop average temperature
for calculations, K
T_NDa = (T_NDh + T_NDc) / 2 # Natural draft loop average
temperature for calculations, K
T_DHXD = 1005.85 # DHX surface temperature on the direct loop
side, K
T_DHXI = 471.30 # DHX surface temperature on the intermediate
loop side, K
T_NDHXI = 400.81 # NDHX surface temperature on the intermediate
loop side, K
T_NDHXNd = 318.561 # NDHX surface temperature on the natural
draft loop side, K
LMTD_DHX = ((T_Dh - T_Ih) - (T_Dc - T_Ic)) / math.log((T_Dh -
T_Ih) / (T_Dc - T_Ic))
# Values used to find cross-flow correction factor
LMTD_R = (T_NDc - T_NDh) / (T_Ic - T_Ih)
LMTD_P = (T_Ic - T_Ih) / (T_NDc - T_Ih)
LMTD_F = 1.0 # cross-flow correction factor, turns out to not be
necessary at the temperatures
LMTD_NDHX = (((T_Ih - T_NDh) - (T_Ic - T_NDc)) / math.log((T_Ih -
T_NDh) / (T_Ic - T_NDc))) * LMTD_F

# Direct loop thermophysical properties
cp_Na = 2706 # ideal diatomic gas specific heat for Nitrogen,
J/(kg K)
cp_Hea = 5193 # ideal monoatomic gas specific heat for Helium,
J/(kg K)
```

```
cp_Da = 0.8 * cp_Hea + 0.2 * cp_Na # direct loop isobaric
specific heat at DHX average temperature, J/(kg K)
k_Hea = 0.5181 # Thermal conductivity of helium at average direct
loop temperature, W/(m K)
k_Na = 0.5181 # Thermal conductivity of nitrogen at average
direct loop temperature, W/(m K)
k_Da = 0.8 * k_Hea + 0.2 * k_Na # Average thermal conductivity of
direct loop fluid, W/(m K)
mu_Heh = 8.277e-5 # dynamic viscosity of Helium at hot direct
loop temperature, Pa s
mu_Hec = 4.876e-5 # dynamic viscosity of Helium at cold direct
loop temperature, Pa s
mu_Hea = 6.663e-5 # dynamic viscosity of Helium at average direct
loop temperature, Pa s
mu_Nh = 7.132e-5 # dynamic viscosity of nitrogen at hot direct
loop temperature, Pa s
mu_Nc = 4.369e-5 # dynamic viscosity of nitrogen at cold direct
loop temperature, Pa s
mu_Na = 5.817e-5 # dynamic viscosity of nitrogen at average
direct loop temperature, Pa s
mu_Dh = 0.8 * mu_Heh + 0.2 * mu_Nh # Direct loop hot dynamic
viscosity, Pa s
mu_Dc = 0.8 * mu_Hec + 0.2 * mu_Nc # Direct loop cold dynamic
viscosity, Pa s
mu_Da = 0.8 * mu_Hea + 0.2 * mu_Na # Direct loop average dynamic
viscosity, Pa s
Pr_Da = mu_Da * cp_Da / k_Da # Prandtl number at average
temperature for direct loop flow over DHX
rho_Da = P_D / (R_D * T_Da) # Direct loop average density, kg/m^3
rho_Dc = P_D / (R_D * T_Dc) # Direct loop cold density, kg/m^3
rho_Dh = P_D / (R_D * T_Dh) # Direct loop hot density, kg/m^3

# Intermediate loop thermophysical properties
cp_Ia = 4332 # specific heat capacity for Water at average
intermediate temperature, J/(kg K)
k_Ia = 0.6714 # Thermal conductivity of water at 300 C and 200
bar, W/(m K)
mu_Ia = 15.84e-5 # Intermediate loop average dynamic viscosity,
Pa s
mu_Ic = 20.98e-5 # Intermediate loop cold dynamic viscosity, Pa s
mu_Ih = 12.74e-5 # Intermediate loop hot dynamic viscosity, Pa s
Pr_Ia = mu_Ia * cp_Ia / k_Ia # Prandtl number at average
temperature for intermediate loop flow through DHX
rho_Ia = 901.1 # Intermediate loop average density, kg/m^3
rho_Ic = 938.6 # Intermediate loop cold density, kg/m^3
rho_Ih = 856.2 # Intermediate loop hot density, kg/m^3

# Natural draft loop thermophysical properties
cp_NDa = 1005 # specific heat capacity for Water at average
intermediate temperature, J/(kg K)
```

```
k_NDa = 0.02661 # Thermal conductivity of water at 300 C and 200
bar, W/(m K)
mu_NDa = 1.917e-5 # Intermediate loop average dynamic viscosity,
Pa s
mu_NDc = 1.872e-5 # Intermediate loop cold dynamic viscosity, Pa
s
mu_NDh = 1.962e-5 # Intermediate loop hot dynamic viscosity, Pa s
Pr_NDa = mu_NDa * cp_NDa / k_NDa # Prandtl number at average
temperature for intermediate loop flow through DHX
rho_NDa = 1.113 # Intermediate loop average density, kg/m^3
rho_NDc = 1.149 # Intermediate loop cold density, kg/m^3
rho_NDh = 1.079 # Intermediate loop hot density, kg/m^3

# Direct loop section data used to calculate the direct loop
resistance number
# Sections are made up of continuous lengths which have the same
temperature and cross sectional area, such that density, dynamic
viscosity, and hydraulic diameter is also constant through each
section.
# Form loss coefficients are summed for each section, i.e. two
elbows are in the first section, the short radius elbow with a
form loss coefficient of 0.3 and long elbow of 0.2, so the total
for that section is 0.5.
L_Ds = [12.345205, 1.016, 0.9144, 0.4064, 0.4064, 5.0625, 0.4064,
7.040581] # Direct loop section lengths, m
A_Ds = [A_Din, 3.133094, 2.404643, 2.559253, 1.502578, 0.4459026,
0.7601879, A_Din] # Direct loop section areas, m^2
rho_Ds = [rho_Dh, rho_Dh, rho_Da, rho_Dc, rho_Dc, rho_Dc, rho_Dc,
rho_Dc] # Direct loop section densities, kg/m^3
mu_Ds = [mu_Dh, mu_Dh, mu_Da, mu_Dc, mu_Dc, mu_Dc, mu_Dc, mu_Dc]
# Direct loop section dynamic viscosity, Pa s
Dh_Ds = [0.7747, 1.8136, 0.5601, 1.1303, 0.7785, 0.2794, 1.0028,
0.7747] # Direct loop section hydraulic diameters, m
K1 = (1 - rho_Ds[0] * A_Ds[0] / (rho_Ds[1] * A_Ds[1]))**2 # form
loss coefficient for section 1, based on area change
K2 = (1 - rho_Ds[1] * A_Ds[1] / (rho_Ds[2] * A_Ds[2]))**2 # form
loss coefficient for section 2, based on area change
K4 = (1 - rho_Ds[3] * A_Ds[3] / (rho_Ds[4] * A_Ds[4]))**2 # form
loss coefficient for section 4, based on area change
K6 = (1 - rho_Ds[5] * A_Ds[5] / (rho_Ds[6] * A_Ds[6]))**2 # form
loss coefficient for section 6, based on area change
K_Ds = [0.5, K1, K2, 0, K4, 0, K6, 0.2] # Direct loop section
form loss coefficients
# Initialize variables for direct loop resistance number
calculation loop
piF_D = 1 # Direct loop resistance number, initial guess
v_Ds = [0,0,0,0,0,0,0,0] # initialize array for section
velocities
Re_Ds = [0,0,0,0,0,0,0,0] # initialize array for section Reynolds
numbers
```

```
f_Ds = [0,0,0,0,0,0,0,0] # initialize array for section friction
factors
piF_Ds = [0,0,0,0,0,0,0,0] # initialize array for section
resistance numbers
this = 'true' # loop break variable
x = 0 # Direct loop resistance number iteration counter

while (this == 'true'):

    x += 1
    v_Din = ((rho_Dc - rho_Dh)* g * L_D / (rho_Dh * piF_D)
)**(0.5) # direct inlet velocity calculated according to equation
revealed in bottom-up scaling analysis

    for i in range(0,8):

        v_Ds[i] = v_Din * A_Din * rho_Dh / (A_Ds[i] * rho_Ds[i])
# calculate velocity for every section based on constant mass
flow rate, m/s
        Re_Ds[i] = rho_Ds[i] * v_Ds[i] * Dh_Ds[i] / mu_Ds[i] #
section Reynolds number
        f_Ds[i] = 64 / Re_Ds[i] # section friction factor,
correlation for laminar pipe flow (Re < 2320)
        piF_Ds[i] =
(K_Ds[i]+f_Ds[i]*L_Ds[i]/Dh_Ds[i])*(rho_Dh*A_Din**2/(rho_Ds[i]*A_
Ds[i]**2)) # Direct loop section resistance number

    if math.fabs(sum(piF_Ds)-piF_D) < 1e-8:

        this = 'false'

    piF_D = sum(piF_Ds)

#print('Values for the direct loop converged after', x,
'iterations.')
#print('Direct loop resistance number: ', piF_D)
#print('Direct maximum velocity: ', max(v_Ds))
#print('Direct minimum velocity: ', min(v_Ds))
#print(' ')

# Intermediate loop section data used to calculate the
intermediate loop resistance number
# Sections are made up of continuous lengths which have the same
temperature and cross sectional area, such that density, dynamic
viscosity, and hydraulic diameter is also constant through each
section.
# Form loss coefficients are summed for each section, i.e. four
elbows are in the first section, each with a form loss
coefficient of 0.2, so the total for that section is 0.8.
```

```
L_Is = [24.76491536, LNDHX, 22.72213728, 0.2032, LDHX, 0.2032] #
Intermediate loop section lengths, m
A_I2 = 0.05177901042 # DHX manifold average area
A_Is = [A_I1, A_I1, A_I1, A_I2, A_DHX, A_I2] # Intermediate loop
section areas, m^2
rho_Is = [rho_Ih, rho_Ia, rho_Ic, rho_Ic, rho_Ia, rho_Ih] #
Intermediate loop section densities, kg/m^3
mu_Is = [mu_Ih, mu_Ia, mu_Ic, mu_Ic, mu_Ia, mu_Ih] # Intermediate
loop section dynamic viscosity, Pa s
Dh_I1 = IDNDHX # 6 inch round pipe hydraulic diameter, m
Dh_I2 = 0.2567626991 # DHX manifold hydraulic diameter, m
Dh_Is = [Dh_I1, Dh_I1, Dh_I1, Dh_I2, IDDHX, Dh_I2] # Intermediate
loop section hydraulic diameters, m
K3 = (1 - rho_Is[2] * A_Is[2] / (rho_Is[4] * A_Is [4]))**2 # form
loss coefficient for section 3, based on area change
K5 = (1 - rho_Is[4] * A_Is[4] / (rho_Is[0] * A_Is [0]))**2 # form
loss coefficient for section 5, based on area change
K_Is = [0.8, 0.6, 0.4, K3, 0, K5] # Intermediate loop section
form loss coefficients
# Initialize variables for intermediate loop resistance number
calculation loop
piF_I = 1 # Intermediate loop resistance number, initial guess
v_Is = [0,0,0,0,0,0] # initialize array for section velocities
Re_Is = [0,0,0,0,0,0] # initialize array for section Reynolds
numbers
piF_Is = [0,0,0,0,0,0] # initialize array for section resistance
numbers
this = 'true' # loop break variable
y = 0 # Intermediate loop resistance number iteration counter

while (this == 'true'):

    f_Isnew = [2,2,2,2,2,2] # initialize array for section
friction factors
    f_Isold = [1,1,1,1,1,1] # initialize array for section
friction factors, must be different so a new friction factor will
be calculated for each outer loop iteration

    y += 1
    v_I1 = ((rho_Ic - rho_Ih)* g * L_I / (rho_Ih * piF_I)
)**(0.5) # intermediate section 1 velocity calculated according
to equation revealed in bottom-up scaling analysis

    for i in range(0,6):

        v_Is[i] = v_I1 * A_I1 * rho_Ih / (A_Is[i] * rho_Is[i]) #
calculate velocity for every section based on constant mass flow
rate, m/s
        Re_Is[i] = rho_Is[i] * v_Is[i] * Dh_Is[i] / mu_Is[i] #
section Reynolds number
```

```
        while math.fabs(f_Isnew[i]-f_Isold[i]) > (1e-6): #
Iteration is required to find the friction factor using the
Colebrook-White equation, for turbulent full pipe flow (Re >
4000)

            f_Isold[i]=f_Isnew[i] # store value from last
iteration to test convergence for while loop

            f_Isnew[i] = (1 / (-2 * math.log10(rough / (3.7 *
Dh_Is[i]) + 2.51 / (Re_Is[i] * (f_Isold[i])**(0.5)))))**2 #
Intermediate loop section friction factor

        piF_Is[i] =
(K_Is[i]+f_Isnew[i]*L_Is[i]/Dh_Is[i])*(rho_Ih*A_I1**2/(rho_Is[i]*
A_Is[i]**2)) # Direct loop section resistance number

    if math.fabs(sum(piF_Is)-piF_I) < 1e-8: # check convergence
of the intermediate loop resistance number

        this = 'false'

    piF_I = sum(piF_Is) # store value of intermediate loop
resistance number

#print('Values for the intermediate loop converged after', y,
'iterations.')
#print('Intermediate loop resistance number: ', piF_I)
#print('Intermediate maximum velocity: ', max(v_Is))
#print('Intermediate minimum velocity: ', min(v_Is))
#print(' ')

# Natural draft loop section data used to calculate the direct
loop resistance number
# Sections are made up of continuous lengths which have the same
temperature and cross sectional area, such that density, dynamic
viscosity, and hydraulic diameter is also constant through each
section.
# Form loss coefficients are summed for each section, as before
L_NDs = [8.25, 0.15348, 0.19304, 0.15348, 22.98097039] # Natural
draft loop section lengths, m
A_NDs = [78.75, 70, 63.39128569, 70, 78.75] # Natural draft loop
section areas, m^2
rho_NDs = [rho_NDc, rho_NDc, rho_NDa, rho_NDh, rho_NDh] # Natural
draft loop section densities, kg/m^3
mu_NDs = [mu_NDc, mu_NDc, mu_NDa, mu_NDh, mu_NDh] # Natural draft
loop section dynamic viscosity, Pa s
Dh_NDs = [8.75, 8.235294118, 1.483359383, 8.235294118, 8.75] #
Natural draft loop section hydraulic diameters, m
```

```
K1 = (1 - rho_NDs[0] * A_NDs[0] / (rho_NDs[1] * A_NDs[1]))**2 #
form loss coefficient for section 1, based on area change
K2 = (1 - rho_NDs[1] * A_NDs[1] / (rho_NDs[2] * A_NDs[2]))**2 #
form loss coefficient for section 2, based on area change
K3 = (1 - rho_NDs[2] * A_NDs[2] / (rho_NDs[3] * A_NDs[3]))**2 #
form loss coefficient for section 3, based on area change
K4 = (1 - rho_NDs[3] * A_NDs[3] / (rho_NDs[4] * A_NDs[4]))**2 +
0.5 # form loss coefficient for section 4, based on area change
and sharp 45deg bend
K_NDs = [1.3, K1, K2, K3, K4] # Natural draft loop section form
loss coefficients
# Initialize variables for natural draft loop resistance number
calculation loop
piF_ND = 1 # Natural draft loop resistance number, initial guess
v_NDs = [0,0,0,0,0] # initialize array for section velocities
Re_NDs = [0,0,0,0,0] # initialize array for section Reynolds
numbers
f_NDs = [0,0,0,0,0] # initialize array for section friction
factors
piF_NDs = [0,0,0,0,0] # initialize array for section resistance
numbers
this = 'true' # loop break variable
z = 0 # Natural draft loop resistance number iteration counter

while (this == 'true'):
    f_NDsnew = [2,2,2,2,2,2] # initialize array for section
friction factors
    f_NDsold = [1,1,1,1,1,1] # initialize array for section
friction factors, must be different so a new friction factor will
be calculated for each outer loop iteration
    z += 1
    v_NDin = ((rho_NDc - rho_NDh)* g * L_ND / (rho_NDc * piF_ND)
)**(0.5) # natural draft inlet velocity calculated according to
equation revealed in bottom-up scaling analysis

    for i in range(0,5):

        v_NDs[i] = v_NDin * A_NDs[0] * rho_NDc / (A_NDs[i] *
rho_NDs[i]) # calculate velocity for every section based on
constant mass flow rate, m/s
        Re_NDs[i] = rho_NDs[i] * v_NDs[i] * Dh_NDs[i] / mu_NDs[i]
# section Reynolds number

        while math.fabs(f_NDsnew[i]-f_NDsold[i]) > (1e-6): #
Iteration is required to find the friction factor using the
Colebrook-White equation, for turbulent full pipe flow (Re >
4000)

            f_NDsold[i]=f_NDsnew[i] # store value from last
iteration to test convergence for while loop
```

```
            f_NDsnew[i] = (1 / (-2 * math.log10(rough / (3.7 *
Dh_NDs[i]) + 2.51 / (Re_NDs[i] * (f_NDsold[i])**(0.5)))))**2 #
Intermediate loop section friction factor

        piF_NDs[i] =
(K_NDs[i]+f_NDs[i]*L_NDs[i]/Dh_NDs[i])*(rho_NDc*A_NDs[0]**2/(rho_
NDs[i]*A_NDs[i]**2)) # natural draft loop section resistance
number

    if math.fabs(sum(piF_NDs)-piF_ND) < 1e-8:

        this = 'false'

    piF_ND = sum(piF_NDs)

print('Values for the natural draft loop converged after', z,
'iterations.')
print('Natural draft loop resistance number: ', piF_ND)
print('Natural draft maximum velocity: ', max(v_NDs))
print('Natural draft minimum velocity: ', min(v_NDs))
print(' ')

h_DDHX = 0.683 * Re_Ds[2]**(0.466) * Pr_Da**(1/3) * k_Da / ODDHX
# average heat transfer coefficient on the direct side of the
DHX, W/(m^2 K)
h_IDHX = 0.023 * Re_Is[4]**(4/5) * Pr_Ia**(0.40) * k_Ia / IDDHX #
average heat transfer coefficient on the intermediate side of the
DHX, W/(m^2 K)
h_INDHX = 0.023 * Re_Is[1]**(4/5) * Pr_Ia**(0.30) * k_Ia / IDNDHX
# average heat transfer coefficient on the intermdiate side of
the NDHX, W/(m^2 K)
h_NdNDHX = 0.027 * Re_NDs[2]**(0.805) * Pr_NDa**(1/3) * k_NDa /
ODNDHX # What the natural draft side of the NDHX loop heat
transfer coefficient must be, W/(m^2 K)

q_DDHX = h_DDHX * As_DDHX * (T_Da - T_DHXD) # heat transfer rate
from the direct loop to the DHX, W
q_DHX = kDHX / tDHX * As_DHX * LMTD_DHX # heat transfer rate
through the DHX tubes, W
q_IDHX = h_IDHX * As_IDHX * (T_DHXI - T_Ia) # heat transfer rate
from the DHX to the intermediate loop, W
q_INDHX = h_INDHX * As_INDHX * (T_Ia - T_NDHXI) # heat transfer
rate from the intermediate loop to the NDHX, W
q_NDHX = kNDHX / tNDHX * As_NDHX * LMTD_NDHX # heat transfer rate
through the NDHX tubes, W
q_NdNDHX = h_NdNDHX * As_NdNDHX * (T_NDHXNd - T_NDa) # heat
transfer rate from the NDHX to the natural draft loop, W
```

```
UA_DHX = 1 / (1 / (h_DDHX * As_DDHX) + tDHX / (kDHX * As_DHX) + 1
/ (h_IDHX * As_IDHX)) # overall heat transfer coefficient for the
hot half of the system
UA_NDHX = 1 / (1 / (h_INDHX * As_INDHX) + tNDHX / (kNDHX *
As_NDHX) + 1 / (h_NdNDHX * As_NdNDHX)) # overall heat transfer
coefficient for the cold half of the system
q_System = (T_Dh - T_NDc) * (1 / (1 / UA_DHX + 1 / UA_NDHX)) #
total heat transfer rate across the entire system

print('Heat transfer rate direct side DHX:        ', '%.3e' %
q_DDHX)
print('Heat transfer rate through DHX:            ', '%.3e' %
q_DHX)
print('Heat transfer rate intermediate side DHX:  ', '%.3e' %
q_IDHX)
print('Heat transfer rate intermediate side NDHX: ', '%.3e' %
q_INDHX)
print('Heat transfer rate through NDHX:           ', '%.3e' %
q_NDHX)
print('Heat transfer rate natural draft side NDHX:', '%.3e' %
q_NdNDHX)
print('Heat transfer rate through the system:     ', '%.3e' %
q_System)

mfr_D = v_Din * rho_Dh * A_Din # mass flow rate through the
direct loop, kg/s
mfr_I = v_I1 * rho_Ih * A_I1 # mass flow rate through the
intermediate loop, kg/s
mfr_ND = v_NDin * rho_NDc * A_NDs[0] # mass flow rate through the
natural draft loop, kg/s

q_t = 5e6 # target heat transfer rate (approximate amount of
decay power at the time when core outlet temperature reaches its
maximum value divided by two (only one DRACS module vs. two in
EM2))
T_Dct = T_Dh - q_t / (mfr_D * cp_Da) # target direct loop cold
temperature, K
T_DHXDt = T_Da - q_t / (h_DDHX * As_DDHX) # target DHX surface
temperature on the direct loop side, K
T_Iat = (T_Da + T_NDa * (UA_NDHX / UA_DHX)) / (1 + (UA_NDHX /
UA_DHX)) # target average intermediate loop temperature, K
T_Idelt = q_t / (mfr_I * cp_Ia) # target difference between hot
and cold temperature in the intermediate loop, K
T_Iht = T_Iat + T_Idelt / 2 # target intermeidate loop hot
temperature, K
T_Ict = T_Iat - T_Idelt / 2 # target intermediate loop cold
temperature, K
T_DHXIt = T_Ia + q_t / (h_IDHX * As_IDHX) # target DHX surface
temperature on the intermediate loop side, K
```

```
T_NDHXIt = T_Ia - q_t / (h_INDHX * As_INDHX) # target NDHX
surface temperature on the intermediate loop side, K
T_NDht = T_NDc + q_t / (mfr_ND * cp_NDa) # target natural draft
loop hot temperature, K
T_NDHXNdt = T_NDa + q_t / (h_NdNDHX * As_NdNDHX) # target NDHX
surface temperature on the natural draft loop side, K
k_DHXt = q_t * tDHX / (LMTD_DHX * As_DHX) # target thermal
conductivity through DHX tubes, W/(m K)
k_NDHXt = q_t * tNDHX / (LMTD_NDHX * As_NDHX) # target thermal
conductivity through NDHX tubes, W/(m K)

#print(T_Dct)
#print(T_DHXDt)
#print(T_Ict)
#print(T_Iht)
#print(T_DHXIt)
#print(T_NDHXIt)
#print(T_NDht)
#print(T_NDHXNdt)
#print(k_DHXt)
#print(k_NDHXt)
```

8.2.Appendix B: Engineering Equation Solver script

```
T_Dh = 2273.15[K]
T_Dc = 1080.38[K]
T_Da =(T_Dh + T_Dc) / 2

P_D = 4.5 [bar]
T_Ic = 407.07 [K]
T_Ih = 488.31 [K]
T_Ia = (T_Ih + T_Ic) / 2
P_I = 140 [bar]

T_NDc = 303.15 [K]
T_NDh = 322.77 [K]
T_NDa = (T_NDh + T_NDc) / 2
P_ND = 1 [bar]

mu_Heh=Viscosity(Helium,T=T_Dh,P=P_D)
mu_Hec=Viscosity(Helium,T=T_Dc,P=P_D)
mu_Hea=Viscosity(Helium,T=T_Da,P=P_D)
cp_Hea=Cp(Helium,T=T_Da,P=P_D)
k_Hea=Conductivity(Helium,T=T_Da,P=P_D)
mu_Nh=Viscosity(Nitrogen,T=T_Dh,P=P_D)
mu_Nc=Viscosity(Nitrogen,T=T_Dc,P=P_D)
mu_Na=Viscosity(Nitrogen,T=T_Da,P=P_D)
cp_Na=Cp(Water,T=T_Da,P=P_D)
k_Na=Conductivity(Helium,T=T_Da,P=P_D)

rho_Ih=Density(Water,T=T_Ih,P=P_I)
rho_Ic=Density(Water,T=T_Ic,P=P_I)
rho_Ia=Density(Water,T=T_Ia,P=P_I)
mu_Ih=Viscosity(Water,T=T_Ih,P=P_I)
mu_Ic=Viscosity(Water,T=T_Ic,P=P_I)
mu_Ia=Viscosity(Water,T=T_Ia,P=P_I)
k_Ia=Conductivity(Water,T=T_Ia,P=P_I)
cp_Ia=Cp(Water,T=T_Ia,P=P_I)

rho_NDh=Density(Air,T=T_NDh,P=P_ND)
rho_NDc=Density(Air,T=T_NDc,P=P_ND)
rho_NDa=Density(Air,T=T_NDa,P=P_ND)
mu_NDh=Viscosity(Air,T=T_NDh)
mu_NDc=Viscosity(Air,T=T_NDc)
mu_NDa=Viscosity(Air,T=T_NDa)
k_NDa=Conductivity(Air,T=T_NDa)
cp_NDa=Cp(Air,T=T_NDa)
```

8.3. Appendix C: RELAP5-3D model description

8.3.1. Direct loop model specifics

The direct loop nodalization, shown in Figure 5-5, contains 9 hydrodynamic volume components and 8 junction components. Boundary volumes are used rather than modeling the primary system, and the piping matches the orientations and relative dimensions of the SolidWorks model of the scaled-down DRACS module. Each hydrodynamic volume will be described briefly with values presented for both the scaled-down and full-scale models. Junctions will not be described individually as each gives information on the mass flow rate, which remains constant throughout the loop, and the flow area, which is always the minimum flow area of the volumes connected.

8.3.1.1. Boundary cells, volumes (101) and (117)

The boundary volumes are used to model boundary conditions from and to the primary system, and are connected to each end of the direct loop piping as modeled in SolidWorks for the scaled-down model. The inlet was chosen to be the first elbow which is seen in the inlet of the direct loop, rather than the flange or reducer because this would more closely match the full-scale prototype, which does not have to change the size of piping in the direct loop due to port availability. The inlet and outlet boundary volumes share the flow area of the inlet and outlet piping, and both use the same length. Surface roughness is not necessary as friction calculations are not completed by RELAP5-3D in time-dependent volumes. The boundary condition for mass flow rate, set by the time-dependent junction at the inlet, is also included in the table. All conditions

are evaluated at the peak core outlet temperature during a D-LOFC for conservatism, approximated from Figure 5-4.

Table 8-1: Direct loop boundary volume information, volumes (101) and (117)

Characteristic	Full-scale	Scaled-down
Direct inlet temperature, (101)	2000° C	2000° C
Direct outlet temperature, (117)	816.55° C	816.55° C
Direct loop pressure, (101) & (117)	4.5 bar	4.5 bar
Direct boundary flow area, (101) & (117)	0.4713646324 m^2	0.0294602895 m^2
Direct boundary length, (101) & (117)	1 m	0.25 m
Hydraulic diameter, (101) & (117)	0.7747 m	0.193675 m
Direct mass flow rate, (102)	0.8996861798 kg/s	0.028116606 kg/s
Direct loop height, system quantity	19.643 m	4.91075 m

8.3.1.2. Direct inlet pipe, volume (103)

The direct inlet pipe is made up of the direct inlet elbow, direct inlet horizontal pipe, and the flange which connects this pipe to the direct inlet on the DHX module. It is modeled as a pipe component in RELAP5-3D, with one volume for the vertical distance covered by the elbow, and two volumes which equally cover the horizontal distance covered by elbow, pipe, and flange. Although pictures of the EM^2 depict the DRACS as having a concentric duct all the way to the DHX module which is attached to the pressure vessel at a different place, the model in RELAP5-3D was built for full-scale to match the geometry of the scaled-down model in order to eliminate variables that could lead to negative results. An analysis could be done of the effects that the different flow path has on the flow characteristics with a more complete knowledge of the full-scale

prototype. For now, the scaling analysis is the primary concern so the design was kept as simple as possible. Relevant information for this component is shown in Table 8-2.

Table 8-2: Direct inlet pipe information, volume (103)

Characteristic	Full-scale	Scaled-down
Flow area	0.4713646324 m^2	0.0294602895 m^2
Section length	1.2192 m [1], 2.2198076 m [2,3]	0.3048 m [1], 0.5549519 m [2,3]
Horizontal angle	0°	0°
Vertical angle	90° [1], 0° [2,3]	90° [1], 0° [2,3]
Elevation change	1.2192 m [1], 0 m [2,3]	0.3048 m [1], 0 m [2,3]
Hydraulic diameter	0.7747 m	0.193675 m
Pressure	4.5 bar	4.5 bar
Temperature	2000° C	2000° C

The component number is surrounded by parentheses and the volume number within the component is surrounded by square brackets to differentiate in this and following tables. The surface roughness on this component and every other in the entire system is 15 µm, which was a value found for stainless steel pipe [71]. This value was kept the same in both full-scale and scaled-down because it is a material property and is assumed to remain constant. There are ways to finish a pipe with different surface roughness, such as polishing, but that is not taken into account. Volume and junction flags used are default values except that the water packing scheme is turned off, as there is no water present in the direct loop. No choking model is used, which is

recommended where there is a sharp area change and choking behavior is expected [68].

8.3.1.3. Direct DHX inlet pipe, volume (105)

It was desired that the DHX module would be a system that is manufactured such that it can be picked up and connected to the various pipes by flanges. The RELAP5-3D model kept the DHX module separate by breaking the inlet pipe at the flange face such that although volumes (103) and (105) have the same flow area and hydraulic diameter, they are distinct components from the direct inlet piping to the inlet piping within the DHX module.

There is one horizontal section made up by the flange and the horizontal distance of the DHX inlet elbow, while the vertical distance covered by the DHX inlet elbow and the concentric inlet pipe are broken into two equal vertical sections. Another horizontal section follows which is used to model the turnaround of fluid from the inlet to the outlet through the DHX plenum. Originally the plenum was modeled separately as a branch, but was added as an extra volume in this pipe while trying to fix some errors that had arisen in the direct loop. This change was not the one that fixed the errors, but it did not create any either, and it was a simpler model than having a separate component. The same volume and junction flags area again used as discussed for volume (103).

Table 8-3: Direct DHX inlet pipe information, volume (105)

Characteristic	Full-scale	Scaled-down
Flow area	0.4713646324 m^2	0.02946028953 m^2
Section length	1.257808 m [1], 3.150362 m [2,3], 1.44145 m [4]	0.314452 m [1], 0.7875905 m [2,3], 0.3603625 m [4]
Horizontal angle	0°	0°
Vertical angle	0° [1,4], 90° [2,3]	0° [1,4], 90° [2,3]
Elevation change	0 m [1,4], 3.150362 m [2,3]	0 m [1,4], 0.7875905 m [2,3]
Hydraulic diameter	0.7747 m	0.193675 m
Pressure	4.5 bar	4.5 bar
Temperature	2000° C	2000° C

8.3.1.4. Direct flow over DHX tubes, volume (107)

Volume (107) is the only volume in the direct loop in which heat transfer occurs; the only volume connected to a heat structure. The flow length was divided into four sections for this reason, and so a temperature gradient could be established. The temperature gradient is evenly spaced along the four volumes, with the inlet section having the same temperature as the previous volumes, and the outlet section having the same temperature as the following volumes.

The inner diameter of the outer concentric section was chosen to accommodate the space taken up by the helical DHX tubes within this volume. In a helical coil, like a toroid, there exists a major and minor diameter. The minor diameter for all tubes is the diameter of the tube itself, and where the direct loop is concerned, this is the outer diameter. The major diameter is the diameter of the helical wrap around the inner

concentric pipe. For each tube, the major diameter is different. There are six tubes which make up the helical coil, and they are in a staggered array. There is a separate stream-wise and a transverse pitch which explain the relationship between each consecutive tube. The first row of three tubes are separated by the transverse pitch from the adjacent tube. The innermost of these three is separated from the outer wall of the inner pipe by half of the stream-wise pitch, such that the major diameter of the first tube is the stream-wise pitch larger than the outer diameter of the inner pipe. The second row of three tubes are staggered from the first by half of a stream-wise pitch, such that they sit directly between consecutive tubes in the first row. The third tube in the second row therefore has the largest major diameter. The inner diameter of the outer concentric section was chosen to be that of the smallest typical pipe size that would provide the same separation from the outermost major diameter as was imposed on the first tube from the inner pipe. In the scaled-down model, this resulted in a 22" schedule 80 pipe. The diameters were simply scaled up by the diameter scaling factor for the full-scale model.

$$A = \pi\left(\left(\frac{ID_L}{2}\right)^2 - \left(\frac{OD_S}{2}\right)^2\right) - A_{DHXtube} \tag{8.1}$$

The flow area for this volume was calculated by equation (8.1). The helical tubes of the DHX provide a more complicated section of the area blocked as they are in a helical coil, and this area obstruction is accounted for by the last term in equation (8.1). It was decided to compute the area blocked by these tubes by calculating the total volume

taken up by the DHX tubes and dividing that volume by the height of volume (107). The large inner diameter is that of the outer annulus and the small outer diameter is that of the inner pipe, being the other two variables in equation (8.1).

$$D_e = \frac{4A}{\pi(ID_L + OD_S) + P_{DHXtube}} \tag{8.2}$$

The hydraulic diameter was similarly calculated to equation (8.2), where the area is calculated as described in the paragraph above, and the perimeter on the bottom uses the same diameters as in equation (8.1). The average perimeter addition from the DHX tubes is also accounted for in the denominator. This perimeter addition was calculated by finding the total surface area of the 6 tubes which make the DHX, and dividing that surface area by the height of volume (107). Table 8-4 below contains the results of these calculations. Volume and junction control flags for volume (107) are the same as those described for volume (103).

Table 8-4: Direct flow over DHX tubes information, volume (107)

Characteristic	**Full-scale**	**Scaled-down**
Flow area	2.404642573 m^2	0.1502901608 m^2
Section length	0.2286 m	0.05715 m
Vertical angle	-90°	-90°
Elevation change	-0.2286 m	-0.05715 m
Hydraulic diameter	0.5601010397 m	0.1400252599 m
Pressure	4.5 bar	4.5 bar
Temperature	2000° C [1], 1605.517° C [2], 1211.033° C [3], 816.55° C [4]	2000° C [1], 1605.517° C [2], 1211.033° C [3], 816.55° C [4]

8.3.1.5. DHX check valve reducer, volume (109)

In the prototypical DRACS DHX module cutaway, as shown in Figure 4-3, there is a reducer below the DHX tubes which has a check valve called out at that point. For this reason, this volume is called the check valve reducer, although it was modeled as a pipe rather than a check valve. The flow direction is governed by the time dependent junction, so this volume just models the effects of the flow area reduction. Also shown in Figure 4-3 is some space between where the DHX tubes end and this reducer begin. Without dimensions, specifics could not be modeled, so the height of this empty space and the reducer were estimated.

As discussed in section 5.2.2, the reducer itself is broken into two volumes, one with the larger area and one with the smaller area. The empty space above is a third volume with constant flow area. Through running both RELAP5-3D models, it became clear that the nodalization with values from the SolidWorks model resulted in unstable geometry, due to the low length to diameter ratio. The length of the two reducers, this and volume (113), were increased in order to stabilize the problem. The length which was added to volume (109) was subtracted from volume (111), and the length added to volume (113) was subtracted from volume (115) in order to preserve the overall distance covered by the outlet piping. The flow area and hydraulic diameter of each section are calculated according to equations (8.1) and (8.2), where the terms accounting for the DHX tubes are set to zero. The results are shown below in Table 8-5.

Table 8-5: DHX check valve reducer information, volume (109)

Characteristic	Full-scale	Scaled-down
Flow area	2.5592528 m^2 [1,2], 0.4459025816 m^2 [3]	0.1599533 m^2 [1,2], 0.02786891135 m^2 [3]
Section length	0.4064 m [1], 1.0 m [2,3]	0.1016 m [1], 0.25 m [2,3]
Vertical angle	-90°	-90°
Elevation change	-0.4064 m [1], -1.0 m [2,3]	-0.1016 m [1], -0.25 m [2,3]
Hydraulic diameter	1.1303 m [1,2], 0.2794 m [3]	0.282575 m [1,2], 0.06985 m [3]
Pressure	4.5 bar	4.5 bar
Temperature	816.55° C	816.55° C

8.3.1.6. DHX outlet annulus, volume (111)

The DHX outlet annulus is the outer annulus around the DHX inlet pipe, from the point where it joins by means of the elbow, as contained in volume (105). This annulus ends at an elevation of just below the bottom-most elevation of said elbow, a half-inch below the outer diameter in the scaled-down model and two inches below in the full-scale model. The inner diameter was selected to provide a flow area very similar to that of the inner pipe. The length was adjusted in order to get the proper direct loop height, or elevation difference between the center of the core and the DHX. All of these design features were completed for the scaled-down model in SolidWorks and scaled up for the full-scale model for RELAP5-3D. The length of volume (111) is divided equally into the two sections. The volume and junction flags are the same as described for volume (103).

Table 8-6: DHX outlet annulus information, volume (111)

Characteristic	Full-scale	Scaled-down
Flow area	0.4459025816 m^2	0.02786891135 m^2
Section length	1.734437 m	0.47360925 m
Vertical angle	-90°	-90°
Elevation change	-1.734437 m	-0.47360925 m
Hydraulic diameter	0.2794 m	0.06985 m
Pressure	4.5 bar	4.5 bar
Temperature	816.55° C	816.55° C

8.3.1.7. DHX direct outlet reducer, volume (113)

Volume (113) is made up of the reducer which takes the diameter from the outlet annulus diameter to the outlet pipe diameter, and the direct DHX outlet flange. This volume functions similar to volume (109) except that the section with constant flow area follows the reducer rather than preceding it. This reducer does not have an analogous component in the prototype because the flow path from the RPV to the DHX module in that case is concentric the whole way. Length had to be added to the reducer sections in order to increase the length to diameter ratio for stability of the model as discussed in section 8.3.1.5. The volume and junction flags are the same that are described for volume (103). Table 8-7 contains the relevant information for this volume.

Table 8-7: DHX direct outlet reducer information, volume (113)

Characteristic	Full-scale	Scaled-down
Flow area	1.049011159 m^2 [1], 0.4713646324 m^2 [2,3]	0.06556319741 m^2 [1], 0.02946029853 m^2 [2,3]
Section length	0.6096 m [1,2], 0.445008 m [3]	0.1524 m [1,2], 0.111252 m [3]
Vertical angle	-90°	-90°
Elevation change	-0.6096 m [1,2], -0.445008 m [3]	-0.1524 m [1,2], -0.111252 m [3]
Hydraulic diameter	1.1557 m [1], 0.7747 m [2,3]	0.288925 m [1], 0.193675 m [2,3]
Pressure	4.5 bar	4.5 bar
Temperature	816.55° C	816.55° C

8.3.1.8. Direct outlet pipe, volume (115)

The direct outlet pipe is that which is needed to connect the outlet of the DHX module to the port selected to be the outlet for the direct loop. It is made up of a flange, a vertical pipe, an elbow, and another flange. The vertical section is divided into two even sections, and the horizontal section is one section.

This horizontal section is the only one in the loop with a horizontal angle other than zero, and it is set at the angle necessary to make the connection to the proper port. The volume and junction flags are the same as described for volume (103). Relevant information for this volume is contained in Table 8-8.

Table 8-8: Direct outlet pipe information, volume (115)

Characteristic	Full-scale	Scaled-down
Flow area	0.4713646324 m^2	0.02946029853 m^2
Section length	2.320925 m [1,2], 1.664208 m [3]	0.58023125 m [1,2], 0.416052 m [3]
Horizontal angle	0° [1,2], 182.94072° [3]	0° [1,2], 182.94072° [3]
Vertical angle	-90° [1,2], 0° [3]	-90° [1,2], 0° [3]
Elevation change	-2.320925 m [1,2], 0 m [3]	-0.58023125 m [1,2], 0 m [3]
Hydraulic diameter	0.7747 m	0.193675 m
Pressure	4.5 bar	4.5 bar
Temperature	816.55° C	816.55° C

8.3.2. Intermediate loop model specifics

The intermediate loop nodalization, shown in Figure 5-6, includes 8 volume components and 8 junction components as it is a closed loop. Water in this intermediate loop flows through the tubes which make up both the DHX and NDHX, and so 2 volumes have attached heat structures. The inlet and outlet manifold components for the DHX tubes are very similar and so will be described together. All other components will be briefly described individually.

There are certain system quantities which remain the same throughout the intermediate loop, such as the mass flow rate, the surface roughness, pressure, and the volume and junction flags within each volume component. The defaults are used for each of these, with water packing enabled, although the code only applies the water packing scheme to vertically oriented volumes. There is no choking model used except

at two places because the flow area remains constant through much of the loop, and otherwise area changes are smooth, except where the DHX tubes meet the manifolds on either end. For these two junctions, the standard choking model is enabled with an abrupt area change. The system pressure is set just below the pressure rating of schedule 80 stainless steel pipe for a 6-inch pipe, which is the full-scale model diameter, and the rating is higher for the scaled-down pipe. The system pressure is maintained in these RELAP5-3D models by the addition of a time-dependent volume in the loop.

8.3.2.1. DHX intermediate outlet pipe, volume (201)

The DHX intermediate outlet pipe consists of an elbow, a vertical pipe, and a flange which start at the outlet of the DHX outlet manifold, go through the DHX plenum, and end on the outside of the plenum. One section is used for the horizontal component of the elbow, and one section is used for all of the vertical piping. The flow area remains the same for the entire volume, as is the case for most of the intermediate loop.

Table 8-9: DHX intermediate outlet pipe information, volume (201)

Characteristic	Full-scale	Scaled-down
Flow area	0.01824146925 m^2	0.001140091828 m^2
Section length	0.2286 m [1], 1.38303 m [2]	0.05715 m [1], 0.3457575 m [2]
Horizontal	0°	0°
Vertical angle	0° [1], 90° [2]	0° [1], 90° [2]
Elevation change	0 m [1], 1.38303 m [2]	0 m [1], 0.3457575 m [2]
Hydraulic diameter	0.1524 m	0.0381 m
Pressure	140 bar	140 bar
Temperature	215.23° C	215.23° C
Mass flow rate	9.313552723 kg/s	0.2910485226 kg/s

8.3.2.2. Intermediate loop hot pipe, volume (203)

The intermediate loop hot pipe is made up of all the piping between the intermediate outlet flange on the DHX module and the NDHX tube inlet. A total of 10 sections are made up of 5 horizontal and 5 vertical sections. The first 4 horizontal sections of pipe make up the difference along the y-axis between the DHX outlet and the NDHX inlet such that there is no distance to be covered along that axis between the NDHX outlet and the DHX inlet. The piping is well insulated such that the temperature remains constant at the high temperature for the loop.

Table 8-10: Intermediate loop hot pipe information, volume (203)

Characteristic	Full-scale	Scaled-down
Flow area	0.01824146925 m^2	0.001140091828 m^2
Section length	0.50165 m [1], 2.9194125 m [2-5], 2.7844623 m [6-9], 0.2286 m [10]	0.1254125 m [1], 0.7267870013 m [2-5], 0.696115575 m [6-9], 0.05715 m [10]
Horizontal	0° [1], 143.1716637° [2-5], 0° [6-9], 180° [10]	0° [1], 143.1716637° [2-5], 0° [6-9], 180° [10]
Vertical angle	90° [1], 0° [2-5], 90° [6-9], 0° [10]	90° [1], 0° [2-5], 90° [6-9], 0° [10]
Elevation change	0.50165 m [1], 0 m [2-5], 2.7844623 m [6-9], 0 m [10]	0.1254125 m [1], 0 m [2-5], 0.696115575 m [6-9], 0 m [10]
Hydraulic diameter	0.1524 m	0.0381 m
Pressure	140 bar	140 bar
Temperature	215.23° C	215.23° C
Mass flow rate	9.313552723 kg/s	0.2910485226 kg/s

8.3.2.3. Intermediate side of NDHX tube, volume (205)

The specifics of the NDHX tubes are not known for the full-scale prototype. Overall dimensions of the heat exchangers are given, it is known that the inlet and outlet both connect on the same side at opposite ends, and it sits horizontally. All of these things have been preserved in the model in RELAP5-3D and SolidWorks. The piping has been designed with 3 bends, each of equal size, and the overall dimensions were scaled down for the SolidWorks model, and scaled back up to be used in the full-scale RELAP5-3D model. The bends are long gradual bends to reduce form loss through the heat exchanger.

Table 8-11: Intermediate side of NDHX tube information, volume (205)

Characteristic	Full-scale	Scaled-down
Flow area	0.01824146925 m^2	0.001140091828 m^2
Section length	1.4722094 m [1-6,23-28], 2.3334472 m [7,8,14,15,21,22], 1.49266656 m [9-13,16-20]	0.36805235 m [1-6,23-28], 0.5833618 m [7,8,14,15,21,22], 0.37316664 m [9-13,16-20]
Horizontal	180° [1-6,16-20], 210° [7,15,21], 330° [8,14,22], 0° [9-13,23-28]	180° [1-6,16-20], 210° [7,15,21], 330° [8,14,22], 0° [9-13,23-28]
Vertical angle	0°	0°
Hydraulic diameter	0.1524 m	0.0381 m
Pressure	140 bar	140 bar
Temperature	215.23° C, 212.58° C, 209.93° C, 207.27° C, 204.62° C, 201.97° C, 197.76° C, 193.56° C, 190.87° C, 188.18° C, 185.49° C, 182.80° C, 180.12° C, 175.91° C, 171.71° C, 169.02° C, 166.33° C, 163.34° C, 160.95° C, 158.26° C, 154.06° C, 149.85° C, 147.2° C, 144.55° C, 141.9° C, 139.24° C, 136.59° C, 133.94° C	215.23° C, 212.58° C, 209.93° C, 207.27° C, 204.62° C, 201.97° C, 197.76° C, 193.56° C, 190.87° C, 188.18° C, 185.49° C, 182.80° C, 180.12° C, 175.91° C, 171.71° C, 169.02° C, 166.33° C, 163.34° C, 160.95° C, 158.26° C, 154.06° C, 149.85° C, 147.2° C, 144.55° C, 141.9° C, 139.24° C, 136.59° C, 133.94° C

The overall length of tube in the heat exchanger is quite large compared to all of the other components in the intermediate loop, so the tube is divided into quite a few sections. The temperature is reduced through the heat structure attached to this volume, and so there are a lot of separate temperatures to input. The temperature distribution was computed using length weighting. Each bend was modeled as two sections at reflected angles to make up the horizontal distance. All of the relevant input information for volume (205) is shown above in Table 8-11.

8.3.2.4. Intermediate loop cold pipe, volume (207)

The intermediate loop cold pipe is much like the hot pipe, although it has more vertical distance to cover and does not cover any distance along the y-axis. The first section is the horizontal component of an elbow, followed by five vertical sections, and then three horizontal sections leading up to the intermediate DHX module inlet flange.

Table 8-12: Intermediate loop cold pipe information, volume (207)

Characteristic	Full-scale	Scaled-down
Flow area	0.01824146925 m^2	0.001140091828 m^2
Section length	0.2286 m [1], 2.79551384 m [2-6], 2.372783333 m [7-9]	0.05715 m [1], 0.69887846 m [2-6], 0.5931958333 m [7-9]
Horizontal	0°	0°
Vertical angle	0° [1], -90° [2-6], 0° [7-9]	0° [1], -90° [2-6], 0° [7-9]
Elevation change	0 m [1,7-9], -2.79551384 m [2-6]	0 m [1,7-9], -0.69887846 m [2-6]
Hydraulic diameter	0.1524 m	0.0381 m
Pressure	140 bar	140 bar
Temperature	133.94° C	133.94° C
Mass flow rate	9.313552723 kg/s	0.2910485226 kg/s

8.3.2.5. DHX intermediate inlet pipe, volume (209)

The DHX intermediate inlet pipe is made up of the intermediate DHX module inlet flange and a small length of pipe that leads to the inlet DHX manifold. This pipe is modeled as a branch component. The overall length was short enough that only one volume is required, and the time-dependent volume (238) is connected here in order to regulate the pressure throughout the loop. The three junctions that connect to this volume then make it necessary to use a branch component. Junction [1] connects volume (207) to (209). Junction [2] connects volume (209) to (211). Junction [3] connects volume (238) to (209). These junction numbers are reflected in Table 8-13 for the flow rates. Junction [3] uses a junction flag value of 1 for the v flag, which specifies that a vertical intake volume is connected to a horizontal component.

Table 8-13: DHX intermediate inlet pipe information, volume (209)

Characteristic	Full-scale	Scaled-down
Flow area	0.01824146925 m^2	0.001140091828 m^2
Section length	1.59385 m	0.3984625 m
Horizontal	0°	0°
Vertical angle	0°	0°
Elevation change	0 m	0 m
Hydraulic diameter	0.1524 m	0.0381 m
Pressure	140 bar	140 bar
Temperature	133.94° C	133.94° C
Mass flow rate	9.313552723 kg/s [1,2], 0 kg/s [3]	0.2910485226 kg/s [1,2], 0 kg/s [3]

8.3.2.6. DHX tube manifolds, volumes (211) and (215)

The DHX tube manifolds are very similar components, with some reflection depending on inlet or outlet. The shape on the tube side is made to provide a smooth shape with only some extra distance around the outside of the tubes such that there is enough room to have a wall. On the pipe side of each manifold, the shape is simply the dimensions of the pipe which it connects to, which is that piping used throughout the rest of the intermediate loop. The center of the tube is offset in the vertical direction from the center of the tube side of the manifold in order to avoid interference with the tube bundle. This leads to a small elevation increase for each manifold. The inlet manifold is at the bottom of the tube bundle, and therefore the pipe end needs to be lower to avoid interference with the tubes. The outlet manifold is at the top of the tube bundle, so the pipe end needs to be higher to avoid interference with the tubes. Round cuts from the side which is closest to the tube bundle on the tube side of each manifold were necessary to avoid interference with the adjacent layer of tubes. This leads to a unique manifold shape, seen below in Figure 8-1. The manifold pictured is the outlet manifold, although the inlet manifold loos similar, just with the cuts on the top side. The shape in between these two ends was created using the lofted boss/base button in SolidWorks, so a smooth curve was fitted between the two sketches.

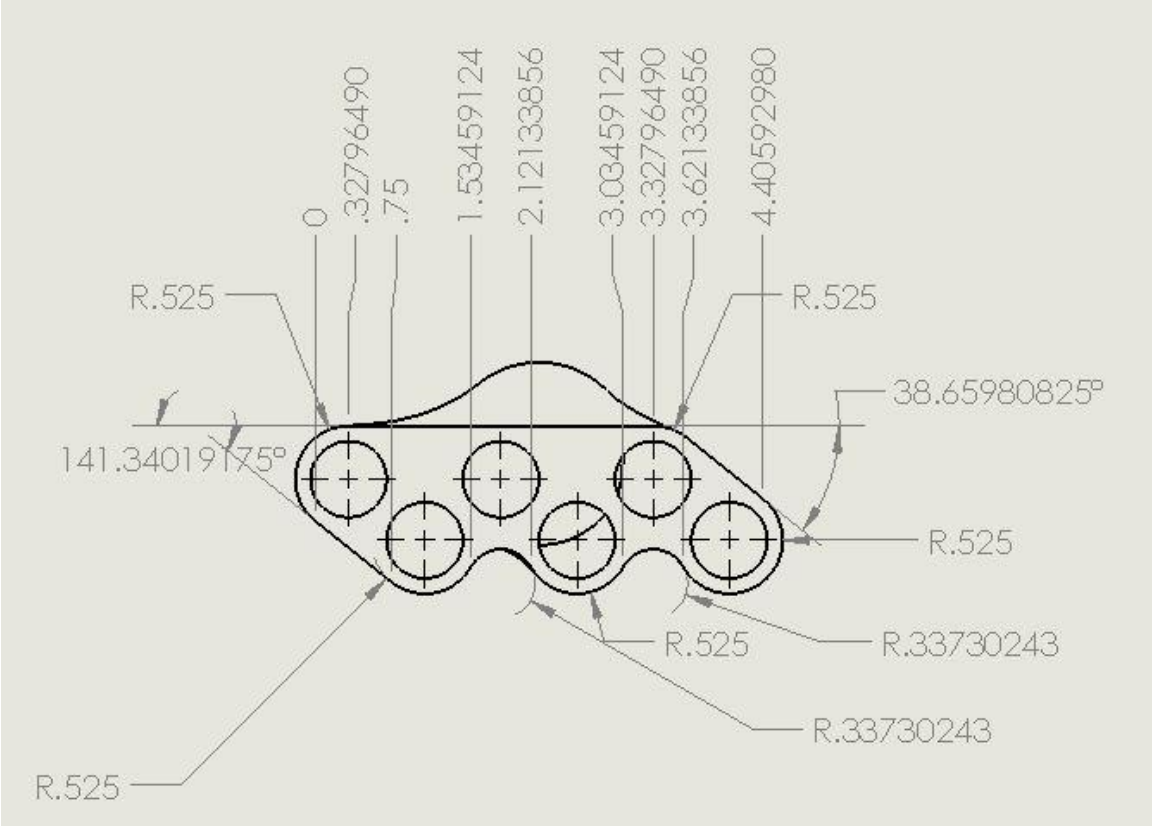

Figure 8-1: DHX outlet manifold with dimensions

The hydraulic diameter for the tube side of these manifolds was calculated by finding the perimeter on the inside and dividing by pi for an equivalent diameter. This equivalent diameter was also used to find the flow area on this end, as the geometry is very complicated. In the table below, the numbers which specify section [1] refers to the pipe side for both manifolds, while section [2] refers to the tube sheet side, although the actual section number for each end depends on whether it is the inlet or outlet manifold.

Table 8-14: DHX tube manifolds information, volumes (211) and (215)

Characteristic	Full-scale	Scaled-down
Flow area	0.01824146925 m^2 [1], 0.1024249944 m^2 [2]	0.001140091828 m^2 [1], 0.006401562149 m^2 [2]
Section length	0.1016 m	0.0254 m
Horizontal	0°	0°
Vertical angle	5.710593137°	5.710593137°
Elevation change	0.01016 m	0.00254 m
Hydraulic diameter	0.1524 m [1], 0.3611253 m [2]	0.0381 m [1], 0.0902813496 m [2]
Pressure	140 bar	140 bar
Temperature	133.94° C (211), 215.23° C (215)	133.94° C (211), 215.23° C (215)
Mass flow rate	9.313552723 kg/s	0.2910485226 kg/s

8.3.2.7. DHX tubes intermediate side, volume (213)

There are six tubes which make up the multi-tube helical coil DHX. RELAP5-3D models parallel flow channels more easily by combining them into a single component with an increased flow area. In a four loop PWR, three loops are combined into one loop in RELAP5-3D and only the loop which contains the pressurizer is kept separate. This example is shown in volume 5 of the RELAP5-3D manual, while demonstrating nodalization. Another application of this principle is in modeling steam generator tube ruptures, intact tubes are lumped together, while the ruptured tube is modeled separately. Multiple flow channels through the reactor core might be similarly lumped, while the hot channel is modeled separately. The purpose of the model determines what components are important enough to model separately.

In this case, all six tubes function the same and are modeled with an overall length which is the average of the six tubes. The flow areas are summed for one total flow area. The hydraulic diameter is the same as a single tube because while the flow area of six tubes are combined, so are the perimeters of those six tubes. The length of each tube is calculated using its major diameter and the number of turns from inlet to outlet. Each tube makes seven turns in total. The separation between a single tube from one layer to the next is twice the stream-wise pitch, which was discussed in section 5.2.3.5. Because of the helical tube wrap, the length of the tubes on the intermediate side is much greater than the length of the flow past the tubes on the direct side.

There is not a way in RELAP5-3D to model a constantly curving tube like a helical coil properly, so a choice must be made on what assumptions to make. A report out of Idaho National Lab describes some simplifications necessary to model a helical-coil steam generator, and how the simplifications affected the problem modeled. All of the tubes were combined similarly into a single tube, with equivalent flow area, hydraulic diameter, heat transfer area, and heated hydraulic diameter. The single tube was modeled as a horizontal pipe inclined with the same inclination angle as the tube bundle. This resulted in reduced heat transfer from the coiled tubes, and the mass flow rate had to be adjusted to get the proper temperature drop across the tubes, as well as a heat transfer multiplier [72]. This problem was discussed briefly during the advanced thermal hydraulics course with Dr. Qiao Wu, and he argued that modeling a helical coil

heat exchanger with an entirely vertical pipe matches the flow dynamics properly so the heat transfer multiplier and adjustment of mass flow rate will not be necessary.

Helical coil heat exchangers increase heat transfer because the shape causes constant acceleration of the fluid toward the center leading to more mixing. A straight pipe inclined at the same angle will have issues with stratified two-phase flow where the inclination angle leads to gravity affecting liquid water more than steam, which can cause chugging, or at least greater interfacial drag. This issue is not present in a helical coil due to the mixing discussed above, and a vertical pipe does not suffer from any stratified flow, so more closely matches.

The helical coil is therefore modeled in this work as a single pipe which preserves the flow area, heat transfer area, hydraulic diameter and heated hydraulic diameter. This single pipe is fully vertical, and the flow length matches that of the helical tube bundle, while the elevation change is also set to be what it would be if the pipe were at the proper inclination angle. Thus the reduced elevation change leads to the proper loop elevations preserved, and the flow length is still preserved. RELAP5-3D limits the elevation change to be less than or equal to the flow length, so this reduction in elevation change is allowed.

All information necessary for volume (213) is entered in Table 8-15 below. The temperature changes between sections are again listed sequentially without section

numbers called out next to each temperature. The temperature distribution in this component is evenly distributed as each section is of the same length.

Table 8-15: DHX tubes intermediate side information, volume (213)

Characteristic	Full-scale	Scaled-down
Flow area	0.02055205535 m^2	0.00128450346 m^2
Section length	1.550046107 m	0.3875115268 m
Horizontal	0°	0°
Vertical angle	90°	90°
Elevation change	0.04572 m	0.01143 m
Hydraulic diameter	0.06604 m	0.01651 m
Pressure	140 bar	140 bar
Temperature	133.94° C, 138.22° C, 142.50° C, 146.78° C, 151.05° C, 155.33° C, 159.61° C, 163.89° C, 168.17° C, 172.45° C, 176.72° C, 181.00° C, 185.28° C, 198.56° C, 193.84° C, 198.12° C, 202.39° C, 206.67° C, 210.95° C, 215.23° C	133.94° C, 138.22° C, 142.50° C, 146.78° C, 151.05° C, 155.33° C, 159.61° C, 163.89° C, 168.17° C, 172.45° C, 176.72° C, 181.00° C, 185.28° C, 198.56° C, 193.84° C, 198.12° C, 202.39° C, 206.67° C, 210.95° C, 215.23° C
Mass flow rate	9.313552723 kg/s	0.2910485226 kg/s

8.3.3. Natural draft loop model specifics

The natural draft loop is modeled as a single pipe component surrounded by time-dependent junctions and time-dependent volumes. These time-dependent components serve to create boundary conditions for the inlet and outlet of this pipe component, and these boundary conditions are steady-state in this case. The full-scale model uses a NDDCT to cool the NDHX, while the scaled-down model is designed with a forced draft air-cooled NDHX instead. The flow through the heat exchanger is then modeled by the

pipe component, and the rest of this loop is different depending on full-scale or scaled-down model, so it is omitted.

8.3.3.1. Natural draft loop boundaries, volumes (301) and (305)

The inlet velocity was calculated for the full-scale model using the python script, and the mass flow rate was determined therefrom. The boundary temperatures were also determined using said python script. This information is used as the boundary conditions.

The dimensions were given for the full-scale prototype NDHX, but not for the air duct that leads to and from the NDHX. In Figure 1-4, it can be seen that the area decreases through the NDHX, but not by how much. Half of a meter was added in each direction to the full-scale model for the air ducts above and below the NDHX as a rough estimate, and the overall dimensions is scaled by the length scale for the scaled-down model. The angle of the air duct on the outlet side was taken to be 45° for calculations of friction and form loss in the python script. These boundary volumes, however, both have a vertical angle of 90°, with the same flow area and length.

The area change into and out of the DHX looks to be smooth in Figure 1-4, so no choking model is applied in the boundary junctions.

Table 8-16: Natural draft boundaries information, volumes (301) and (305)

Characteristic	Full-scale	Scaled-down
Flow area	78.75 m^2	4.921875 m^2
Section length	1 m	0.25 m
Horizontal	0°	0°
Vertical angle	90°	90°
Elevation change	1 m	0.25 m
Hydraulic diameter	8.75 m	2.1875 m
Pressure	1 bar	1 bar
Temperature	30° C (301), 49.62° C (305)	30° C (301), 49.62° C (305)
Mass flow rate	253.5775529 kg/s	7.924298528 kg/s

8.3.3.2. Natural draft NDHX reject heat air flow, volume (303)

The overall height of the NDHX in the full-scale prototype is called out in Figure 1-4, and the height is greater than the outer diameter of the NDHX tube. The NDHX is therefore assumed to be a finned-tube heat exchanger in the prototype. Calculations in the python script without fins revealed that the temperature rise across the NDHX would have to be greater than the maximum possible, such that the hot temperature in the natural draft loop would be greater than the hot temperature in the intermediate loop. Heat only transfers from high to low temperature, so this is impossible without another source of heat. Fins were added to the full-scale and scaled-down model in order to increase the heat transfer area on the natural draft side of the NDHX, thus allowing for a smaller temperature rise in the fluid with the same heat transfer rate. The boundary temperatures shown in Table 8-16 are based on this finned-tube NDHX.

Volume (303) is a pipe component divided into three sections. The center section is the part that contains the NDHX tubes and fins, while the two outer sections contain only fins. The height of the center section is equal to the outer diameter of the NDHX tube. The remaining vertical dimension as called out in Figure 1-4 is then split equally between the two outer sections. The overall area is also called out in the same figure for this NDHX pipe section, and the flow area was determined for each section by taking that number and removing the area obstructions. For the outer sections, only the fins cause an area obstruction. For the center sections, this was the fins and tube. The area obstruction due to the NDHX tube was found the same way as the area obstruction due to the DHX tubes for volume (107). The volume occupied by both fin and tube in the center section was divided by the length of the center section.

Table 8-17: Natural draft NDHX reject heat air flow information, volume (303)

Characteristic	Full-scale	Scaled-down
Flow area	49.112 m^2 [1,3], 44.31294158 m^2 [2]	3.0695 m^2 [1,3], 2.769558849 m^2 [2]
Section length	0.15348 m [1,3], 0.19304 m [2]	0.03837 m [1,3], 0.04826 m [2]
Horizontal	0°	0°
Vertical angle	90°	90°
Elevation change	0.15348 m [1,3], 0.19304 m [2]	0.03837 m [1,3], 0.04826 m [2]
Hydraulic diameter	0.009389542109 m [1,3], 0.009226199359 m [2]	0.002347385527 m [1,3], 0.00230654984 m [2]
Pressure	1 bar	1 bar
Temperature	30° C, 39.81° C, 49.62° C	30° C, 39.81° C, 49.62° C
Mass flow rate	253.5775529 kg/s	7.924298528 kg/s

The hydraulic diameter for each of these sections was also found similarly to the method described for volume (107). The large number of fins attached to tubes led to some more complicated calculations, but the concept is the same. The temperature variation across the volumes was found similarly to volume (205), using length weighting. The results of these calculations are listed in Table 8-17.

8.3.4. Heat structure model specifics

Heat structures are the components in RELAP5-3D which are used for heat generation and heat transfer. They do not have to communicate with a hydrodynamic volume, but they can. Fuel pins and steam generators are both heat structures that would be included in a full reactor system model, as well as any solid structures such as the thermal shield which are expected to have heat transferred across them.

A heat structure is broken into axial sections much like a pipe component in order to allow custom information for each section while still maintaining similarities throughout the heat structure. A heat structure is also divided radially in order to describe different layers, such as fuel, gap, and clad in a fuel pin. The axial break down allows the heat structure to communicate with multiple hydrodynamic volumes, while the radial break down allows each axial section to communicate with up to two separate hydrodynamic volumes. Multiple axial sections can communicate with a single hydrodynamic volume or section, but each axial section can only communicate with one hydrodynamic volume. Thus a heat structure should be broken down axially according to the

hydrodynamic volume it needs to share information with, there need to be at minimum the same number of axial sections as there are in the hydrodynamic volume.

In the case of this RELAP5-3D model of the DRACS, it has been assumed that all piping is well insulated, such that heat transfer only occurs across the two heat exchangers, the DHX and NDHX. Some description of the heat structure input information for each of these heat exchangers follows.

8.3.4.1. DRACS heat exchanger, heat structure (1213)

The DHX communicates with hydrodynamic volumes on both sides of the heat structure; volume (107) in the direct loop deposits heat, while volume (213) in the intermediate loop absorbs heat. Both heat structures were numbered according to the hydrodynamic volumes with which they communicate in the intermediate loop. Volume (107) has 4 sections to communicate with the DHX. Volume (213) has 20 sections to communicate with the DHX. The heat structure was broken into 20 axial sections in order to communicate with volume (213), and 5 axials sections were assigned to each of the 4 sections in volume (107). The DHX only has two radial mesh points, so only one material is described to separate the left boundary, volume (213), from the right boundary, volume (107).

No heat generation occurs within the DHX, and the default convection boundary condition type is used on both boundaries. The flow of the direct loop is opposite that of the intermediate loop past the DHX, thus it is a counter-flow heat exchanger. The axial heat structure numbers match that of the sections of volume (213), and the fourth

section of volume (107) is attached to the first five axial sections of the heat structure, and so on, to specify this counter-flow. No grid spacers are present in the DHX, so all associated values are not used. The boiling factor and heat transfer coefficient foul factors are set to default values for both boundaries. The forward and reverse heated lengths were found according to the guidelines in volume 2 appendix A of the RELAP5-3D user's manual [73]. All other relevant information for this heat structure is contained in Table 8-18.

Table 8-18: DHX information, heat structure (1213)

Characteristic	Full-scale	Scaled-down
Left boundary	0.03302 m	0.008255 m
Right boundary	0.0381 m	0.009525 m
Heated surf. area LB	0.3215892731 m^2	0.02009932957 m^2
Heated surf. area RB	0.3710645459 m^2	0.02319153412 m^2
Temperature on LB	198.15° C	198.15° C
Temperature on RB	732.7° C	732.7° C
Heated hyd. diam. LB	0.06604 m	0.01651 m
Heated hyd. diam. RB	1.185133526 m	0.2962833815 m
Natural circ. length LB	0.06604 m	0.01651 m
Natural circ. length RB	0.04572 m	0.01143 m
Pitch-to-diameter LB	1.477644055	1.477644055
Pitch-to-diameter RB	1.280624847	1.280624847

8.3.4.2. Natural draft heat exchanger, heat structure (1205)

The NDHX also communicates with hydrodynamic volumes on both sides of the heat structure; volume (205) in the intermediate loop deposits heat, while volume (303) in

the natural draft loop absorbs heat. The intermediate loop volume (205) again has a greater number of sections than the other side of the heat exchanger, so dictates the number of axial heat structures. In this case, volume (205) has 28 sections, while volume (303) has 3 sections. The allocation of axial heat structures to the sections in volume (303) is discussed later. Because of the horizontal orientation of the NDHX, the flow paths though the hydrodynamic volumes are orthogonal, thus it is a cross-flow heat exchanger. The NDHX only has two radial mesh points, so only one material is described to separate the left boundary, volume (205), from the right boundary, volume (303). The pitch-to diameter ratio for both boundaries are set to the maximum value of 1.6 because the tube spacing is very large compared to the diameter.

No heat generation occurs within the NDHX, and the default convection boundary condition type is used on both boundaries. No grid spacers are present in the DHX, so all associated values are not used. The boiling factor is set to the default value on both boundaries. The heat transfer coefficient foul factor is set to the default on the left boundary, but is used to compensate for heat transfer area on the right boundary, as discussed below. The forward and reverse heated lengths were found according to the guidelines in volume 2 appendix A of the RELAP5-3D user's manual [73]. All other relevant information for this heat structure is contained in Table 8-18.

Originally, the NDHX heat structure was built to try and model the fins attached to the tube on the natural draft side of the heat exchanger, affecting all three sections of volume (303). RELAP5-3D output an error that the surface area on the left and right

boundaries did not consistently match the geometry type. In order to eliminate this error, the extra surface area added by the fins was eliminated, and the heat transfer coefficient foul factor was used to compensate for the difference in surface area. According to equation (72), which is derived from Newton's law of cooling, the rate of heat transferred from a surface is the product of the difference in temperature between the object and its surroundings, the heated surface area, and the heat transfer coefficient. Thus the heat transfer rate and temperature difference can remain constant if the heat transfer coefficient is raised by the same factor that the surface area is lowered by. The ratio of finned-tube surface area to tube only surface area was found, and this ratio was used as the heat transfer coefficient foul factor. The result is that the error was eliminated, and the heat transfer rate should be calculated the same anyway.

Table 8-19: NDHX information, heat structure (1205)

Characteristic	Full-scale	Scaled-down
Left boundary	0.0762 m	0.01905 m
Right boundary	0.09652 m	0.02413 m
Heated surf. area LB	0.7453437193 m^2	0.04658398246 m^2
Heated surf. area RB	0.9441020445 m^2	0.05900637778 m^2
Temperature on LB	127.66° C	127.66° C
Temperature on RB	45.50° C	45.50° C
Heated hyd. diam. LB	0.1524 m	0.0381 m
Heated hyd. diam. RB	1.294377369 m	0.3235943422 m
Natural circ. length LB	0.1524 m	0.0381 m
Natural circ. length RB	0.006894285714 m	0.001723571429 m
Pitch-to-diameter LB	1.6	1.6
Pitch-to-diameter RB	1.6	1.6

The removal of the fins from the heat structure means that the outer sections of volume (303), which only touch fins, will no longer communicate with the heat structure, and all heat absorbed from the NDHX by the natural draft fluid must occur in the center section of volume (303), where the tubes are. Thus all 28 axial heat structures communicate with section [2] of volume (303).

8.4.Appendix D: Full-scale RELAP5-3D model deck

```
=DRACS prototype

**============================================================
=============**
** RELAP5-3D model of a Direct Reactor Auxiliary Cooling System
for a GFR     **
** Completed as a portion of the work to contribute to the thesis
as part of  **
** the degree requirements for a Master of Science degree in
Nuclear          **
** Engineering. The flow path is based on a scaled model designed
by me in    **
** order to compare outputs from two separate RELAP5-3D decks to
the scaling  **
** analysis. The two decks are identical except the input values
are scaled   **
** according to the scaling choices between model and prototype,
outlined in  **
** chapter 3 of said thesis.
**
**============================================================
=============**
** Author: Grant Blake
**
** Deck start date: 08/24/2016
**
** Deck end date: 09/10/2016
**
** Current version: 2.1
**
** Version updates: Fixed the order of minor edit outputs to
match model      **
**============================================================
=============**



**============================================================
=============**
** Miscellaneous Control Cards
**
**============================================================
=============**


**=======*===============*====================================
=============**
** Card 100, problem type and option
```

```
*        Problem type     Problem option
0000100  newath           transnt


** Card 102, units selection
*        Input units      Output units
0000102  si               si
**=======*================*=====================================
=============**


**=======*================*================*================*====
==========*==**
** Card 110, noncondensable gas species
*        Noncondensable gas type (enter up to 5)
0000110  helium           nitrogen         air


** Card 115, noncondensable mass fractions
*        Mass fraction for each gas type
0000115  0.8              0.2              0.0
**=======*================*================*================*====
==========*==**


**=======*================*================*================*====
==========*==**
** Card 120, hydrodynamic system control, direct loop
*        Ref. vol #       Ref. elevation   Fluid type       Name
g
0000120  107030000        0.0              he
Direct         0


** Card 121, hydrodynamic system control, intermediate loop
*        Ref. vol #       Ref. elevation   Fluid type       Name
g
0000121  213110000        0.0              h2o              Int-
Loop       1


** Card 122, hydrodynamic system control, air cooling loop
*        Ref. vol #       Ref. elevation   Fluid type       Name
g
0000122  303020000        13.5             n2               Air-
Loop       0
**=======*================*================*================*====
==========*==**
```

```
**=======*===============*===============*===============*=============**
** Card 201, time step control
*        End time         Min time step    Max time step    ssdtt
*        (sec)            (sec)            (sec)
0000201  1.6+4            1.0-5            20.0             00000
+        100              2000             2000000
*        ^                ^                ^
*        Minor frequency  Major frequency  restart frequency
*        (# of dt)        (# of dt)        (# of dt)
**=======*===============*===============*===============*=============**


**=========================================================================**
** Minor edit requests
**
**=========================================================================**

*        pressure         volume #
0000301  p                103010000
0000302  p                201010000
0000303  p                303030000

*        temperature      volume #
0000304  tempg            103010000
0000305  tempg            115030000
0000306  tempf            201010000
0000307  tempf            207010000
0000308  tempg            303030000
0000309  tempg            303010000

*        density          volume #
0000310  rho              103010000
0000311  rho              115030000
0000312  rho              201010000
0000313  rho              207010000
0000314  rho              303030000
0000315  rho              303010000

*        viscosity        volume #
0000316  viscg            103010000
0000317  viscf            201010000
0000318  viscg            303010000
0000334  viscf            207010000

*        velocity         volume #
0000319  velg             103010001
```

```
0000320  velf             201010001
0000321  velg             303010001
0000332  velf             238010001
0000333  velf             207010001
0000337  velf             207050001
0000338  velf             207090001

*        thermal cond.    volume #
0000322  thcong           103010000
0000323  thconf           201010000
0000324  thcong           303010000
0000335  thconf           207010000

*        heat tran rate   control variable/volume #
0000325  cntrlvar         001
0000326  cntrlvar         002
0000327  cntrlvar         003
0000328  q                303020000

*        specific heat    volume #
0000329  csubpg           103010000
0000330  csubpf           201010000
0000331  csubpg           303030000
0000336  csubpf           207010000



**=============================================================
=============**
** Hydrodynamic Components, Direct loop
**
**=============================================================
=============**


**=======*===============*===============*===============*====
==========*==**
** Volume 101, direct inlet boundary

*        Component name   Component type
1010000  DirInlet         tmdpvol

*        flow area        flow length      volume
horiz. angle   vert. angle
*        (m2)             (m)              (m3)             (deg)
(deg)
*         elev. chng.      roughness        hydraulic diam.  vol-
flag
*         (m)              (m)              (m)
tlpvbfe
```

```
1010101  0.4713646324     1.0               0.0               0.0
90.0
+         1.0              0.0               0.7747
0000000

*        ebt
1010200  004

*        time             pressure          temperature
static quality
*        (sec)            (Pa)              (K)               (dry
non-con.)
1010201  0.0              4.5+5             2273.15           0.0
**=======*================*================*================*====
==========*==**


**=======*================*================*================*====
============**
** Junction 102, direct inlet junction

*        Component name   Component type
1020000  DirInJnc         tmdpjun

*        from vol.        to vol.          jun. area         jun-
flag
*                                          (m2)
jefvcahs
1020101  101010000        103000000        0.4713646324
00000000

*        mass flow rates
1020200  1

*        time             liquid flow      vapor flow
interface vel.
*        (sec)            (kg/sec)         (kg/sec)
(m/sec)
1020201  0.0              0.0              0.8996961798      0.0
**=======*================*================*================*====
============**


**=======*=====*==========*================*================*====
=*=====*=====**
** Volume 103, direct inlet pipe

*        Component name   Component type
1030000  DirInPip         pipe
```

```
*        nv, # of volumes
1030001  3

*        flow area        vol #
*        (m2)
1030101  0.4713646324     3

*        flow length      vol #
*        (m)
1030301  1.2192           1
1030302  2.2198076        3

*        Horiz. angle     vol #
*        (deg)
1030501  0.0              3

*        Vert. angle      vol #
*        (deg)
1030601  90.0             1
1030602   0.0             3

*        Elev. change     vol #
*        (m)
1030701  1.2192           1
1030702  0.0              3

*        roughness        hydrlc.diam.     vol #
*        (m)              (m)
1030801  1.5-5            0.7747           3

*        vol-flag         vol #
*        tlpvbfe
1031001  0010000          3

*        jun-flag         jun #
*        jefvcahs
1031101  00001000         2

*        ebt   pressure   temperature      static quality   0.0
0.0   vol #
*              (Pa)       (K)              (dry non-con.)
1031201  004   4.5+5      2273.15          0.0              0.0
0.0   3

*        mass flow rates
1031300  1

*        liquid flow      vapor flow       interface vel.   jun #
*        (kg/sec)         (kg/sec)         (m/sec)
1031301  0.0              0.8996961798     0.0              2
```

```
**=======*=====*==========*===============*===============*====
=*=====*=====**


**=======*===============*===============*===============*====
=*=====*=====**
** Junction 104, DHX direct inlet flange face

*        Component name   Component type
1040000  DDHXInFl         sngljun

*        from vol.        to vol.          jun. area        A_F
A_R   jun-flag
*                                          (m2)
jefvcahs
1040101  103010000        105000000        0.4713646324     0.0
0.0   00001000

*        mass flow rates  liquid flow      vapor flow
interface vel.
*                         (kg/sec)         (kg/sec)
(m/sec)
1040201  1                0.0              0.8996961798     0.0
**=======*===============*===============*===============*====
=*=====*=====**


**=======*=====*==========*===============*===============*====
=*=====*=====**
** Volume 105, DHX inlet pipe

*        Component name   Component type
1050000  DHXInPip         pipe

*        nv, # of volumes
1050001  4

*        flow area        vol #
*        (m2)
1050101  0.4713646324     4

*        flow length      vol #
*        (m)
1050301  1.257808         1
1050302  3.150362         3
1050303  1.44145          4

*        Horiz. angle     vol #
*        (deg)
1050501  0.0              4
```

```
*        Vert. angle      vol #
*        (deg)
1050601   0.0             1
1050602  90.0             3
1050603   0.0             4

*        Elev. change     vol #
*        (m)
1050701  0.0              1
1050702  3.150362         3
1050703  0.0              4

*        roughness        hydrlc.diam.     vol #
*        (m)              (m)
1050801  1.5-5            0.7747           4

*        vol-flag         vol #
*        tlpvbfe
1051001  0010000          4

*        jun-flag         jun #
*        jefvcahs
1051101  00001000         3

*        ebt   pressure   temperature      static quality   0.0
0.0   vol #
*              (Pa)       (K)              (dry non-con.)
1051201  004   4.5+5      2273.15          0.0              0.0
0.0   4

*        mass flow rates
1051300  1

*        liquid flow      vapor flow       interface vel.   jun #
*        (kg/sec)         (kg/sec)         (m/sec)
1051301  0.0              0.8996961798     0.0              3
**=======*=====*==========*================*================*====
=*=====*=====**


**=======*================*================*================*====
=*=====*=====**
** Junction 106, direct entrance to flow over DHX tubes

*        Component name   Component type
1060000  InDHXJnc         sngljun

*        from vol.        to vol.          jun. area        A_F
A_R   jun-flag
```

```
*                                                (m2)
jefvcahs
1060101  105010000        107000000        0.4713646324     0.0
0.0   00001000

*        mass flow rates  liquid flow      vapor flow
interface vel.
*                         (kg/sec)         (kg/sec)
(m/sec)
1060201  1                0.0              0.8996961798     0.0
**=======*================*================*================*====
=*=====*======**


**=======*=====*==========*================*================*====
=*=====*======**
** Volume 107, direct flow over DHX tubes

*        Component name   Component type
1070000  DDHXTube         annulus

*        nv, # of volumes
1070001  4

*        flow area        vol #
*        (m2)
1070101  2.404642573      4

*        flow length      vol #
*        (m)
1070301  0.2286           4

*        Vert. angle      vol #
*        (deg)
1070601  -90.0            4

*        Elev. change     vol #
*        (m)
1070701  -0.2286          4

*        roughness        hydrlc.diam.     vol #
*        (m)              (m)
1070801  1.5-5            0.5601010397     4

*        vol-flag         vol #
*        tlpvbfe
1071001  0010000          4

*        jun-flag         jun #
*        jefvcahs
```

```
1071101  00001000         3

*        ebt   pressure   temperature      static quality   0.0
0.0   vol #
*              (Pa)       (K)              (dry non-con.)
1071201  004   4.5+5      2273.15          0.0              0.0
0.0   1
1071202  004   4.5+5      1878.667         0.0              0.0
0.0   2
1071203  004   4.5+5      1484.183         0.0              0.0
0.0   3
1071204  004   4.5+5      1089.70          0.0              0.0
0.0   4

*        mass flow rates
1071300  1

*        liquid flow      vapor flow       interface vel.   jun #
*        (kg/sec)         (kg/sec)         (m/sec)
1071301  0.0              0.8996961798     0.0              3
**=======*=====*==========*================*================*====
=*=====*=====**


**=======*================*================*================*====
=*=====*=====**
** Junction 108, direct end of flow over DHX tubes

*        Component name   Component type
1080000  OutDHXJn         sngljun

*        from vol.        to vol.          jun. area        A_F
A_R   jun-flag
*                                          (m2)
jefvcahs
1080101  107010000        109000000        2.404642573      0.0
0.0   00001000

*        mass flow rates  liquid flow      vapor flow
interface vel.
*                         (kg/sec)         (kg/sec)
(m/sec)
1080201  1                0.0              0.8996961798     0.0
**=======*================*================*================*====
=*=====*=====**


**=======*=====*==========*================*================*====
=*=====*=====**
** Volume 109, DHX check valve reducer
```

```
*        Component name   Component type
1090000  DHXChkVl         annulus

*        nv, # of volumes
1090001  3

*        flow area        vol #
*        (m2)
1090101  2.5592528        2
1090102  0.4459025816     3

*        flow length      vol #
*        (m)
1090301  0.4064           1
1090302  1.0              3

*        Vert. angle      vol #
*        (deg)
1090601  -90.0            3

*        Elev. change     vol #
*        (m)
1090701  -0.4064          1
1090702  -1.0             3

*        roughness        hydrlc.diam.     vol #
*        (m)              (m)
1090801  1.5-5            1.1303           2
1090802  1.5-5            0.2794           3

*        vol-flag         vol #
*        tlpvbfe
1091001  0010000          3

*        jun-flag         jun #
*        jefvcahs
1091101  00001000         2

*        ebt   pressure   temperature      static quality   0.0
0.0   vol #
*              (Pa)       (K)              (dry non-con.)
1091201  004   4.5+5      1089.7           0.0              0.0
0.0   3

*        mass flow rates
1091300  1

*        liquid flow      vapor flow       interface vel.   jun #
*        (kg/sec)         (kg/sec)         (m/sec)
```

```
1091301  0.0               0.8996961798     0.0               2
**=======*=====*==========*================*================*====
=*=====*=====**


**=======*===============*===============*================*====
=*=====*=====**
** Junction 110, DHX check valve out

*        Component name   Component type
1100000  DHXCVOut         sngljun

*        from vol.        to vol.          jun. area        A_F
A_R   jun-flag
*                                          (m2)
jefvcahs
1100101  109010000        111000000        0.4459025816     0.0
0.0   00001000

*        mass flow rates  liquid flow      vapor flow
interface vel.
*                         (kg/sec)         (kg/sec)
(m/sec)
1100201  1                0.0              0.8996961798     0.0
**=======*================*================*================*====
=*=====*=====**


**=======*=====*==========*================*================*====
=*=====*=====**
** Volume 111, DHX outlet annulus

*        Component name   Component type
1110000  DHXOutAn         annulus

*        nv, # of volumes
1110001  2

*        flow area        vol #
*        (m2)
1110101  0.4459025816     2

*        flow length      vol #
*        (m)
1110301  1.734437         2

*        Vert. angle      vol #
*        (deg)
1110601  -90.0            2
```

```
*        Elev. change     vol #
*        (m)
1110701  -1.734437        2

*        roughness        hydrlc.diam.     vol #
*        (m)              (m)
1110801  1.5-5            0.2794           2

*        vol-flag         vol #
*        tlpvbfe
1111001  0010000          2

*        jun-flag         jun #
*        jefvcahs
1111101  00001000         1

*        ebt   pressure   temperature      static quality   0.0
0.0   vol #
*              (Pa)       (K)              (dry non-con.)
1111201  004   4.5+5      1089.7           0.0              0.0
0.0   2

*        mass flow rates
1111300  1

*        liquid flow      vapor flow       interface vel.   jun #
*        (kg/sec)         (kg/sec)         (m/sec)
1111301  0.0              0.8996961798     0.0              1
**=======*=====*==========*================*================*====
=*=====*=====**


**=======*===============*================*================*====
=*=====*=====**
** Junction 112, end of DHX annulus

*        Component name   Component type
1120000  DHXEndAn         sngljun

*        from vol.        to vol.          jun. area        A_F
A_R   jun-flag
*                                          (m2)
jefvcahs
1120101  111010000        113000000        0.4459025816     0.0
0.0   00001000

*        mass flow rates  liquid flow      vapor flow
interface vel.
*                         (kg/sec)         (kg/sec)
(m/sec)
```

```
1120201  1                0.0              0.8996961798     0.0
**=======*================*================*================*====
=*=====*=====**


**=======*=====*==========*================*================*====
=*=====*=====**
** Volume 113, DHX diret outlet reducer

*        Component name   Component type
1130000  DHXOutRd         pipe

*        nv, # of volumes
1130001  3

*        flow area        vol #
*        (m2)
1130101  1.0490111586     1
1130102  0.4713646324     3

*        flow length      vol #
*        (m)
1130301  0.6096           2
1130302  0.445008         3

*        Vert. angle      vol #
*        (deg)
1130601  -90.0            3

*        Elev. change     vol #
*        (m)
1130701  -0.6096          2
1130702  -0.445008        3

*        roughness        hydrlc.diam.     vol #
*        (m)              (m)
1130801  1.5-5            1.1557           1
1130802  1.5-5            0.7747           3

*        vol-flag         vol #
*        tlpvbfe
1131001  0010000          3

*        jun-flag         jun #
*        jefvcahs
1131101  00001000         2

*        ebt   pressure   temperature      static quality   0.0
0.0   vol #
*              (Pa)       (K)              (dry non-con.)
```

```
1131201  004   4.5+5      1089.7           0.0              0.0
0.0   3

*        mass flow rates
1131300  1

*        liquid flow      vapor flow       interface vel.   jun #
*        (kg/sec)         (kg/sec)         (m/sec)
1131301  0.0              0.8996961798     0.0              2
**=======*=====*==========*================*================*====
=*=====*=====**


**=======*================*================*================*====
=*=====*=====**
** Junction 114, DHX direct outlet flange face

*        Component name   Component type
1140000  DDHXOutF         sngljun

*        from vol.        to vol.          jun. area        A_F
A_R   jun-flag
*                                          (m2)
jefvcahs
1140101  113010000        115000000        0.4713646324     0.0
0.0   00001000

*        mass flow rates  liquid flow      vapor flow
interface vel.
*                         (kg/sec)         (kg/sec)
(m/sec)
1140201  1                0.0              0.8996961798     0.0
**=======*================*================*================*====
=*=====*=====**


**=======*=====*==========*================*================*====
=*=====*=====**
** Volume 115, direct outlet pipe

*        Component name   Component type
1150000  DirOutPi         pipe

*        nv, # of volumes
1150001  3

*        flow area        vol #
*        (m2)
1150101  0.4713646324     3
```

```
*        flow length      vol #
*        (m)
1150301  2.320925         2
1150302  1.664208         3

*        Horiz. angle     vol #
*        (deg)
1150501    0.0            2
1150502  182.940720339    3

*        Vert. angle      vol #
*        (deg)
1150601  -90.0            2
1150602    0.0            3

*        Elev. change     vol #
*        (m)
1150701  -2.320925        2
1150702   0.0             3

*        roughness        hydrlc.diam.     vol #
*        (m)              (m)
1150801  1.5-5            0.7747           3

*        vol-flag         vol #
*        tlpvbfe
1151001  0010000          3

*        jun-flag         jun #
*        jefvcahs
1151101  00001000         2

*        ebt   pressure   temperature      static quality   0.0
0.0   vol #
*               (Pa)      (K)              (dry non-con.)
1151201  004   4.5+5      1089.7           0.0              0.0
0.0   3

*        mass flow rates
1151300  1

*        liquid flow      vapor flow       interface vel.   jun #
*        (kg/sec)         (kg/sec)         (m/sec)
1151301  0.0              0.8996961798     0.0              2
**=======*=====*==========*================*================*====
=*=====*=====**


**=======*================*================*================*====
=*=====*=====**
```

```
** Junction 116, direct outlet junction

*        Component name   Component type
1160000  DirOutJn         sngljun

*        from vol.        to vol.          jun. area        A_F
A_R   jun-flag
*                                          (m2)
jefvcahs
1160101  115010000        117000000        0.4713646324     0.0
0.0   00000000

*        mass flow rates  liquid flow      vapor flow
interface vel.
*                         (kg/sec)         (kg/sec)
(m/sec)
1160201  1                0.0              0.8996961798     0.0
**=======*================*================*================*====
=*=====*=====**


**=======*================*================*================*====
==========*==**
** Volume 117, direct outlet boundary

*        Component name   Component type
1170000  DirOutlt         tmdpvol

*        flow area        flow length      volume
horiz. angle   vert. angle
*        (m2)             (m)              (m3)             (deg)
(deg)
*         elev. chng.      roughness        hydraulic diam.  vol-
flag
*         (m)              (m)              (m)
tlpvbfe
1170101  0.4713646324     1.0              0.0
182.940720339  0.0
+         0.0              0.0              0.7747
0000000

*        ebt
1170200  004

*        time             pressure         temperature
static quality
*        (sec)            (Pa)             (K)              (dry
non-con.)
1170201  0.0              4.5+5            1089.7           0.0
```

```
**=======*===============*===============*===============*====
==========*==**


**=================================================================
=============**
** Hydrodynamic Components, Intermediate loop
**
**=================================================================
=============**


**=======*===============*===============*===============*====
*====*======***
** Volume 201, DHX intermediate outlet pipe

*        Component name   Component type
2010000  IDHXOPip         pipe

*        nv, # of volumes
2010001  2

*        flow area        vol #
*        (m2)
2010101  0.01824146925    2

*        flow length      vol #
*        (m)
2010301  0.2286           1
2010302  1.38303          2

*        Horiz. angle     vol #
*        (deg)
2010501  0.0              2

*        Vert. angle      vol #
*        (deg)
2010601   0.0             1
2010602  90.0             2

*        Elev. change     vol #
*        (m)
2010701  0.0              1
2010702  1.38303          2

*        roughness        hydrlc.diam.     vol #
*        (m)              (m)
2010801  1.5-5            0.1524           2
```

```
*        vol-flag         vol #
*        tlpvbfe
2011001  0000000          2

*        jun-flag         jun #
*        jefvcahs
2011101  00001000         1

*        ebt              pressure         temperature      0.0
0.0  0.0    vol #
*                         (Pa)             (K)
2011201  003              140.0+5          488.38           0.0
0.0  0.0    2

*        mass flow rates
2011300  1

*        liquid flow      vapor flow       interface vel.   jun #
*        (kg/sec)         (kg/sec)         (m/sec)
2011301  9.313552723      0.0              0.0              1
**=======*================*================*================*====
*====*======***


**=======*================*================*================*====
=*=====*=====**
** Junction 202, DHX intermediate outlet flange face
*        Component name   Component type
2020000  IDHXOutF         sngljun

*        from vol.        to vol.          jun. area        A_F
A_R   jun-flag
*                                          (m2)
jefvcahs
2020101  201010000        203000000        0.01824146925    0.0
0.0   00001000

*        mass flow rates  liquid flow      vapor flow
interface vel.
*                         (kg/sec)         (kg/sec)
(m/sec)
2020201  1                9.313552723      0.0              0.0
**=======*================*================*================*====
=*=====*=====**


**=======*================*================*================*====
*====*======***
** Volume 203, intermediate loop hot pipe
```

```
*        Component name   Component type
2030000  IHotPipe         pipe

*        nv, # of volumes
2030001  10

*        flow area        vol #
*        (m2)
2030101  0.01824146925    10

*        flow length      vol #
*        (m)
2030301  0.50165           1
2030302  2.9194125         5
2030303  2.7844623         9
2030304  0.2286           10

*        Horiz. angle     vol #
*        (deg)
2030501    0.0             1
2030502  143.1716637       5
2030503    0.0             9
2030504  180.0            10

*        Vert. angle      vol #
*        (deg)
2030601  90.0              1
2030602   0.0              5
2030603  90.0              9
2030604   0.0             10

*        Elev. change     vol #
*        (m)
2030701  0.50165           1
2030702  0.0               5
2030703  2.7844623         9
2030704  0.0              10

*        roughness        hydrlc.diam.     vol #
*        (m)              (m)
2030801  1.5-5            0.1524           10

*        vol-flag         vol #
*        tlpvbfe
2031001  0000000          10

*        jun-flag         jun #
*        jefvcahs
2031101  00001000         9
```

```
*        ebt               pressure          temperature       0.0
0.0  0.0    vol #
*                          (Pa)              (K)
2031201  003               140.0+5           488.38            0.0
0.0  0.0    10

*        mass flow rates
2031300  1

*        liquid flow       vapor flow        interface vel.    jun #
*        (kg/sec)          (kg/sec)          (m/sec)
2031301  9.313552723       0.0               0.0               9
**=======*================*================*================*====
*====*======***


**=======*================*================*================*====
=*=====*=====**
** Junction 204, intermediate NDHX tube inlet

*        Component name    Component type
2040000  INDHXTin           sngljun

*        from vol.         to vol.           jun. area         A_F
A_R   jun-flag
*                                            (m2)
jefvcahs
2040101  203010000         205000000         0.01824146925     0.0
0.0   00001000

*        mass flow rates   liquid flow       vapor flow
interface vel.
*                          (kg/sec)          (kg/sec)
(m/sec)
2040201  1                 9.313552723       0.0               0.0
**=======*================*================*================*====
=*=====*=====**


**=======*================*================*================*====
*====*======***
** Volume 205, intermediate side of NDHX tube

*        Component name    Component type
2050000  INDHXTub          pipe

*        nv, # of volumes
2050001  28

*        flow area         vol #
```

```
*        (m2)
2050101  0.01824146925    28

*        flow length      vol #
*        (m)
2050301  1.4722094         6
2050302  2.3334472         8
2050303  1.49266656       13
2050304  2.3334472        15
2050305  1.49266656       20
2050306  2.3334472        22
2050307  1.4722094        28

*        Horiz. angle     vol #
*        (deg)
2050501  180.0             6
2050502  210.0             7
2050503  330.0             8
2050504    0.0            13
2050505  330.0            14
2050506  210.0            15
2050507  180.0            20
2050508  210.0            21
2050509  330.0            22
2050510    0.0            28

*        Vert. angle      vol #
*        (deg)
2050601  0.0              28

*        Elev. change     vol #
*        (m)
2050701  0.0              28

*        roughness        hydrlc.diam.     vol #
*        (m)              (m)
2050801  1.5-5            0.1524           28

*        vol-flag         vol #
*        tlpvbfe
2051001  0000000          28

*        jun-flag         jun #
*        jefvcahs
2051101  00001000         27

*        ebt              pressure         temperature      0.0
0.0  0.0    vol #
*                         (Pa)             (K)
```

```
2051201  003            140.0+5          488.38           0.0
0.0  0.0     1
2051202  003            140.0+5          485.73           0.0
0.0  0.0     2
2051203  003            140.0+5          483.08           0.0
0.0  0.0     3
2051204  003            140.0+5          480.42           0.0
0.0  0.0     4
2051205  003            140.0+5          477.77           0.0
0.0  0.0     5
2051206  003            140.0+5          475.12           0.0
0.0  0.0     6
2051207  003            140.0+5          470.91           0.0
0.0  0.0     7
2051208  003            140.0+5          466.71           0.0
0.0  0.0     8
2051209  003            140.0+5          464.02           0.0
0.0  0.0     9
2051210  003            140.0+5          461.33           0.0
0.0  0.0    10
2051211  003            140.0+5          458.64           0.0
0.0  0.0    11
2051212  003            140.0+5          455.95           0.0
0.0  0.0    12
2051213  003            140.0+5          453.27           0.0
0.0  0.0    13
2051214  003            140.0+5          449.06           0.0
0.0  0.0    14
2051215  003            140.0+5          444.86           0.0
0.0  0.0    15
2051216  003            140.0+5          442.17           0.0
0.0  0.0    16
2051217  003            140.0+5          439.48           0.0
0.0  0.0    17
2051218  003            140.0+5          436.79           0.0
0.0  0.0    18
2051219  003            140.0+5          434.10           0.0
0.0  0.0    19
2051220  003            140.0+5          431.41           0.0
0.0  0.0    20
2051221  003            140.0+5          427.21           0.0
0.0  0.0    21
2051222  003            140.0+5          423.00           0.0
0.0  0.0    22
2051223  003            140.0+5          420.35           0.0
0.0  0.0    23
2051224  003            140.0+5          417.70           0.0
0.0  0.0    24
2051225  003            140.0+5          415.05           0.0
0.0  0.0    25
```

```
2051226  003              140.0+5          412.39           0.0
0.0  0.0    26
2051227  003              140.0+5          409.74           0.0
0.0  0.0    27
2051228  003              140.0+5          407.09           0.0
0.0  0.0    28

*        mass flow rates
2051300  1

*        liquid flow      vapor flow       interface vel.   jun #
*        (kg/sec)         (kg/sec)         (m/sec)
2051301  9.313552723      0.0              0.0              27
**=======*================*================*================*====
*====*======***


**=======*================*================*================*====
=*=====*=====**
** Junction 206, intermediate NDHX tube outlet

*        Component name   Component type
2060000  INDHXTou         sngljun

*        from vol.        to vol.          jun. area        A_F
A_R   jun-flag
*                                          (m2)
jefvcahs
2060101  205010000        207000000        0.01824146925    0.0
0.0   00001000

*        mass flow rates  liquid flow      vapor flow
interface vel.
*                         (kg/sec)         (kg/sec)
(m/sec)
2060201  1                9.313552723      0.0              0.0
**=======*================*================*================*====
=*=====*=====**


**=======*================*================*================*====
*====*======***
** Volume 207, intermediate loop cold pipe

*        Component name   Component type
2070000  IColdPip         pipe

*        nv, # of volumes
2070001  9
```

```
*        flow area        vol #
*        (m2)
2070101  0.01824146925    9

*        flow length      vol #
*        (m)
2070301  0.2286           1
2070302  2.79551384       6
2070303  2.372783333      9

*        Horiz. angle     vol #
*        (deg)
2070501  0.0              9

*        Vert. angle      vol #
*        (deg)
2070601    0.0            1
2070602  -90.0            6
2070603    0.0            9

*        Elev. change     vol #
*        (m)
2070701   0.0             1
2070702  -2.79551384      6
2070703   0.0             9

*        roughness        hydrlc.diam.     vol #
*        (m)              (m)
2070801  1.5-5            0.1524           9

*        vol-flag         vol #
*        tlpvbfe
2071001  0000000          9

*        jun-flag         jun #
*        jefvcahs
2071101  00001000         8

*        ebt              pressure         temperature      0.0
0.0  0.0    vol #
*                         (Pa)             (K)
2071201  003              140.0+5          407.09           0.0
0.0  0.0    9

*        mass flow rates
2071300  1

*        liquid flow      vapor flow       interface vel.   jun #
*        (kg/sec)         (kg/sec)         (m/sec)
2071301  9.313552723      0.0              0.0              8
```

```
**=======*===============*===============*===============*====
*====*======***


**=======*===============*===============*===============*====
*====*======***
** Volume 209, DHX intermediate inlet pipe

*        Component name   Component type
2090000  IDHXInPi          branch

*        nj, # of juncs.  mass flow rates
2090001  3                1

*        flow area        flow length      volume
horiz. angle   vert. angle
*        (m2)             (m)              (m3)             (deg)
(deg)
*         elev. chng.      roughness        hydraulic diam.  vol-
flag
*         (m)              (m)              (m)
tlpvbfe
2090101  0.01824146925    1.59385          0.0              0.0
0.0
+         0.0              1.5-5            0.1524
0000000

*        ebt              pressure         temperature
*                         (Pa)             (K)
2090200  003              140.0+5          407.09

*        from vol.        to vol.          jun. area        A_F
A_R   jun-flag
*                                          (m2)
jefvcahs
2091101  207010000        209000000        0.01824146925    0.0
0.0   00001000
2092101  209010000        211000000        0.01824146925    0.0
0.0   00001000
2093101  238010000        209000000        0.01824146925    0.0
0.0   00011000

*        hydrlc.diam.     flooding corr.   vapor inter.     slope
*        (m)
2091110  0.1524           0.0              1.0              1.0
2092110  0.1524           0.0              1.0              1.0
2093110  0.1524           0.0              1.0              1.0

*        liquid flow      vapor flow       interface vel.
*        (kg/sec)         (kg/sec)         (m/sec)
```

```
2091201  9.313552723      0.0              0.0
2092201  9.313552723      0.0              0.0
2093201  0.0              0.0              0.0
**=======*================*================*================*====
==========*==**


**=======*================*================*================*====
*====*======***
** Volume 211, DHX tube inlet manifold

*        Component name   Component type
2110000  DHXInMan         pipe

*        nv, # of volumes
2110001  2

*        flow area        vol #
*        (m2)
2110101  0.01824146925    1
2110102  0.1024249944     2

*        flow length      vol #
*        (m)
2110301  0.1016           2

*        Horiz. angle     vol #
*        (deg)
2110501  0.0              2

*        Vert. angle      vol #
*        (deg)
2110601  5.710593137      2

*        Elev. change     vol #
*        (m)
2110701  0.01016          2

*        roughness        hydrlc.diam.     vol #
*        (m)              (m)
2110801  1.5-5            0.1524           1
2110801  1.5-5            0.3611253982     2

*        vol-flag         vol #
*        tlpvbfe
2111001  0000000          2

*        jun-flag         jun #
*        jefvcahs
2111101  00001000         1
```

```
*        ebt               pressure          temperature       0.0
0.0  0.0    vol #
*                          (Pa)              (K)
2111201  003               140.0+5           407.09            0.0
0.0  0.0    2

*        mass flow rates
2111300  1

*        liquid flow       vapor flow        interface vel.    jun #
*        (kg/sec)          (kg/sec)          (m/sec)
2111301  9.313552723       0.0               0.0               1
**=======*================*================*================*====
*====*======***


**=======*================*================*================*====
=*=====*=====**
** Junction 212, DHX tube inlet

*        Component name    Component type
2120000  DHXTubIn          sngljun

*        from vol.         to vol.           jun. area         A_F
A_R   jun-flag
*                                            (m2)
jefvcahs
2120101  211010000         213000000         0.02055205535     0.0
0.0   00001000

*        mass flow rates   liquid flow       vapor flow
interface vel.
*                          (kg/sec)          (kg/sec)
(m/sec)
2120201  1                 9.313552723       0.0               0.0
**=======*================*================*================*====
=*=====*=====**


**=======*================*================*================*====
*====*======***
** Volume 213, intermediate flow through DHX tubes

*        Component name    Component type
2130000  IDHXTube          pipe

*        nv, # of volumes
2130001  20
```

```
*        flow area        vol #
*        (m2)
2130101  0.02055205535    20

*        flow length      vol #
*        (m)
2130301  1.550046107      20

*        Vert. angle      vol #
*        (deg)
2130601  90.0             20

*        Elev. change     vol #
*        (m)
2130701  0.04572          20

*        roughness        hydrlc.diam.     vol #
*        (m)              (m)
2130801  1.5-5            0.06604          20

*        vol-flag         vol #
*        tlpvbfe
2131001  0000000          20

*        jun-flag         jun #
*        jefvcahs
2131101  00001000         19

*        ebt              pressure         temperature      0.0
0.0  0.0    vol #
*                         (Pa)             (K)
2131201  003              140.0+5          407.09           0.0
0.0  0.0     1
2131202  003              140.0+5          411.37           0.0
0.0  0.0     2
2131203  003              140.0+5          415.65           0.0
0.0  0.0     3
2131204  003              140.0+5          419.93           0.0
0.0  0.0     4
2131205  003              140.0+5          424.20           0.0
0.0  0.0     5
2131206  003              140.0+5          428.48           0.0
0.0  0.0     6
2131207  003              140.0+5          432.76           0.0
0.0  0.0     7
2131208  003              140.0+5          437.04           0.0
0.0  0.0     8
2131209  003              140.0+5          441.32           0.0
0.0  0.0     9
```

```
2131210  003              140.0+5          445.60           0.0
0.0  0.0    10
2131211  003              140.0+5          449.87           0.0
0.0  0.0    11
2131212  003              140.0+5          454.15           0.0
0.0  0.0    12
2131213  003              140.0+5          458.43           0.0
0.0  0.0    13
2131214  003              140.0+5          462.71           0.0
0.0  0.0    14
2131215  003              140.0+5          466.99           0.0
0.0  0.0    15
2131216  003              140.0+5          471.27           0.0
0.0  0.0    16
2131217  003              140.0+5          475.54           0.0
0.0  0.0    17
2131218  003              140.0+5          479.82           0.0
0.0  0.0    18
2131219  003              140.0+5          484.10           0.0
0.0  0.0    19
2131220  003              140.0+5          488.38           0.0
0.0  0.0    20


*        mass flow rates
2131300  1

*        liquid flow      vapor flow       interface vel.   jun #
*        (kg/sec)         (kg/sec)         (m/sec)
2131301  9.313552723      0.0              0.0              19
**=======*================*================*================*====
*====*=======***


**=======*================*================*================*====
=*=====*======**
** Junction 214, DHX tube outlet

*        Component name   Component type
2140000  DHXTubOu         sngljun

*        from vol.        to vol.          jun. area        A_F
A_R   jun-flag
*                                          (m2)
jefvcahs
2140101  213010000        215000000        0.02055205535    0.0
0.0   00001000

*        mass flow rates  liquid flow      vapor flow
interface vel.
```

```
*                          (kg/sec)         (kg/sec)
(m/sec)
2140201  1                 9.313552723      0.0               0.0
**=======*================*================*================*====
=*=====*=====**


**=======*================*================*================*====
*====*======***
** Volume 215, DHX tube outlet manifold

*        Component name   Component type
2150000  DHXOuMan         pipe

*        nv, # of volumes
2150001  2

*        flow area        vol #
*        (m2)
2150101  0.1024249944     1
2150102  0.01824146925    2

*        flow length      vol #
*        (m)
2150301  0.1016           2

*        Horiz. angle     vol #
*        (deg)
2150501  0.0              2

*        Vert. angle      vol #
*        (deg)
2150601  5.710593137      2

*        Elev. change     vol #
*        (m)
2150701  0.01016          2

*        roughness        hydrlc.diam.     vol #
*        (m)              (m)
2150801  1.5-5            0.3611253982     1
2150802  1.5-5            0.1524           2

*        vol-flag         vol #
*        tlpvbfe
2151001  0000000          2

*        jun-flag         jun #
*        jefvcahs
2151101  00001000         1
```

```
*        ebt               pressure          temperature       0.0
0.0  0.0    vol #
*                          (Pa)              (K)
2151201  003               140.0+5           488.38            0.0
0.0  0.0    2

*        mass flow rates
2151300  1

*        liquid flow       vapor flow        interface vel.    jun #
*        (kg/sec)          (kg/sec)          (m/sec)
2151301  9.313552723       0.0               0.0               1
**=======*================*================*================*====
*====*======***


**=======*================*================*================*====
=*=====*=====**
** Junction 216, DHX manifold outlet junction

*        Component name    Component type
2160000  DHXManOJ          sngljun

*        from vol.         to vol.           jun. area         A_F
A_R   jun-flag
*                                            (m2)
jefvcahs
2160101  215010000         201000000         0.01824146925     0.0
0.0   00001000

*        mass flow rates   liquid flow       vapor flow
interface vel.
*                          (kg/sec)          (kg/sec)
(m/sec)
2160201  1                 9.313552723       0.0               0.0
**=======*================*================*================*====
=*=====*=====**


**=======*================*================*================*====
==========*==**
** Volume 238, intermediate pressure control boundary

*        Component name    Component type
2380000  IntPress          tmdpvol

*        flow area         flow length       volume
horiz. angle   vert. angle
```

```
*        (m2)              (m)               (m3)              (deg)
(deg)
*         elev. chng.       roughness         hydraulic diam.  vol-
flag
*         (m)               (m)               (m)
tlpvbfe
2380101  0.01824146925    0.40              0.0               0.0
-90.0
+         -0.4              0.0               0.1524
0000000

*        ebt
2380200  003

*        time              pressure          temperature
*        (sec)             (Pa)              (K)
2380201  0.0               140.0+5           314.45
**=======*================*================*================*====
==========*==**



**=============================================================
=============**
** Hydrodynamic Components, Natural draft loop
**
**=============================================================
=============**


**=======*================*================*================*====
==========*==**
** Volume 301, natural draft inlet boundary

*        Component name   Component type
3010000  NDrInlet         tmdpvol

*        flow area        flow length      volume
horiz. angle   vert. angle
*        (m2)              (m)               (m3)              (deg)
(deg)
*         elev. chng.       roughness         hydraulic diam.  vol-
flag
*         (m)               (m)               (m)
tlpvbfe
3010101  78.75             1.0               0.0               0.0
90.0
+         1.0               1.5-5             8.75
0000000
```

```
*        ebt
3010200  004

*        time              pressure          temperature
static quality
*        (sec)             (Pa)              (K)               (dry
non-con.)
3010201  0.0               1.0+5             303.15            0.0

*        helium            nitrogen          air
*        (mass frac.)      (mass frac.)      (mass frac.)
3010301  0.0               0.0               1.0
**=======*================*================*================*====
==========*==**


**=======*================*================*================*====
=============**
** Junction 302, natural draft inlet junction

*        Component name    Component type
3020000  NDInJunc          tmdpjun

*        from vol.         to vol.           jun. area         jun-
flag
*                                            (m2)
jefvcahs
3020101  301010000         303000000         78.75
00000000

*        mass flow rates
3020200  1

*        time              liquid flow       vapor flow
interface vel.
*        (sec)             (kg/sec)          (kg/sec)
(m/sec)
3020201  0.0               0.0               253.5775529       0.0
**=======*================*================*================*====
=============**


**=======*=====*==========*================*================*====
=*=====*======**
** Volume 303, natural draft NDHX reject heat air flow

*        Component name    Component type
3030000  NDNDHXRj          pipe

*        nv, # of volumes
```

```
3030001  3

*        flow area        vol #
*        (m2)
3030101  49.098           1
3030102  44.30015448      2
3030103  49.098           3

*        flow length      vol #
*        (m)
3030301  0.15348          1
3030302  0.19304          2
3030303  0.15348          3

*        Horiz. angle     vol #
*        (deg)
3030501  0.0              3

*        Vert. angle      vol #
*        (deg)
3030601  90.0             3

*        Elev. change     vol #
*        (m)
3030701  0.15348          1
3030702  0.19304          2
3030703  0.15348          3

*        roughness        hydrlc.diam.     vol #
*        (m)              (m)
3030801  1.5-5            9.38058846-3     1
3030802  1.5-5            9.217414092-3    2
3030803  1.5-5            9.38058846-3     3

*        vol-flag         vol #
*        tlpvbfe
3031001  0010000          3

*        jun-flag         jun #
*        jefvcahs
3031101  00001000         2

*        ebt   pressure   temperature      static quality   0.0
0.0   vol #
*              (Pa)       (K)              (dry non-con.)
3031201  004   1.0+5      303.15           0.0              0.0
0.0   1
3031202  004   1.0+5      312.96           0.0              0.0
0.0   2
```

```
3031203  004   1.0+5      322.77           0.0              0.0
0.0   3

*        mass flow rates
3031300  1

*        liquid flow      vapor flow       interface vel.   jun #
*        (kg/sec)         (kg/sec)         (m/sec)
3031301  0.0              253.5775529      0.0              2

*        helium           nitrogen         air
additional  vol #
*        (mass frac.)     (mass frac.)     (mass frac.)     mass
frac
3033201  0.0              0.0              1.0              0.0
0.0   3
**=======*=====*==========*================*================*====
=*=====*=====**


**=======*================*================*================*====
=============**
** Junction 304, natural draft outlet junction

*        Component name   Component type
3040000  NDOutJun         tmdpjun

*        from vol.        to vol.          jun. area        jun-
flag
*                                          (m2)
jefvcahs
3040101  303010000        305000000        78.75
00000000

*        mass flow rates
3040200  1

*        time             liquid flow      vapor flow
interface vel.
*        (sec)            (kg/sec)         (kg/sec)
(m/sec)
3040201  0.0              0.0              253.5775529      0.0
**=======*================*================*================*====
=============**


**=======*================*================*================*====
==========*==**
** Volume 305, natural draft outlet boundary
```

```
*        Component name   Component type
3050000  NDOutlet         tmdpvol

*        flow area        flow length      volume
horiz. angle   vert. angle
*        (m2)             (m)              (m3)             (deg)
(deg)
*         elev. chng.      roughness        hydraulic diam.  vol-
flag
*         (m)              (m)              (m)
tlpvbfe
3050101  78.75            1.0              0.0              0.0
90.0
+         1.0              1.5-5            8.75
0000000

*        ebt
3050200  004

*        time             pressure         temperature
static quality
*        (sec)            (Pa)             (K)              (dry
non-con.)
3050201  0.0              1.0+5            322.77           0.0

*        helium           nitrogen         air
*        (mass frac.)     (mass frac.)     (mass frac.)
3050301  0.0              0.0              1.0
**=======*================*================*================*====
==========*==**



**================================================================
=============**
** Heat Structures, DRACS Heat Exchanger, DHX
**
**================================================================
=============**

*        nh, axial mesh   np, rad. mesh    Geom. type       SS
init. flag
*         Left boundary    Reflood flag
*         (m)
12131000 20               2                2                1
+         0.03302          0

*        mesh location    mesh format
12131100 0                1
```

```
*        # of intervals   right coord.
12131101 1                0.0381

*        composition #    interval #
12131201 001              1

*        source Q_in      interval #
12131301 0.0              1

*        temp. entered
12131400 0

*        temperature      mp #
*        (K)
12131401  471.3           1
12131402 1005.85          2

* *LB*   LB volume #      increment        LB cond. type
surface area code
* *LB*    surface area     hs #
*         (m2)
12131501 213010000        10000            101              0
+         0.3215892731     20


* *RB*   RB volume #      increment        RB cond. type
surface area code
* *RB*    surface area     hs #
*         (m2)
12131601 107040000        0                101              0
+         0.3710645459      5
12131602 107030000        0                101              0
+         0.3710645459     10
12131603 107020000        0                101              0
+         0.3710645459     15
12131604 107010000        0                101              0
+         0.3710645459     20


*        power src type   Int src mult     LB direct heat   RB
direct heat   hs #
12131701 0                0.0              0.0              0.0
20

*        twelve-word format
12131800 1

* *LB*   HT hyd. diam.    Ht lngth for     Ht lngth rev     Grd
spcr L for   Grd spcr L rev
```

```
*         (m)                (m)                (m)                (m)
(m)
* *LB*    Grd loss coeff   Grd loss coeff   boiling factor   nat
circ lngth
*         for                rev                                  (m)
* *LB*     pitch-to-diam    HTC foul factor  hs #
12131801 0.06604           0.7750230537    30.22589909      0.0
0.0
+         0.0              0.0              1.0
0.06604
+          1.477644055      1.0              1
12131802 0.06604           2.325069161     28.67585299      0.0
0.0
+         0.0              0.0              1.0
0.06604
+          1.477644055      1.0              2
12131803 0.06604           3.875115268     27.12580688      0.0
0.0
+         0.0              0.0              1.0
0.06604
+          1.477644055      1.0              3
12131804 0.06604           5.425161376     25.57576077      0.0
0.0
+         0.0              0.0              1.0
0.06604
+          1.477644055      1.0              4
12131805 0.06604           6.975207483     24.02571446      0.0
0.0
+         0.0              0.0              1.0
0.06604
+          1.477644055      1.0              5
12131806 0.06604           8.52525359      22.47566856      0.0
0.0
+         0.0              0.0              1.0
0.06604
+          1.477644055      1.0              6
12131807 0.06604          10.0752997       20.92562245      0.0
0.0
+         0.0              0.0              1.0
0.06604
+          1.477644055      1.0              7
12131808 0.06604          11.6253458       19.37557634      0.0
0.0
+         0.0              0.0              1.0
0.06604
+          1.477644055      1.0              8
12131809 0.06604          13.17539191      17.82553023      0.0
0.0
+         0.0              0.0              1.0
0.06604
```

```
+          1.477644055      1.0              9
12131810 0.06604          14.72543802      16.27548413      0.0
0.0
+         0.0              0.0              1.0
0.06604
+          1.477644055      1.0              10
12131811 0.06604          16.27548413      14.72543802      0.0
0.0
+         0.0              0.0              1.0
0.06604
+          1.477644055      1.0              11
12131812 0.06604          17.82553023      13.17539191      0.0
0.0
+         0.0              0.0              1.0
0.06604
+          1.477644055      1.0              12
12131813 0.06604          19.37557634      11.6253458       0.0
0.0
+         0.0              0.0              1.0
0.06604
+          1.477644055      1.0              13
12131814 0.06604          20.92562245      10.0752997       0.0
0.0
+         0.0              0.0              1.0
0.06604
+          1.477644055      1.0              14
12131815 0.06604          22.47566856       8.52525359      0.0
0.0
+         0.0              0.0              1.0
0.06604
+          1.477644055      1.0              15
12131816 0.06604          24.02571446       6.975207483     0.0
0.0
+         0.0              0.0              1.0
0.06604
+          1.477644055      1.0              16
12131817 0.06604          25.57576077       5.425161376     0.0
0.0
+         0.0              0.0              1.0
0.06604
+          1.477644055      1.0              17
12131818 0.06604          27.12580688       3.875115268     0.0
0.0
+         0.0              0.0              1.0
0.06604
+          1.477644055      1.0              18
12131819 0.06604          28.67585299       2.325069161     0.0
0.0
+         0.0              0.0              1.0
0.06604
```

```
+          1.477644055      1.0              19
12131820 0.06604          30.22589909       0.7750230537    0.0
0.0
+         0.0              0.0              1.0
0.06604
+          1.477644055      1.0              20

*        twelve-word format
12131900 1

* *RB*   HT hyd. diam.    Ht lngth for     Ht lngth rev     Grd
spcr L for   Grd spcr L rev
*        (m)              (m)              (m)              (m)
(m)
* *RB*    Grd loss coeff   Grd loss coeff   boiling factor   nat
circ lngth
*         for              rev                               (m)
* *RB*     pitch-to-diam    HTC foul factor  hs #
12131901 1.185133526      0.89154          0.02286          0.0
0.0
+         0.0              0.0              1.0
0.04572
+          1.280624847      1.0              1
12131902 1.185133526      0.84582          0.06858          0.0
0.0
+         0.0              0.0              1.0
0.04572
+          1.280624847      1.0              2
12131903 1.185133526      0.8001           0.1143           0.0
0.0
+         0.0              0.0              1.0
0.04572
+          1.280624847      1.0              3
12131904 1.185133526      0.75438          0.16002          0.0
0.0
+         0.0              0.0              1.0
0.04572
+          1.280624847      1.0              4
12131905 1.185133526      0.70866          0.20574          0.0
0.0
+         0.0              0.0              1.0
0.04572
+          1.280624847      1.0              5
12131906 1.185133526      0.66294          0.25146          0.0
0.0
+         0.0              0.0              1.0
0.04572
+          1.280624847      1.0              6
12131907 1.185133526      0.61722          0.29718          0.0
0.0
```

```
+         0.0              0.0              1.0
0.04572
+          1.280624847      1.0              7
12131908 1.185133526      0.5715           0.3429           0.0
0.0
+         0.0              0.0              1.0
0.04572
+          1.280624847      1.0              8
12131909 1.185133526      0.52578          0.38862          0.0
0.0
+         0.0              0.0              1.0
0.04572
+          1.280624847      1.0              9
12131910 1.185133526      0.48006          0.43434          0.0
0.0
+         0.0              0.0              1.0
0.04572
+          1.280624847      1.0              10
12131911 1.185133526      0.43434          0.48006          0.0
0.0
+         0.0              0.0              1.0
0.04572
+          1.280624847      1.0              11
12131912 1.185133526      0.38862          0.52578          0.0
0.0
+         0.0              0.0              1.0
0.04572
+          1.280624847      1.0              12
12131913 1.185133526      0.3429           0.5715           0.0
0.0
+         0.0              0.0              1.0
0.04572
+          1.280624847      1.0              13
12131914 1.185133526      0.29718          0.61722          0.0
0.0
+         0.0              0.0              1.0
0.04572
+          1.280624847      1.0              14
12131915 1.185133526      0.25146          0.66294          0.0
0.0
+         0.0              0.0              1.0
0.04572
+          1.280624847      1.0              15
12131916 1.185133526      0.20574          0.70866          0.0
0.0
+         0.0              0.0              1.0
0.04572
+          1.280624847      1.0              16
12131917 1.185133526      0.16002          0.75438          0.0
0.0
```

```
+         0.0              0.0              1.0
0.04572
+          1.280624847      1.0              17
12131918 1.185133526      0.1143           0.8001           0.0
0.0
+         0.0              0.0              1.0
0.04572
+          1.280624847      1.0              18
12131919 1.185133526      0.06858          0.84582          0.0
0.0
+         0.0              0.0              1.0
0.04572
+          1.280624847      1.0              19
12131920 1.185133526      0.02286          0.89154          0.0
0.0
+         0.0              0.0              1.0
0.04572
+          1.280624847      1.0              20


**=============================================================
=============**
** Heat Structures, Natural Draft Heat Exchanger, NDHX
**
**=============================================================
=============**


*        nh, axial mesh   np, rad. mesh    Geom. type       SS
init. flag
*         Left boundary    Reflood flag     boundary vol.    max
# axial intervals
*         (m)
12051000 28               2                2                1
+         0.0762           0                *no reflood is used

*        mesh location    mesh format
12051100 0                1

*        # of intervals   right coord.
12051101 1                0.09652

*        composition #    interval #
12051201 002              1

*        source Q_in      interval #
12051301 0.0              1

*        temp. entered
```

```
12051400 0

*        temperature      mesh point #
*        (K)
12051401 400.81           1
12051402 318.651          2

* *LB*   LB volume #      increment        LB cond. type
surface area code
* *LB*    surface area     hs #
*         (m)
12051501 205010000        10000            101              0
+         0.7453437193     28

* *RB*   RB volume #      increment        RB cond. type
surface area code
* *RB*    surface area     hs #
*         (m)
12051601 303020000        0                101              0
+         0.9441020445     28

*        power src type   Int src mult     LB direct heat   RB
direct heat   hs #
12051701 0                0.0              0.0              0.0
28

*        twelve-word format
12051800 1

* *LB*   HT hyd. diam.    Ht lngth for     Ht lngth rev     Grd
spcr L for   Grd spcr L rev
*        (m)              (m)              (m)              (m)
(m)
* *LB*    Grd loss coeff   Grd loss coeff   boiling factor   nat
circ lngth
*         for              rev                                (m)
* *LB*     pitch-to-diam    HTC foul factor  hs #
12051801 0.1524           45.8577569        0.7361047        0.0
0.0
+         0.0              0.0              1.0
0.1524
+          1.6              1.0               1
12051802 0.1524           44.3855475        2.2083141        0.0
0.0
+         0.0              0.0              1.0
0.1524
+          1.6              1.0               2
12051803 0.1524           42.9133381        3.6805235        0.0
0.0
```

```
+          0.0              0.0              1.0
0.1524
+          1.6              1.0                3
12051804 0.1524           41.4411287        5.1527329        0.0
0.0
+          0.0              0.0              1.0
0.1524
+          1.6              1.0                4
12051805 0.1524           39.9689193        6.6249423        0.0
0.0
+          0.0              0.0              1.0
0.1524
+          1.6              1.0                5
12051806 0.1524           38.4967099        8.0971517        0.0
0.0
+          0.0              0.0              1.0
0.1524
+          1.6              1.0                6
12051807 0.1524           36.5938816        9.99998          0.0
0.0
+          0.0              0.0              1.0
0.1524
+          1.6              1.0                7
12051808 0.1524           34.2604344       12.3334272        0.0
0.0
+          0.0              0.0              1.0
0.1524
+          1.6              1.0                8
12051809 0.1524           32.34737752      14.24648408       0.0
0.0
+          0.0              0.0              1.0
0.1524
+          1.6              1.0                9
12051810 0.1524           30.85471096      15.73915064       0.0
0.0
+          0.0              0.0              1.0
0.1524
+          1.6              1.0               10
12051811 0.1524           29.3620444       17.2318172        0.0
0.0
+          0.0              0.0              1.0
0.1524
+          1.6              1.0               11
12051812 0.1524           27.86937784      18.72448376       0.0
0.0
+          0.0              0.0              1.0
0.1524
+          1.6              1.0               12
12051813 0.1524           26.37671128      20.21715032       0.0
0.0
```

```
+          0.0              0.0              1.0
0.1524
+          1.6              1.0               13
12051814 0.1524           24.4636544       22.1302072       0.0
0.0
+          0.0              0.0              1.0
0.1524
+          1.6              1.0               14
12051815 0.1524           22.1302072       24.4636544       0.0
0.0
+          0.0              0.0              1.0
0.1524
+          1.6              1.0               15
12051816 0.1524           20.21715032      26.37671128      0.0
0.0
+          0.0              0.0              1.0
0.1524
+          1.6              1.0               16
12051817 0.1524           18.72448376      27.86937784      0.0
0.0
+          0.0              0.0              1.0
0.1524
+          1.6              1.0               17
12051818 0.1524           17.2318172       29.3620444       0.0
0.0
+          0.0              0.0              1.0
0.1524
+          1.6              1.0               18
12051819 0.1524           15.73915064      30.85471096      0.0
0.0
+          0.0              0.0              1.0
0.1524
+          1.6              1.0               19
12051820 0.1524           14.24648408      32.34737752      0.0
0.0
+          0.0              0.0              1.0
0.1524
+          1.6              1.0               20
12051821 0.1524           12.3334272       34.2604344       0.0
0.0
+          0.0              0.0              1.0
0.1524
+          1.6              1.0               21
12051822 0.1524            9.99998         36.5938816       0.0
0.0
+          0.0              0.0              1.0
0.1524
+          1.6              1.0               22
12051823 0.1524            8.0971517       38.4967099       0.0
0.0
```

```
+         0.0              0.0              1.0
0.1524
+          1.6              1.0              23
12051824 0.1524            6.6249423       39.9689193       0.0
0.0
+         0.0              0.0              1.0
0.1524
+          1.6              1.0              24
12051825 0.1524            5.1527329       41.4411287       0.0
0.0
+         0.0              0.0              1.0
0.1524
+          1.6              1.0              25
12051826 0.1524            3.6805235       42.9133381       0.0
0.0
+         0.0              0.0              1.0
0.1524
+          1.6              1.0              26
12051827 0.1524            2.2083141       44.3855475       0.0
0.0
+         0.0              0.0              1.0
0.1524
+          1.6              1.0              27
12051828 0.1524            0.7361047       45.8577569       0.0
0.0
+         0.0              0.0              1.0
0.1524
+          1.6              1.0              28

*        twelve-word format
12051900 1

* *RB*   HT hyd. diam.    Ht lngth for     Ht lngth rev     Grd
spcr L for   Grd spcr L rev
*        (m)              (m)              (m)              (m)
(m)
* *RB*    Grd loss coeff   Grd loss coeff   boiling factor   nat
circ lngth
*         for              rev                                (m)
* *RB*     pitch-to-diam    HTC foul factor  hs #
12051901 1.294377369      0.1895928571     0.003447142857   0.0
0.0
+         0.0              0.0              1.0
0.006894285714
+          1.6              140.0453858       1
12051902 1.294377369      0.1826985714     0.01034142857    0.0
0.0
+         0.0              0.0              1.0
0.006894285714
+          1.6              140.0453858       2
```

```
12051903 1.294377369      0.1758042857     0.01723571429    0.0
0.0
+         0.0              0.0              1.0
0.006894285714
+          1.6               140.0453858       3
12051904 1.294377369      0.16891          0.02413          0.0
0.0
+         0.0              0.0              1.0
0.006894285714
+          1.6               140.0453858       4
12051905 1.294377369      0.1620157143     0.0310428571     0.0
0.0
+         0.0              0.0              1.0
0.006894285714
+          1.6               140.0453858       5
12051906 1.294377369      0.1551214286     0.03791857143    0.0
0.0
+         0.0              0.0              1.0
0.006894285714
+          1.6               140.0453858       6
12051907 1.294377369      0.1482271429     0.04481285714    0.0
0.0
+         0.0              0.0              1.0
0.006894285714
+          1.6               140.0453858       7
12051908 1.294377369      0.1413328571     0.05170714286    0.0
0.0
+         0.0              0.0              1.0
0.006894285714
+          1.6               140.0453858       8
12051909 1.294377369      0.1344385714     0.05860142857    0.0
0.0
+         0.0              0.0              1.0
0.006894285714
+          1.6               140.0453858       9
12051910 1.294377369      0.1275442857     0.06549571429    0.0
0.0
+         0.0              0.0              1.0
0.006894285714
+          1.6               140.0453858      10
12051911 1.294377369      0.12065          0.07239          0.0
0.0
+         0.0              0.0              1.0
0.006894285714
+          1.6               140.0453858      11
12051912 1.294377369      0.1137557143     0.07928428571    0.0
0.0
+         0.0              0.0              1.0
0.006894285714
+          1.6               140.0453858      12
```

```
12051913 1.294377369      0.1068614286     0.08617857143    0.0
0.0
+         0.0              0.0              1.0
0.006894285714
+          1.6               140.0453858      13
12051914 1.294377369      0.09996714286    0.09307285714    0.0
0.0
+         0.0              0.0              1.0
0.006894285714
+          1.6               140.0453858      14
12051915 1.294377369      0.09307285714    0.09996714286    0.0
0.0
+         0.0              0.0              1.0
0.006894285714
+          1.6               140.0453858      15
12051916 1.294377369      0.08617857143    0.1068614286     0.0
0.0
+         0.0              0.0              1.0
0.006894285714
+          1.6               140.0453858      16
12051917 1.294377369      0.07928428571    0.1137557143     0.0
0.0
+         0.0              0.0              1.0
0.006894285714
+          1.6               140.0453858      17
12051918 1.294377369      0.07239          0.12065          0.0
0.0
+         0.0              0.0              1.0
0.006894285714
+          1.6               140.0453858      18
12051919 1.294377369      0.06549571429    0.1275442857     0.0
0.0
+         0.0              0.0              1.0
0.006894285714
+          1.6               140.0453858      19
12051920 1.294377369      0.05860142857    0.1344385714     0.0
0.0
+         0.0              0.0              1.0
0.006894285714
+          1.6               140.0453858      20
12051921 1.294377369      0.05170714286    0.1413328571     0.0
0.0
+         0.0              0.0              1.0
0.006894285714
+          1.6               140.0453858      21
12051922 1.294377369      0.04481285714    0.1482271429     0.0
0.0
+         0.0              0.0              1.0
0.006894285714
+          1.6               140.0453858      22
```

```
12051923 1.294377369      0.03791857143    0.1551214286     0.0
0.0
+         0.0              0.0              1.0
0.006894285714
+          1.6               140.0453858      23
12051924 1.294377369      0.0310428571     0.1620157143     0.0
0.0
+         0.0              0.0              1.0
0.006894285714
+          1.6               140.0453858      24
12051925 1.294377369      0.02413          0.16891          0.0
0.0
+         0.0              0.0              1.0
0.006894285714
+          1.6               140.0453858      25
12051926 1.294377369      0.01723571429    0.1758042857     0.0
0.0
+         0.0              0.0              1.0
0.006894285714
+          1.6               140.0453858      26
12051927 1.294377369      0.01034142857    0.1826985714     0.0
0.0
+         0.0              0.0              1.0
0.006894285714
+          1.6               140.0453858      27
12051928 1.294377369      0.003447142857   0.1895928571     0.0
0.0
+         0.0              0.0              1.0
0.006894285714
+          1.6               140.0453858      28


**==========================================================
=============**
** Heat Structure Thermal Property Data
**
**==========================================================
=============**


**========*===============*================*==================
=============**
*         material type    therm cond flag  vol ht cap flag
20100100  tbl/fctn         1                1

*         constant value for thermal conductivity (W/m K)
20100101  0.53606

*         constant value for volumetric heat capacity (J/m3 K)
```

```
20100151  1.0
**========*===============*===============*====================
=============**


**========*===============*===============*====================
=============**
*         material type    therm cond flag  vol ht cap flag
20100200  tbl/fctn         1                1

*         constant value for thermal conductivity (W/m K)
20100201  32.44646

*         constant value for volumetric heat capacity (J/m3 K)
20100251  1.0
**========*===============*===============*====================
=============**



**=========================================================================
=============**
** Control system quantities
**
**=========================================================================
=============**


**=======*===============*===============*===============*====
=============**
*        total heat transfer from direct loop fluid to DHX tubes
*        quantity name    control type     scaling factor
20500100 dhxqdsum         sum              1.0              0.0 0

*        a_0  a_1 minor edit1  a_2 minor edit2  a_3 minor edit3
a_4 minor edit4
20500101 0.0  1.0 q 107010000  1.0 q 107020000  1.0 q 107030000
1.0 q 107040000
**=======*====*===============*===============*===============
*============**


**=======*===============*===============*===============*====
=============**
*        total heat transfer from DHX to intermediate loop fluid
*        quantity name    control type     scaling factor
20500200 dhxqisum         sum              1.0              0.0
0
*        a_0  a_1 minor edit1  a_2 minor edit2  a_3 minor edit3
a_4 minor edit4
```

```
20500201 0.0  1.0 q 213010000  1.0 q 213020000  1.0 q 213030000
1.0 q 213040000
+             1.0 q 213050000  1.0 q 213060000  1.0 q 213070000
1.0 q 213080000
20500202      1.0 q 213090000  1.0 q 213100000  1.0 q 213110000
1.0 q 213120000
+             1.0 q 213130000  1.0 q 213140000  1.0 q 213150000
1.0 q 213160000
20500203      1.0 q 213170000  1.0 q 213180000  1.0 q 213190000
1.0 q 213200000
**=======*====*================*================*================
*============**


**=======*================*================*================*====
=============**
*        total heat transfer from intermediate loop fluid
*        quantity name    control type     scaling factor
20500300 ndhxqism         sum              1.0              0.0
0
*        a_0  a_1 minor edit1  a_2 minor edit2  a_3 minor edit3
a_4 minor edit4
20500301 0.0  1.0 q 205010000  1.0 q 205020000  1.0 q 205030000
1.0 q 205040000
+             1.0 q 205050000  1.0 q 205060000  1.0 q 205070000
1.0 q 205080000
20500302      1.0 q 205090000  1.0 q 205100000  1.0 q 205110000
1.0 q 205120000
+             1.0 q 205130000  1.0 q 205140000  1.0 q 205150000
1.0 q 205160000
20500303      1.0 q 205170000  1.0 q 205180000  1.0 q 205190000
1.0 q 205200000
+             1.0 q 205210000  1.0 q 205220000  1.0 q 205230000
1.0 q 205240000
20500204      1.0 q 205250000  1.0 q 205260000  1.0 q 205270000
1.0 q 205280000
**=======*====*================*================*================
*============**
```

.

8.5. Appendix E: Scaled-down RELAP5-3D model deck

```
=DRACS model

**============================================================
=============**
** RELAP5-3D model of a Direct Reactor Auxiliary Cooling System
for a GFR     **
** Completed as a portion of the work to contribute to the thesis
as part of  **
** the degree requirements for a Master of Science degree in
Nuclear          **
** Engineering. The flow path is based on a scaled model designed
by me in    **
** order to compare outputs from two separate RELAP5-3D decks to
the scaling  **
** analysis. The two decks are identical except the input values
are scaled   **
** according to the scaling choices between model and prototype,
outlined in  **
** chapter 3 of said thesis.
**
**============================================================
=============**
** Author: Grant Blake
**
** Deck start date: 08/27/2016
**
** Deck end date: 09/10/2016
**
** Current version: 2.0
**
** Version updates: Adjusted heat structure thermal property data
to match    **
**  scaling factors
**
**============================================================
=============**



**============================================================
=============**
** Miscellaneous Control Cards
**
**============================================================
=============**
```

```
**=======*===============*=====================================
=============**
** Card 100, problem type and option
*        Problem type     Problem option
0000100  newath           transnt


** Card 102, units selection
*        Input units      Output units
0000102  si               si
**=======*===============*=====================================
=============**


**=======*===============*===============*===============*====
==========*==**
** Card 110, noncondensable gas species
*        Noncondensable gas type (enter up to 5)
0000110  helium           nitrogen         air


** Card 115, noncondensable mass fractions
*        Mass fraction for each gas type
0000115  0.8              0.2              0.0
**=======*===============*===============*===============*====
==========*==**


**=======*===============*===============*===============*====
==========*==**
** Card 120, hydrodynamic system control, direct loop
*        Ref. vol #       Ref. elevation   Fluid type       Name
g
0000120  107030000        0.0              he
Direct         0


** Card 121, hydrodynamic system control, intermediate loop
*        Ref. vol #       Ref. elevation   Fluid type       Name
g
0000121  213110000        0.0              h2o              Int-
Loop       1


** Card 122, hydrodynamic system control, air cooling loop
*        Ref. vol #       Ref. elevation   Fluid type       Name
g
0000122  303020000        3.375            n2               Air-
Loop       0
```

```
**=======*===============*===============*===============*====
==========*==**


**=======*===============*===============*===============*====
=============**
** Card 201, time step control
*        End time         Min time step    Max time step    ssdtt
*        (sec)            (sec)            (sec)
*         Minor frequency  Major frequency  restart frequency
*         (# of dt)        (# of dt)        (# of dt)
0000201  8.0+3            1-10             10.0             00000
+         100              1000             1000000
**========*===============*===============*===============*===
=============**


**=============================================================
=============**
** Minor edit requests
**
**=============================================================
=============**

*        pressure         volume #
0000301  p                103010000
0000302  p                201010000
0000303  p                303030000

*        temperature      volume #
0000304  tempg            103010000
0000305  tempg            115030000
0000306  tempf            201010000
0000307  tempf            207010000
0000308  tempg            303030000
0000309  tempg            303010000

*        density          volume #
0000310  rho              103010000
0000311  rho              115030000
0000312  rho              201010000
0000313  rho              207010000
0000314  rho              303030000
0000315  rho              303010000

*        viscosity        volume #
0000316  viscg            103010000
0000317  viscf            201010000
0000318  viscg            303010000
```

```
*        velocity         volume #
0000319  velg             103010001
0000320  velf             201010001
0000321  velg             303010001
0000332  velf             238010001

*        thermal cond.    volume #
0000322  thcong           103010000
0000323  thconf           201010000
0000324  thcong           303010000

*        heat tran rate   control variable/volume #
0000325  cntrlvar         001
0000326  cntrlvar         002
0000327  cntrlvar         003
0000328  q                303020000

*        specific heat    volume #
0000329  csubpg           103010000
0000330  csubpf           201010000
0000331  csubpg           303030000



**=============================================================
=============**
** Hydrodynamic Components, Direct loop
**
**=============================================================
=============**


**=======*===============*===============*================*====
==========*==**
** Volume 101, direct inlet boundary

*        Component name   Component type
1010000  DirInlet         tmdpvol

*        flow area        flow length      volume
horiz. angle   vert. angle
*        (m2)             (m)              (m3)             (deg)
(deg)
*         elev. chng.      roughness        hydraulic diam.  vol-
flag
*         (m)              (m)              (m)
tlpvbfe
1010101  0.02946028953    0.25             0.0              0.0
90.0
```

```
+         0.25             3.75-6           0.193675
0000000

*        ebt
1010200  004

*        time             pressure         temperature
static quality
*        (sec)            (Pa)             (K)               (dry
non-con.)
1010201  0.0              4.5+5            2273.15           0.0
**=======*================*================*================*====
==========*==**


**=======*================*================*================*====
=============**
** Junction 102, direct inlet junction

*        Component name   Component type
1020000  DirInJnc         tmdpjun

*        from vol.        to vol.          jun. area         jun-
flag
*                                          (m2)
jefvcahs
1020101  101010000        103000000        0.02946028953
00000000

*        mass flow rates
1020200  1

*        time             liquid flow      vapor flow
interface vel.
*        (sec)            (kg/sec)         (kg/sec)
(m/sec)
1020201  0.0              0.0              0.02811550562     0.0
**=======*================*================*================*====
=============**


**=======*=====*==========*================*================*====
=*=====*=====**
** Volume 103, direct inlet pipe

*        Component name   Component type
1030000  DirInPip         pipe

*        nv, # of volumes
1030001  3
```

```
*        flow area        vol #
*        (m2)
1030101  0.02946028953    3

*        flow length      vol #
*        (m)
1030301  0.3048           1
1030302  0.5549519        3

*        Horiz. angle     vol #
*        (deg)
1030501  0.0              3

*        Vert. angle      vol #
*        (deg)
1030601  90.0             1
1030602   0.0             3

*        Elev. change     vol #
*        (m)
1030701  0.3048           1
1030702  0.0              3

*        roughness        hydrlc.diam.     vol #
*        (m)              (m)
1030801  3.75-6           0.193675         3

*        vol-flag         vol #
*        tlpvbfe
1031001  0010000          3

*        jun-flag         jun #
*        jefvcahs
1031101  00001000         2

*        ebt   pressure   temperature      static quality   0.0
0.0   vol #
*              (Pa)       (K)              (dry non-con.)
1031201  004   4.5+5      2273.15          0.0              0.0
0.0   3

*        mass flow rates
1031300  1

*        liquid flow      vapor flow       interface vel.   jun #
*        (kg/sec)         (kg/sec)         (m/sec)
1031301  0.0              0.02811550562    0.0              2
**=======*=====*==========*================*================*====
=*=====*=====**
```

```
**=======*===============*===============*===============*====
=*=====*=====**
** Junction 104, DHX direct inlet flange face

*        Component name   Component type
1040000  DDHXInFl         sngljun

*        from vol.        to vol.          jun. area        A_F
A_R   jun-flag
*                                          (m2)
jefvcahs
1040101  103010000        105000000        0.02946028953    0.0
0.0   00001000

*        mass flow rates  liquid flow      vapor flow
interface vel.
*                         (kg/sec)         (kg/sec)
(m/sec)
1040201  1                0.0              0.02811550562    0.0
**=======*===============*===============*===============*====
=*=====*=====**


**=======*=====*==========*===============*===============*====
=*=====*=====**
** Volume 105, DHX inlet pipe

*        Component name   Component type
1050000  DHXInPip         pipe

*        nv, # of volumes
1050001  4

*        flow area        vol #
*        (m2)
1050101  0.02946028953    4

*        flow length      vol #
*        (m)
1050301  0.314452         1
1050302  0.7875905        3
1050303  0.3603625        4

*        Horiz. angle     vol #
*        (deg)
1050501  0.0              4

*        Vert. angle      vol #
```

```
*        (deg)
1050601   0.0             1
1050602  90.0             3
1050603   0.0             4

*        Elev. change     vol #
*        (m)
1050701  0.0              1
1050702  0.7875905        3
1050703  0.0              4

*        roughness        hydrlc.diam.     vol #
*        (m)              (m)
1050801  3.75-6           0.193675         4

*        vol-flag         vol #
*        tlpvbfe
1051001  0010000          4

*        jun-flag         jun #
*        jefvcahs
1051101  00001000         3

*        ebt   pressure   temperature      static quality   0.0
0.0   vol #
*              (Pa)       (K)              (dry non-con.)
1051201  004   4.5+5      2273.15          0.0              0.0
0.0   4

*        mass flow rates
1051300  1

*        liquid flow      vapor flow       interface vel.   jun #
*        (kg/sec)         (kg/sec)         (m/sec)
1051301  0.0              0.02811550562    0.0              3
**=======*=====*==========*================*================*====
=*=====*=====**


**=======*================*================*================*====
=*=====*=====**
** Junction 106, direct entrance to flow over DHX tubes

*        Component name   Component type
1060000  InDHXJnc         sngljun

*        from vol.        to vol.          jun. area        A_F
A_R   jun-flag
*                                          (m2)
jefvcahs
```

```
1060101  105010000        107000000        0.02946028953    0.0
0.0   00001000

*        mass flow rates  liquid flow      vapor flow
interface vel.
*                         (kg/sec)         (kg/sec)
(m/sec)
1060201  1                0.0              0.02811550562    0.0
**=======*================*================*================*====
=*=====*=====**


**=======*=====*==========*================*================*====
=*=====*=====**
** Volume 107, direct flow over DHX tubes

*        Component name   Component type
1070000  DDHXTube         annulus

*        nv, # of volumes
1070001  4

*        flow area        vol #
*        (m2)
1070101  0.1502901608     4

*        flow length      vol #
*        (m)
1070301  0.05715          4

*        Vert. angle      vol #
*        (deg)
1070601  -90.0            4

*        Elev. change     vol #
*        (m)
1070701  -0.05715         4

*        roughness        hydrlc.diam.     vol #
*        (m)              (m)
1070801  3.75-6           0.1400252599     4

*        vol-flag         vol #
*        tlpvbfe
1071001  0010000          4

*        jun-flag         jun #
*        jefvcahs
1071101  00001000         3
```

```
*        ebt   pressure   temperature      static quality   0.0
0.0   vol #
*              (Pa)       (K)              (dry non-con.)
1071201  004   4.5+5      2273.15          0.0              0.0
0.0   1
1071202  004   4.5+5      1878.667         0.0              0.0
0.0   2
1071203  004   4.5+5      1484.183         0.0              0.0
0.0   3
1071204  004   4.5+5      1089.70          0.0              0.0
0.0   4

*        mass flow rates
1071300  1

*        liquid flow      vapor flow       interface vel.   jun #
*        (kg/sec)         (kg/sec)         (m/sec)
1071301  0.0              0.02811550562    0.0              3
**=======*=====*==========*================*================*====
=*=====*=====**


**=======*================*================*================*====
=*=====*=====**
** Junction 108, direct end of flow over DHX tubes

*        Component name   Component type
1080000  OutDHXJn         sngljun

*        from vol.        to vol.          jun. area        A_F
A_R   jun-flag
*                                          (m2)
jefvcahs
1080101  107010000        109000000        0.150290160796   0.0
0.0   00001000

*        mass flow rates  liquid flow      vapor flow
interface vel.
*                         (kg/sec)         (kg/sec)
(m/sec)
1080201  1                0.0              0.02811550562    0.0
**=======*================*================*================*====
=*=====*=====**


**=======*=====*==========*================*================*====
=*=====*=====**
** Volume 109, DHX check valve reducer

*        Component name   Component type
```

```
1090000  DHXChkVl         annulus

*        nv, # of volumes
1090001  3

*        flow area        vol #
*        (m2)
1090101  0.1599533        2
1090102  0.02786891135    3

*        flow length      vol #
*        (m)
1090301  0.1016           1
1090302  0.2              3

*        Vert. angle      vol #
*        (deg)
1090601  -90.0            3

*        Elev. change     vol #
*        (m)
1090701  -0.1016          1
1090702  -0.2             3

*        roughness        hydrlc.diam.     vol #
*        (m)              (m)
1090801  3.75-6           0.282575         2
1090802  3.75-6           0.06985          3

*        vol-flag         vol #
*        tlpvbfe
1091001  0010000          3

*        jun-flag         jun #
*        jefvcahs
1091101  00001000         2

*        ebt   pressure   temperature      static quality   0.0
0.0   vol #
*              (Pa)       (K)              (dry non-con.)
1091201  004   4.5+5      1089.7           0.0              0.0
0.0   3

*        mass flow rates
1091300  1

*        liquid flow      vapor flow       interface vel.   jun #
*        (kg/sec)         (kg/sec)         (m/sec)
1091301  0.0              0.02811550562    0.0              2
```

```
**=======*=====*==========*===============*===============*====
=*=====*=====**


**=======*===============*===============*===============*====
=*=====*=====**
** Junction 110, DHX check valve out

*        Component name   Component type
1100000  DHXCVOut         sngljun

*        from vol.        to vol.          jun. area        A_F
A_R   jun-flag
*                                          (m2)
jefvcahs
1100101  109010000        111000000        0.02786891135    0.0
0.0   00001000

*        mass flow rates  liquid flow      vapor flow
interface vel.
*                         (kg/sec)         (kg/sec)
(m/sec)
1100201  1                0.0              0.02811550562    0.0
**=======*===============*===============*===============*====
=*=====*=====**


**=======*=====*==========*===============*===============*====
=*=====*=====**
** Volume 111, DHX outlet annulus

*        Component name   Component type
1110000  DHXOutAn         annulus

*        nv, # of volumes
1110001  2

*        flow area        vol #
*        (m2)
1110101  0.02786891135    2

*        flow length      vol #
*        (m)
1110301  0.47360925       2

*        Vert. angle      vol #
*        (deg)
1110601  -90.0            2

*        Elev. change     vol #
```

```
*        (m)
1110701  -0.47360925      2

*        roughness        hydrlc.diam.     vol #
*        (m)              (m)
1110801  3.75-6           0.06985          2

*        vol-flag         vol #
*        tlpvbfe
1111001  0010000          2

*        jun-flag         jun #
*        jefvcahs
1111101  00001000         1

*        ebt   pressure   temperature      static quality   0.0
0.0   vol #
*              (Pa)       (K)              (dry non-con.)
1111201  004   4.5+5      1089.7           0.0              0.0
0.0   2

*        mass flow rates
1111300  1

*        liquid flow      vapor flow       interface vel.   jun #
*        (kg/sec)         (kg/sec)         (m/sec)
1111301  0.0              0.02811550562    0.0              1
**=======*=====*==========*================*================*====
=*=====*=====**


**=======*===============*================*================*====
=*=====*=====**
** Junction 112, end of DHX annulus

*        Component name   Component type
1120000  DHXEndAn         sngljun

*        from vol.        to vol.          jun. area        A_F
A_R   jun-flag
*                                          (m2)
jefvcahs
1120101  111010000        113000000        0.02786891135    0.0
0.0   00001000

*        mass flow rates  liquid flow      vapor flow
interface vel.
*                         (kg/sec)         (kg/sec)
(m/sec)
1120201  1                0.0              0.02811550562    0.0
```

```
**=======*===============*===============*===============*====
=*=====*=====**


**=======*=====*==========*===============*===============*====
=*=====*=====**
** Volume 113, DHX diret outlet reducer

*        Component name   Component type
1130000  DHXOutRd         pipe

*        nv, # of volumes
1130001  3

*        flow area        vol #
*        (m2)
1130101  0.06556319741    1
1130102  0.02946028953    3

*        flow length      vol #
*        (m)
1130301  0.1524           2
1130302  0.111252         3

*        Vert. angle      vol #
*        (deg)
1130601  -90.0            3

*        Elev. change     vol #
*        (m)
1130701  -0.1524          2
1130702  -0.111252        3

*        roughness        hydrlc.diam.     vol #
*        (m)              (m)
1130801  3.75-6           0.288925         1
1130802  3.75-6           0.193675         3

*        vol-flag         vol #
*        tlpvbfe
1131001  0010000          3

*        jun-flag         jun #
*        jefvcahs
1131101  00001000         2

*        ebt   pressure   temperature      static quality   0.0
0.0   vol #
*              (Pa)       (K)              (dry non-con.)
```

```
1131201  004   4.5+5      1089.7           0.0              0.0
0.0   3

*        mass flow rates
1131300  1

*        liquid flow      vapor flow       interface vel.   jun #
*        (kg/sec)         (kg/sec)         (m/sec)
1131301  0.0              0.02811550562    0.0              2
**=======*=====*==========*================*================*====
=*=====*=====**


**=======*================*================*================*====
=*=====*=====**
** Junction 114, DHX direct outlet flange face

*        Component name   Component type
1140000  DDHXOutF         sngljun

*        from vol.        to vol.          jun. area        A_F
A_R   jun-flag
*                                          (m2)
jefvcahs
1140101  113010000        115000000        0.02946028953    0.0
0.0   00001000

*        mass flow rates  liquid flow      vapor flow
interface vel.
*                         (kg/sec)         (kg/sec)
(m/sec)
1140201  1                0.0              0.02811550562    0.0
**=======*================*================*================*====
=*=====*=====**


**=======*=====*==========*================*================*====
=*=====*=====**
** Volume 115, direct outlet pipe

*        Component name   Component type
1150000  DirOutPi         pipe

*        nv, # of volumes
1150001  3

*        flow area        vol #
*        (m2)
1150101  0.02946028953    3
```

```
*        flow length      vol #
*        (m)
1150301  0.58023125       2
1150302  0.416052         3

*        Horiz. angle     vol #
*        (deg)
1150501    0.0            2
1150502  182.940720339    3

*        Vert. angle      vol #
*        (deg)
1150601  -90.0            2
1150602    0.0            3

*        Elev. change     vol #
*        (m)
1150701  -0.58023125      2
1150702   0.0             3

*        roughness        hydrlc.diam.     vol #
*        (m)              (m)
1150801  3.75-6           0.193675         3

*        vol-flag         vol #
*        tlpvbfe
1151001  0010000          3

*        jun-flag         jun #
*        jefvcahs
1151101  00001000         2

*        ebt   pressure   temperature      static quality   0.0
0.0   vol #
*               (Pa)      (K)              (dry non-con.)
1151201  004   4.5+5      1089.7           0.0              0.0
0.0   3

*        mass flow rates
1151300  1

*        liquid flow      vapor flow       interface vel.   jun #
*        (kg/sec)         (kg/sec)         (m/sec)
1151301  0.0              0.02811550562    0.0              2
**=======*=====*==========*================*================*====
=*=====*=====**


**=======*================*================*================*====
=============**
```

```
** Junction 116, direct outlet junction

*        Component name   Component type
1160000  DirOutJn         sngljun

*        from vol.        to vol.          jun. area        A_F
A_R   jun-flag
*                                          (m2)
jefvcahs
1160101  115010000        117000000        0.02946028953    0.0
0.0   00000000

*        mass flow rates  liquid flow      vapor flow
interface vel.
*                         (kg/sec)         (kg/sec)
(m/sec)
1160201  1                0.0              0.02811550562    0.0
**=======*================*================*================*====
=============**


**=======*================*================*================*====
==========*==**
** Volume 117, direct outlet boundary

*        Component name   Component type
1170000  DirOutlt         tmdpvol

*        flow area        flow length      volume
horiz. angle   vert. angle
*        (m2)             (m)              (m3)             (deg)
(deg)
*         elev. chng.      roughness        hydraulic diam.  vol-
flag
*         (m)              (m)              (m)
tlpvbfe
1170101  0.02946028953    0.25             0.0
182.940720339  0.0
+         0.0              3.75-6           0.193675
0000000

*        ebt
1170200  004

*        time             pressure         temperature
static quality
*        (sec)            (Pa)             (K)              (dry
non-con.)
1170201  0.0              4.5+5            1089.7           0.0
```

```
**=======*===============*===============*===============*====
==========*==**


**=================================================================
=============**
** Hydrodynamic Components, Intermediate loop
**
**=================================================================
=============**


**=======*===============*===============*===============*====
*====*======***
** Volume 201, DHX intermediate outlet pipe

*        Component name   Component type
2010000  IDHXOPip         pipe

*        nv, # of volumes
2010001  2

*        flow area        vol #
*        (m2)
2010101  1.140091828125-3 2

*        flow length      vol #
*        (m)
2010301  0.05715          1
2010302  0.3457575        2

*        Horiz. angle     vol #
*        (deg)
2010501  0.0              2

*        Vert. angle      vol #
*        (deg)
2010601   0.0             1
2010602  90.0             2

*        Elev. change     vol #
*        (m)
2010701  0.0              1
2010702  0.3457575        2

*        roughness        hydrlc.diam.     vol #
*        (m)              (m)
2010801  3.75-6           0.0381           2
```

```
*        vol-flag         vol #
*        tlpvbfe
2011001  0000000          2

*        jun-flag         jun #
*        jefvcahs
2011101  00001000         1

*        ebt              pressure         temperature      0.0
0.0  0.0    vol #
*                         (Pa)             (K)
2011201  003              140.0+5          488.38           0.0
0.0  0.0    2

*        mass flow rates
2011300  1

*        liquid flow      vapor flow       interface vel.   jun #
*        (kg/sec)         (kg/sec)         (m/sec)
2011301  0.2910485226     0.0              0.0              1
**=======*================*================*================*====
*====*======***


**=======*================*================*================*====
=*=====*=====**
** Junction 202, DHX intermediate outlet flange face
*        Component name   Component type
2020000  IDHXOutF         sngljun

*        from vol.        to vol.          jun. area        A_F
A_R   jun-flag
*                                          (m2)
jefvcahs
2020101  201010000        203000000        1.140091828125-3 0.0
0.0   00001000

*        mass flow rates  liquid flow      vapor flow
interface vel.
*                         (kg/sec)         (kg/sec)
(m/sec)
2020201  1                0.2910485226     0.0              0.0
**=======*================*================*================*====
=*=====*=====**


**=======*================*================*================*====
*====*======***
** Volume 203, intermediate loop hot pipe
```

```
*        Component name   Component type
2030000  IHotPipe         pipe

*        nv, # of volumes
2030001  10

*        flow area        vol #
*        (m2)
2030101  1.140091828125-3 10

*        flow length      vol #
*        (m)
2030301  0.1254125         1
2030302  0.728953125       5
2030303  0.696115575       9
2030304  0.05715          10

*        Horiz. angle     vol #
*        (deg)
2030501    0.0             1
2030502  143.1716637       5
2030503    0.0             9
2030504  180.0            10

*        Vert. angle      vol #
*        (deg)
2030601  90.0              1
2030602   0.0              5
2030603  90.0              9
2030604   0.0             10

*        Elev. change     vol #
*        (m)
2030701  0.1254125         1
2030702  0.0               5
2030703  0.696115575       9
2030704  0.0              10

*        roughness        hydrlc.diam.     vol #
*        (m)              (m)
2030801  3.75-6           0.0381           10

*        vol-flag         vol #
*        tlpvbfe
2031001  0000000          10

*        jun-flag         jun #
*        jefvcahs
2031101  00001000         9
```

```
*        ebt               pressure          temperature       0.0
0.0  0.0    vol #
*                          (Pa)              (K)
2031201  003               140.0+5           488.38            0.0
0.0  0.0    10

*        mass flow rates
2031300  1

*        liquid flow       vapor flow        interface vel.    jun #
*        (kg/sec)          (kg/sec)          (m/sec)
2031301  0.2910485226      0.0               0.0               9
**=======*================*================*================*====
*====*======***


**=======*================*================*================*====
=*=====*=====**
** Junction 204, intermediate NDHX tube inlet

*        Component name    Component type
2040000  INDHXTin           sngljun

*        from vol.         to vol.           jun. area         A_F
A_R   jun-flag
*                                            (m2)
jefvcahs
2040101  203010000         205000000         1.140091828125-3  0.0
0.0   00001000

*        mass flow rates   liquid flow       vapor flow
interface vel.
*                          (kg/sec)          (kg/sec)
(m/sec)
2040201  1                 0.2910485226      0.0               0.0
**=======*================*================*================*====
=*=====*=====**


**=======*================*================*================*====
*====*======***
** Volume 205, intermediate side of NDHX tube

*        Component name    Component type
2050000  INDHXTub          pipe

*        nv, # of volumes
2050001  28

*        flow area         vol #
```

```
*        (m2)
2050101  1.140091828125-3 28

*        flow length      vol #
*        (m)
2050301  0.36805235        6
2050302  0.5833618         8
2050303  0.37316664       13
2050304  0.5833618        15
2050305  0.37316664       20
2050306  0.5833618        22
2050307  0.36805235       28

*        Horiz. angle     vol #
*        (deg)
2050501  180.0             6
2050502  210.0             7
2050503  330.0             8
2050504    0.0            13
2050505  330.0            14
2050506  210.0            15
2050507  180.0            20
2050508  210.0            21
2050509  330.0            22
2050510    0.0            28

*        Vert. angle      vol #
*        (deg)
2050601  0.0              28

*        Elev. change     vol #
*        (m)
2050701  0.0              28

*        roughness        hydrlc.diam.     vol #
*        (m)              (m)
2050801  3.75-6           0.0381           28

*        vol-flag         vol #
*        tlpvbfe
2051001  0000000          28

*        jun-flag         jun #
*        jefvcahs
2051101  00001000         27

*        ebt              pressure         temperature      0.0
0.0  0.0    vol #
*                         (Pa)             (K)
```

```
2051201  003            140.0+5          488.38           0.0
0.0  0.0     1
2051202  003            140.0+5          485.73           0.0
0.0  0.0     2
2051203  003            140.0+5          483.08           0.0
0.0  0.0     3
2051204  003            140.0+5          480.42           0.0
0.0  0.0     4
2051205  003            140.0+5          477.77           0.0
0.0  0.0     5
2051206  003            140.0+5          475.12           0.0
0.0  0.0     6
2051207  003            140.0+5          470.91           0.0
0.0  0.0     7
2051208  003            140.0+5          466.71           0.0
0.0  0.0     8
2051209  003            140.0+5          464.02           0.0
0.0  0.0     9
2051210  003            140.0+5          461.33           0.0
0.0  0.0    10
2051211  003            140.0+5          458.64           0.0
0.0  0.0    11
2051212  003            140.0+5          455.95           0.0
0.0  0.0    12
2051213  003            140.0+5          453.27           0.0
0.0  0.0    13
2051214  003            140.0+5          449.06           0.0
0.0  0.0    14
2051215  003            140.0+5          444.86           0.0
0.0  0.0    15
2051216  003            140.0+5          442.17           0.0
0.0  0.0    16
2051217  003            140.0+5          439.48           0.0
0.0  0.0    17
2051218  003            140.0+5          436.79           0.0
0.0  0.0    18
2051219  003            140.0+5          434.10           0.0
0.0  0.0    19
2051220  003            140.0+5          431.41           0.0
0.0  0.0    20
2051221  003            140.0+5          427.21           0.0
0.0  0.0    21
2051222  003            140.0+5          423.00           0.0
0.0  0.0    22
2051223  003            140.0+5          420.35           0.0
0.0  0.0    23
2051224  003            140.0+5          417.70           0.0
0.0  0.0    24
2051225  003            140.0+5          415.05           0.0
0.0  0.0    25
```

```
2051226  003              140.0+5          412.39           0.0
0.0  0.0    26
2051227  003              140.0+5          409.74           0.0
0.0  0.0    27
2051228  003              140.0+5          407.09           0.0
0.0  0.0    28

*        mass flow rates
2051300  1

*        liquid flow      vapor flow       interface vel.   jun #
*        (kg/sec)         (kg/sec)         (m/sec)
2051301  0.2910485226     0.0              0.0              27
**=======*================*================*================*====
*====*======***


**=======*================*================*================*====
=*=====*=====**
** Junction 206, intermediate NDHX tube outlet

*        Component name   Component type
2060000  INDHXTou         sngljun

*        from vol.        to vol.          jun. area        A_F
A_R   jun-flag
*                                          (m2)
jefvcahs
2060101  205010000        207000000        1.140091828125-3 0.0
0.0   00001000

*        mass flow rates  liquid flow      vapor flow
interface vel.
*                         (kg/sec)         (kg/sec)
(m/sec)
2060201  1                0.2910485226     0.0              0.0
**=======*================*================*================*====
=*=====*=====**


**=======*================*================*================*====
*====*======***
** Volume 207, intermediate loop cold pipe

*        Component name   Component type
2070000  IColdPip         pipe

*        nv, # of volumes
2070001  9
```

```
*        flow area        vol #
*        (m2)
2070101  1.140091828125-3 9

*        flow length      vol #
*        (m)
2070301  0.05715          1
2070302  0.69887846       6
2070303  0.59319583325    9

*        Horiz. angle     vol #
*        (deg)
2070501  0.0              9

*        Vert. angle      vol #
*        (deg)
2070601    0.0            1
2070602  -90.0            6
2070603    0.0            9

*        Elev. change     vol #
*        (m)
2070701   0.0             1
2070702  -0.69887846      6
2070703   0.0             9

*        roughness        hydrlc.diam.     vol #
*        (m)              (m)
2070801  3.75-6           0.0381           9

*        vol-flag         vol #
*        tlpvbfe
2071001  0000000          9

*        jun-flag         jun #
*        jefvcahs
2071101  00001000         8

*        ebt              pressure         temperature      0.0
0.0  0.0    vol #
*                         (Pa)             (K)
2071201  003              140.0+5          407.09           0.0
0.0  0.0    9

*        mass flow rates
2071300  1

*        liquid flow      vapor flow       interface vel.   jun #
*        (kg/sec)         (kg/sec)         (m/sec)
2071301  0.2910485226     0.0              0.0              8
```

```
**=======*===============*===============*===============*====
*====*======***


**=======*===============*===============*===============*====
==========*==**
** Volume 209, DHX intermediate inlet pipe

*        Component name   Component type
2090000  IDHXInPi          branch

*        nj, # of juncs.  mass flow rates
2090001  3                1

*        flow area        flow length      volume
horiz. angle   vert. angle
*        (m2)             (m)              (m3)             (deg)
(deg)
*         elev. chng.      roughness        hydraulic diam.  vol-
flag
*         (m)              (m)              (m)
tlpvbfe
2090101  1.140091828125-3 0.3984625        0.0              0.0
0.0
+         0.0              3.75-6           0.0381
0000000

*        ebt              pressure         temperature
*                         (Pa)             (K)
2090200  003              140.0+5          407.09

*        from vol.        to vol.          jun. area        A_F
A_R   jun-flag
*                                          (m2)
jefvcahs
2091101  207010000        209000000        0.001140091828   0.0
0.0   00001000
2092101  209010000        211000000        0.001140091828   0.0
0.0   00001000
2093101  238010000        209000000        0.001140091828   0.0
0.0   00011000

*        hydrlc.diam.     flooding corr.   vapor inter.     slope
*        (m)
2091110  0.0381           0.0              1.0              1.0
2092110  0.0381           0.0              1.0              1.0
2093110  0.0381           0.0              1.0              1.0

*        liquid flow      vapor flow       interface vel.
*        (kg/sec)         (kg/sec)         (m/sec)
```

```
2091201  0.2910485226     0.0              0.0
2092201  0.2910485226     0.0              0.0
2093201  0.0              0.0              0.0
**=======*================*================*================*====
=*=====*=====**


**=======*================*================*================*====
*====*======***
** Volume 211, DHX tube inlet manifold

*        Component name   Component type
2110000  DHXInMan         pipe

*        nv, # of volumes
2110001  2

*        flow area        vol #
*        (m2)
2110101  1.140091828125-3 1
2110102  0.00640156215    2

*        flow length      vol #
*        (m)
2110301  0.0254           2

*        Horiz. angle     vol #
*        (deg)
2110501  0.0              2

*        Vert. angle      vol #
*        (deg)
2110601  5.710593137      2

*        Elev. change     vol #
*        (m)
2110701  0.00254          2

*        roughness        hydrlc.diam.     vol #
*        (m)              (m)
2110801  3.75-6           0.0381           1
2110801  3.75-6           0.09028134955    2

*        vol-flag         vol #
*        tlpvbfe
2111001  0000000          2

*        jun-flag         jun #
*        jefvcahs
2111101  00001000         1
```

```
*        ebt               pressure          temperature       0.0
0.0  0.0    vol #
*                          (Pa)              (K)
2111201  003               140.0+5           407.09            0.0
0.0  0.0    2

*        mass flow rates
2111300  1

*        liquid flow       vapor flow        interface vel.    jun #
*        (kg/sec)          (kg/sec)          (m/sec)
2111301  0.2910485226      0.0               0.0               1
**=======*================*================*================*====
*====*======***


**=======*================*================*================*====
=*=====*=====**
** Junction 212, DHX tube inlet

*        Component name    Component type
2120000  DHXTubIn          sngljun

*        from vol.         to vol.           jun. area         A_F
A_R   jun-flag
*                                            (m2)
jefvcahs
2120101  211010000         213000000         1.284503459375-3  0.0
0.0   00001000

*        mass flow rates   liquid flow       vapor flow
interface vel.
*                          (kg/sec)          (kg/sec)
(m/sec)
2120201  1                 0.2910485226      0.0               0.0
**=======*================*================*================*====
=*=====*=====**


**=======*================*================*================*====
*====*======***
** Volume 213, intermediate flow through DHX tubes

*        Component name    Component type
2130000  IDHXTube          pipe

*        nv, # of volumes
2130001  20
```

```
*        flow area        vol #
*        (m2)
2130101  1.284503459375-3 20

*        flow length      vol #
*        (m)
2130301  0.38751152675    20

*        Vert. angle      vol #
*        (deg)
2130601  90.0             20

*        Elev. change     vol #
*        (m)
2130701  0.01143          20

*        roughness        hydrlc.diam.     vol #
*        (m)              (m)
2130801  3.75-6           0.01651          20

*        vol-flag         vol #
*        tlpvbfe
2131001  0000000          20

*        jun-flag         jun #
*        jefvcahs
2131101  00001000         19

*        ebt              pressure         temperature      0.0
0.0  0.0    vol #
*                         (Pa)             (K)
2131201  003              140.0+5          407.09           0.0
0.0  0.0     1
2131202  003              140.0+5          411.37           0.0
0.0  0.0     2
2131203  003              140.0+5          415.65           0.0
0.0  0.0     3
2131204  003              140.0+5          419.93           0.0
0.0  0.0     4
2131205  003              140.0+5          424.20           0.0
0.0  0.0     5
2131206  003              140.0+5          428.48           0.0
0.0  0.0     6
2131207  003              140.0+5          432.76           0.0
0.0  0.0     7
2131208  003              140.0+5          437.04           0.0
0.0  0.0     8
2131209  003              140.0+5          441.32           0.0
0.0  0.0     9
```

```
2131210  003              140.0+5          445.60           0.0
0.0  0.0    10
2131211  003              140.0+5          449.87           0.0
0.0  0.0    11
2131212  003              140.0+5          454.15           0.0
0.0  0.0    12
2131213  003              140.0+5          458.43           0.0
0.0  0.0    13
2131214  003              140.0+5          462.71           0.0
0.0  0.0    14
2131215  003              140.0+5          466.99           0.0
0.0  0.0    15
2131216  003              140.0+5          471.27           0.0
0.0  0.0    16
2131217  003              140.0+5          475.54           0.0
0.0  0.0    17
2131218  003              140.0+5          479.82           0.0
0.0  0.0    18
2131219  003              140.0+5          484.10           0.0
0.0  0.0    19
2131220  003              140.0+5          488.38           0.0
0.0  0.0    20


*        mass flow rates
2131300  1

*        liquid flow      vapor flow       interface vel.   jun #
*        (kg/sec)         (kg/sec)         (m/sec)
2131301  0.2910485226     0.0              0.0              19
**=======*================*================*================*====
*====*=======***


**=======*================*================*================*====
=*=====*======**
** Junction 214, DHX tube outlet

*        Component name   Component type
2140000  DHXTubOu         sngljun

*        from vol.        to vol.          jun. area        A_F
A_R   jun-flag
*                                          (m2)
jefvcahs
2140101  213010000        215000000        1.284503459375-3 0.0
0.0   00001000

*        mass flow rates  liquid flow      vapor flow
interface vel.
```

```
*                          (kg/sec)         (kg/sec)
(m/sec)
2140201  1                 0.2910485226     0.0               0.0
**=======*================*================*================*====
=*=====*=====**


**=======*================*================*================*====
*====*======***
** Volume 215, DHX tube outlet manifold

*        Component name   Component type
2150000  DHXOuMan         pipe

*        nv, # of volumes
2150001  2

*        flow area        vol #
*        (m2)
2150101  0.00640156215    1
2150102  1.140091828125-3 2

*        flow length      vol #
*        (m)
2150301  0.0254           2

*        Horiz. angle     vol #
*        (deg)
2150501  0.0              2

*        Vert. angle      vol #
*        (deg)
2150601  5.710593137      2

*        Elev. change     vol #
*        (m)
2150701  0.00254          2

*        roughness        hydrlc.diam.     vol #
*        (m)              (m)
2150801  3.75-6           0.09028134955    1
2150802  3.75-6           0.0381           2

*        vol-flag         vol #
*        tlpvbfe
2151001  0000000          2

*        jun-flag         jun #
*        jefvcahs
2151101  00001000         1
```

```
*        ebt               pressure          temperature       0.0
0.0  0.0    vol #
*                          (Pa)              (K)
2151201  003               140.0+5           488.38            0.0
0.0  0.0    2

*        mass flow rates
2151300  1

*        liquid flow       vapor flow        interface vel.    jun #
*        (kg/sec)          (kg/sec)          (m/sec)
2151301  0.2910485226      0.0               0.0               1
**=======*================*================*================*====
*====*======***


**=======*================*================*================*====
=*=====*=====**
** Junction 216, DHX manifold outlet junction

*        Component name    Component type
2160000  DHXManOJ          sngljun

*        from vol.         to vol.           jun. area         A_F
A_R   jun-flag
*                                            (m2)
jefvcahs
2160101  215010000         201000000         1.140091828125-3  0.0
0.0   00001000

*        mass flow rates   liquid flow       vapor flow
interface vel.
*                          (kg/sec)          (kg/sec)
(m/sec)
2160201  1                 0.2910485226      0.0               0.0
**=======*================*================*================*====
=*=====*=====**


**=======*================*================*================*====
==========*==**
** Volume 238, intermediate pressure control boundary

*        Component name    Component type
2380000  IntPress          tmdpvol

*        flow area         flow length       volume
horiz. angle   vert. angle
```

```
*        (m2)              (m)               (m3)              (deg)
(deg)
*         elev. chng.       roughness         hydraulic diam.  vol-
flag
*         (m)               (m)               (m)
tlpvbfe
2380101  1.140091828125-3 0.10              0.0               0.0
-90.0
+         -0.1              3.75-6            0.0381
0000000

*        ebt
2380200  003

*        time              pressure          temperature
*        (sec)             (Pa)              (K)
2380201  0.0               140.0+5           320.74
**=======*================*================*================*====
==========*==**



**=============================================================
=============**
** Hydrodynamic Components, Natural draft loop
**
**=============================================================
=============**


**=======*================*================*================*====
==========*==**
** Volume 301, natural draft inlet boundary

*        Component name   Component type
3010000  NDrInlet         tmdpvol

*        flow area        flow length      volume
horiz. angle   vert. angle
*        (m2)              (m)               (m3)              (deg)
(deg)
*         elev. chng.       roughness         hydraulic diam.  vol-
flag
*         (m)               (m)               (m)
tlpvbfe
3010101  4.921875         0.25              0.0               0.0
90.0
+         0.25              3.75-6            2.1875
0000000
```

```
*        ebt
3010200  004

*        time              pressure          temperature
static quality
*        (sec)             (Pa)              (K)               (dry
non-con.)
3010201  0.0               1.0+5             303.15            0.0

*        helium            nitrogen          air
*        (mass frac.)      (mass frac.)      (mass frac.)
3010301  0.0               0.0               1.0
**=======*================*================*================*====
==========*==**


**=======*================*================*================*====
=============**
** Junction 302, natural draft inlet junction

*        Component name    Component type
3020000  NDInJunc          tmdpjun

*        from vol.         to vol.           jun. area         jun-
flag
*                                            (m2)
jefvcahs
3020101  301010000         303000000         4.921875
00000000

*        mass flow rates
3020200  1

*        time              liquid flow       vapor flow
interface vel.
*        (sec)             (kg/sec)          (kg/sec)
(m/sec)
3020201  0.0               0.0               7.924298528       0.0
**=======*================*================*================*====
=============**


**=======*=====*==========*================*================*====
=*=====*=====**
** Volume 303, natural draft NDHX reject heat air flow

*        Component name    Component type
3030000  NDNDHXRj          pipe

*        nv, # of volumes
```

```
3030001  3

*        flow area        vol #
*        (m2)
3030101  3.0695           1
3030102  2.769558849      2
3030103  3.0695           3

*        flow length      vol #
*        (m)
3030301  0.03837          1
3030302  0.04826          2
3030303  0.03837          3

*        Horiz. angle     vol #
*        (deg)
3030501  0.0              3

*        Vert. angle      vol #
*        (deg)
3030601  90.0             3

*        Elev. change     vol #
*        (m)
3030701  0.03837          1
3030702  0.04826          2
3030703  0.03837          3

*        roughness        hydrlc.diam.     vol #
*        (m)              (m)
3030801  3.75-6           2.347385527-3    1
3030802  3.75-6           2.30654984-3     2
3030803  3.75-6           2.347385527-3    3

*        vol-flag         vol #
*        tlpvbfe
3031001  0010000          3

*        jun-flag         jun #
*        jefvcahs
3031101  00001000         2

*        ebt   pressure   temperature      static quality   0.0
0.0   vol #
*              (Pa)       (K)              (dry non-con.)
3031201  004   1.0+5      303.15           0.0              0.0
0.0   1
3031202  004   1.0+5      312.96           0.0              0.0
0.0   2
```

```
3031203  004   1.0+5      322.77           0.0              0.0
0.0   3

*        mass flow rates
3031300  1

*        liquid flow      vapor flow       interface vel.   jun #
*        (kg/sec)         (kg/sec)         (m/sec)
3031301  0.0              7.924298528      0.0              2

*        helium           nitrogen         air
additional  vol #
*        (mass frac.)     (mass frac.)     (mass frac.)     mass
frac
3033201  0.0              0.0              1.0              0.0
0.0   3
**=======*=====*==========*================*================*====
=*=====*=====**


**=======*================*================*================*====
=============**
** Junction 304, natural draft outlet junction

*        Component name   Component type
3040000  NDOutJun         tmdpjun

*        from vol.        to vol.          jun. area        jun-
flag
*                                          (m2)
jefvcahs
3040101  303010000        305000000        4.921875
00000000

*        mass flow rates
3040200  1

*        time             liquid flow      vapor flow
interface vel.
*        (sec)            (kg/sec)         (kg/sec)
(m/sec)
3040201  0.0              0.0              7.924298528      0.0
**=======*================*================*================*====
=============**


**=======*================*================*================*====
==========*==**
** Volume 305, natural draft outlet boundary
```

```
*        Component name   Component type
3050000  NDOutlet         tmdpvol

*        flow area        flow length      volume
horiz. angle   vert. angle
*        (m2)             (m)              (m3)             (deg)
(deg)
*         elev. chng.      roughness        hydraulic diam.  vol-
flag
*         (m)              (m)              (m)
tlpvbfe
3050101  4.921875         0.25             0.0              0.0
90.0
+         0.25             3.75-6           2.1875
0000000

*        ebt
3050200  004

*        time             pressure         temperature
static quality
*        (sec)            (Pa)             (K)              (dry
non-con.)
3050201  0.0              1.0+5            322.77           0.0

*        helium           nitrogen         air
*        (mass frac.)     (mass frac.)     (mass frac.)
3050301  0.0              0.0              1.0
**=======*================*================*================*====
==========*==**



**================================================================
=============**
** Heat Structures, DRACS Heat Exchanger, DHX
**
**================================================================
=============**

*        nh, axial mesh   np, rad. mesh    Geom. type       SS
init. flag
*         Left boundary    Reflood flag
*         (m)
12131000 20               2                2                1
+         0.008255         0

*        mesh location    mesh format
12131100 0                1
```

```
*        # of intervals   right coord.
12131101 1                0.009525

*        composition #    interval #
12131201 001              1

*        source Q_in      interval #
12131301 0.0              1

*        temp. entered
12131400 0

*        temperature      mp #
*        (K)
12131401  471.3           1
12131402 1005.85          2

* *LB*   LB volume #      increment        LB cond. type
surface area code
* *LB*    surface area     hs #
*         (m2)
12131501 213010000        10000            101              0
+         0.02009932957    20


* *RB*   RB volume #      increment        RB cond. type
surface area code
* *RB*    surface area     hs #
*         (m2)
12131601 107040000        0                101              0
+         0.02319153412     5
12131602 107030000        0                101              0
+         0.02319153412    10
12131603 107020000        0                101              0
+         0.02319153412    15
12131604 107010000        0                101              0
+         0.02319153412    20


*        power src type   Int src mult     LB direct heat   RB
direct heat   hs #
12131701 0                0.0              0.0              0.0
20

*        twelve-word format
12131800 1

* *LB*   HT hyd. diam.    Ht lngth for     Ht lngth rev     Grd
spcr L for   Grd spcr L rev
```

```
*         (m)                (m)                (m)                (m)
(m)
* *LB*    Grd loss coeff   Grd loss coeff   boiling factor   nat
circ lngth
*         for                rev                                  (m)
* *LB*     pitch-to-diam    HTC foul factor  hs #
12131801 0.01651          0.1937557634     7.556474773      0.0
0.0
+         0.0               0.0               1.0
0.01651
+          1.477644055       1.0               1
12131802 0.01651          0.5812672902     7.168963246      0.0
0.0
+         0.0               0.0               1.0
0.01651
+          1.477644055       1.0               2
12131803 0.01651          0.9687788171     6.78045172       0.0
0.0
+         0.0               0.0               1.0
0.01651
+          1.477644055       1.0               3
12131804 0.01651          1.356290344      6.393940193      0.0
0.0
+         0.0               0.0               1.0
0.01651
+          1.477644055       1.0               4
12131805 0.01651          1.743801871      6.006428666      0.0
0.0
+         0.0               0.0               1.0
0.01651
+          1.477644055       1.0               5
12131806 0.01651          2.131313398      5.618917139      0.0
0.0
+         0.0               0.0               1.0
0.01651
+          1.477644055       1.0               6
12131807 0.01651          2.518824924      5.231405612      0.0
0.0
+         0.0               0.0               1.0
0.01651
+          1.477644055       1.0               7
12131808 0.01651          2.906336451      4.843894085      0.0
0.0
+         0.0               0.0               1.0
0.01651
+          1.477644055       1.0               8
12131809 0.01651          3.293847978      4.456382559      0.0
0.0
+         0.0               0.0               1.0
0.01651
```

```
+          1.477644055      1.0              9
12131810 0.01651          3.681359505      4.068871032      0.0
0.0
+         0.0              0.0              1.0
0.01651
+          1.477644055      1.0              10
12131811 0.01651          4.068871032      3.681359505      0.0
0.0
+         0.0              0.0              1.0
0.01651
+          1.477644055      1.0              11
12131812 0.01651          4.456382559      3.293847978      0.0
0.0
+         0.0              0.0              1.0
0.01651
+          1.477644055      1.0              12
12131813 0.01651          4.843894085      2.906336451      0.0
0.0
+         0.0              0.0              1.0
0.01651
+          1.477644055      1.0              13
12131814 0.01651          5.231405612      2.518824924      0.0
0.0
+         0.0              0.0              1.0
0.01651
+          1.477644055      1.0              14
12131815 0.01651          5.618917139      2.131313398      0.0
0.0
+         0.0              0.0              1.0
0.01651
+          1.477644055      1.0              15
12131816 0.01651          6.006428666      1.743801871      0.0
0.0
+         0.0              0.0              1.0
0.01651
+          1.477644055      1.0              16
12131817 0.01651          6.393940193      1.356290344      0.0
0.0
+         0.0              0.0              1.0
0.01651
+          1.477644055      1.0              17
12131818 0.01651          6.78045172       0.9687788171     0.0
0.0
+         0.0              0.0              1.0
0.01651
+          1.477644055      1.0              18
12131819 0.01651          7.168963246      0.5812672902     0.0
0.0
+         0.0              0.0              1.0
0.01651
```

```
+          1.477644055      1.0              19
12131820 0.01651          7.556474773      0.1937557634     0.0
0.0
+         0.0              0.0              1.0
0.01651
+          1.477644055      1.0              20

*        twelve-word format
12131900 1

* *RB*   HT hyd. diam.    Ht lngth for     Ht lngth rev     Grd
spcr L for   Grd spcr L rev
*        (m)              (m)              (m)              (m)
(m)
* *RB*    Grd loss coeff   Grd loss coeff   boiling factor   nat
circ lngth
*         for              rev                               (m)
* *RB*     pitch-to-diam    HTC foul factor  hs #
12131901 0.2962833815     0.222885         0.005715         0.0
0.0
+         0.0              0.0              1.0
0.01143
+          1.280624847      1.0              1
12131902 0.2962833815     0.211455         0.017145         0.0
0.0
+         0.0              0.0              1.0
0.01143
+          1.280624847      1.0              2
12131903 0.2962833815     0.200025         0.028575         0.0
0.0
+         0.0              0.0              1.0
0.01143
+          1.280624847      1.0              3
12131904 0.2962833815     0.188595         0.040005         0.0
0.0
+         0.0              0.0              1.0
0.01143
+          1.280624847      1.0              4
12131905 0.2962833815     0.177165         0.051435         0.0
0.0
+         0.0              0.0              1.0
0.01143
+          1.280624847      1.0              5
12131906 0.2962833815     0.165735         0.062885         0.0
0.0
+         0.0              0.0              1.0
0.01143
+          1.280624847      1.0              6
12131907 0.2962833815     0.154305         0.074295         0.0
0.0
```

```
+         0.0              0.0              1.0
0.01143
+          1.280624847      1.0               7
12131908 0.2962833815     0.142875         0.085725         0.0
0.0
+         0.0              0.0              1.0
0.01143
+          1.280624847      1.0               8
12131909 0.2962833815     0.131445         0.097155         0.0
0.0
+         0.0              0.0              1.0
0.01143
+          1.280624847      1.0               9
12131910 0.2962833815     0.120015         0.108585         0.0
0.0
+         0.0              0.0              1.0
0.01143
+          1.280624847      1.0              10
12131911 0.2962833815     0.108585         0.120015         0.0
0.0
+         0.0              0.0              1.0
0.01143
+          1.280624847      1.0              11
12131912 0.2962833815     0.097155         0.131445         0.0
0.0
+         0.0              0.0              1.0
0.01143
+          1.280624847      1.0              12
12131913 0.2962833815     0.085725         0.142875         0.0
0.0
+         0.0              0.0              1.0
0.01143
+          1.280624847      1.0              13
12131914 0.2962833815     0.074295         0.154305         0.0
0.0
+         0.0              0.0              1.0
0.01143
+          1.280624847      1.0              14
12131915 0.2962833815     0.062885         0.165735         0.0
0.0
+         0.0              0.0              1.0
0.01143
+          1.280624847      1.0              15
12131916 0.2962833815     0.051435         0.177165         0.0
0.0
+         0.0              0.0              1.0
0.01143
+          1.280624847      1.0              16
12131917 0.2962833815     0.040005         0.188595         0.0
0.0
```

```
+         0.0              0.0              1.0
0.01143
+          1.280624847      1.0              17
12131918 0.2962833815     0.028575         0.200025         0.0
0.0
+         0.0              0.0              1.0
0.01143
+          1.280624847      1.0              18
12131919 0.2962833815     0.017145         0.211455         0.0
0.0
+         0.0              0.0              1.0
0.01143
+          1.280624847      1.0              19
12131920 0.2962833815     0.005715         0.222885         0.0
0.0
+         0.0              0.0              1.0
0.01143
+          1.280624847      1.0              20


**==========================================================
=============**
** Heat Structures, Natural Draft Heat Exchanger, NDHX
**
**==========================================================
=============**


*        nh, axial mesh   np, rad. mesh    Geom. type       SS
init. flag
*         Left boundary    Reflood flag     boundary vol.    max
# axial intervals
*         (m)
12051000 28               2                2                1
+         0.0762           0                *no reflood is used

*        mesh location    mesh format
12051100 0                1

*        # of intervals   right coord.
12051101 1                0.09652

*        composition #    interval #
12051201 002              1

*        source Q_in      interval #
12051301 0.0              1

*        temp. entered
```

```
12051400 0

*        temperature      mesh point #
*        (K)
12051401 400.81           1
12051402 318.651          2

* *LB*   LB volume #      increment        LB cond. type
surface area code
* *LB*    surface length   hs #
*         (m)
12051501 205010000        10000            101              0
+         0.04658398246    28

* *RB*   RB volume #      increment        RB cond. type
surface area code
* *RB*    surface length   hs #
*         (m)
12051601 303020000        0                101              0
+         0.05900637778    28

*        power src type   Int src mult     LB direct heat   RB
direct heat   hs #
12051701 0                0.0              0.0              0.0
28

*        twelve-word format
12051800 1

* *LB*   HT hyd. diam.    Ht lngth for     Ht lngth rev     Grd
spcr L for   Grd spcr L rev
*        (m)              (m)              (m)              (m)
(m)
* *LB*    Grd loss coeff   Grd loss coeff   boiling factor   nat
circ lngth
*         for              rev                               (m)
* *LB*     pitch-to-diam    HTC foul factor  hs #
12051801 0.0381           11.46443923       0.184026175      0.0
0.0
+         0.0              0.0              1.0
0.0381
+          1.6              1.0               1
12051802 0.0381           11.09638688       0.552078525      0.0
0.0
+         0.0              0.0              1.0
0.0381
+          1.6              1.0               2
12051803 0.0381           10.72833453       0.920130875      0.0
0.0
```

```
+          0.0              0.0              1.0
0.0381
+           1.6              1.0                3
12051804 0.0381           10.36028218       1.288183225     0.0
0.0
+          0.0              0.0              1.0
0.0381
+           1.6              1.0                4
12051805 0.0381           9.992229825       1.656235575     0.0
0.0
+          0.0              0.0              1.0
0.0381
+           1.6              1.0                5
12051806 0.0381           9.624177475       2.024287925     0.0
0.0
+          0.0              0.0              1.0
0.0381
+           1.6              1.0                6
12051807 0.0381           9.1484704         2.49995         0.0
0.0
+          0.0              0.0              1.0
0.0381
+           1.6              1.0                7
12051808 0.0381           8.5651086         3.0833568       0.0
0.0
+          0.0              0.0              1.0
0.0381
+           1.6              1.0                8
12051809 0.0381           8.08684438        3.56162102      0.0
0.0
+          0.0              0.0              1.0
0.0381
+           1.6              1.0                9
12051810 0.0381           7.71367774        3.93478766      0.0
0.0
+          0.0              0.0              1.0
0.0381
+           1.6              1.0               10
12051811 0.0381           7.3405111         4.3079543       0.0
0.0
+          0.0              0.0              1.0
0.0381
+           1.6              1.0               11
12051812 0.0381           6.96734446        4.68112094      0.0
0.0
+          0.0              0.0              1.0
0.0381
+           1.6              1.0               12
12051813 0.0381           6.59417782        5.05428758      0.0
0.0
```

```
+          0.0              0.0              1.0
0.0381
+           1.6              1.0              13
12051814 0.0381           6.1159136        5.5325518        0.0
0.0
+          0.0              0.0              1.0
0.0381
+           1.6              1.0              14
12051815 0.0381           5.5325518        6.1159136        0.0
0.0
+          0.0              0.0              1.0
0.0381
+           1.6              1.0              15
12051816 0.0381           5.05428758       6.59417782       0.0
0.0
+          0.0              0.0              1.0
0.0381
+           1.6              1.0              16
12051817 0.0381           4.68112094       6.96734446       0.0
0.0
+          0.0              0.0              1.0
0.0381
+           1.6              1.0              17
12051818 0.0381           4.3079543        7.3405111        0.0
0.0
+          0.0              0.0              1.0
0.0381
+           1.6              1.0              18
12051819 0.0381           3.93478766       7.71367774       0.0
0.0
+          0.0              0.0              1.0
0.0381
+           1.6              1.0              19
12051820 0.0381           3.56162102       8.08684438       0.0
0.0
+          0.0              0.0              1.0
0.0381
+           1.6              1.0              20
12051821 0.0381           3.0833568        8.5651086        0.0
0.0
+          0.0              0.0              1.0
0.0381
+           1.6              1.0              21
12051822 0.0381           2.49995          9.1484704        0.0
0.0
+          0.0              0.0              1.0
0.0381
+           1.6              1.0              22
12051823 0.0381           2.024287925      9.624177475      0.0
0.0
```

```
+         0.0              0.0              1.0
0.0381
+          1.6              1.0               23
12051824 0.0381            1.656235575      9.992229825     0.0
0.0
+         0.0              0.0              1.0
0.0381
+          1.6              1.0               24
12051825 0.0381            1.288183225     10.36028218      0.0
0.0
+         0.0              0.0              1.0
0.0381
+          1.6              1.0               25
12051826 0.0381            0.920130875     10.72833453      0.0
0.0
+         0.0              0.0              1.0
0.0381
+          1.6              1.0               26
12051827 0.0381            0.552078525     11.09638688      0.0
0.0
+         0.0              0.0              1.0
0.0381
+          1.6              1.0               27
12051828 0.0381            0.184026175     11.46443923      0.0
0.0
+         0.0              0.0              1.0
0.0381
+          1.6              1.0               28

*        twelve-word format
12051900 1

* *RB*   HT hyd. diam.    Ht lngth for     Ht lngth rev     Grd
spcr L for   Grd spcr L rev
*        (m)              (m)              (m)              (m)
(m)
* *RB*    Grd loss coeff   Grd loss coeff   boiling factor   nat
circ lngth
*         for              rev                               (m)
* *RB*     pitch-to-diam    HTC foul factor  hs #
12051901 0.3235943422     0.04739821429    0.0008617857143  0.0
0.0
+         0.0              0.0              1.0
0.001723571429
+          1.6              140.0453858       1
12051902 0.3235943422     0.04567464286    0.002585357143   0.0
0.0
+         0.0              0.0              1.0
0.001723571429
+          1.6              140.0453858       2
```

```
12051903 0.3235943422     0.04395107143    0.004308928571   0.0
0.0
+         0.0              0.0              1.0
0.001723571429
+          1.6               140.0453858       3
12051904 0.3235943422     0.0422275        0.0060325        0.0
0.0
+         0.0              0.0              1.0
0.001723571429
+          1.6               140.0453858       4
12051905 0.3235943422     0.04050392857    0.007756071429   0.0
0.0
+         0.0              0.0              1.0
0.001723571429
+          1.6               140.0453858       5
12051906 0.3235943422     0.03878035714    0.009479642857   0.0
0.0
+         0.0              0.0              1.0
0.001723571429
+          1.6               140.0453858       6
12051907 0.3235943422     0.03705678571    0.01120321429    0.0
0.0
+         0.0              0.0              1.0
0.001723571429
+          1.6               140.0453858       7
12051908 0.3235943422     0.03533321429    0.01292678571    0.0
0.0
+         0.0              0.0              1.0
0.001723571429
+          1.6               140.0453858       8
12051909 0.3235943422     0.03360964286    0.01465035714    0.0
0.0
+         0.0              0.0              1.0
0.001723571429
+          1.6               140.0453858       9
12051910 0.3235943422     0.03188607143    0.01637392857    0.0
0.0
+         0.0              0.0              1.0
0.001723571429
+          1.6               140.0453858      10
12051911 0.3235943422     0.0301625        0.0180975        0.0
0.0
+         0.0              0.0              1.0
0.001723571429
+          1.6               140.0453858      11
12051912 0.3235943422     0.02843892857    0.01982107143    0.0
0.0
+         0.0              0.0              1.0
0.001723571429
+          1.6               140.0453858      12
```

```
12051913 0.3235943422     0.02671535714    0.02154464286    0.0
0.0
+         0.0              0.0              1.0
0.001723571429
+          1.6               140.0453858      13
12051914 0.3235943422     0.02499178571    0.02326821429    0.0
0.0
+         0.0              0.0              1.0
0.001723571429
+          1.6               140.0453858      14
12051915 0.3235943422     0.02326821429    0.02499178571    0.0
0.0
+         0.0              0.0              1.0
0.001723571429
+          1.6               140.0453858      15
12051916 0.3235943422     0.02154464286    0.02671535714    0.0
0.0
+         0.0              0.0              1.0
0.001723571429
+          1.6               140.0453858      16
12051917 0.3235943422     0.01982107143    0.02843892857    0.0
0.0
+         0.0              0.0              1.0
0.001723571429
+          1.6               140.0453858      17
12051918 0.3235943422     0.0180975        0.0301625        0.0
0.0
+         0.0              0.0              1.0
0.001723571429
+          1.6               140.0453858      18
12051919 0.3235943422     0.01637392857    0.03188607143    0.0
0.0
+         0.0              0.0              1.0
0.001723571429
+          1.6               140.0453858      19
12051920 0.3235943422     0.01465035714    0.03360964286    0.0
0.0
+         0.0              0.0              1.0
0.001723571429
+          1.6               140.0453858      20
12051921 0.3235943422     0.01292678571    0.03533321429    0.0
0.0
+         0.0              0.0              1.0
0.001723571429
+          1.6               140.0453858      21
12051922 0.3235943422     0.01120321429    0.03705678571    0.0
0.0
+         0.0              0.0              1.0
0.001723571429
+          1.6               140.0453858      22
```

```
12051923 0.3235943422     0.009479642857   0.03878035714    0.0
0.0
+         0.0              0.0              1.0
0.001723571429
+          1.6              140.0453858      23
12051924 0.3235943422     0.007756071429   0.04050392857    0.0
0.0
+         0.0              0.0              1.0
0.001723571429
+          1.6              140.0453858      24
12051925 0.3235943422     0.0060325        0.0422275        0.0
0.0
+         0.0              0.0              1.0
0.001723571429
+          1.6              140.0453858      25
12051926 0.3235943422     0.004308928571   0.04395107143    0.0
0.0
+         0.0              0.0              1.0
0.001723571429
+          1.6              140.0453858      26
12051927 0.3235943422     0.002585357143   0.04567464286    0.0
0.0
+         0.0              0.0              1.0
0.001723571429
+          1.6              140.0453858      27
12051928 0.3235943422     0.0008617857143  0.04739821429    0.0
0.0
+         0.0              0.0              1.0
0.001723571429
+          1.6              140.0453858      28



**==========================================================
=============**
** Heat Structure Thermal Property Data
**
**==========================================================
=============**


**========*===============*================*=================
=============**
*         material type    therm cond flag  vol ht cap flag
20100100  tbl/fctn         1                1

*         constant value for thermal conductivity (W/m K)
20100101  0.01655

*         constant value for volumetric heat capacity (J/m3 K)
```

```
20100151  1.0
**========*===============*===============*====================
=============**


**========*===============*===============*====================
=============**
*         material type    therm cond flag  vol ht cap flag
20100200  tbl/fctn         1                1

*         constant value for thermal conductivity (W/m K)
20100201  11.4203

*         constant value for volumetric heat capacity (J/m3 K)
20100251  0.015625
**========*===============*===============*====================
=============**



**=================================================================
=============**
** Control system quantities
**
**=================================================================
=============**


**=======*===============*===============*===============*====
=============**
*        total heat transfer from direct loop fluid to DHX tubes
*        quantity name    control type     scaling factor
20500100 dhxqdsum         sum              1.0              0.0 0

*        a_0  a_1 minor edit1  a_2 minor edit2  a_3 minor edit3
a_4 minor edit4
20500101 0.0  1.0 q 107010000  1.0 q 107020000  1.0 q 107030000
1.0 q 107040000
**=======*====*===============*===============*===============
*============**


**=======*===============*===============*===============*====
=============**
*        total heat transfer from DHX to intermediate loop fluid
*        quantity name    control type     scaling factor
20500200 dhxqisum         sum              1.0              0.0
0
*        a_0  a_1 minor edit1  a_2 minor edit2  a_3 minor edit3
a_4 minor edit4
```

```
20500201 0.0  1.0 q 213010000  1.0 q 213020000  1.0 q 213030000
1.0 q 213040000
+             1.0 q 213050000  1.0 q 213060000  1.0 q 213070000
1.0 q 213080000
20500202      1.0 q 213090000  1.0 q 213100000  1.0 q 213110000
1.0 q 213120000
+             1.0 q 213130000  1.0 q 213140000  1.0 q 213150000
1.0 q 213160000
20500203      1.0 q 213170000  1.0 q 213180000  1.0 q 213190000
1.0 q 213200000
**=======*====*================*================*================
*============**


**=======*================*================*================*====
=============**
*        total heat transfer from intermediate loop fluid
*        quantity name    control type     scaling factor
20500300 ndhxqism         sum              1.0              0.0
0
*        a_0  a_1 minor edit1  a_2 minor edit2  a_3 minor edit3
a_4 minor edit4
20500301 0.0  1.0 q 205010000  1.0 q 205020000  1.0 q 205030000
1.0 q 205040000
+             1.0 q 205050000  1.0 q 205060000  1.0 q 205070000
1.0 q 205080000
20500302      1.0 q 205090000  1.0 q 205100000  1.0 q 205110000
1.0 q 205120000
+             1.0 q 205130000  1.0 q 205140000  1.0 q 205150000
1.0 q 205160000
20500303      1.0 q 205170000  1.0 q 205180000  1.0 q 205190000
1.0 q 205200000
+             1.0 q 205210000  1.0 q 205220000  1.0 q 205230000
1.0 q 205240000
20500204      1.0 q 205250000  1.0 q 205260000  1.0 q 205270000
1.0 q 205280000
**=======*====*================*================*================
*============**



.
```

8.6.Appendix F: SolidWorks model part drawings

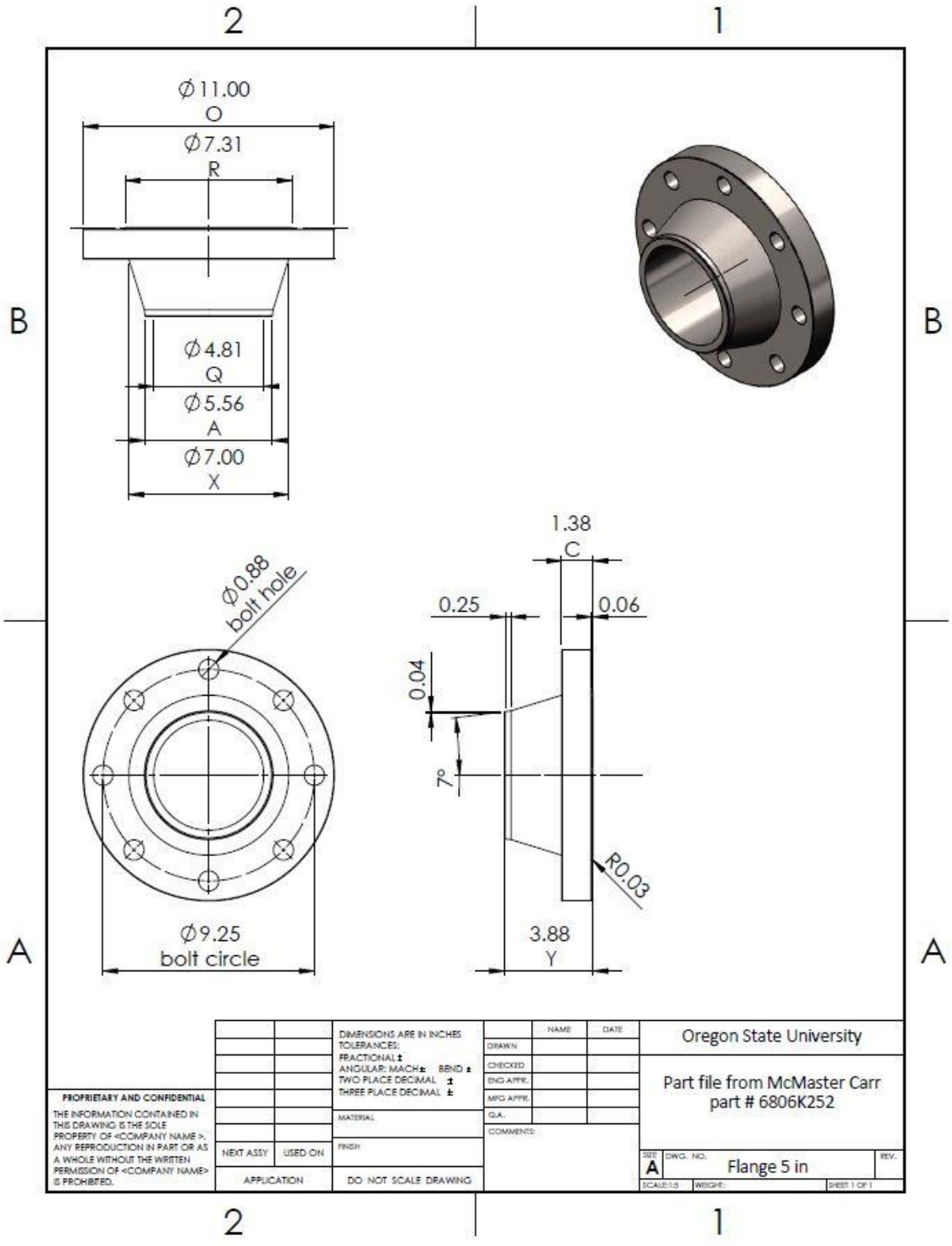

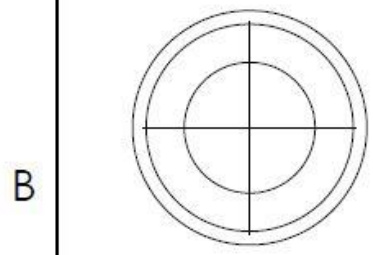

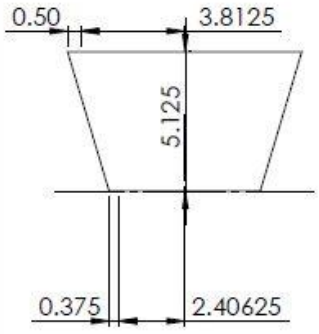

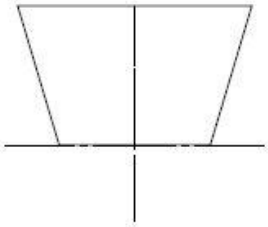

		DIMENSIONS ARE IN INCHES TOLERANCES: FRACTIONAL ± ANGULAR: MACH ± BEND ± TWO PLACE DECIMAL ± THREE PLACE DECIMAL ±		NAME	DATE
			DRAWN		
			CHECKED		
			ENG APPR.		
			MFG APPR.		
			Q.A.		
		MATERIAL	COMMENTS:		
NEXT ASSY	USED ON	FINISH			
APPLICATION		DO NOT SCALE DRAWING			

PROPRIETARY AND CONFIDENTIAL

THE INFORMATION CONTAINED IN THIS DRAWING IS THE SOLE PROPERTY OF <COMPANY NAME >. ANY REPRODUCTION IN PART OR AS A WHOLE WITHOUT THE WRITTEN PERMISSION OF <COMPANY NAME> IS PROHIBITED.

Oregon State University

Original work by Grant C. Blake

SIZE	DWG. NO.	REV.
A	Direct inlet reducer	
SCALE:1:5	WEIGHT:	SHEET 1 OF 1

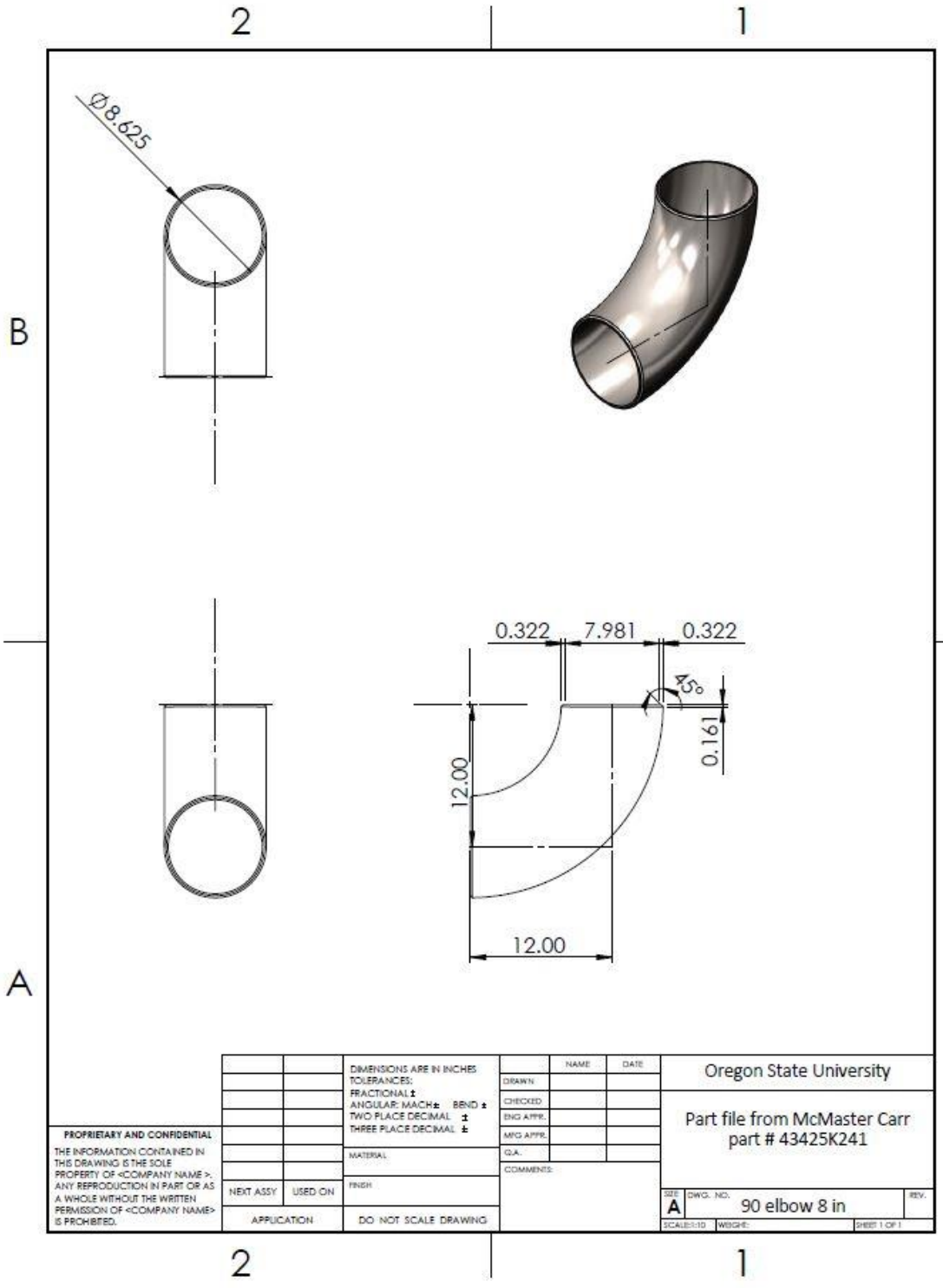
2
1
B
A
Ø8.625
0.322
7.981
0.322
45°
0.161
12.00
12.00
PROPRIETARY AND CONFIDENTIAL
THE INFORMATION CONTAINED IN THIS DRAWING IS THE SOLE PROPERTY OF <COMPANY NAME >. ANY REPRODUCTION IN PART OR AS A WHOLE WITHOUT THE WRITTEN PERMISSION OF <COMPANY NAME> IS PROHIBITED.
NEXT ASSY
USED ON
APPLICATION
DIMENSIONS ARE IN INCHES
TOLERANCES:
FRACTIONAL ±
ANGULAR: MACH ± BEND ±
TWO PLACE DECIMAL ±
THREE PLACE DECIMAL ±
MATERIAL
FINISH
DO NOT SCALE DRAWING
NAME
DATE
DRAWN
CHECKED
ENG APPR.
MFG APPR.
Q.A.
COMMENTS:
Oregon State University
Part file from McMaster Carr
part # 43425K241
SIZE
A
DWG. NO.
90 elbow 8 in
REV.
SCALE:1:10
WEIGHT:
SHEET 1 OF 1

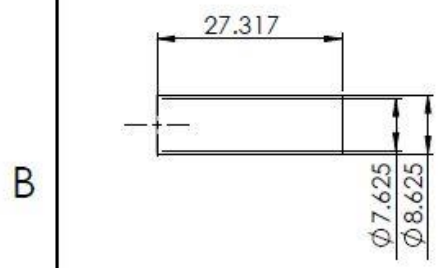

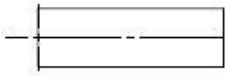

		DIMENSIONS ARE IN INCHES TOLERANCES: FRACTIONAL ± ANGULAR: MACH ± BEND ± TWO PLACE DECIMAL ± THREE PLACE DECIMAL ±		NAME	DATE	Oregon State University
			DRAWN			
			CHECKED			Original work by Grant C. Blake
			ENG APPR.			
			MFG APPR.			
		MATERIAL	Q.A.			
			COMMENTS:			
NEXT ASSY	USED ON	FINISH				SIZE A DWG. NO. Direct inlet horizontal pipe REV.
APPLICATION		DO NOT SCALE DRAWING				SCALE:1:10 WEIGHT: SHEET 1 OF 1

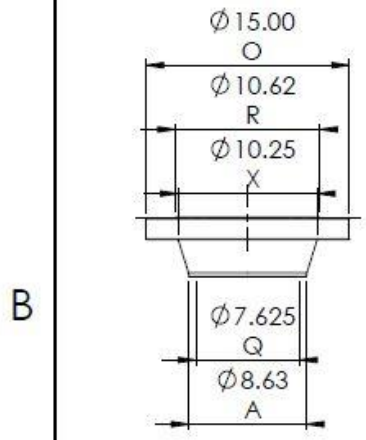

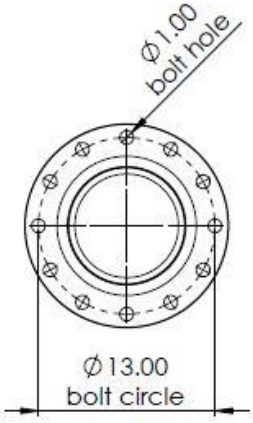

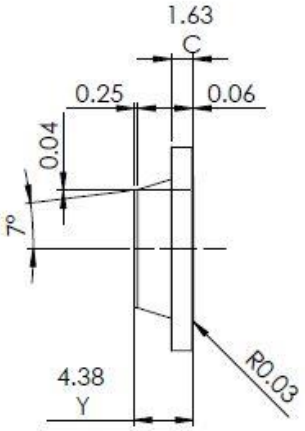

		DIMENSIONS ARE IN INCHES TOLERANCES: FRACTIONAL ± ANGULAR: MACH ± BEND ± TWO PLACE DECIMAL ± THREE PLACE DECIMAL ±		NAME	DATE
			DRAWN		
			CHECKED		
			ENG APPR.		
			MFG APPR.		
			Q.A.		
		MATERIAL	COMMENTS:		
NEXT ASSY	USED ON	FINISH			
APPLICATION		DO NOT SCALE DRAWING			

Oregon State University

Part file from McMaster Carr
part # 6806K253

SIZE	DWG. NO.	REV.
A	Flange 8 in	
SCALE:1:5	WEIGHT:	SHEET 1 OF 1

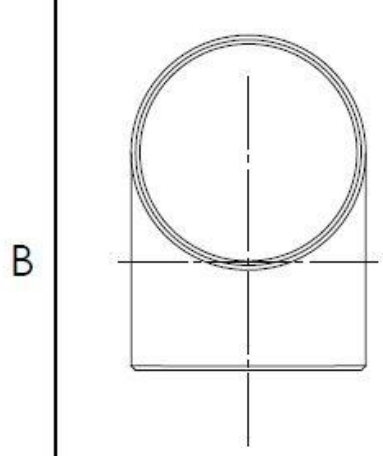

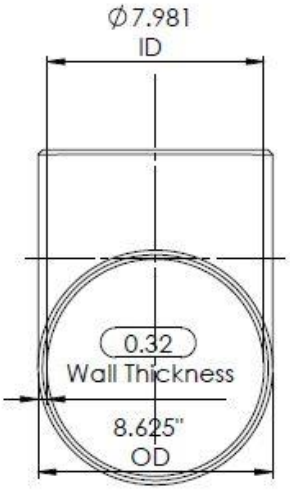

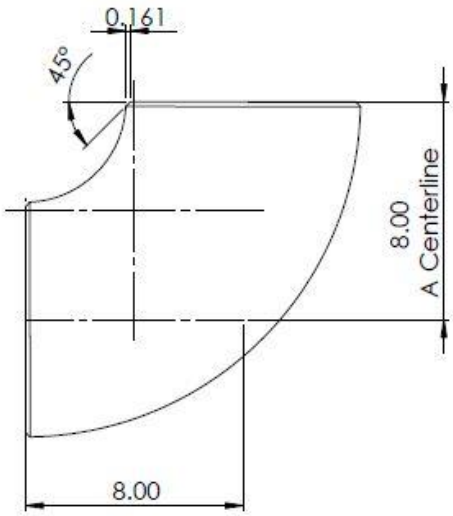

		DIMENSIONS ARE IN INCHES TOLERANCES: FRACTIONAL ± ANGULAR: MACH ± BEND ± TWO PLACE DECIMAL ± THREE PLACE DECIMAL ±		NAME / DATE	Oregon State University
			DRAWN		
			CHECKED		Part file from McMaster Carr part # 43425K247
			ENG APPR.		
			MFG APPR.		
			Q.A.		
		MATERIAL	COMMENTS:		
NEXT ASSY	USED ON	FINISH			SIZE A — DWG. NO. 90 elbow 8 in short — REV.
APPLICATION		DO NOT SCALE DRAWING			SCALE:1:5 — WEIGHT: — SHEET 1 OF 1

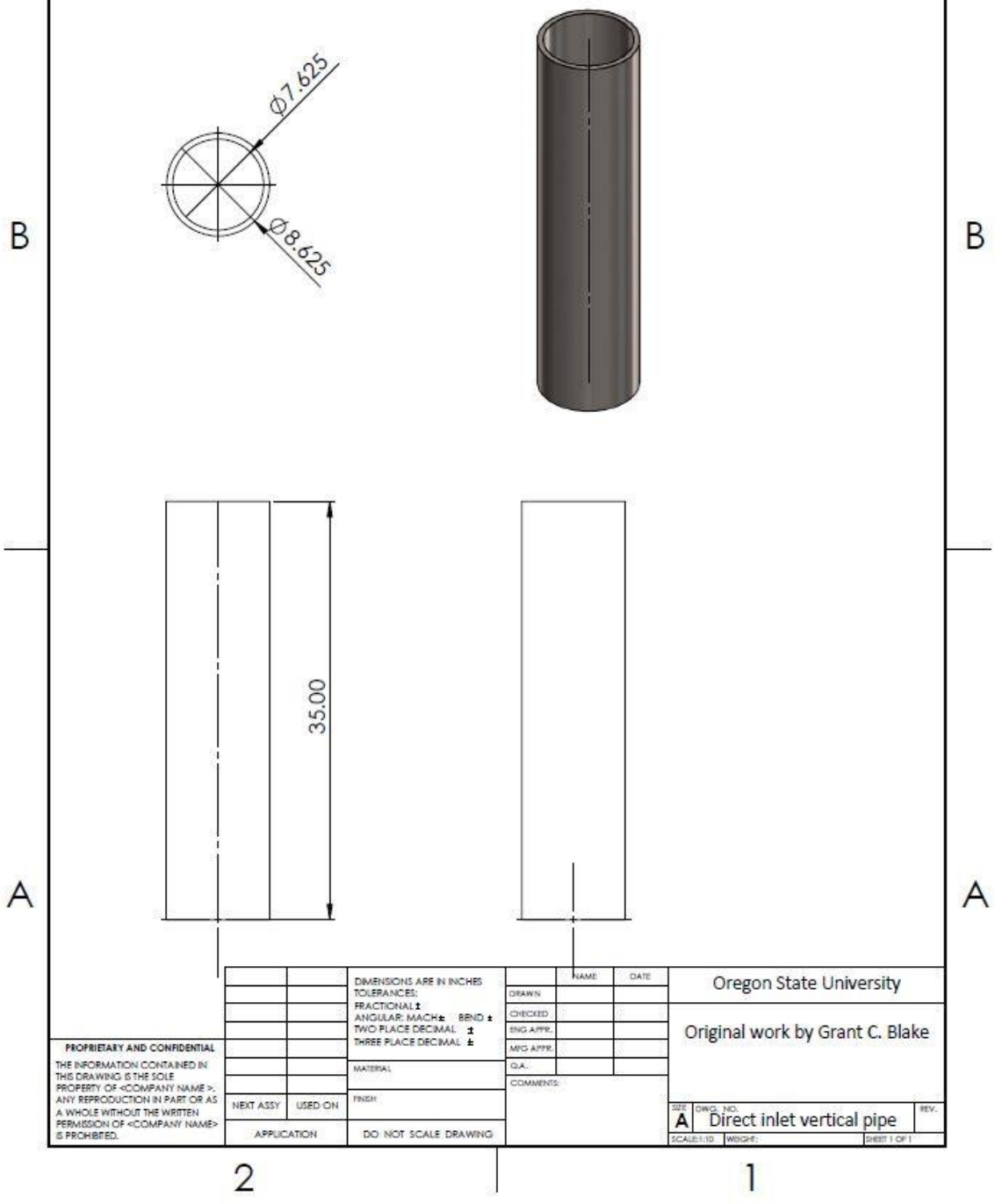
2
1
B
B
A
A
Ø7.625
Ø8.625
35.00
PROPRIETARY AND CONFIDENTIAL
THE INFORMATION CONTAINED IN THIS DRAWING IS THE SOLE PROPERTY OF <COMPANY NAME >. ANY REPRODUCTION IN PART OR AS A WHOLE WITHOUT THE WRITTEN PERMISSION OF <COMPANY NAME> IS PROHIBITED.
NEXT ASSY
USED ON
APPLICATION
DIMENSIONS ARE IN INCHES
TOLERANCES:
FRACTIONAL ±
ANGULAR: MACH ± BEND ±
TWO PLACE DECIMAL ±
THREE PLACE DECIMAL ±
MATERIAL
FINISH
DO NOT SCALE DRAWING
NAME
DATE
DRAWN
CHECKED
ENG APPR.
MFG APPR.
Q.A.
COMMENTS:
Oregon State University
Original work by Grant C. Blake
SIZE
A
DWG. NO.
Direct inlet vertical pipe
REV.
SCALE:1:10
WEIGHT:
SHEET 1 OF 1

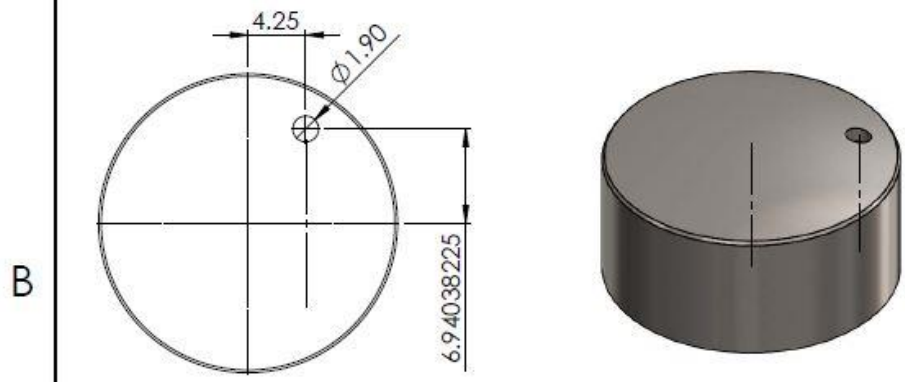

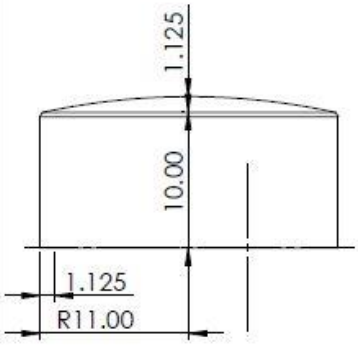

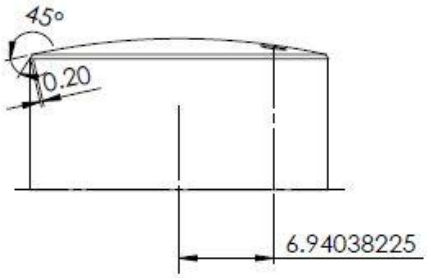

		DIMENSIONS ARE IN INCHES TOLERANCES: FRACTIONAL ± ANGULAR: MACH ± BEND ± TWO PLACE DECIMAL ± THREE PLACE DECIMAL ±		NAME	DATE
			DRAWN		
			CHECKED		
			ENG APPR.		
			MFG APPR.		
		MATERIAL	Q.A.		
			COMMENTS:		
NEXT ASSY	USED ON	FINISH			
APPLICATION		DO NOT SCALE DRAWING			

PROPRIETARY AND CONFIDENTIAL

THE INFORMATION CONTAINED IN THIS DRAWING IS THE SOLE PROPERTY OF <COMPANY NAME >. ANY REPRODUCTION IN PART OR AS A WHOLE WITHOUT THE WRITTEN PERMISSION OF <COMPANY NAME> IS PROHIBITED.

Oregon State University

Original work by Grant C. Blake

SIZE	DWG. NO.	REV.
A	Direct loop plenum	
SCALE:1:10	WEIGHT:	SHEET 1 OF 1

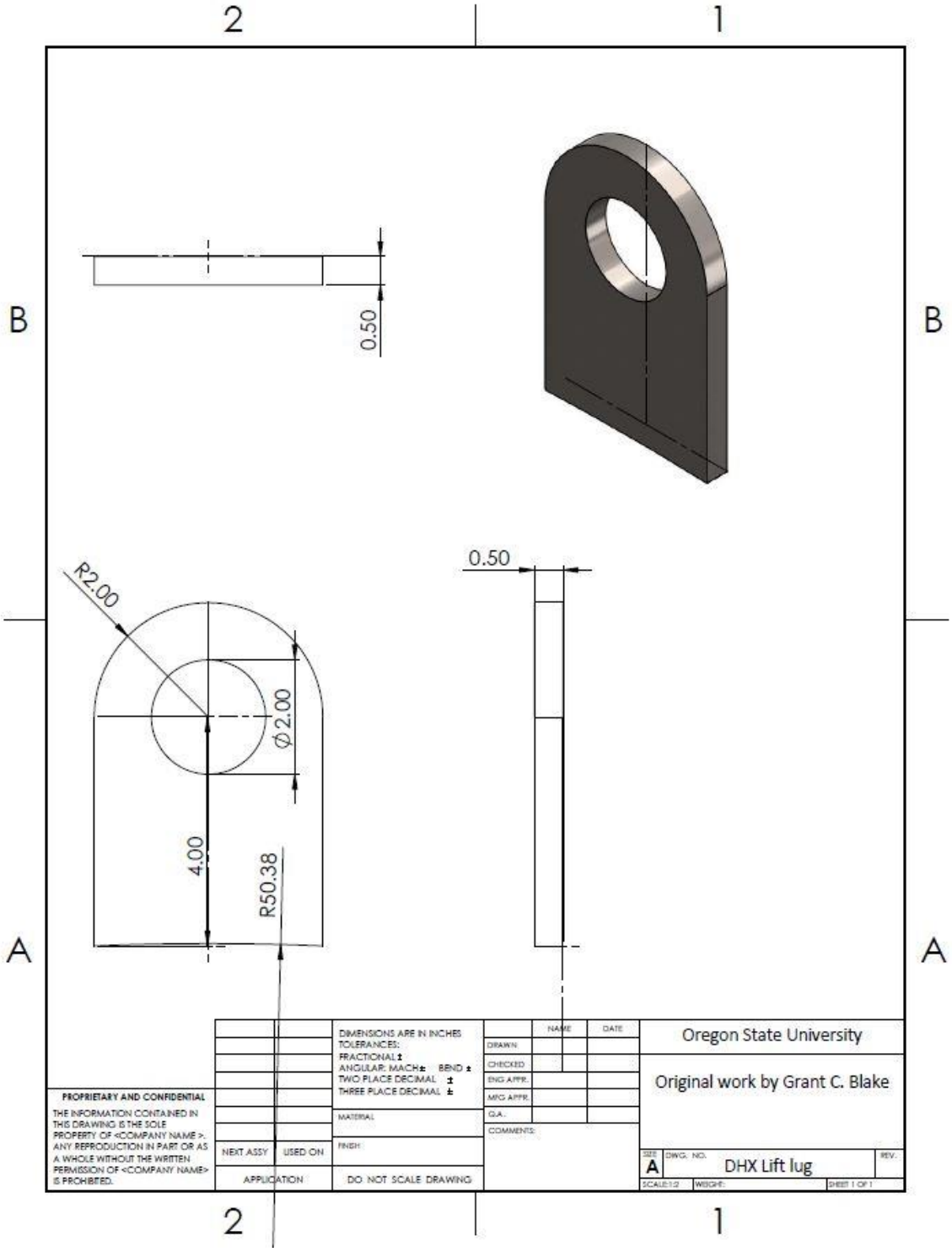
2
1
B
B
0.50
R2.00
Ø2.00
4.00
R50.38
0.50
A
A
2
1
PROPRIETARY AND CONFIDENTIAL
THE INFORMATION CONTAINED IN THIS DRAWING IS THE SOLE PROPERTY OF <COMPANY NAME >. ANY REPRODUCTION IN PART OR AS A WHOLE WITHOUT THE WRITTEN PERMISSION OF <COMPANY NAME> IS PROHIBITED.
DIMENSIONS ARE IN INCHES
TOLERANCES:
FRACTIONAL ±
ANGULAR: MACH ± BEND ±
TWO PLACE DECIMAL ±
THREE PLACE DECIMAL ±
MATERIAL
FINISH
DO NOT SCALE DRAWING
NAME
DATE
DRAWN
CHECKED
ENG APPR.
MFG APPR.
Q.A.
COMMENTS:
NEXT ASSY
USED ON
APPLICATION
Oregon State University
Original work by Grant C. Blake
SIZE A
DWG. NO.
DHX Lift lug
REV.
SCALE:1:2
WEIGHT:
SHEET 1 OF 1

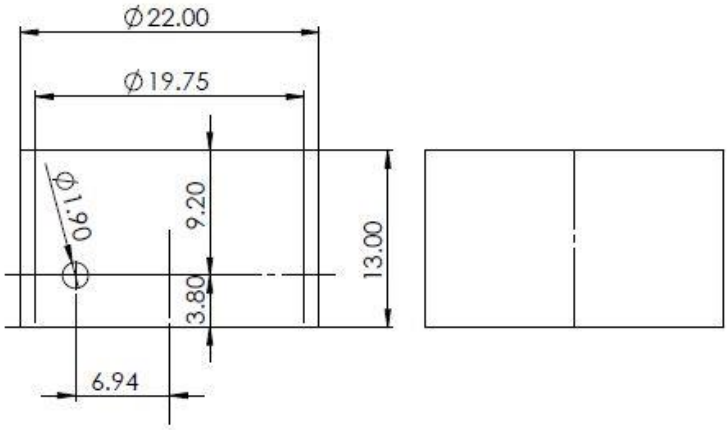

		DIMENSIONS ARE IN INCHES TOLERANCES: FRACTIONAL ± ANGULAR: MACH ± BEND ± TWO PLACE DECIMAL ± THREE PLACE DECIMAL ±		NAME	DATE
			DRAWN		
			CHECKED		
			ENG APPR.		
			MFG APPR.		
			Q.A.		
		MATERIAL	COMMENTS:		
NEXT ASSY	USED ON	FINISH			
APPLICATION		DO NOT SCALE DRAWING			

Oregon State University

Original work by Grant C. Blake

SIZE	DWG. NO.	REV.
A	Direct flow over DHX	
SCALE:1:10	WEIGHT:	SHEET 1 OF 1

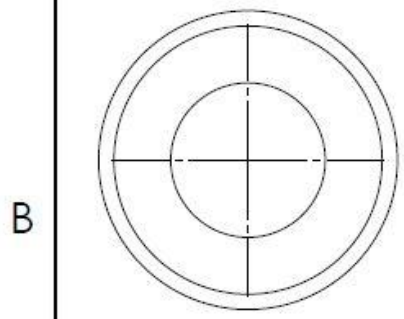

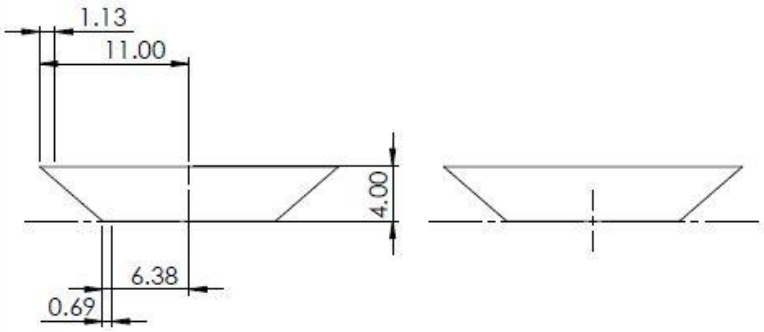

		DIMENSIONS ARE IN INCHES TOLERANCES: FRACTIONAL ± ANGULAR: MACH ± BEND ± TWO PLACE DECIMAL ± THREE PLACE DECIMAL ±		NAME	DATE
			DRAWN		
			CHECKED		
			ENG APPR.		
			MFG APPR.		
		MATERIAL	Q.A.		
			COMMENTS:		
NEXT ASSY	USED ON	FINISH			
APPLICATION		DO NOT SCALE DRAWING			

Oregon State University

Original work by Grant C. Blake

SIZE	DWG. NO.	REV.
A	Direct outlet reducer 1	
SCALE:1:10	WEIGHT:	SHEET 1 OF 1

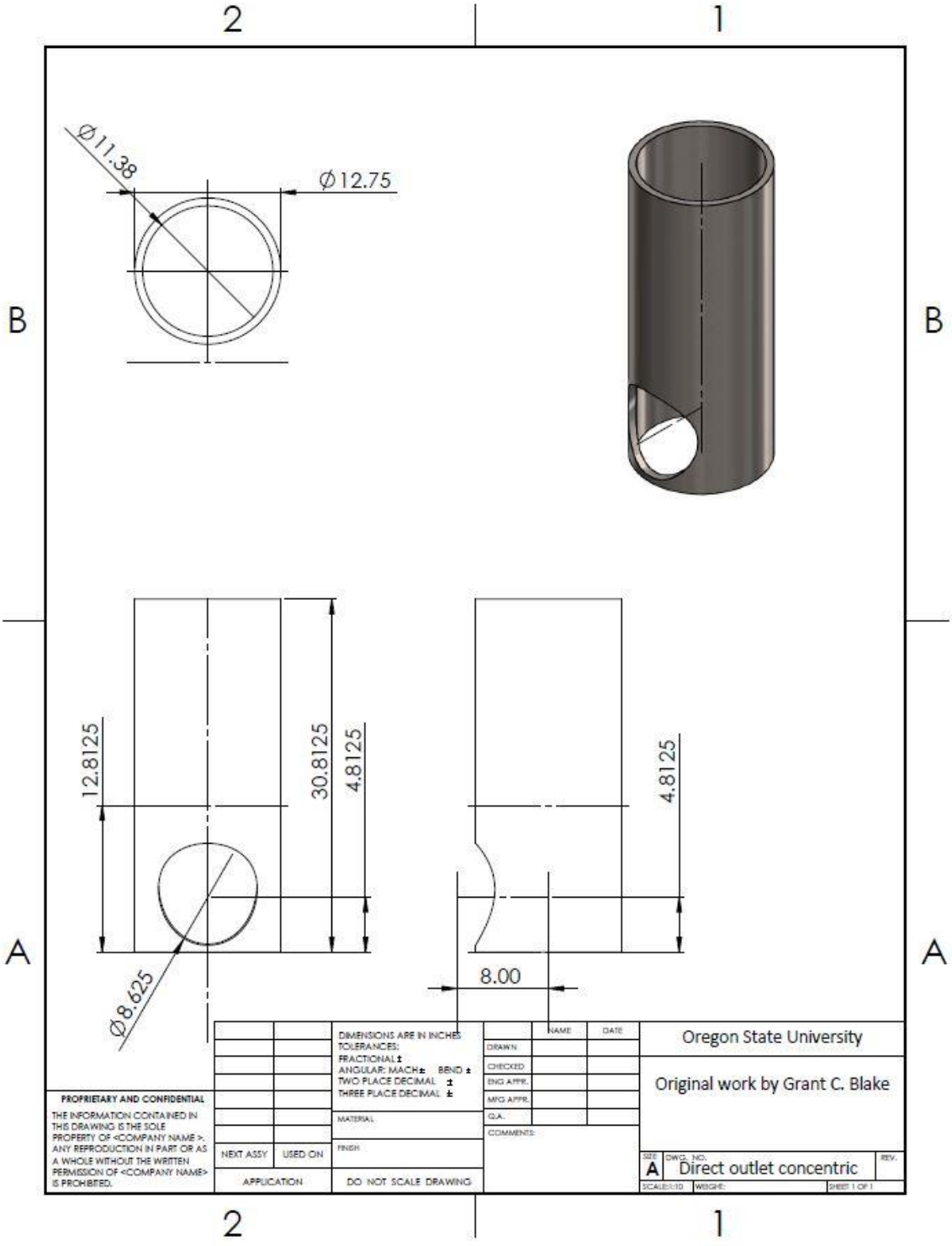
2
1
B
A
Ø11.38
Ø12.75
12.8125
30.8125
4.8125
4.8125
8.00
Ø8.625
PROPRIETARY AND CONFIDENTIAL
THE INFORMATION CONTAINED IN THIS DRAWING IS THE SOLE PROPERTY OF <COMPANY NAME >. ANY REPRODUCTION IN PART OR AS A WHOLE WITHOUT THE WRITTEN PERMISSION OF <COMPANY NAME> IS PROHIBITED.
NEXT ASSY
USED ON
APPLICATION
DIMENSIONS ARE IN INCHES
TOLERANCES:
FRACTIONAL ±
ANGULAR: MACH ± BEND ±
TWO PLACE DECIMAL ±
THREE PLACE DECIMAL ±
MATERIAL
FINISH
DO NOT SCALE DRAWING
NAME
DATE
DRAWN
CHECKED
ENG APPR.
MFG APPR.
Q.A.
COMMENTS:
Oregon State University
Original work by Grant C. Blake
SIZE
A
DWG. NO.
Direct outlet concentric
REV.
SCALE:1:10
WEIGHT:
SHEET 1 OF 1

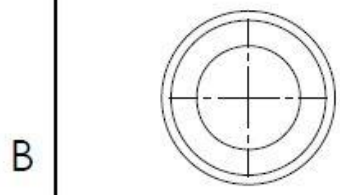

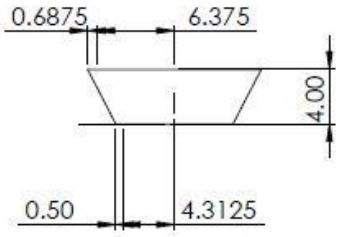

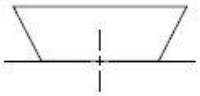

		DIMENSIONS ARE IN INCHES TOLERANCES: FRACTIONAL ± ANGULAR: MACH ± BEND ± TWO PLACE DECIMAL ± THREE PLACE DECIMAL ±		NAME	DATE
			DRAWN		
			CHECKED		
			ENG APPR.		
			MFG APPR.		
			Q.A.		
		MATERIAL	COMMENTS:		
NEXT ASSY	USED ON	FINISH			
APPLICATION		DO NOT SCALE DRAWING			

Oregon State University

Original work by Grant C. Blake

SIZE	DWG. NO.	REV.
A	Direct outlet reducer 2	
SCALE:1:10	WEIGHT:	SHEET 1 OF 1

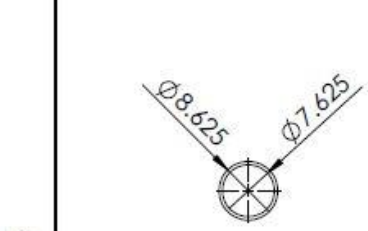

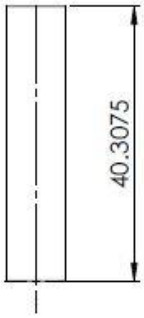

		DIMENSIONS ARE IN INCHES TOLERANCES: FRACTIONAL ± ANGULAR: MACH ± BEND ± TWO PLACE DECIMAL ± THREE PLACE DECIMAL ±		NAME	DATE
			DRAWN		
			CHECKED		
			ENG APPR.		
			MFG APPR.		
			Q.A.		
		MATERIAL	COMMENTS:		
NEXT ASSY	USED ON	FINISH			
APPLICATION		DO NOT SCALE DRAWING			

Oregon State University

Original work by Grant C. Blake

SIZE A | DWG. NO. Direct outlet vertical pipe | REV.

SCALE:1:10 | WEIGHT: | SHEET 1 OF 1

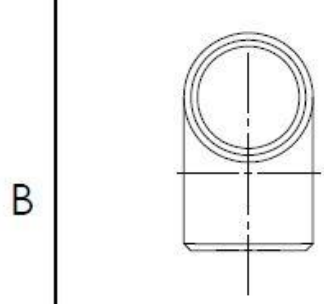

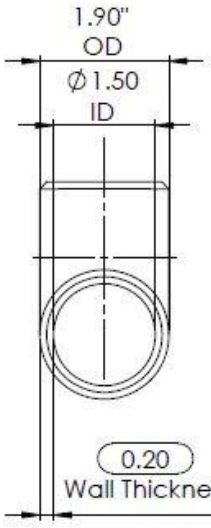

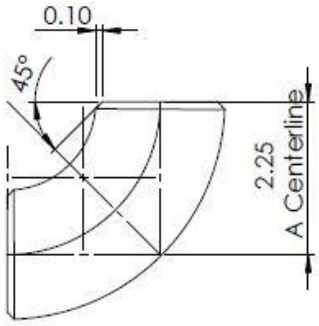

		DIMENSIONS ARE IN INCHES TOLERANCES: FRACTIONAL ± ANGULAR: MACH ± BEND ± TWO PLACE DECIMAL ± THREE PLACE DECIMAL ±		NAME / DATE	Oregon State University
			DRAWN		
			CHECKED		Part file from McMaster Carr part # 1739K12
			ENG APPR.		
			MFG APPR.		
			Q.A.		
		MATERIAL	COMMENTS:		
NEXT ASSY	USED ON	FINISH			SIZE A · DWG. NO. 90 elbow 1.5 in · REV.
APPLICATION		DO NOT SCALE DRAWING			SCALE: 1:2 · WEIGHT: · SHEET 1 OF 1

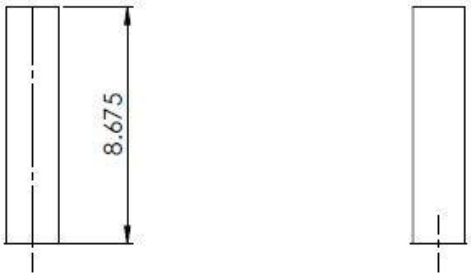

		DIMENSIONS ARE IN INCHES TOLERANCES: FRACTIONAL ± ANGULAR: MACH ± BEND ± TWO PLACE DECIMAL ± THREE PLACE DECIMAL ±		NAME	DATE
			DRAWN		
			CHECKED		
			ENG APPR.		
			MFG APPR.		
			QA:		
		MATERIAL	COMMENTS:		
NEXT ASSY	USED ON	FINISH			
APPLICATION		DO NOT SCALE DRAWING			

PROPRIETARY AND CONFIDENTIAL

THE INFORMATION CONTAINED IN THIS DRAWING IS THE SOLE PROPERTY OF <COMPANY NAME >. ANY REPRODUCTION IN PART OR AS A WHOLE WITHOUT THE WRITTEN PERMISSION OF <COMPANY NAME> IS PROHIBITED.

Oregon State University

Original work by Grant C. Blake

SIZE A | DWG. NO. Int. DHX outlet riser pipe | REV.

SCALE:1:2 | WEIGHT: | SHEET 1 OF 1

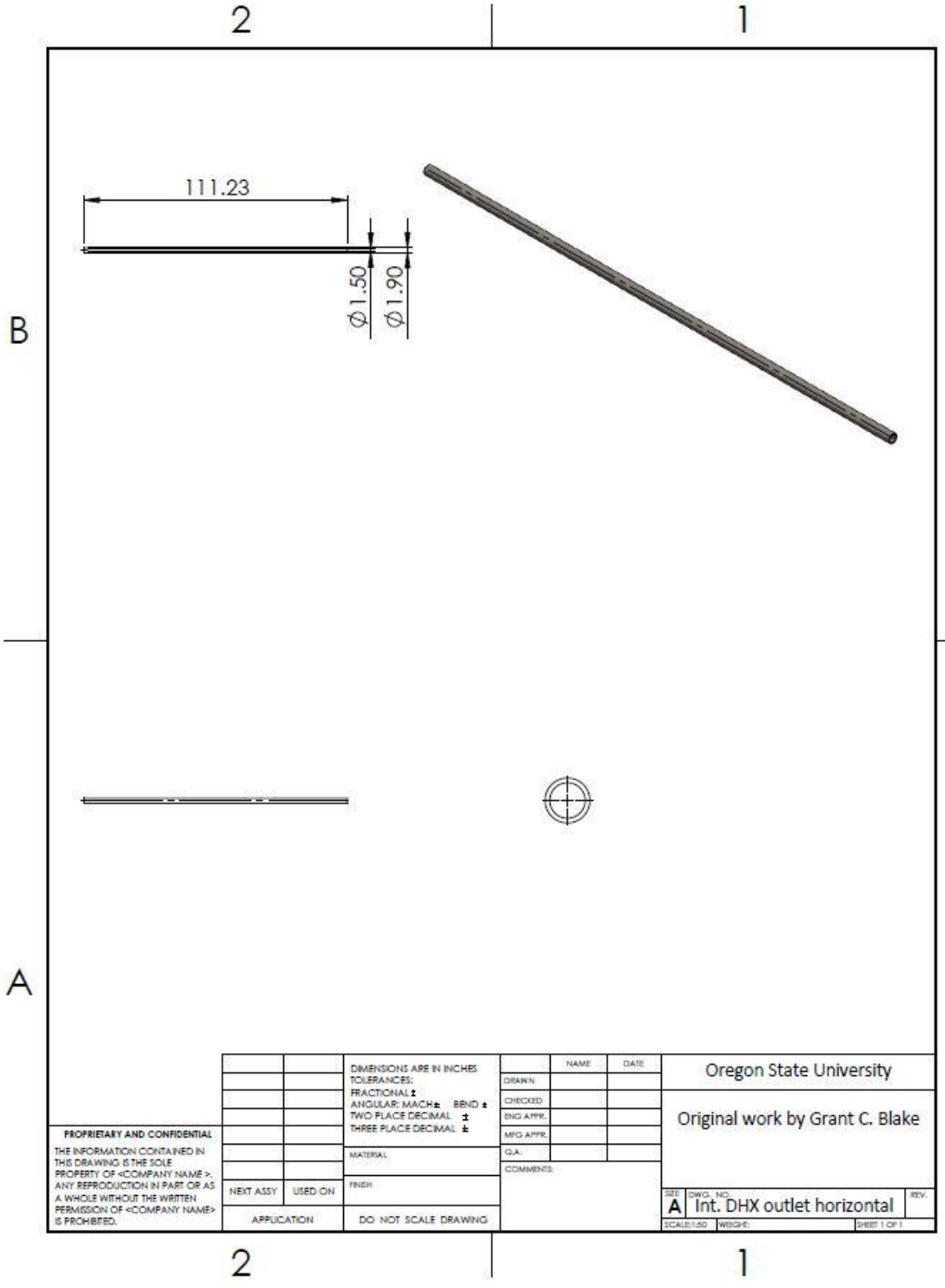
2
1
B
A
111.23
Ø1.50
Ø1.90
PROPRIETARY AND CONFIDENTIAL
THE INFORMATION CONTAINED IN THIS DRAWING IS THE SOLE PROPERTY OF <COMPANY NAME >. ANY REPRODUCTION IN PART OR AS A WHOLE WITHOUT THE WRITTEN PERMISSION OF <COMPANY NAME> IS PROHIBITED.
NEXT ASSY
USED ON
APPLICATION
DIMENSIONS ARE IN INCHES
TOLERANCES:
FRACTIONAL ±
ANGULAR: MACH ± BEND ±
TWO PLACE DECIMAL ±
THREE PLACE DECIMAL ±
MATERIAL
FINISH
DO NOT SCALE DRAWING
NAME
DATE
DRAWN
CHECKED
ENG APPR.
MFG APPR.
Q.A.
COMMENTS:
Oregon State University
Original work by Grant C. Blake
SIZE
A
DWG. NO.
Int. DHX outlet horizontal
REV.
SCALE:1:50
WEIGHT:
SHEET 1 OF 1

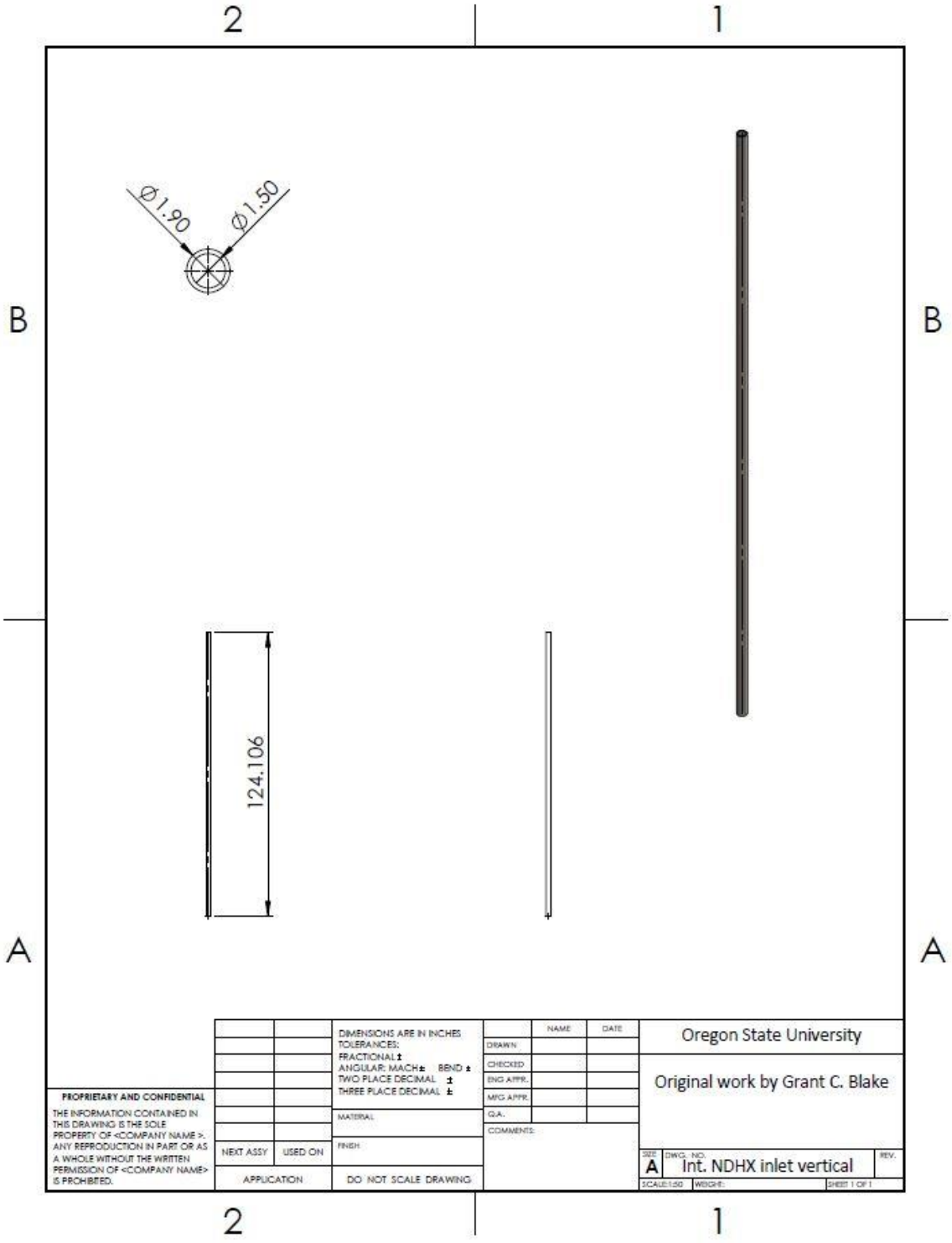

		DIMENSIONS ARE IN INCHES TOLERANCES: FRACTIONAL ± ANGULAR: MACH ± BEND ± TWO PLACE DECIMAL ± THREE PLACE DECIMAL ±		NAME	DATE
			DRAWN		
			CHECKED		
			ENG APPR.		
			MFG APPR.		
			Q.A.		
		MATERIAL	COMMENTS:		
NEXT ASSY	USED ON	FINISH			
APPLICATION		DO NOT SCALE DRAWING			

Oregon State University

Original work by Grant C. Blake

SIZE	DWG. NO.	REV.
A	Int. NDHX inlet vertical	
SCALE: 1:50	WEIGHT:	SHEET 1 OF 1

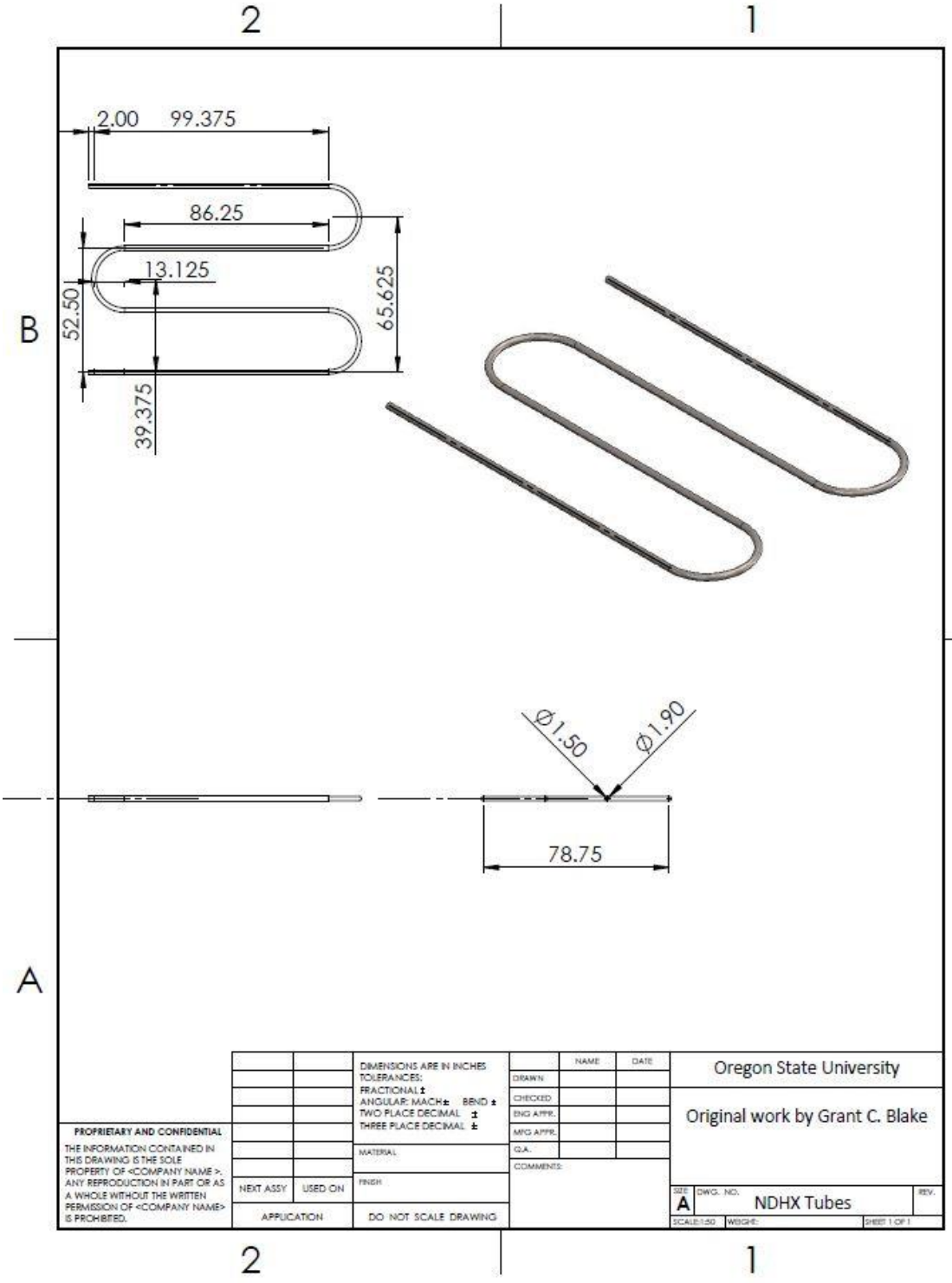

		DIMENSIONS ARE IN INCHES TOLERANCES: FRACTIONAL ± ANGULAR: MACH ± BEND ± TWO PLACE DECIMAL ± THREE PLACE DECIMAL ±		NAME	DATE
			DRAWN		
			CHECKED		
			ENG APPR.		
			MFG APPR.		
			Q.A.		
		MATERIAL	COMMENTS:		
NEXT ASSY	USED ON	FINISH			
APPLICATION		DO NOT SCALE DRAWING			

Oregon State University

Original work by Grant C. Blake

SIZE	DWG. NO.	REV.
A	NDHX Tubes	
SCALE:1:50	WEIGHT:	SHEET 1 OF 1

		DIMENSIONS ARE IN INCHES TOLERANCES: FRACTIONAL ± ANGULAR: MACH ± BEND ± TWO PLACE DECIMAL ± THREE PLACE DECIMAL ±		NAME	DATE
			DRAWN		
			CHECKED		
			ENG APPR.		
			MFG APPR.		
			Q.A.		
		MATERIAL	COMMENTS:		
NEXT ASSY	USED ON	FINISH			
APPLICATION		DO NOT SCALE DRAWING			

Oregon State University

Original work by Grant C. Blake

SIZE	DWG. NO.	REV.
A	NDHX fins	
SCALE:1:50	WEIGHT:	SHEET 1 OF 1

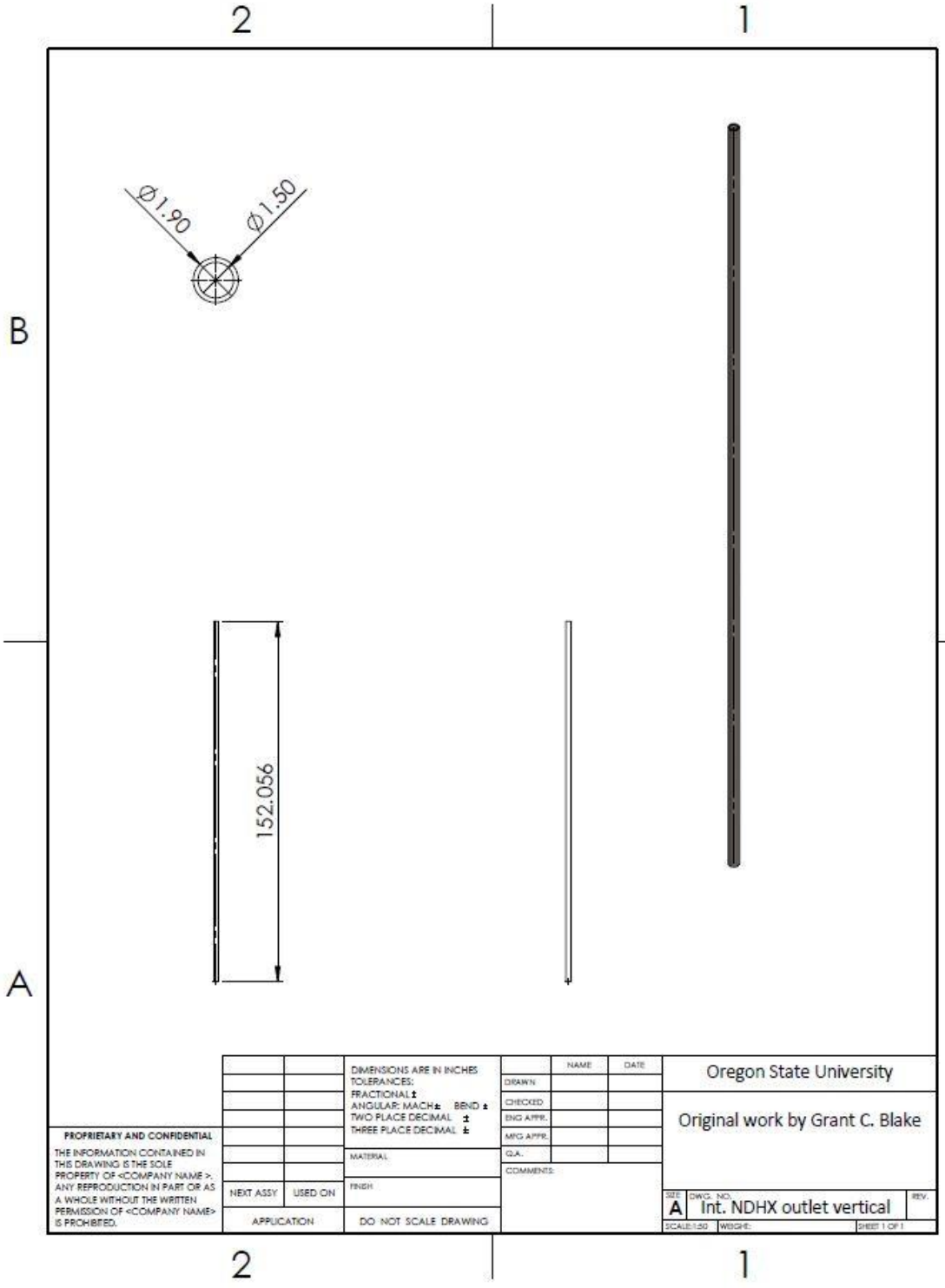
2
1
B
A
Ø1.90
Ø1.50
152.056
PROPRIETARY AND CONFIDENTIAL
THE INFORMATION CONTAINED IN THIS DRAWING IS THE SOLE PROPERTY OF <COMPANY NAME >. ANY REPRODUCTION IN PART OR AS A WHOLE WITHOUT THE WRITTEN PERMISSION OF <COMPANY NAME> IS PROHIBITED.
NEXT ASSY
USED ON
APPLICATION
DIMENSIONS ARE IN INCHES
TOLERANCES:
FRACTIONAL ±
ANGULAR: MACH ± BEND ±
TWO PLACE DECIMAL ±
THREE PLACE DECIMAL ±
MATERIAL
FINISH
DO NOT SCALE DRAWING
NAME
DATE
DRAWN
CHECKED
ENG APPR.
MFG APPR.
Q.A.
COMMENTS:
Oregon State University
Original work by Grant C. Blake
SIZE A
DWG. NO. Int. NDHX outlet vertical
REV.
SCALE:1:50
WEIGHT:
SHEET 1 OF 1

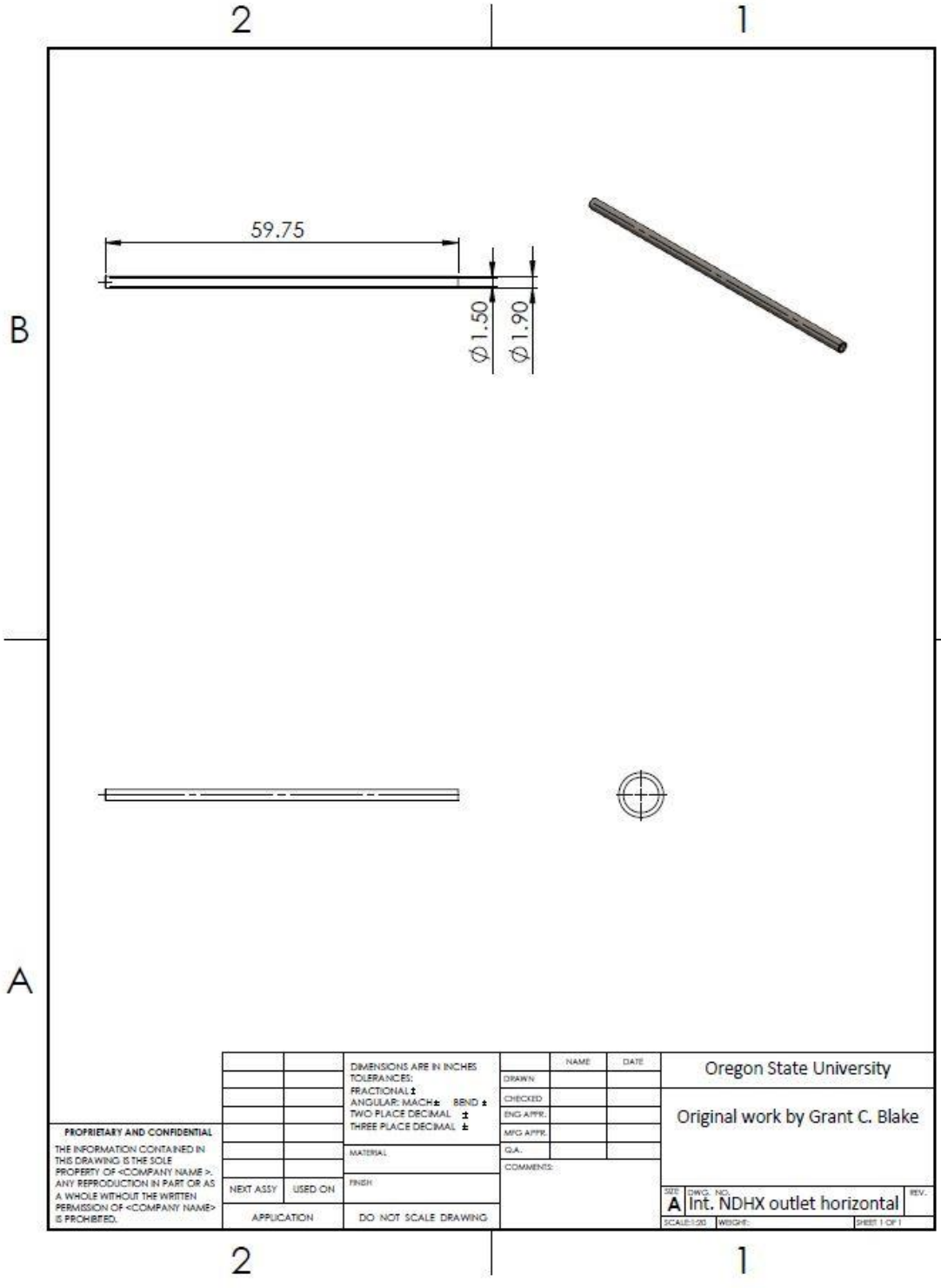

		DIMENSIONS ARE IN INCHES TOLERANCES: FRACTIONAL ± ANGULAR: MACH ± BEND ± TWO PLACE DECIMAL ± THREE PLACE DECIMAL ±		NAME	DATE
			DRAWN		
			CHECKED		
			ENG APPR.		
			MFG APPR.		
		MATERIAL	Q.A.		
			COMMENTS:		
NEXT ASSY	USED ON	FINISH			
APPLICATION		DO NOT SCALE DRAWING			

Oregon State University

Original work by Grant C. Blake

SIZE	DWG. NO.	REV.
A	Int. NDHX outlet horizontal	
SCALE:1:20	WEIGHT:	SHEET 1 OF 1

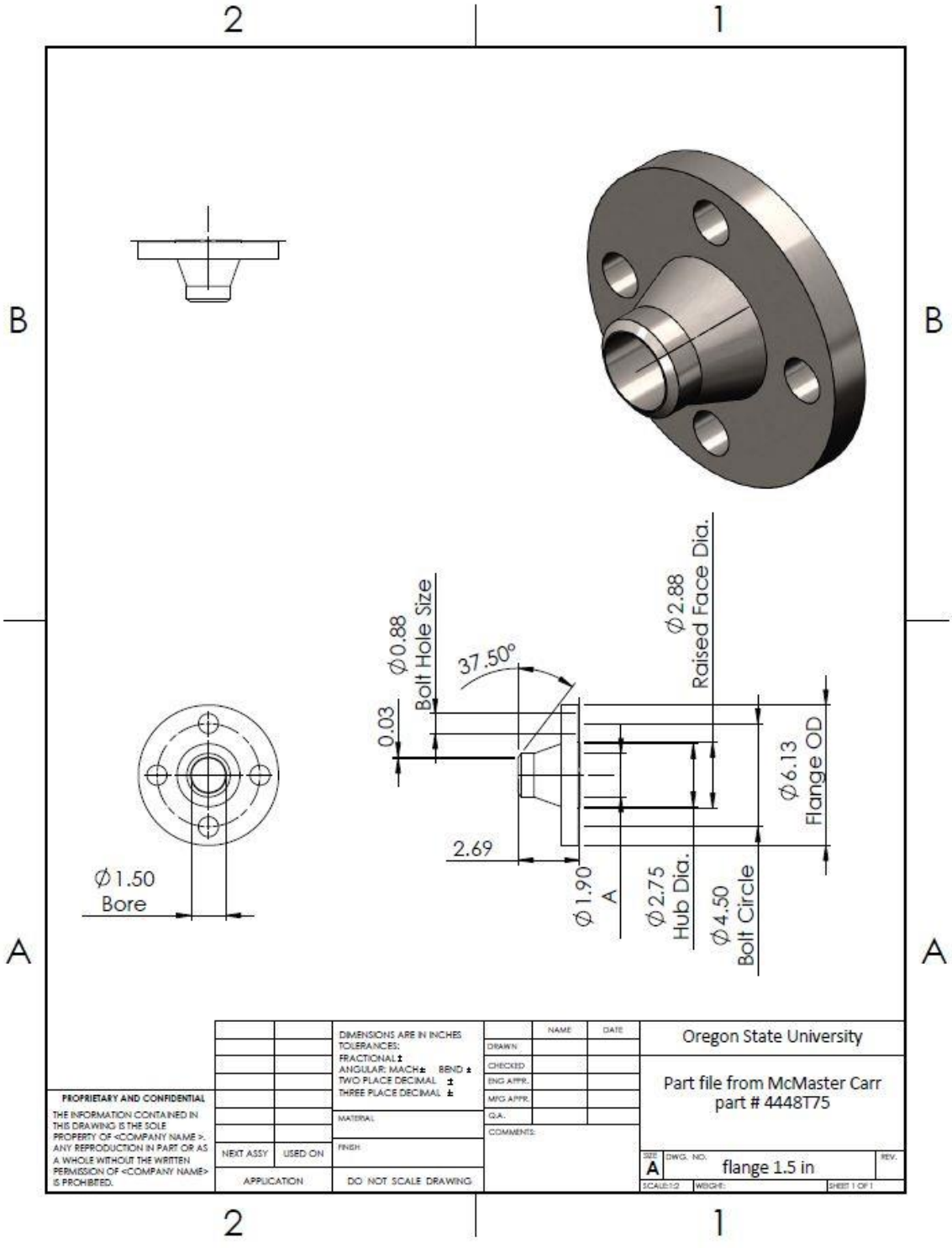
2
1
B
A
Ø0.88
Bolt Hole Size
37.50°
Ø2.88
Raised Face Dia.
0.03
Ø6.13
Flange OD
2.69
Ø1.90
A
Ø2.75
Hub Dia.
Ø4.50
Bolt Circle
Ø1.50
Bore
PROPRIETARY AND CONFIDENTIAL
THE INFORMATION CONTAINED IN THIS DRAWING IS THE SOLE PROPERTY OF <COMPANY NAME >. ANY REPRODUCTION IN PART OR AS A WHOLE WITHOUT THE WRITTEN PERMISSION OF <COMPANY NAME> IS PROHIBITED.
NEXT ASSY
USED ON
APPLICATION
DIMENSIONS ARE IN INCHES
TOLERANCES:
FRACTIONAL ±
ANGULAR: MACH ± BEND ±
TWO PLACE DECIMAL ±
THREE PLACE DECIMAL ±
MATERIAL
FINISH
DO NOT SCALE DRAWING
NAME
DATE
DRAWN
CHECKED
ENG APPR.
MFG APPR.
Q.A.
COMMENTS:
Oregon State University
Part file from McMaster Carr
part # 4448T75
SIZE
A
DWG. NO.
flange 1.5 in
REV.
SCALE:1:2
WEIGHT:
SHEET 1 OF 1

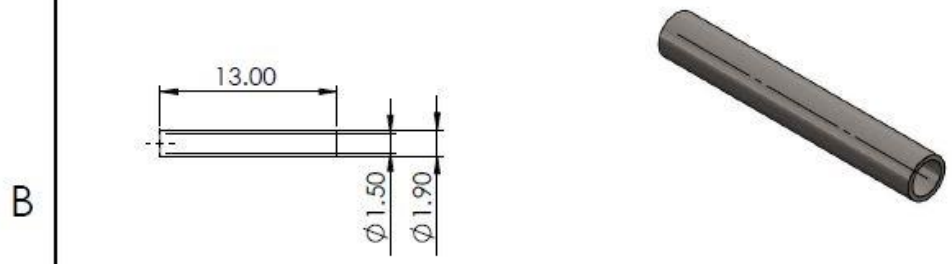

		DIMENSIONS ARE IN INCHES TOLERANCES: FRACTIONAL ± ANGULAR: MACH ± BEND ± TWO PLACE DECIMAL ± THREE PLACE DECIMAL ±		NAME	DATE	Oregon State University
			DRAWN			
			CHECKED			Original work by Grant C. Blake
			ENG APPR.			
			MFG APPR.			
			Q.A.			
		MATERIAL	COMMENTS:			
NEXT ASSY	USED ON	FINISH				SIZE A DWG. NO. Int. DHX inlet horizontal REV.
APPLICATION		DO NOT SCALE DRAWING				SCALE:1:5 WEIGHT: SHEET 1 OF 1

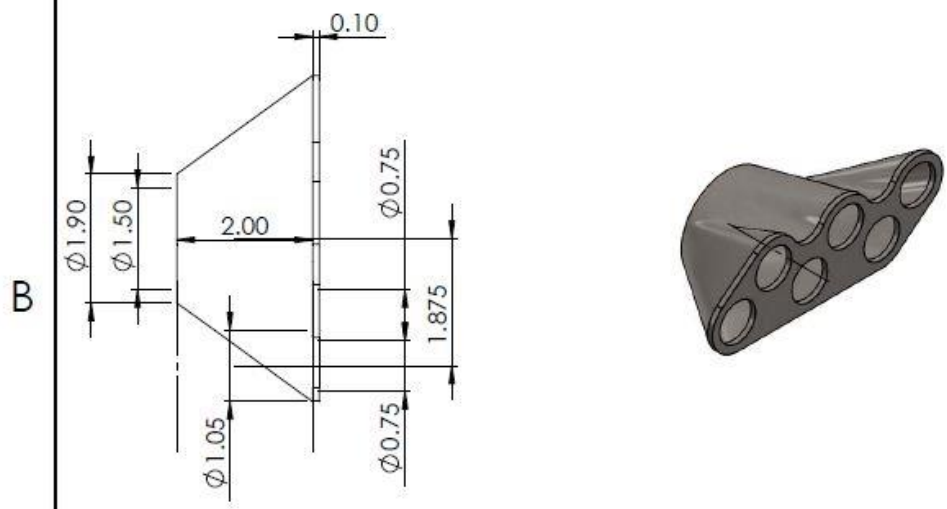

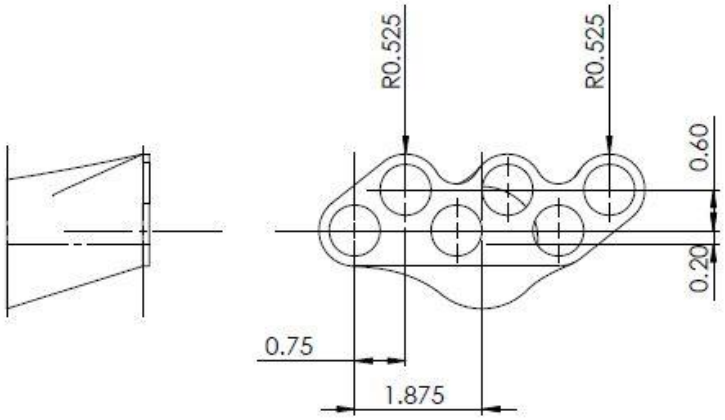

		DIMENSIONS ARE IN INCHES TOLERANCES: FRACTIONAL ± ANGULAR: MACH ± BEND ± TWO PLACE DECIMAL ± THREE PLACE DECIMAL ±		NAME	DATE	Oregon State University
			DRAWN			
			CHECKED			Original work by Grant C. Blake
			ENG APPR.			
			MFG APPR.			
			Q.A.			
		MATERIAL	COMMENTS:			
		FINISH				SIZE A — DWG. NO. DHX inlet manifold — REV.
NEXT ASSY	USED ON					
APPLICATION		DO NOT SCALE DRAWING				SCALE:1:2 — WEIGHT: — SHEET 1 OF 1

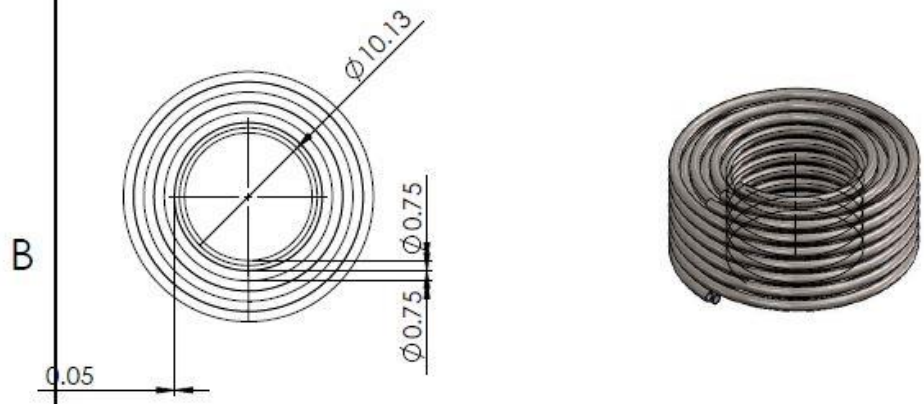

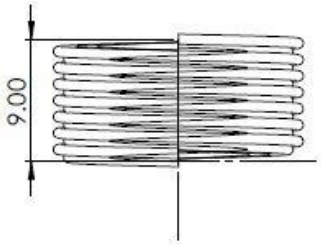

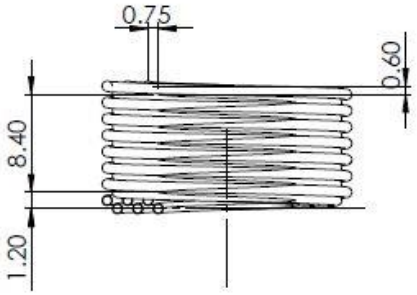

		DIMENSIONS ARE IN INCHES TOLERANCES: FRACTIONAL ± ANGULAR: MACH ± BEND ± TWO PLACE DECIMAL ± THREE PLACE DECIMAL ±		NAME	DATE
			DRAWN		
			CHECKED		
			ENG APPR.		
			MFG APPR.		
			Q.A.		
		MATERIAL	COMMENTS:		
NEXT ASSY	USED ON	FINISH			
APPLICATION		DO NOT SCALE DRAWING			

Oregon State University

Original work by Grant C. Blake

SIZE A | DWG. NO. Helical coil tube bundle | REV.

SCALE:1:10 | WEIGHT: | SHEET 1 OF 1

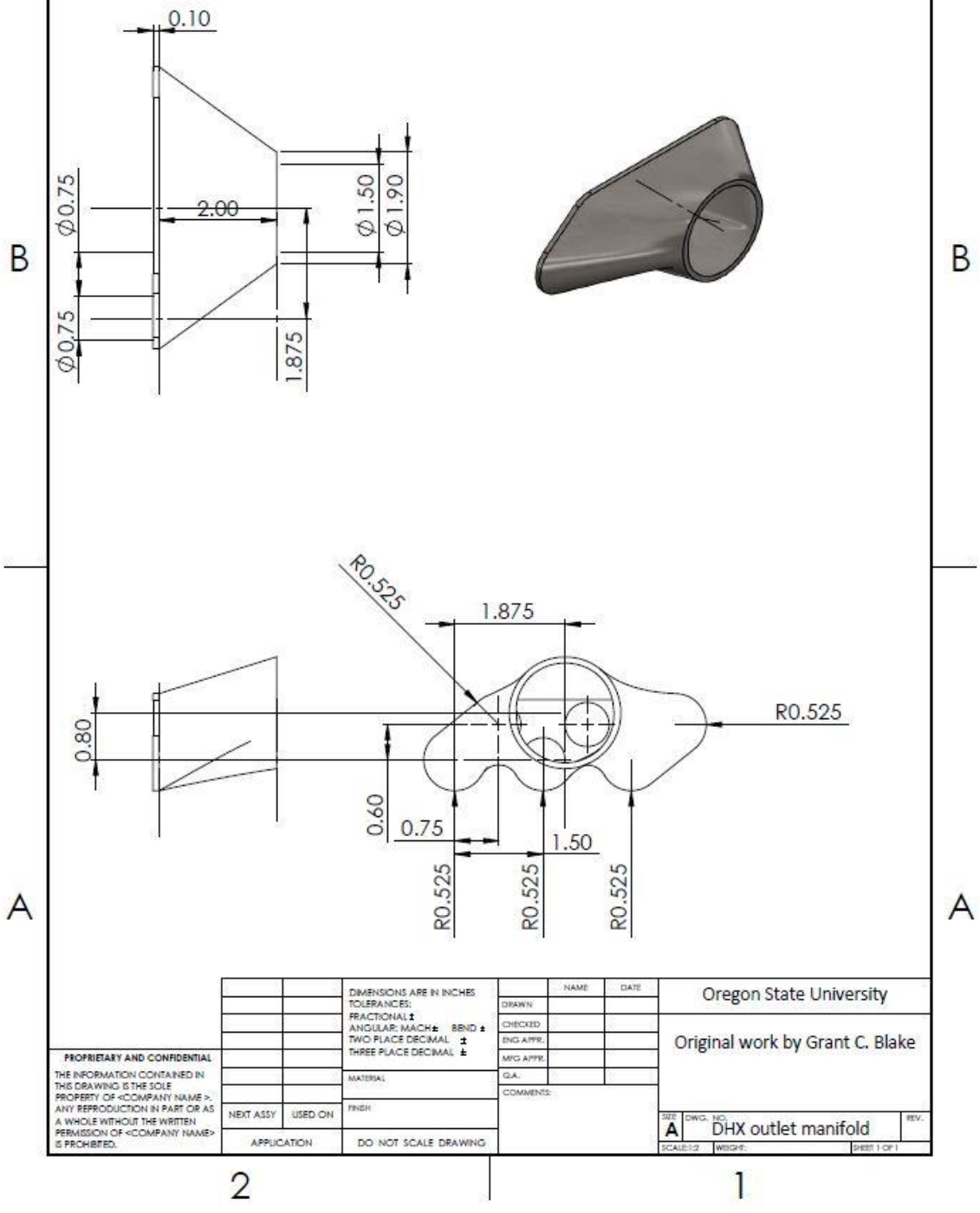
2
1
B
A
0.10
Ø0.75
2.00
Ø1.50
Ø1.90
Ø0.75
1.875
R0.525
1.875
R0.525
0.80
0.60
0.75
1.50
R0.525
R0.525
R0.525
PROPRIETARY AND CONFIDENTIAL
THE INFORMATION CONTAINED IN THIS DRAWING IS THE SOLE PROPERTY OF <COMPANY NAME >. ANY REPRODUCTION IN PART OR AS A WHOLE WITHOUT THE WRITTEN PERMISSION OF <COMPANY NAME> IS PROHIBITED.
DIMENSIONS ARE IN INCHES
TOLERANCES:
FRACTIONAL ±
ANGULAR: MACH ± BEND ±
TWO PLACE DECIMAL ±
THREE PLACE DECIMAL ±
MATERIAL
FINISH
NEXT ASSY
USED ON
APPLICATION
DO NOT SCALE DRAWING
NAME
DATE
DRAWN
CHECKED
ENG APPR.
MFG APPR.
Q.A.
COMMENTS:
Oregon State University
Original work by Grant C. Blake
SIZE A
DWG. NO. DHX outlet manifold
REV.
SCALE:1:2
WEIGHT:
SHEET 1 OF 1